Anthropogenic impact on ecosystems and land degradation in the Eastern Mongolian Steppe

Batnyambuu Dashpurev

München 2022

Anthropogenic impact on ecosystems and land degradation in the Eastern Mongolian Steppe

Dissertation zur Erlangung des Doktorgrades
an der Fakultät für Geowissenschaften
der Ludwig-Maximilians-Universität München

Vorgelegt von
Batnyambuu Dashpurev
aus Bulgan, Mongolei

München, den 31. März 2022

Erstgutachter/in: Prof. Dr. Lukas Lehnert
Zweitgutachter/in: Prof. Dr. Jörg Bendix

Tag der mündlichen Prüfung: 15. Juli 2022

Acknowledgements

The research work presented this thesis would have not been possible without the support, efforts, time and guidance of my supervisors, colleagues, friends and family. My journey to a PhD was not only my study in academic; it has also been a journey for my entire family member to learn new culture, language and education. My PhD journey started with the wonderful one-year time in Marburg and then came to Munich. During the last four years at the Philipps University of Marburg and Ludwig Maximilians University of Munich, I have received lots of opportunities, care, support and inspiration from many people who made me to successfully complete this research.

First and foremost, I want to express my deepest appreciation to my supervisors, Prof. Dr. Lukas Lehnert and Prof. Dr. Jörg Bendix for giving me this wonderful opportunity to conduct my research under your kind supervision in the Philipps University of Marburg and Ludwig Maximilian University of Munich in Germany. Thank you for your continuous supervision, valuable advice, encouragement and support that helped me to successfully accomplish this PhD research project.

I want to express my special appreciation to my supervisor Prof. Dr. Lukas Lehnert for giving me the opportunity to start this PhD project and to join the part of MORE STEP project. He gave me orientation on how to think in a professional way, how to write the scientific research project, how to conduct the scientific research and how to write the scientific articles. I benefited a great deal from his experience and deep understanding of ecology, remote sensing and programming languages. Lukas also granted me the freedom to work on my interests and to develop my ideas and provided me with the valuable opportunity to conduct fieldwork in the eastern Mongolian steppe and to communicate with the botanists and other experts in the MORE STEP project. Additionally, Lukas who not only provided academic advices for my research but also has been a mentor giving me friendly advice on my career. I am so grateful for the valuable advice on both research and on my career.

I would also like to extent my sincere appreciation to my supervisor Prof. Dr. Jörg Bendix for generously accepting to be my supervisor, for giving me a chance to join his working group, and his support, guidance and encouragement. Despite his crowded agenda, he always took time for giving me advice and reviewing my research proposal, report and manuscripts. In this line, I would also like to thank the colleagues of Laboratory for Climatology and Remote Sensing (LCRS) in the Philipps University of Marburg for providing such a friendly, nice and welcoming atmosphere during my stay at the LCRS. I would particularly like to thank Birgit Kühne-Bialozyt and Nazli Turini for their valuable advice and guidance and for being such friendly and nice office roommates. I further would like to thank Ms. Heidi Wiegand (Welcome center, International Office and Family Services in the Philipps University of Marburg) who kindly helped me to find suitable accommodation for my family and a kindergarten and school place for my sons. My first year in Marburg, Germany could never be better without her relocation service, guidance and help.

This research has performed under a PhD scholarship provided by the German Academic Exchange Service (DAAD), Research Grants—Doctoral Programmes in Germany, 2018/19 (57381412), Grant ref. no.: 91691130. I sincerely appreciate to DAAD particularly Ms. Saint

Michelle Jeremy, for her full support and advice. This research was financially supported by the research project "MORE STEP – Mobility at risk: Sustaining the Mongolian Steppe Ecosystem" (Phase I: 01.03.2019 - 28.02.2022 and Phase II: 01.03.2022 - 29.02.2024) funded by the German Ministry for Education and Research (BMBF) (Grant number 01LC1820B). I would like to express my deep gratitude for the financial support of the MORE STEP project.

I would also like to extend my sincere thankfulness to my project collaborators and co-authors. My special gratitude goes to Prof. Dr. Karsten Wesche for his valuable advice, guidance and practical recommendations in fieldwork as well as writing paper. The fieldwork in eastern Mongolia steppe was impossible to conduct without help as Munkhzul Oyunbileg for her valuable help and support. I would particularly like to thank Dr. Yun Jäschke and Oyundelger Khurelpurev for their help and support in field data collection, species determination and writing paper. As well as I would like to extent my sincere appreciation to Prof. Dr. Battsengel Vandansambuu for his valuable advice and support on my study and career.

I would like to express further thankfulness to all my great colleagues from the department of Geography in the LMU, who created a very good and positive working environment. My special thanks to Dr. Phan Thanh Noi, I really appreciated and enjoyed our coffee breaks, lunches and fresh-air breaks on the institute balcony as well as all adventure time we shared together in field campaigns in Mongolia. Moreover, thank you for your valuable contributions to my publications and for sharing your thoughts and experiences with me. Particular thanks to my office roommates, Amarachi Kalu, Yawei Wang and Yueli Chen, who made a friendly and nice atmosphere. As well as I would like to say thanks to all other unnamed colleagues of our remote sensing working group.

Finally, I want to thank my wife, Ulziimaa Dashkhuu, with all my heart. Thank you for giving me the supportive background and persistent encouragement that really made it possible for me to come to this point and thank you for your patience and love. Special thanks are to my lovely sons, Batbilegt Batnyambuu and Tugsbilegt Batnyambuu, who filled my life with greater joy. I would also like to say thanks to all my friends for their support and encouragement. As well as I would like to express my deepest personal gratitude to all my family, especially my lovely mother Badarch Bazarjav, parents-in-law Dashkhuu Dagva and Ichinkhorloo Deevii, brother Myagmardorj Dashpurev, brother Batjargal Dashpurev, sister Tuya Dashpurev and niece Oyunnyambuu Maksad for their enduring love, help, support and encouragement.

To the memory of my father, Dashpurev Dendev, who taught me the hard-working attitudes that have been and continue to be a major source of strength and of inspiration to me.

Summary

The Eastern Mongolian Steppes are one of the last remaining intact temperate grasslands in the world. During the last two decades, a continuous rise in anthropogenic drivers has become one of the most important ecological issues in the eastern Mongolia steppe. Especially, ongoing land degradation poses many serious challenges to ecosystems and sustainable livelihoods over Mongolian steppes. Although few studies exist on the land degradation assessments of eastern Mongolia steppes, none of them investigated the effects of anthropogenic drivers such as land use/cover change, dirt road, transportation corridors and steppe fire on surrounding grasslands and its contribution into degradation process. Because the associated change in land cover and ecosystem is spatially highly variable, it is more difficult to detect degradation drivers and estimate their impact in large and remote areas, such as the eastern Mongolian steppe. This difficulty results to obstruct the identification of land degradation status, as well as to consider its anthropogenic drivers at regional scales. Consequently, the aims of this thesis are (i) to monitor the spatiotemporal changes of land use/cover due to oil exploitation with associated dirt roads and transportation corridors, (ii) to investigate the consequences of dirt road corridors and linear infrastructure on the steppe ecosystems, (iii) to map the current vegetation cover and land degradation status and (iv) to analyze the relationship between land degradation proxy and potential drivers in the eastern Mongolian steppe. To achieve these aims, this thesis developed a remote sensing based approach and extensively evaluated the contribution of modern machine learning methods, multi-spatial and multi-spectral remote sensing datasets and its derived products and field measurements for land degradation assessment. The main research statements and findings are briefly summarized in the following.

The background of the first part of the study was that there is practically no permanent infrastructure in eastern Mongolia. This results in a spatio-temporally highly variable network of unpaved roads with unknown and unmonitored changes. Therefore, the capabilities and limitations of using high and medium spatial resolution satellite imagery with a random forest approach to detect relatively narrow linear features such as roads and dirt tracks were developed. This showed that the new PlanetScope and RapidEye satellites provide suitable imagery, which has a high potential to detect narrow linear features such as dirt roads. However, such data are only available for recent years. Therefore, these high-resolution data were combined with data from long-term archives such as Landsat, which allowed long-term changes in infrastructure to be revealed. The resulting spatio-temporal land use/land cover maps showed that the area of pristine steppe converted to land for oil production and associated unpaved roads and infrastructure has increased by 88%, with the largest expansion of 47% during 2005-2010.

After identifying changes in land use/cover due to the expansion of oil exploitation and exploration, the ecological impacts of dirt roads, transportation corridors and wildfires were investigated using field vegetation measurements and UAV surveys at four sites in the far eastern Mongolian steppe. These plot-scale field data sets were then integrated to multi-temporal PlanetScope imagery for creating large-scale maps of coverage values of plant functional groups. In this context, this study proposed a model to minimize scale issues that often impede classification and regression analysis. The estimates of plant functional group cover revealed that the ecological effects of dirt roads and railroads extended up to 60–120 m into the adjacent, otherwise less degraded steppe vegetation. In addition, a comparison analysis found that wildfires affected the composition of plant functional groups in reducing

the fractional cover of graminoids and forbs, and that increasing cover of bare ground leads to a distinct and patchy mosaic of different vegetation types.

The current land degradation status of the eastern Mongolian steppe was investigated combining remote sensing, geographic information systems and machine learning in this thesis. To gain a better understanding of the land degradation process, this thesis gives greater attention to estimate the proxies of land degradation that support to explain the independent land degradation map of the eastern Mongolian steppe. Therefore, fractional vegetation cover (FVC) and aboveground biomass (AGB) were estimated by Random Forest regressions using Sentinel-2 imagery and 256 field measurements of vegetation in eastern Mongolian steppe. To detect vegetation cover trends, Mann-Kendall trend tests were applied NDVI time series of Landsat. To detect drivers of land degradation, twenty potential variables were selected based on the literature review. These can be grouped into ecological, geomorphometric, environmental and anthropogenic variables. Subsequently, Random Forest classification model was used to predict the land degradation status based on all potential variables and field measurements of degradation rates as response variable in eastern Mongolian steppe. As a result, the land degradation map revealed that most parts of the steppe were affected by some degree of degradation, with more than 36% of the area falling into moderate, heavy and severe degradation classes. Regarding the spatial configuration of degradation, the moderately, heavily and severely degraded land was spatially concentrated in the central parts of the study area where moderate dry steppe and dry steppe occur. Those areas have the least vegetation cover and aboveground biomass that are clearly discriminated in the estimated maps of fractional vegetation cover and aboveground biomass in this thesis. Similarly, the trend test for the changes in vegetation cover found that two-thirds of the eastern Mongolian steppe experienced statistically significant decreasing trends. Additionally, a large proportion of moderately and severely degraded grasslands together with significantly decreasing NDVI trends were located in areas that are mostly used for oil exploration and exploitation, the administration center of the province, and areas along the transportation corridors to border crossings. To understand factors driving biomass in Eastern Mongolia, relationships between AGB and all other land degradation drivers except FVC were examined using Spearman correlation analysis in a running moving window of 500 x 500 pixels in size. Overall results indicate that no strong relationship between AGB and other land degradation drivers could be found over the entire study area; on the contrary, strong correlations have been detected at local scales. Thus, results indicate that the driving forces are not constant over the entire study area. Focusing on certain areas of the study region, AGB is positively correlated with elevation, NDVI trends, distance to mining and oil exploitation sites, distance to road network, soil types, distance to water body, precipitation sum, precipitation change and road corridors, but some of these drivers are negatively correlated with AGB at other locations.

Overall, this thesis delivers new insights into the assessment and mapping of human-induced land degradation and its drivers on the eastern Mongolian steppe using combined methods of field surveys, GIS, remote sensing and machine learning, and develops the state of methodology in identifying ecological effects of anthropogenic drivers on grasslands. In this thesis, ecological effects of transportation corridors on surrounding ecosystem were estimated in eastern Mongolian steppe, which never estimated before in Mongolia. Subsequently, land degradation map estimated by machine learning approach in this thesis revealed that most part of eastern Mongolian steppe is generally affected by some degree of degradation; especially moderate dry steppe and dry steppe are mainly occurred moderate and sever degradation. Furthermore, spatiotemporal land use/cover maps confirm that oil exploitation areas and associated dirt road corridors increased dramatically in dry steppes, where severe land degradation currently occurred. Additionally, the relationship between land degradation proxy

and potential drivers was analyzed to clarify the role and contribution of drivers to ongoing degradation, that has not been extensively analyzed before in land degradation studies in Mongolian steppes.

Zusammenfassung

Die ostmongolische Steppe ist eines der letzten noch intakten gemäßigten Grasländer der Welt. In den letzten zwei Jahrzehnten hat sich der kontinuierliche Anstieg der anthropogenen Einflüsse zu einem der wichtigsten ökologischen Probleme in der ostmongolischen Steppe entwickelt. Vor allem die fortschreitende Degradation ist eine ernsthafte Herausforderung in Bezug auf den Erhalt der Ökosysteme und die nachhaltige Sicherung der Lebensgrundlage in den mongolischen Steppen. Obwohl es wenige Studien zur Bewertung der Degradation in den Steppen der östlichen Mongolei gibt, hat keine von ihnen die Auswirkungen anthropogener Faktoren wie Landnutzungs-/Bodenbedeckungsänderungen, unbefestigter Straßen, Transportkorridore und Steppenfeuer auf das umliegende Grasland und deren Beitrag zum Degradationsprozess untersucht. Da die damit verbundenen Veränderungen der Bodenbedeckung und des Ökosystems räumlich sehr variabel sind, ist es in großen und abgelegenen Gebieten wie der ostmongolischen Steppe schwieriger, Degradationsfaktoren zu erkennen und ihre Auswirkungen abzuschätzen. Diese Schwierigkeit erschwert die Ermittlung des Zustands der Bodendegradation und die Berücksichtigung ihrer anthropogenen Ursachen auf regionaler Ebene. Die Ziele dieser Arbeit sind daher (i) die Beobachtung der raum-zeitlichen Veränderungen der Landnutzung und -bedeckung aufgrund der Erdölförderung und der damit verbundenen unbefestigten Straßen und Transportkorridore, (ii) die Untersuchung der Auswirkungen der unbefestigten Straßenkorridore und der linearen Infrastruktur auf die Steppenökosysteme, (iii) die Kartierung der aktuellen Vegetationsbedeckung und des Zustands der Landdegradierung und (iv) die Analyse der Beziehung zwischen der Landdegradation und deren potenzieller Einflussfaktoren in der ostmongolischen Steppe. Um diese Ziele zu erreichen, wurde in dieser Arbeit ein fernerkundungsbasierter Ansatz auf Basis moderner maschineller Lernmethoden entwickelt, der die Degradation unter Einbeziehung multiskalarer Fernerkundungsdatensätze und daraus abgeleiteter Produkte sowie von Feldmessungen umfassend bewertet. Die wichtigsten Forschungsergebnisse werden im Folgenden kurz zusammengefasst.

Hintergrund des ersten Teils der Studie war, dass in der Ostmongolei praktisch keine permanente Infrastruktur existiert. Dadurch entsteht ein raum-zeitlich höchst variables Netz aus unbefestigten Wegen, über deren Lage und Veränderung keinerlei Informationen existieren. Daher wurden die Möglichkeiten und Grenzen der Verwendung von Satellitenbildern mit hoher und mittlerer räumlicher Auflösung mit einem Random-Forest-Ansatz zur Erkennung relativ schmaler linearer Merkmale wie Straßen und unbefestigter Wege entwickelt. Dabei zeigte sich, dass die neuen Satelliten PlanetScope und RapidEye Bilder mit hoher räumlicher Auflösung liefern, und somit ein hohes Potenzial haben, schmale lineare Merkmale wie unbefestigte Straßen zu erkennen. Solche Daten sind allerdings nur für die letzten Jahre verfügbar. Daher wurden diese hochauflösenden Daten mit Daten aus Langzeitarchiven wie Landsat kombiniert, wodurch langfristige Veränderungen der Infrastruktur aufgezeigt werden konnten. Die von verschiedenen Satelliten abgeleiteten raum-zeitlichen Landnutzungs-/Bodenbedeckungskarten und die Ergebnisse zeigten, dass die Fläche der unberührten Steppe, die in Land für die Ölförderung und die damit verbundenen

unbefestigten Straßen und Infrastrukturen umgewandelt wurde, um 88 % zugenommen hat, wobei die größte Ausdehnung mit 47 % im Zeitraum 2005-2010 zu verzeichnen war.

Nach der Identifizierung von Veränderungen in der Landnutzung und -bedeckung aufgrund der Ausweitung der Ölförderung und -exploration wurden die ökologischen Auswirkungen von unbefestigten Straßen, Transportkorridoren und Waldbränden mit Hilfe von Vegetationsaufnahmen und UAV-Daten an vier Standorten in der fernöstlichen mongolischen Steppe untersucht. Diese parzellenbezogenen Felddatensätze wurden dann in multitemporale PlanetScope-Bilder integriert, um großmaßstäbliche Karten der Bedeckungswerte von Pflanzenfunktionsgruppen zu erstellen. In diesem Zusammenhang wurde in dieser Studie ein Modell zur Minimierung von Maßstabsproblemen vorgeschlagen, die häufig die Klassifizierung und Regressionsanalyse behindern. Die Schätzungen der Deckung von Pflanzenfunktionsgruppen zeigten, dass die ökologischen Auswirkungen von unbefestigten Straßen und Eisenbahnlinien bis zu 60-120 m in die angrenzende, ansonsten weniger geschädigte Steppenvegetation hineinreichen. Darüber hinaus ergab eine Vergleichsanalyse, dass Buschbrände die Zusammensetzung der funktionellen Pflanzengruppen stark beeinflussen, indem sie den Deckungsgrad von Graminoiden und Gräsern verringern, und dass eine Zunahme offenen Bodens zu einem ausgeprägten und lückenhaften Mosaik verschiedener Vegetationstypen führt.

In dieser Arbeit wurde der aktuelle Zustand der Bodendegradation in der östlichen mongolischen Steppe durch die Kombination von Fernerkundung, geografischen Informationssystemen und maschinellem Lernen untersucht. Um ein besseres Verständnis des Landdegradationsprozesses zu erlangen, wird in dieser Arbeit der Schätzung der Proxies für die Landdegradation größere Aufmerksamkeit gewidmet. Daher wurden die anteiligen Vegetationsbedeckung (FVC) und die oberirdische Biomasse (AGB) durch Random-Forest-Regressionen unter Verwendung von Sentinel-2-Bildern und 256 Feldmessungen der Vegetation in der östlichen mongolischen Steppe geschätzt. Um Trends in der Vegetationsbedeckung zu erkennen, wurden Mann-Kendall-Trendtests auf NDVI-Zeitreihen von Landsat angewendet. Um die Ursachen der Landverschlechterung zu ermitteln, wurden auf der Grundlage einer Literaturrecherche zwanzig potenzielle Variablen ausgewählt. Diese können in ökologische, geomorphometrische, umweltbezogene und anthropogene Variablen unterteilt werden. Anschließend wurde ein Random-Forest-Klassifizierungsmodell verwendet, um den Zustand der Bodendegradation auf der Grundlage aller potenziellen Variablen und Feldmessungen der Degradationsraten in der östlichen mongolischen Steppe vorherzusagen. Im Ergebnis zeigte die Karte der Bodendegradation, dass die meisten Teile der Steppe von einem gewissen Grad der Degradation betroffen waren, wobei mehr als 36 % der Fläche in die Klassen mäßige, starke und schwere Degradation fielen. Was die räumliche Verteilung der Degradation betrifft, so konzentrierten sich die mäßig, stark und schwer degradierten Flächen in den zentralen Teilen des Untersuchungsgebiets, wo mäßig trockene Steppen und Trockensteppen vorkommen. Diese Gebiete weisen die geringste Vegetationsbedeckung und oberirdische Biomasse auf, was in den geschätzten Karten der anteiligen Vegetationsbedeckung und der oberirdischen Biomasse in dieser Arbeit deutlich zu erkennen ist. Ebenso ergab der Trendtest für die Veränderungen der Vegetationsbedeckung, dass zwei Drittel der ostmongolischen Steppe statistisch signifikant abnehmende Trends aufweisen. Darüber hinaus befand sich ein großer Teil des mäßig und stark degradierten Graslands zusammen mit signifikant abnehmenden NDVI-Trends in Gebieten, die hauptsächlich für die

Ölexploration und -gewinnung genutzt werden, im Verwaltungszentrum der Provinz und in Gebieten entlang der Transportkorridore zu den Grenzübergängen. Um die Faktoren zu verstehen, die die Biomasse in der östlichen Mongolei beeinflussen, wurden die Beziehungen zwischen AGB und allen anderen Faktoren der Landverschlechterung mit Ausnahme von FVC mit Hilfe der Spearman-Korrelationsanalyse in einem laufenden gleitenden Fenster von 500 x 500 Pixeln Größe untersucht. Die Gesamtergebnisse deuten darauf hin, dass im gesamten Untersuchungsgebiet keine starke Beziehung zwischen AGB und anderen Faktoren der Landdegradation festgestellt werden konnte; im Gegenteil, starke Korrelationen wurden auf lokaler Ebene entdeckt. Die Ergebnisse deuten also darauf hin, dass die treibenden Kräfte nicht im gesamten Untersuchungsgebiet konstant sind. In bestimmten Gebieten der Untersuchungsregion ist die AGB positiv korreliert mit der Höhe, dem NDVI-Trend, der Entfernung zu Bergbau- und Ölförderstätten, der Entfernung zum Straßennetz, den Bodentypen, der Entfernung zu Gewässern, der Niederschlagssumme, der Niederschlagsänderung und den Straßenkorridoren, während einige dieser Faktoren an anderen Orten negativ mit der AGB korreliert sind.

Insgesamt liefert diese Arbeit neue Einblicke in die Bewertung und Kartierung der vom Menschen verursachten Bodendegradation und ihrer Einflussfaktoren in der ostmongolischen Steppe unter Verwendung kombinierter Methoden von Feldstudien, GIS, Fernerkundung und maschinellem Lernen und entwickelt eine Methodik zur Ermittlung der ökologischen Auswirkungen anthropogener Einflussfaktoren auf Grasland. In dieser Arbeit wurden die ökologischen Auswirkungen von Verkehrskorridoren auf das umgebende Ökosystem in der ostmongolischen Steppe abgeschätzt, was bisher in der Mongolei noch nie der Fall war. Die in dieser Arbeit mit Hilfe von maschinellem Lernen erstellte Karte der Landdegradation zeigt, dass der größte Teil der ostmongolischen Steppe im Allgemeinen von einem gewissen Grad der Degradation betroffen ist; vor allem mäßig trockene Steppen und Trockensteppen sind von mäßiger und starker Degradation betroffen. Darüber hinaus bestätigen raum-zeitliche Landnutzungs-/Bodenbedeckungskarten, dass die Ölfördergebiete und die damit verbundenen unbefestigten Straßenkorridore in den Trockensteppen, in denen derzeit eine starke Bodendegradation stattfindet, drastisch zunehmen. Darüber hinaus wurde die Beziehung zwischen den Indikatoren für die Bodendegradation und den potenziellen Ursachen analysiert, um die Rolle und den Beitrag der Ursachen zur fortschreitenden Degradation zu klären, was bisher in Studien zur Bodendegradation in der mongolischen Steppe noch nicht umfassend untersucht wurde.

Table of content

List of Figures

List of Tables

Abbreviations

The following abbreviations are used in this thesis:

Abbreviations	Description
ACC	Active chromaticity color
AGB	Aboveground biomass
CL	Chlorophyll index
DEM	Digital elevation model
GLCM	Grey level co-occurrence matrix
LD	Land degradation
MAUP	Modifiable areal unit problem
MK	Mann-Kendall trend test
NDVI	Normalized difference vegetation index
OBIA	Object-based image analysis
PFG	Plant functional group
FVC	Fractional vegetation cover
PVI	Perpendicular vegetation index
RF	Random forest
SAVI	Soil-adjusted vegetation index
SPA	Strictly protected areas
SR	Simple ratio
SWIR	Shortwave infrared
UAV	Unmanned aerial vehicles
VARI	Visible atmospherically resistant index

Chapter 1. Introduction

Grasslands are vitally important ecosystems, providing a wide range of valuable socioeconomic and ecosystem resources on which human communities and native wildlife are dependent (Bengtsson et al., 2019; Reading et al., 2010; Stevens, 2018). Grasslands cover some 26–40 percent of the Earth's terrestrial surface, representing some of the richest and most diverse ecosystems in the world (Suttie et al., 2005). They are found in diverse locations on all continents of the earth and normally occur between forest and deserts (Dudley et al., 2020; Suttie et al., 2005). In temperate regions such as Eurasian Steppes, North-American Prairies etc., there are vast connected grasslands (Suttie et al., 2005). Mongolia hosts an important part of the largest natural grassland regions in the world that is home to one of the last intact steppe ecosystems with traditional land use and significant biodiversity (Batsaikhan et al., 2014; Pfeiffer et al., 2021; Pfeiffer et al., 2020). Mongolian steppes span between the Siberian taiga in the north and Gobi Desert in the south and provide critical and diverse services and values to unique pastoral social-ecological systems (Pfeiffer et al., 2020; Reading et al., 2010).

Globally, grasslands are facing serious threats caused by ongoing land degradation, consequently, almost half of global total grasslands have been degraded due to land use/cover change, climate change, aridity, human activities and artificial overload such as overgrazing (Bardgett et al., 2021; Dudley et al., 2020), but estimates are still rough especially on local scales. Similarly, land degradation poses many serious challenges to ecosystems and sustainable livelihoods on Mongolia steppes in the last two decades (Girvetz et al., 2014; Reading et al., 2010). Land degradation is a complex and global phenomenon; therefore, existing definitions of land degradation differ. The latest report of the United Nations on the Global land outlook stated that "…Land degradation is the reduction or loss of the biological or economic productivity and complexity of rainfed cropland, irrigated cropland, or range, pasture, forest, and woodlands resulting from land uses or from a process or combination of processes arising from human activities" (UNCCD, 2017). The negative consequences of land degradation are not only limited to the loss of land productivity; it also encompasses the deterioration of environmental quality, loss of biodiversity, and increasing risks to human well-being and sustainable livelihood (Gerber et al., 2014; Langdon et al., 2006; UNCCD, 2017). For grasslands, land degradation leads to negative changes in ecosystem functions and services through reducing aboveground biomass, altering plant communities, declining biodiversity and negatively influencing soil properties (Bardgett et al., 2021). Consequently, grassland degradation leads to many severe environmental challenges, for instance, it results in increases and intensification of dust storms in semi-arid and arid regions (Han et al., 2021).

As the process of land degradation is complex, the drivers of land degradation are numerous which are divided into proximate and underlying driving forces (UNCCD, 2017). Proximate drivers are related to the result of natural processes (e.g., landslides, drought, and floods) and anthropogenic activities (e.g., mining, overgrazing, urbanization, deforestation). Underlying drivers are defined as the interactions of socio-economic, policy, governance, land tenure, land-based goods/services etc., that indirectly or latterly influence the direct drivers of land degradation (Mirzabaev et al., 2015). As multiple drivers lead to land degradation, several broad methodologies for monitoring and assessing land degradation were developed based on the accumulated knowledge of experts, literature reviews, field observations, remote sensing

and modeling approaches, which were designed to be applicable at local, regional, national and global levels (Caspari et al., 2015; Gibbs et al., 2015; Kapalanga, 2008). The methodologies for land degradation assessment have been continuously improved since the 1990s (Bai et al., 2008; Biancalani et al., 2013; Caspari et al., 2015; Millennium Ecosystem Assessment, 2005; Oldeman et al., 1990). In the context of global land degradation assessments, remote sensing plays an important role to estimate the improved or degraded area and to identify land degradation drivers (Dubovyk, 2017a). Remote sensing technologies have continuously advanced in terms of spatial, spectral, radiometric and temporal resolutions (Anderson et al., 2015; Kirui et al., 2021; Van et al., 2001). Furthermore, trends of vegetation indices derived from remotely sensed data have been widely used as a proxy for land degradation changes (Bai et al., 2008; Easdale et al., 2018). Such vegetation indices are effective and simple methods with low-cost to quantitatively and qualitatively evaluate vegetation status. Especially, the Normalized Difference Vegetation Index (NDVI), which effectively distinguishes healthy green vegetation from background features, is the most popular index used for land degradation assessment at micro to global scales (Bai et al., 2008; Huang et al., 2021). Besides that, a wide range of remote sensing products including fractional vegetation cover, aboveground biomass, net primary productivity, soil moisture etc., play leading roles in land degradation assessments (Dubovyk, 2017b; Le et al., 2015; Zika et al., 2009).

Land ecosystems provide the principal basis for many ecosystem functions and services, and human livelihoods and well-being (Shukla et al., 2019). The latest global land degradation assessment reported that 33% of global land area is degraded (Food and Agricultural Organization, 2015). Detailed estimates vary in approaches and outcome; for instance, Gibbs et.al (2015) assessed the world's degraded land by comparing the estimates of four major approaches that included expert opinion, satellite-derived net primary productivity, biophysical models and mapping abandoned cropland. Consequently they found that global estimates of total degraded land range widely from less than 1 billion ha to over 6 billion ha (Gibbs et al., 2015). Furthermore, Le et.al (2015) mapped global land degradation hotpots using the long-term trends of biomass productivity as a proxy of land degradation at global scale and showed that land degradation occurred at about 29% of global land area. Moreover, the estimation of land productivity dynamics derived from high-resolution satellite imagery for the period 1999-2013 found that approximately 20.4 % of the Earth's vegetated land surface experienced a persistent declining trend in productivity (Cherlet et al., 2018). The negative consequences of land degradation on environment and socio-economic are vast, including land productivity decline, soil loss, degradation of ecosystem services, loss of biodiversity and an increase of environmental vulnerability etc. (Pacheco et al., 2018). Besides that, land degradation through human activities is negatively affecting the livelihoods and food security of billions of people. According to the recent global assessment of land degradation and restoration (Montanarella et al., 2018), the well-being of at least 3.2 billion people is affected by land degradation worldwide. During the last decade, several studies estimated the global cost of land degradation based on the terrestrial ecosystem services values and agriculture approaches (ELD Initiative, 2015; Nkonya et al., 2015; Pacheco et al., 2018; Sutton et al., 2016). In the global assessment report of the economics of land degradation (Nkonya et al., 2015), the global loss of ecosystem service values due to land degradation is estimated ranging between USD 6.3 and 10.6 trillion per annum, equivalent to 10-17% of global gross domestic product. The report points out that the impact of land

degradation is especially severe on livelihoods of the rural communities, smallholder farmers and low-income population heavily depending on natural resources.

Almost all terrestrial ecosystem services are directly or indirectly impacted by land degradation. Likewise, about half of global total grassland has been degraded due to ongoing land use/cover change, aridity and artificial overload such as overgrazing (Bardgett et al., 2021; Gang et al., 2014; Montanarella, L., Scholes, R., Brainich, 2018). Grasslands provide multiple ecosystem services including support (e.g., water and nutrient cycling), provisioning (e.g., food production), regulating (e.g., climate regulation), cultural (e.g. recreational), biocontrol (e.g., source of predatory organisms) services and providing a home to thousands of species of flora and fauna (Bengtsson et al., 2019; Egoh et al., 2018; Murray et al., 2013). Recent estimates suggested that the loss of net primary productivity occurred on about 49.2 percent of total global grasslands, especially affecting arid and semi-arid grasslands (Gang et al., 2014; Liu et al., 2019). The drivers of land degradation in general comprise all those external factors which change structures, functions, services, compositions and productivities of terrestrial ecosystems (Montanarella et al., 2018).

The drivers of land degradation are generally grouped into direct and indirect drivers based on the causes (Mirzabaev et al., 2015; Montanarella et al., 2018; UNCCD, 2017), however, any combination of direct and indirect drivers lead to complex ways of land degradation (Cherlet et al., 2018). Existing global land degradation assessment reports summarized numerous drivers (Fig. 1) that lead to land degradation (Cherlet et al., 2018; Food and Agricultural Organization, 2015; Millennium Ecosystem Assessment, 2005; Montanarella et al., 2018; Nkonya et al., 2015; UNCCD, 2017). According to those reports, the direct drivers comprise natural and anthropogenic factors that directly affect terrestrial ecosystems. Some of the most significant direct causes of land degradation are population growth, deforestation, overgrazing, and the expansion of agricultural, industrial, infrastructural and urban areas. Population growth, also known as demographic driver, is critical regarding the ongoing land degradation (Behrend, 2016; Bilsborrow, 1992; D'Odorico et al., 2016; Mortimore, 1993). Rapid population growth and the rising living standards cause expansion and intensification of agriculture and livestock grazing. Furthermore, the needs and consumption of a rapidly increasing population is fostering land use/change, extractive industries, energy production and the expansion of infrastructure area etc. This strongly contributes to land degradation (Food and Agricultural Organization, 2015; IPBES, 2019; Millennium Ecosystem Assessment, 2005; UNCCD, 2017). Besides, rapid population growth in urban area due to a mass migration of populations from rural to urban areas also significantly contributes to land degradation (UNCCD, 2017). More specifically, urbanization directly affects land use change due to expansion of built-up areas, and is one of the key drivers for many environmental issues (Gao et al., 2020; Nuissl et al., 2021). By 2007, urban and rural populations were almost exactly equal at 3.33 billion each. Until 2020, urban populations increased to 4.3 billion while rural population had increased to 3.4 billion worldwide (United Nations, 2021). Furthermore, continuous growth of population causes an increasing global demand for food. Estimates based on the projection of population growth showed that agriculture would need to produce 50 percent more food by 2050 in order to meet increasing food demand (FAO, 2017). As a result of increase in agricultural production, the expansion and intensification of agriculture also pose threats to all terrestrial ecosystems and contributes to degradation (Zabel et al., 2019). The continuous land conversion to agriculture is a major driver of biodiversity

loss, deforestation, soil deterioration and land degradation. Agricultural land currently accounts for approximately five billion hectares, or about 38% of the world's land surface (Foley, 2011; World Food and Agriculture, 2021). Of those, about one third is used for cropland while the remaining two third is grazing land. Between 1985 and 2005, the croplands and grazing lands increased by 154 million hectares or about 3% world's land (Foley et al., 2011) and this increase has directly led to deforestation mainly due to forest clearings, especially in tropical and subtropical regions (Hosonuma et al., 2012). Consequently, cropland expansion has caused about 50% of total estimated soil erosion worldwide (Borrelli et al., 2017). Grazing by domestic animals is also an important driver that leads to the alteration in the floristic composition, changes vegetation cover, soil forms and properties, and, thus influences biodiversity of landscape in meadows and pastures (Dregne, 2002; Greenwood et al., 2001; Kairis et al., 2015). Globally, about 7.5% of grasslands have been degraded because of overgrazing (Conant, 2012).

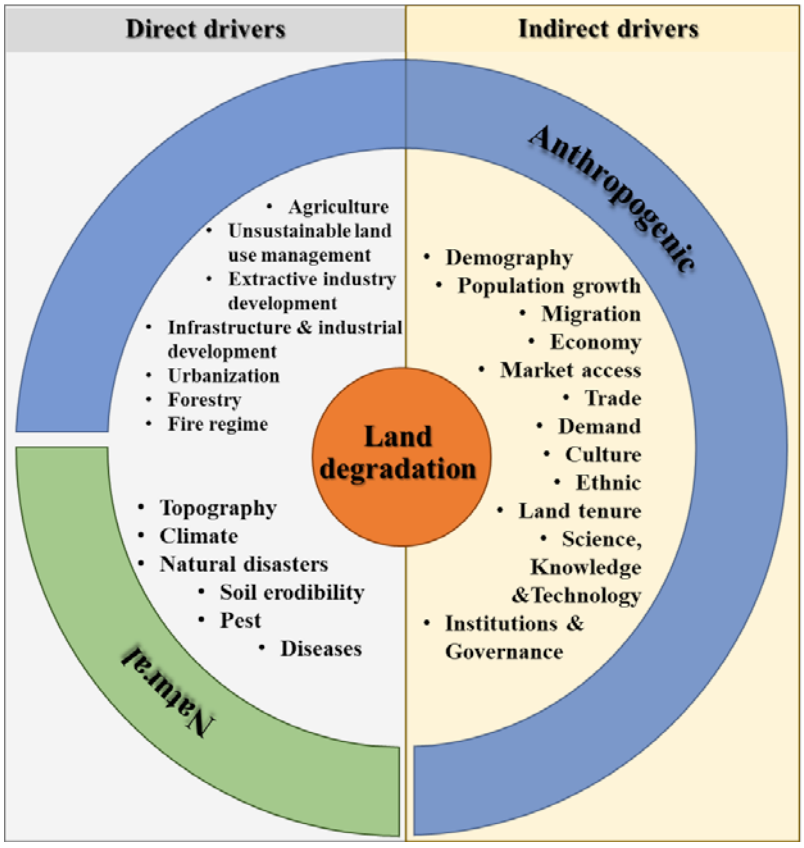

Figure 1. *Drivers of land degradation* (ELD Initiative, 2015; Mirzabaev et al., 2015; Montanarella et al., 2018; UNCCD, 2017).

Worldwide, all forms of mineral extraction including energy minerals, metals, construction minerals and industrial minerals are continuously growing to supply for the demand of population (Cherlet et al., 2021). The mineral extractive sector directly causes a wide range of social and environmental impacts around the world, for instance, expansion of mining and quarrying directly leads to increase in land disturbance, environmental pollution, land degradation and land use change (Agboola et al., 2020; Widana, 2019). According to the most recent global-scale data set of mining areas, the area used for mineral extraction is approximately 57,277 km^2 (Maus et al., 2020). For the land area globally impacted by mineral extraction, it ranges between 300 000 and 800 000 km^2 (Cherlet et al., 2018).

1.1 Study Area

This section briefly introduces the geographical features of Mongolia and fully describes eastern Mongolian grassland steppes. In addition, this section also gives an overview of land degradation status in Mongolia.

1.1.1 Brief overview of Mongolia

Mongolia is a landlocked country and is located in the eastern part of the Asian continent, bordering with Russia in the north and China in the south. Mongolia has a total area of 1.56 million km^2, and it has very diverse geographical features and natural landscapes (Fig. 2). The whole country is part of the Mongolian Plateau. The country's territory is featured with mountains mixed with steppe and vast plains, with an average elevation of about 1580 meters above sea level. The northern and western parts of country are characterized by high mountain chains and vast river valleys. The three major mountain ranges are the Mongol Altai Mountains, the Khangai Mountains and the Khentii Mountains. The southern part of the country is the high plateau of the Gobi Desert with occasional oases that covers over 400,200 km^2. Gobi region is commonly featured with vast plains, sand dunes, sandy strips, red-stone cliffs and canyons, and Saxual forests. Extensive grasslands spread over the eastern part of the country where the steppe mainly consists of broad plains and rolling hills. For the altitudinal and latitudinal zones, the country can be divided into six general natural zones and belts: alpine and mountain taiga, mixed and deciduous forests, forest steppe, steppe, Gobi (desert steppe), and desert zones (Dorjgotov, 2009; Ginin et al., 2019; Yembuu, 2021a).

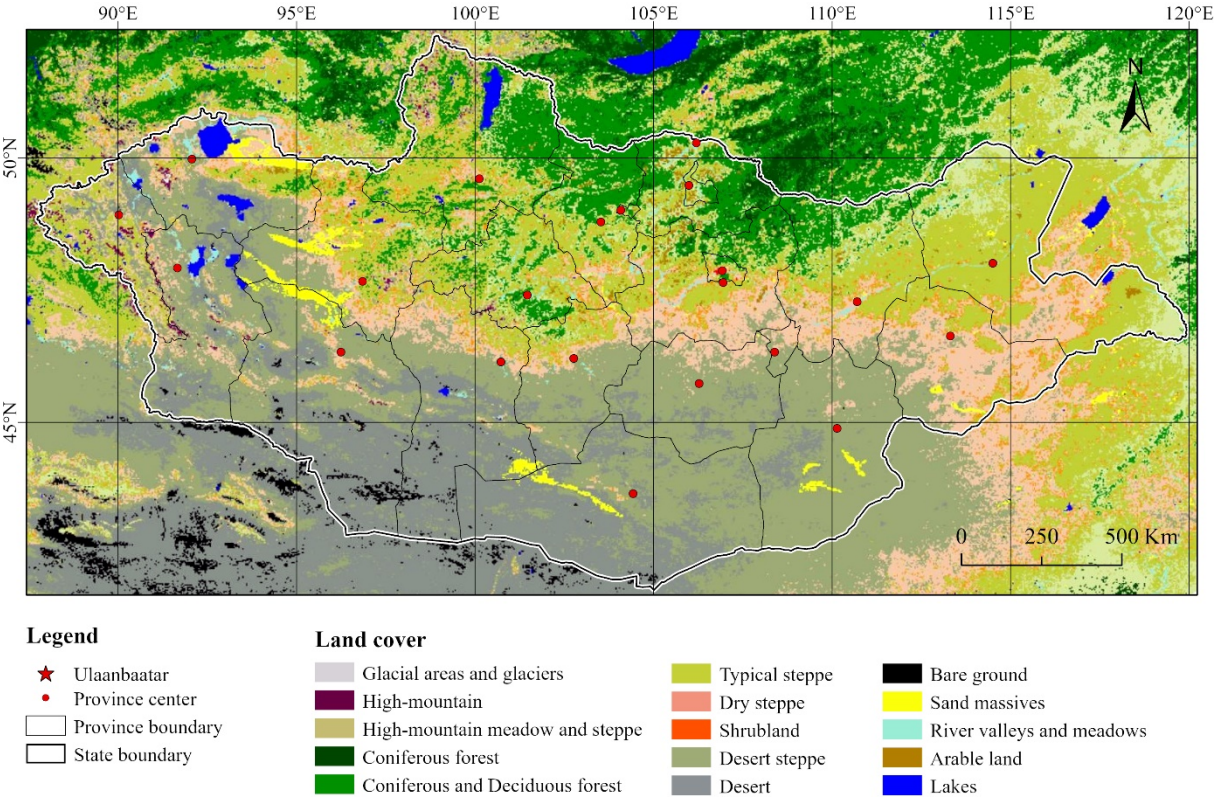

Figure 2. *Land cover map of Mongolia, 2015. Source: Environmental Information center Mongolia* (Environmental Information Center Mongolia, 2021).

The territory of Mongolia is isolated from the seas, located at about 1,000 km from the nearest part of the Pacific Ocean. Consequently, the country has an extreme continental, semi-arid climate with low precipitation and high temperature fluctuations. The average annual temperature ranges from 2 to -8℃. In the highlands, annual average temperature is about -7.8 ℃, while it is about 8.5 ℃ in Gobi region. Average temperatures over most of the country are below 0 ℃ from mid-October through March. The average monthly temperature minimum reaches −31.1 to −55.3℃ in January; the average maximum monthly temperatures of +28.5 to +44.0℃ occur in July. The night temperatures in winter can drop to -40 ℃ in most years while the summer extremes can reach as high as +38℃ in the southern Gobi region. Annual temperature fluctuates at 70-80℃ in most areas. Most of the precipitation falls during the summer and is highest in the north, which receives on an average 350-500 mm of precipitation per year, and lowest in the south, which receives 100-200 mm, while some regions of Gobi Desert in the south receive less than 50 mm of precipitation at all in most years. In the eastern steppe region, precipitation is 200-300 mm (National Statistical Office of Mongolia, 2020; Yembuu, 2021a). The latest assessment confirmed that Mongolia observed an annual mean temperature increase of 2.24°C between 1940 and 2015. The observed rates of warming in Mongolia are much higher than the global average. Warming intensity is spatially variable, for instance, mountainous regions observed higher rise in temperature while these were less in the steppe and Gobi regions. During this period, the annual precipitation slightly decreased by 5.2%. It is reported that the warm season precipitation was mainly declined in the country's central and eastern regions (The World Bank Group and the Asian Development Bank, 2021).

1.1.2 Eastern Mongolian grassland steppe

Mongolia hosts some of the world's largest and most intact steppe regions (Batsaikhan et al., 2014). In total, Mongolia has approximately 1.0 million km^2 steppes including forest steppes, grass steppes and desert steppes (Pfeiffer et al., 2020). The Mongolian steppe is one of the last remaining intact temperate grasslands in the world. The temperate grasslands in Mongolian steppe is the Mongolian portion of the following terrestrial ecoregions: Mongolia-Manchurian grasslands and Daurian forest steppes (Olson et al., 2001; Olson et al., 2002) (Fig. 3). The eastern Mongolia steppe is characterized by an extremely continental climate. The average monthly temperature minimum reaches −20 to −26°C in January; the average maximum monthly temperatures of 19–21°C occur in July. Average annual precipitation amounts to 300-350 mm in Mongolian Daurian forest steppe and 200–300 mm in Eastern Mongolian steppe and Numrug forest steppe, with monthly maxima mainly occurring in summer (Girvetz et al., 2014; Pfeiffer et al., 2021; Shukherdorj et al., 2019; Yembuu, 2021a).

1.1.2.1 Ecoregions, vegetation and wildlife on the eastern Mongolian steppe

The eastern Mongolia steppe has three distinct ecoregions: the Mongolian Daurian (or Mongol Daguur) forest steppe, the Eastern Mongolian typical steppe and the Numrug forest steppe. The Mongolian Daurian forest steppe covers the northern part of the eastern Mongolia steppe and marginal branches of the Khentii Mountain Range and plains. The dominant vegetation is composed by representative species of Daurian forest and mountain steppe and meadow steppe (Table 1), with the mid-sized mountains reaches 1400-1800 m while the mean altitude of valleys is 1100-1200 m above sea level (Hilbig et al., 2016; Pfeiffer et al., 2021; Pfeiffer et al., 2020; Shukherdorj et al., 2019). The eastern Mongolian typical steppe

comprises vast plains and rolling hills where the feather grass *Stipa baicalensis* is dominant alone or together with *Stipa krylovii*. It is composed of moderately dry steppe, dry steppe and moist lowland meadow steppe, with an average altitude of about 800 meters above sea level. In the dry steppe, the vegetation is dominated by bunch grasses like *Stipa krylovii* and *Cleistogenes squarrosa* (Hilbig et al., 2016; Pfeiffer et al., 2021; Pfeiffer et al., 2020; Shukherdorj et al., 2019). The Numrug forest steppe, the far eastern part of the eastern Mongolia steppe, comprises marginal branches of the Greater Khingan Mountains, foothills and plains. The mountain steppe of Numrug receives relatively high amounts precipitation and thus is covered with tall grass steppes. The vegetation is represented by meadow steppe, lowland steppe, and communities of rocky outcrops, mountain steppes, and floodplain vegetation, with the mid-sized mountains reaches 900-1500 m above sea level (Hilbig et al., 2016; Pfeiffer et al., 2021; Pfeiffer et al., 2020; Shukherdorj et al., 2019).

Table 1. *Main steppe types and characteristic species of eastern Mongolia steppes (Pfeiffer et al., 2020).*

Steppe type	Characteristic species
Zonal vegetation of lower elevations:	
Meadow steppe	*Stipa baicalensis, Allium senescens, Filifolium sibirica, Stellera chamaejasme*
Typical steppe	*Leymus chinensis, Stipa baicalensis, S. krylovii, Agropyron cristatum*
Dry steppe	*Stipa krylovii, Cleistogenes squarrosa, Koeleria cristata, Carex duriuscula, Caragana microphylla, C. stenophylla*
Steppe of high mountains:	
Mountain steppe	*Carex korshinskyi, Poa attenuata, Festuca lenensis, Potentilla sericea, Thymus gobicus, Artemisia commutata, Alyssum lenense*

The temperate grasslands in eastern Mongolia support a large assemblage of endemic wildlife such as the endangered Mongolian gazelle. The total population of Mongolian gazelle (*Procapra gutturosa*) is estimated around one million (843,000 – 1,500,000) (Olson et al., 2011); its annual migration is one of the last large-scale migrations in the northern hemisphere (Olson et al., 2010). Beside Mongolian gazelles, other globally and regionally threatened species are occurring at the eastern landscape including mammals such as Pallas's cat, Gray wolf, Corsac fox, Red fox, and birds such as White-naped Crane, Great Bustard, Steppe Eagle, Saker Falcon, Cinereous Vulture, Swan Goose, Japanese Quail, Black-tailed Gadwit, Asian Dowitcher and Yellowbreasted Bunting (Food and Agriculture Organization, 2020).

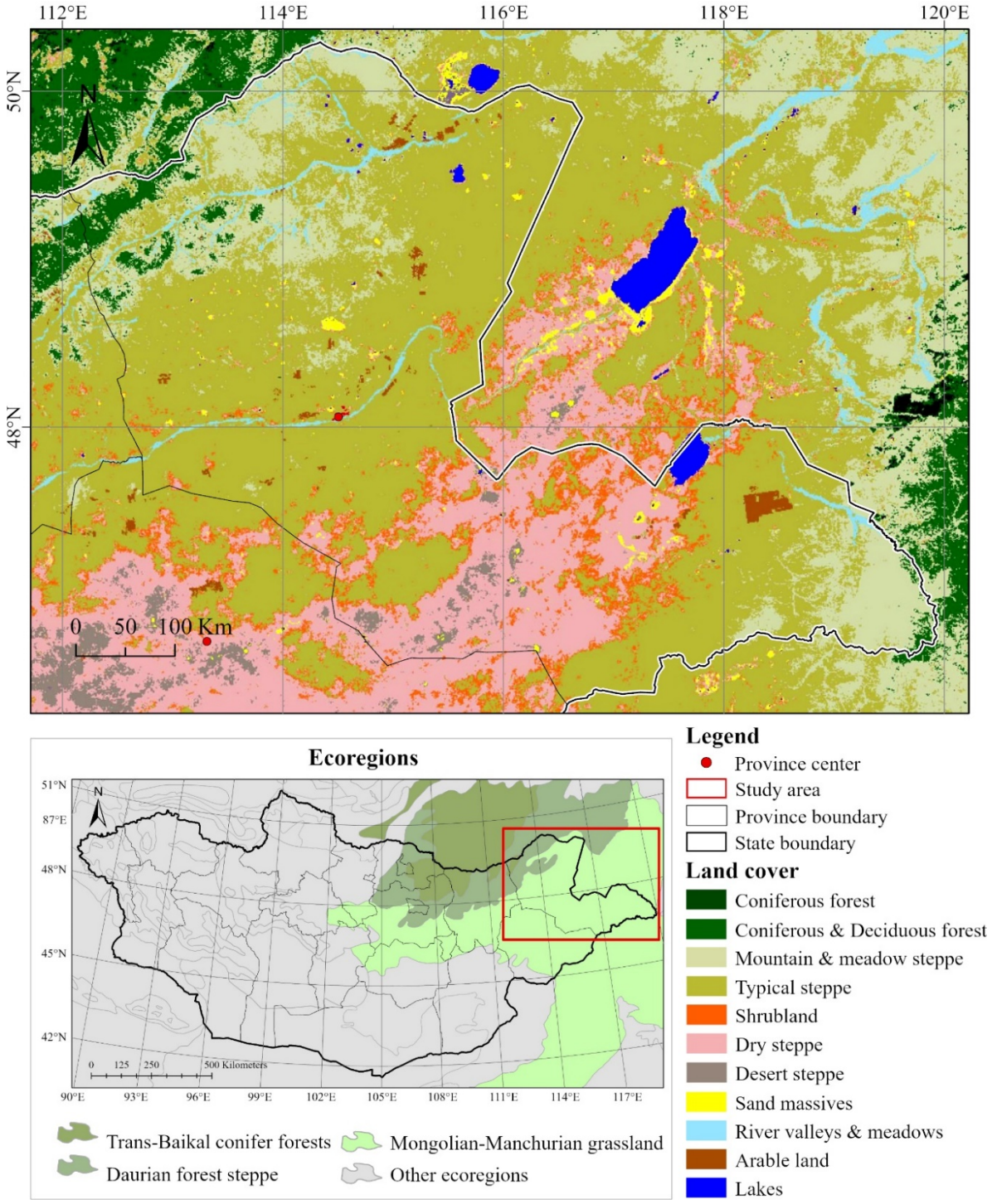

Figure 3. *Eastern Mongolian Steppe ecoregions. Source: Environmental Information center Mongolia* (Environmental Information Center Mongolia, 2021) *and Terrestrial ecoregions of the world* (Olson et al., 2001; Olson et al., 2002).

1.1.2.2 Ecosystem services

Mongolia's grasslands provide multiple ecosystem services (Fig. 4), such as water supply and flow regulation, carbon storage, erosion control, climate mitigation, pollination, cultural, and they are providing a home to thousands of species of flora and fauna (Asian Development Bank, 2014). Mongolian steppe ecosystems are primarily used for domestic livestock grazing

to produce a range of livestock products, and the production of livestock products generate livelihoods for over 22,000 families of nomadic herders in Eastern Mongolia region (Mehring et al., 2018; National Statistical Office of Mongolia, 2020).

Figure 4. *Main ecosystem services of grasslands* (Lemaire et al., 2011; Millennium Ecosystem Assessment, 2005; Zhao et al., 2020).

The primary livestock products are food products and other products such as sheep wool, cashmere, hide and skin. Beside these provisioning services, the steppe provides many cultural services that are also important components on livelihoods of the rural communities' incomes. For instance, the pristine steppe of eastern Mongolia has a range of recreation resources including natural and cultural attractions (Bayarsaikhan et al., 2020).

1.1.2.3 Land use and nature conservation

Mongolian pastoral ecosystems have experienced sustainable and adapted traditional land use for grazing domestic livestock in extreme climatic situations for thousands of years (Fernandez-Gimenez, 2006; Sheehy, 1993). During this long period and different historical era, Mongolian steppes were mainly used for traditional nomadic pastoralism with minimal ecological impact on stability of steppe ecosystems (Endicott, 2012). This form of land use favors communal use by traditional livestock pastoralists, which has changed remarkably little up to the present. The main grazing livestock animals are sheep, goat, cattle and horse in typical steppes, and camels in the dry and desert steppes. Typically, herder families move with grazing livestock animals between seasonal camps each year. In contrast to these short-distance movements, it is also common that herders move over long distances to search fresh forage for livestock animals (Otor). During the 20th century, several changes in Mongolian society and economy occurred that resulted in changes of land use policy and tenure. For instance, the advent of socialist economy resulted in herds becoming state-owned during the period 1930s-1990s (Fernandez-Gimenez, 2006). Moreover, the country's development program of socialist economy led to a number of changes in land use structure through converting pristine steppes to urban areas, mining, industrial land, infrastructure and agricultural land. After institutional and societal changes in the 1990s, also known as transition to democracy and market economy, current land use policy and tenure were formed (Endicott, 2012; Tsedev, 2021), as well as herders were allowed to privatize their herds

(Endicott, 2012). The major land use types in eastern Mongolian steppe are rangelands, strictly protected areas, agricultural land, mines, oil exploration, infrastructure, urban and settlement area. Approximately 80% of the total land in eastern Mongolia are rangelands used for traditional livestock herding (National Statistical Office of Mongolia, 2020). In the eastern Mongolia steppe, there are three strictly protected areas (SPA) and three nature reserves (NR): Mongol Daguur (or Mongolian Daurian) SPA, Numrug SPA, Dornod Mongol SPA, Ugtam NR, Yahi lake NR and Toson khulstai NR (Chimed-Ochir et al., 2010). Mongol Daguur, Dornod Mongol and Toson khulstai are biosphere reserves of the World Network of Biosphere Reserves in UNESCO (UNESCO, 2021).

1.1.3 Land degradation in Mongolia – Brief overview

Mongolia is sparsely populated and one of the biggest continental inland countries with widely varying landscapes, including high mountains, vast steppes, large deserts and dense forests (Yembuu, 2021a). Most of the country's land are government-owned pastures used by traditional livestock pastoralists, followed by arable land, urban areas as well as lands for special needs (National Statistical Office of Mongolia, 2020). In recent few decades, much attention has been given to Mongolian grasslands concerning land degradation, particularly grazing land quality. Because Mongolia is facing land degradation and related environmental challenges due to massive overgrazing, rapid growth of mining, rapid expansion of dirt roads and ongoing global warming. During the last two decades, there have been many efforts at land degradation assessments of Mongolia (Batkhishig, 2013; Dagvadorj et al., 2009; Elbegjargal et al., 2014; Lamchin et al., 2016; Meng et al., 2021; Nyamtseren et al., 2015; Sainnemekh et al., 2022; Sternberg et al., 2011). According to the most recent report (United Nations Convention to Combat Desertification, 2019), about 77.8 percent of Mongolian territory experienced different degrees of degradation. Approximately 22.2 percent of the total land area was not degraded, whereas slightly degraded grasslands occupied 35.3 percent, moderately degraded 25.9 percent, severely degraded 6.7 percent and extremely degraded 9.9 percent, respectively. Furthermore, land degradation is different according to Mongolia’s ecoregions. For instance, the latest report estimated that approximately 40 percent of Mongolian forest area are already suffering from degradation (Ykhanbai, 2010). For the grasslands, the recent estimate based on field monitoring data suggests that as much as 58% of Mongolia's grasslands has been degraded to some extent (Densambuu et al., 2018). Moreover, an analysis of spatiotemporal patterns in Mongolia revealed that the trend of land change in eastern Mongolia steppe was dominated by land degradation in 1990-2020 (Meng et al., 2021; Wang et al., 2020). Particularly, Nasanbat et.al (2018) found that the moderate dry and dry steppes of Eastern Mongolia experienced decreasing NDVI trends in 2000-2016 based on the Mann-Kendall trend analysis. Decreasing trends were especially observed for the months June and July during the same period (Nasanbat et al., 2018).

Scholars suggested that the major causes of ongoing land degradation in Mongolia are deforestation, overgrazing, mining and associated infrastructure development, quarrying, oil exploitation, migration, urbanization and the expansion of agricultural, industrial and infrastructural areas (Batkhishig, 2013; Dudley et al., 2020; Kowal et al., 2021; United Nations Economic Commission for Europe, 2019). Furthermore, migration, centralization, recreation activities and soil erosion of arable lands also contribute to ongoing land degradation (Batkhishig, 2013). These anthropogenic drivers could be strongly related to

Mongolia's socio-economic and institutional change, weak governance in the management of natural resources and the development concept for country's economy growth during the last three decades (UNDP, 2021, 2011). Since Mongolia's transition to a market economy in 1990s, much attention has been paid to develop its main economic sectors including livestock, crop production, extraction of coal, mineral and petroleum and improve transport systems. As a result, country's main economic sectors put significant pressure on its ecosystems, consequently leading to all forms of land degradation (UNDP, 2021, 2011). Furthermore, global climate change also poses a threat to the ecosystems of Mongolia, as it may cause and accelerate land degradation processes (Kowal et al., 2021; Miao et al., 2017). Additionally, Mongolia has experienced substantial impact from global warming, with increasing average summer temperatures by over 2°C and decreasing annual precipitation by 7% between 1940 and 2015 (The World Bank Group and the Asian Development Bank, 2021). The main potential drivers of land degradation in eastern Mongolian steppe will be described in Section 1.2.2.

Land degradation processes strongly influence the sustainable livelihood, economy and environment in Mongolia. An assessment of economic impacts of land degradation in Mongolia showed that the total annual cost of land degradation is estimated at 2.1 billion USD, equivalent to 43% of the country's gross domestic product (Global Mechanism of the UNCCD, 2018). Main economic sectors, especially livestock production, are negatively affected by decline in land productivity. In particular, about 73.5% of the country's territory is used for agricultural production, of which 96.2%, or 1.1 million km^2, is categorized as pastureland which supports over 188,000 nomadic herder families (National Statistical Office of Mongolia, 2020). The livestock sector plays an important role in the economy of Mongolia and food security of its population. The negative impact of land degradation is especially severe for herders who are directly dependent on grassland productivity. For instance, several studies have pointed out that land degradation increases livelihood vulnerability of herders through declining forage biomass and quality and increasing death rates among livestock (Asian Development Bank, 2013; Ulziibaatar et al., 2021). In the meantime, global warming is increasingly influencing the vulnerability of pastoral social-ecological systems in Mongolia, which accelerates degradation processes in grasslands (Chuluun et al., 2017). In particular, the shrinkage and drying up of surface water sources due to climate change is progressing rapidly, which directly threatens Mongolian herder's livelihood (Tao et al., 2015). Arid and semi-arid ecosystems in Mongolia are very sensitive to any changes in water resources; therefore, the drying up of water sources is reducing the available pasture area, forage biomass and pasture yields (Chuluun et al., 2017). Besides that, climate change come along with an increase in frequencies and severities of extreme climate events such as heatwaves, droughts and harsh winters (Dzuds) (IFRC, 2021; The World Bank Group and the Asian Development Bank, 2021). In addition, other agricultural sectors such as crop production are also affected by the decline in land productivity. Some studies pointed out that the arable land erosion could be primary cause for decrease in crop yields in Mongolia (Batkhishig, 2013; Gantumur et al., 2018; Priess et al., 2015). All forms of soil erosion have a detrimental effect on soil quality that results in a reduction of basic functions of soils such as water storage capacity, nutrients availability and rooting space provisioning (Lal et al., 1987). Recent estimates showed that land productivity has already declined on about 4.7% of total croplands in Mongolia (Ministry of Environment and Tourism of Mongolia, 2018). Another study reported that about 46.9% of total arable land in main agricultural regions of Mongolia experienced different degrees of

erosion (Batkhishig, 2013). Land degradation also poses a threat to public health through air pollution, as it causes dust storm. In recent decades, the combined effects of climate change and human-induced land degradation have been contributing to an increase of dust storm events in Mongolian steppes (Nandintsetseg et al., 2015). Generally, Mongolian grasslands experience seasonal wind erosion; however, dust events have become increasingly severe in grasslands and in the Gobi region due to declining vegetation cover, changes in soil structure and moisture and drying out surface water (Gemma et al., 2016; Han et al., 2021; Yong et al., 2021). The hazardous component of sand and dust storms are particulate matters including large coarse (>10 micrometers), coarse (PM2.5–10) and fine (PM2.5) particulate matter (Gemma et al., 2016). Recent studies have reported that the occurrence of eye and respiratory diseases can be related to dust storms the inhabitants are exposed to (Mu et al., 2011; Otani et al., 2017). Dust storm events are not only harmful to human health, but also have a long-term impact on animal health and lead to livestock mortality in Mongolia (Mu et al., 2013).

1.2 Degradation of grasslands on the eastern Mongolian steppe

This section presents the description of grassland degradation processes in the steppe region and explains both main and potential drivers of land degradation. Additionally, this section also gives the detailed description of problem statements that is related to land degradation in eastern Mongolian steppe.

1.2.1 The state of research

The major outcome of land degradation are changes in plants community structure, species composition and functions in grassland ecosystems (Shukla et al., 2019). Therefore, approaches based on plant functional groups have been widely used to investigate and describe land degradation in many grassland ecosystems in the past decades (Luo et al., 2018). A plant functional group (PFGs) is a combination of species that possess similar characteristic and act to cope with similar environments (Gitay et al., 1997). Globally, plant species in grassland communities are commonly classified into PFGs using an *a priori* scheme that considers growth form, life history, and other morphological characteristics (Gitay et al., 1997; Thomas et al., 2019; Wright et al., 2006). In the Mongolian grassland steppes, plants are most commonly categorized by functional similarity based on the growth form (shrub, grass and forbs), life forms and broader taxonomic groups (e.g. graminoids), and plant lifespan (annual and perennial). Usually, PFGs differently respond to different types of degradation drivers and intensities of degradation. Literature reviews suggest that the cover ratio of shrubs, perennial forbs, annual forbs and graminoids is in close relationship with land degradation in temperate grasslands (Kouba et al., 2021; Luo et al., 2018; Zainelabdeen et al., 2020). For Mongolian grassland steppes, several studies have been conducted to determine the responses of PFGs to grazing disturbance (Danzhalova et al., 2012; Fernandez-Gimenez et al., 2001; Lkhagva et al., 2013; Munkhzul et al., 2021; Tuvshintogtokh et al., 2013) and their investigation revealed that heavy grazing directly alters the species of PFGs through reducing the aboveground biomass of palatable graminoids and forbs. For example, an experimental study of the effects of different grazing intensities on pasture also showed that heavy livestock grazing results in a decrease in the ratio of aboveground biomass of palatable plants compared to other plants while annual forbs and unpalatable perennial shrubs are fostered (Nakano et al., 2020). Other detailed studies also revealed that heavy grazing leads to an increase in the dominance of the dwarf shrubs *Artemisia frigida* and *Ephedra sinica* as well as the true shrubs *Caragana microphylla* and *Caragana pygmaea* in Mongolian steppe ecosystems (Bazha et al., 2012; Gunin et al., 2012). Similarly, the disturbance associated dirt road transportation effects to alter surrounding vegetation community (Coffin et al., 2021; Forman et al., 1998; Trombulak et al., 2000). For instance, in a vegetation survey around abandoned and active dirt roads, in central Mongolian typical grassland, showed that the aboveground biomass of *Artemisia* genera significantly increased at the abandoned dirt road and around the active tracks, consequently, those low-palatable species of *Artemisia* genera spreads to the pristine steppe through producing many shoots (Kinugasa et al., 2015). Other studies also reported that the dwarf shrub *Artemisia frigida* showed increased abundance along abandoned tracks and spread into the surrounding, formerly intact vegetation (Bazha et al., 2012; Li et al., 2006). Considering these responses of PFGs to disturbances, the distribution of shrubs and annual forbs indicates degradation, whereas species of other taxonomic groups are typical for healthy steppes. In degradation studies, the PFGs are mostly determined and monitored based

on the ground survey with traditional vegetation sampling methods. These ground-based approaches are important in evaluating land degradation processes, but these methods are costly and time-consuming for large areas. On the other hand, remote sensing methods including high spatial resolution satellite and an unmanned aerial vehicle (UAV) have emerged as a cost-effective alternative to successfully identify species of PFG (Kaneko et al., 2014; Zhao et al., 2021).

During the last four decades, substantial research has been done to gain knowledge of the theoretical basis for using satellite-derived vegetation indices such as a Normalized Difference Vegetation Index (NDVI) for monitoring Earth's vegetation cover and dynamics (Huang et al., 2021; Yengoh et al., 2015a). Such indices derived from remotely sensed satellite-derived data allow delineating the distribution of vegetation and soil based on the characteristic reflectance patterns of green vegetation. The NDVI is a simple numerical indicator that can be used to analyze the remote sensing measurements, from a remote platform and assess whether the target or object being observed contains live green vegetation or not (Kriegler et al., 1969). There are many studies that have proven advantages and benefits in the use of NDVI to assess the vegetation cover and land degradation (Huang et al., 2021). In addition, the NDVI correlates directly with vegetation productivity (Tucker et al., 1986) and the index is easily calculated from spectral bands encompassing long time series. Moreover, the rapid advancements in remote sensing technology and application are making the use of NDVI more popular for vegetation cover assessments (Yengoh et al., 2015b). For reasons related to its strong correlation with vegetation productivity, simplicity, and availability of remote sensing data, changes in NDVI time series have become a proxy for land degradation assessments at global, regional, national and local level (Bai et al., 2008; Huang et al., 2021). Nonetheless, a direct use of NDVI to discriminate between degraded and non-degraded area can be misleading because of several challenges and limitations. The reasons are that the NDVI is not in direct relationship with vegetation degradation, for instance, species changes in plant community occur due to land degradation that leads to increase within some species called degradation indicator species. Strong spread of indicator plants might cause higher NDVI values because these species tend to have high aboveground productivity in Mongolian steppes (Kinugasa et al., 2015; Nakano et al., 2020). Contrarily, species changes in sparsely vegetated area such as semi-dry and dry grasslands may result in low or moderate NDVI values, but this does not always indicate more severe degradation (Li et al., 2020). Therefore, map products that highly discriminate the distribution between degradation indicator plants and other taxonomic group are needed for land degradation assessment in Mongolian grassland steppes.

In land degradation studies, there are proxies for vegetation cover assessments that can directly be derived from both remote sensing data and field measurements (Bao Le et al., 2016). For instance, the fractional vegetation cover (FVC) is an important parameter describing the vegetation degradation and soil erosion, and is often used to evaluate and monitor land degradation status (Chu, 2020; Liang et al., 2020a). FVC has emerged as a measure of ground covered by green leaves and can serve as proxy to assess vegetation condition (Carlson et al., 1997). Moreover, long term changes in FVC can reveal the dynamics of vegetation expansion or loss. FVC can be calculated easily from remote sensing data or by combining field measurement and remote sensing data (Gao et al., 2020). Previously, many researchers have examined the usage of FVC on degradation studies and

soil erosion and confirmed that FVC has a high potential to describe the both land degradation process and soil erosion (Anees et al., 2022; Liang et al., 2020a; Liu et al., 2021; Meusburger et al., 2010). Although FVC is easily calculated from remote sensing data and field measurements, not many studies have conducted to estimate land degradation using FVC in Mongolia (Jaebeom Kim et al., 2020). Besides that, aboveground biomass (AGB) is also a critical ecological variable for understanding the land degradation process and the determining drivers of the degradation (Shukla et al., 2019). AGB is a mass of living vegetation and dead plant material above the soil and is mainly estimated by traditional field measurements or remote sensing methods (Kumar et al., 2017; Liang et al., 2020b). AGB in Mongolian grasslands is dependent on many internal and external factors, such as terrain factors, climate conditions, soil properties and land use (Chen et al., 2007; John et al., 2018; Nanzad et al., 2021). In other words, it is possible to understand land degradation process and drivers through analyzing the relationship and interaction between the spatial patterns of AGB and those many factors. Scholars showed that there have been few efforts at AGB mapping over Mongolia (John et al., 2018; Otgonbayar et al., 2019). However, there is no study on analyzing the relationship between AGB and land degradation drivers for determining potential drivers of land degradation in Mongolian grasslands.

Generally, there are numerous potential natural and anthropogenic forces, which may cause land degradation over Mongolian steppes. These have been widely discussed by several studies, but seldom is their effect quantified in a spatially-explicit manner. Overall, these previous studies suggested that major drivers of land degradation are an increase of human pressure (Batkhishig, 2013; M. Pfeiffer et al., 2021), land use change due to mining and oil exploitation (Batkhishig, 2013; Elbegjargal et al., 2014; Han et al., 2021; Ma et al., 2021), an expansion of dirt roads (Batkhishig, 2013; Keshkamat et al., 2013, 2012; Kinugasa et al., 2015), overgrazing (Batkhishig, 2013; Lkhagva et al., 2013; Munkhzul et al., 2021; Pfeiffer et al., 2021; Sainnemekh et al., 2022), climate variability (Elbegjargal et al., 2014; Han et al., 2021; Liu et al., 2013; Nandintsetseg et al., 2021; Pfeiffer et al., 2021), soil erosion (Batkhishig, 2013; Han et al., 2021; Jugder et al., 2018; Jungrack Kim et al., 2020) and topography (Meng et al., 2021; Xiaoyu et al., 2020). Furthermore, migration, centralization, recreation activities and soil loss of arable lands also contribute to ongoing land degradation (Batkhishig, 2013; Elbegjargal et al., 2014). For mapping land degradation using these drivers, only few studies and national assessments have made an effort to identify the contributions and interactions of major drivers on the ongoing land degradation in Mongolian steppes (Elbegjargal et al., 2014; Meng et al., 2021; Xiaoyu et al., 2020). However, despite these efforts, no comprehensive and spatially-explicit study exists, which considers all above-mentioned potential drivers in Mongolia. For instance, some major anthropogenic drivers have not been considered partly because of the lack of data such as the expansion of dirt road. This may lead to an inaccurate description of land degradation process in eastern Mongolian steppe.

1.2.2 Main and potential drivers of land degradation

Overgrazing. Eastern Mongolian steppe has long been used as pastureland for the nomadic pastoral system (Sheehy, 1993). The livestock grazing pressure largely influences land degradation in Mongolia (Batkhishig, 2013; Tuvshintogtokh et al., 2013), which leads to altered floristic compositions and structure of vegetation cover, species richness, aboveground

biomass, and soil properties and compaction in steppes (Densambuu et al., 2018; Hilker et al., 2014; Kowal et al., 2021; Munkhzul et al., 2021; Na et al., 2018; Sainnemekh et al., 2022). After Mongolia's transition to a market-based system in the early 1990s, herders were allowed to privatize their herds and the number of livestock has increased dramatically. Data from statistical yearbooks (National Statistical Office of Mongolia, 2020; National Statistics Office of Mongolia, 2021) show that the number of livestock increased from 25.8 million to 67.0 million heads between 1990 and 2020 in Mongolia. For eastern Mongolia, the number of livestock has increased almost four times from 3.1 million to 11.3 million heads during this period. Consequently, continuous growth of livestock numbers causes pasturelands to vastly exceed their carrying capacities (Tumur et al., 2020). A recent systematic review summarized the state of research in grazing effects on Mongolian steppe vegetation and found that overall domestic livestock grazing effects negatively in the most of Mongolian steppes except meadow and mountain steppes, especially grazing had a stronger effect on the vegetation of dry steppe as the eastern Mongolia steppe (Munkhzul et al., 2021).

Land use change due to mining and oil exploitation. Within the past several decades, mining has been an important driver of Mongolia's economic growth and investment (Suzuki, 2013). After the shift to a market economy in 1990s, the development concept and strategy for Mongolia's economy growth has become mainly based on the extraction of mineral resources and petroleum (Goyal, 1999; UNDP, 2011). By the mid-2000s Mongolia was emerging as a significant mining country (World Bank Group, 2017), consequently, about 31.3% of country's territory was issued for mineral and coal exploration licenses. In meantime, approximately 0.3% of total territory was issued as operation licenses for mining (Mineral Resources Authority of Mongolia, 2015). Since 2009, Mongolian government has been implementing the restriction policy for mining expansion in order to decrease mining environmental impacts. For instance, several laws were adopted to stop mining activities in upstream river and forested areas (Batkhishig, 2013; United Nations Economic Commission for Europe, 2019). Most recent statistics of mining and geology shows that percent of total licensed area in Mongolia's territory is 4.7 percent, of which 3.7 percent is exploration and 1.0 percent as mining operation (Mineral Resources Authority of Mongolia, 2021). In the meantime, steppes in eastern Mongolia have been intensively used owing to the rapid growth of natural resource extraction, including mining, quarrying and oil extraction, as the extractive sector has become a major part of the economy of Mongolia (Mongolia EITI, 2020). Eastern Mongolia is one of the richest regions in the country in term of raw materials. According to the mining and geology statistics, Dornod aimag (or province) had rich deposits of coal, gold, uranium, petroleum and other metallic ores (Mineral Resources Authority of Mongolia, 2016; Plaza-Toled, 2018). However, much attention has focused on oil exploitation of Tamsag sedimentary basin and large-scale oil exploration projects in Choibalsan sedimentary basin and sub basins of Tamsag and East Gobi sedimentary basin in the Eastern Mongolia region (Tully et al., 2014). Most parts of steppe area in Dornod province are subject to oil exploration licenses under the production sharing contract divided into several blocks encompassing different areas granted in different years. For instance, Mongolia fourteenth EITI reconciliation report 2019 (Mongolia EITI, 2020) documented that five active exploration projects were registered in the field of following blocks in Dornod province: Matad XX, Bayantumen XVII, Kherlentokhoi XXVIII, Ar bulag XXIX and Khukh nuur XVIII. These five petroleum exploration blocks occupy approximately 41 thousand km^2 in the province. In addition, two oil extraction sites were constructed in the Toson Uul XIX and

Matad XXI blocks in 2003 and 2005, which cover about 859.2 km^2. Besides petroleum, Dornod province has 162 valid mining licenses at the end of 2021 and these licensed areas cover about 4.3% of total territory (Table 2), of which 75 licenses are granted for mining operation, and exploration licenses accounted as 87 (Mineral Resources Authority of Mongolia, 2021). Activities related to mining, quarrying, oil exploitation and mineral and oil exploration resulted in the conversion of a large area of pristine steppe to lands for mining sites and miners' village, infrastructure, roads, and disturbed lands. Furthermore, environmental impacts of mining and oil exploitation, and associated infrastructure development are not limited to operation sites.

Table 2. *The number of valid mining licenses with size of area*

	In total			Out of which:					
				Mining			Exploration		
	No. of license	Area (thousand ha)	% of licensed area to total territory	No. of license	Area (thousand ha)	% of licensed area to total territory	No. of license	Area (thousand ha)	% of licensed area to total territory
Nationwide	2,668	6,263.3	4.0%	1740	1,762.7	1.1%	928	4,500.6	2.9%
Eastern Mongolia region*	467	1060.9	3.7%	273	183.1	0.6	194	877.7	3.1%
Dornod province	162	528.9	4.3%	75	69.3	0.6%	87	459.6	3.7%

*Eastern Mongolia economic region comprises Khentii, Sukhbaatar and Dornod province.

Expansion of dirt roads. Dirt road expansion is also a potentially important factor for land degradation in Mongolia, which influences soil erosion (Batkhishig, 2013; Keshkamat et al., 2013, 2012). In far eastern Mongolia, oil exploitation and transportation of crude oil from the Tamsag oil basin increased rapidly in the past two decades (Mongolia EITI, 2020). Consequently, an increased number of permitted and informal dirt roads related to oil exploitation activities in eastern Mongolia region caused extensive soil erosion and degradation in the surrounding areas of the oil exploitation sites and along the transportation corridors from the sites to the Mongolian-Chinese border. Further, large-scale oil exploration activities such as gravity, magnetic and two or three-dimensional seismic surveys led to increase dirt roads, trails and linear land disturbance in eastern Mongolia steppe. For instance, Mongolia extractive industries transparency initiative reported (Mongolia EITI, 2020) that 2D and 3D seismic surveys carried out at 12.78 thousand line kilometers of seismic trails and 5.33 thousand km^2 area in Tamsag basin, respectively. Furthermore, all five petroleum blocks in far eastern Mongolia steppe are subject to further geophysical surveys for oil exploration. There are no exact information about impacts of large-scale seismic surveys for surrounding ecosystem over Mongolia; however, some studies documented that seismic exploration programs primarily led to increasing land disturbance, soil erosion and the number of permanent and temporal dirt roads due to off-road vehicle usage (Kemper et al, 2009;

McCarter et al., 2017; Pring et al., 2010; Raynolds et al., 2020). Besides, mining development and the rising living standards in eastern Mongolia result in increasing numbers and usage of privately owned vehicles. The poor infrastructure in the Eastern Mongolian Steppe's rural areas fosters off-road vehicle travel and transport that consequently induces land disturbance. Since many steppe fires are ignited by cars which are driven over long-grass steppes, increases in off-road transportation will presumably lead to higher fire frequencies.

Climate change. Mongolia is one of the countries that are most severely impacted by ongoing climate change. Mongolia has already experienced significant warming and drying as a result of the global climate change (The World Bank Group and the Asian Development Bank, 2021). Since 1960s, the air temperature have increased about 1.4–2.4 °C at weather stations in Mongolia, while the warm season precipitation rapidly declined in the central and eastern parts of Mongolia (Dagvadrj et al., 2014; The World Bank Group and the Asian Development Bank, 2021; Yembuu, 2021b). These changes increase risks of heatwaves, aridity and droughts in semi-arid grassland ecosystems of eastern Mongolia. For instance, recent estimation reveal that climate change leads to an increase in the aridity of Mongolian steppes, which caused an increase in the ecological sensitivity and vulnerability (Nandintsetseg et al., 2021). Increasing aridity of ecosystems is a one of forces behind land degradation, which could accelerate the degradation process due the climate change in Mongolian grasslands (Miao et al., 2017; Yembuu, 2021b). Future projection of drylands under climate change suggested that aridity in Mongolian steppes will increase which will lead to shifts in vegetation zones consequently leading to higher proportions of arid and semi-arid zones in Mongolia (Huang et al., 2016). This study also pointed out that the risk of land degradation and desertification would be exacerbated due to the increasing aridity with other driving forces in the near future in the drylands of developing countries like as Mongolian steppes.

Other potential drivers. Soil erosion, both from water and wind, is one of the important drivers of land degradation in Mongolian steppes (Batkhishig, 2013). Soil erosion is a geomorphic process, however, human activities and associated land use change significantly accelerate all forms of erosion (Borrelli et al., 2017; Guerra et al., 2017). Unfortunately, there is not much research conducted in Mongolian steppes to assess the influence of soil water erosion and its rate. In an experimental study of soil water erosion conducted in Khentii province in eastern Mongolian steppe, observations of sediment yield amounts from two experimental catchments showed that annual average potential soil erosion rates ranging between 0.37 t/ha to 0.02 t/ha (Onda et al., 2007). Global estimates of soil erosion using universal soil loss equation (USLE/RUSLE) suggested that annual average soil water erosion roughly ranged from 0 to 1 t/ha in eastern Mongolia steppes (Borrelli et al., 2017). Besides that, surface wind erosion also contributes to ongoing land degradation; consequently, subsequent dust generation from degraded land is emerging as serious environmental and socio-economical threats to local communities in Mongolian steppes and neighboring regions (Han et al., 2021; Shi et al., 2010). One of the important signs that land has severely degraded is the occurrence and intensification of dust storms; therefore, soil wind erosion is explained as a potential driver of land degradation in arid land (Sterk et al., 2001). Estimation of wind erosion based on field measurement suggested that wind erosion rates estimated 0.64–1.69 $t \cdot ha^{-2} \cdot y^{-1}$ in typical steppes of Mongolia (Qi et al., 2008). Furthermore, modeling estimates of soil wind erosion using wind erosion equation (WEQ) in Mongolia ranged between 10 to 15 t

ha^{-2} y^{-1} for dry steppes and 5 to 10 t ha^{-2} y^{-1} for typical steppes (Mandakh et al., 2016). In the present study, annual soil loss, soil erodibility and soil types were considered as potential drivers for land degradation. In addition, topographical factors, also known as geomorphometric factors, indirectly influence land degradation processes in Mongolian steppes. For instance, a study conducted to evaluate effects of driving factors on vegetation growth in Mongolia found that topographic factors including elevation, slope degree, slope aspect and curvature have significant effects on vegetation cover change in Mongolia (Xiaoyu et al., 2020).

1.2.3 Problem statement

1.2.3.1 Land use change due to oil exploitation and associated dirt road and infrastructure development in far eastern Mongolia

In the last two decades, land degradation due to the intensification of human activities has become one of the most important ecological issues in the semi-arid grasslands of far eastern Mongolia. The region harbors one of the last intact steppe ecosystems with traditional land use and significant biodiversity (Girvetz et al., 2014; Mehring et al., 2018). Since the first crude oil field discovered in the Tamsag basin in 1995, most of eastern Mongolian steppes are subject to ongoing oil exploration and extraction. Testing of oil production began in 1998, while starting from 2005, main oil extraction sites were constructed and started to export crude oil (Mongolia EITI, 2020). As a consequence, the pristine steppe of far eastern Mongolia was converted to oil exploitation sites, associated with dirt roads and other linear infrastructure, miners' villages and quarries. This land use/cover change is not only restricted to operation sites. Rising oil exploration and exploitation activities cause many environmental issues such as extensive land disturbance and oil spills in areas, which are important habitats of Mongolian gazelles in whole far eastern Mongolian steppe (Girvetz et al., 2014; Nandintsetseg et al., 2019). Moreover, the exploration, extraction and transportation of oil in the steppe cause the rural dirt road network to grow in the form of dirt track corridors. In the meantime, the dirt roads negatively affect the environments and lead to significant disturbances such as vegetation and biodiversity loss and soil erosion all resulting in declines in ecosystem productivity. Therefore, the knowledge about the land use/cover change and current expansion of dirt road network is critically required for environmental conservation and combating land degradation in the steppe region.

The presumably increasing area, which is affected by degradation due to oil exploitation activities and associated infrastructure and dirt road expansion, is currently not monitored and estimations of land disturbance through dirt road usage are still challenging. The reasons are that growth of dirt road network is mainly detected and updated using ground-based GPS surveys and manually digitizing from satellite imagery, but these methods are time consuming and cost intensive for mapping large and remote areas as the Eastern Mongolian Steppe. In addition, dirt road networks change rapidly across short time scales, making GPS surveys even less appropriate. Although it is still difficult to gain accurate maps of dirt road networks, the road-mapping methods that combine novel remote sensing platforms and modern machine learning technique have been dramatically improved at detecting roads with reasonable accuracy in recent years. Such a novel remote sensing platform with high spatial resolution allows detecting the dirt road network and linear infrastructures based on the spectral and spatial characteristics. PlanetScope and RapidEye, also known as the CubeSat satellites, are

examples of recently developed remote sensing platforms with high resolution, which open new possibilities in the study of automatical dirt road detection and detailed land use/cover change analysis. An important gap in the ecological impact assessment of dirt roads is the understanding of any potential effects of dirt roads on surrounding ecosystems and landscapes. One of the possible options to fill this gap is the time series of remote sensing data that enables to reveal the land use/cover and dirt road network change over a longer period.

1.2.3.2 Assessing impacts of transportation corridor and associated dirt roads on steppe vegetation change

An increase of transportation corridors and permanent and temporal dirt roads, driven particularly by the expansion of the mining and oil exploitation causes environmental challenges (Batmunkh, 2021; World Bank, 2006), because both mineral and oil extractive industrial sectors lead to an increase of traffic particularly in the Mongolian countryside. Moreover, the rising living standards and changes in nomadic lifestyles in eastern Mongolia result in increasing numbers of vehicles. Besides, the eastern Mongolian steppe is one of the most popular travel destinations in Mongolia (Bayarsaikhan et al., 2020). Increasing number of tourists leads to growth of uncontrolled rural roads in the Eastern Mongolian steppe. Mongolia‘s paved road network progressively increased from 1,250 km in 1992 to 9,834 km in 2020 (National Statistical Office of Mongolia, 2020). Most paved roads are concentrated in the central region of Mongolia around the capital Ulaanbataar and province centers. Unfortunately, the increment of paved road network is insufficient in comparison to the large territory of Mongolia (Asian Development Bank, 2011). Therefore, the dirt road network is increasing in the all regions of Mongolia.

Currently, only rough estimates of the extension of the Mongolian dirt road network exist. According to the most recent statistical yearbook (National Statistical Office of Mongolia, 2020), Mongolia‘s road network comprise 100,000 km of dirt roads and 2000 km of gravel roads in its approximately 111,942 km network. Out of the 111,942 km of the roads, approximately 12,700 km are intensively used as main national routes. Rough estimates suggested that main road network leads to an area of approximately 3 million ha that is subject to degradation (United Nations Economic Commission for Europe, 2019). The width of dirt track corridors varied depending on dirt road condition and usage, and some of these corridors could reach over 4 km in width (Keshkamat et al., 2013). Because frequent and repeated usage of a track reduces the dirt road condition and leads to the generation of large ruts and corrugations (Keshkamat et al., 2012), drivers avoid the usage of bad conditioned old dirt roads and introduce new ones increasing dramatically the area affected by road transportation year by year.

Relatively few studies have examined the effects of dirt roads on surrounding vegetation on Mongolian steppes (Li et al., 2006) and its consequences for instance on the land degradation and environmental impact (Keshkamat et al., 2013, 2012). Some of these studies were only focused to determine widths of dirt road corridors and investigated the cause of dirt road widening over Mongolia (Keshkamat et al., 2013). For a case study conducted in the central Mongolian steppe, it was investigated that vehicle travel causes the destruction of the surface vegetation, soil compaction, loss of soil aggregation, changes in soil texture, partial or complete removal of the top layer of soil, and loss of soil organisms (Li et al., 2006).

However, important research gaps still remain in the impact assessment of dirt road corridors on surrounding steppe vegetation such as an integrated understanding of the area affected ecologically by dirt roads. Due to this gap, most of past national land degradation assessments roughly estimated the impact and contribution of dirt road corridors to land degradation in Mongolia (United Nations Economic Commission for Europe, 2019). Furthermore, assessing impacts of dirt roads over remote and large territory as Mongolian steppes is costly and time-consuming, therefore, cost-effective methods for assessment are also required.

1.2.3.3 Mapping vegetation cover, biomass and land degradation in eastern Mongolia

In the context of land degradation assessment, fractional vegetation cover and aboveground biomass are the most important parameters (Chu, 2020; Kumar et al., 2017; Liang and Wang, 2020b), which are mainly used as key indicators for determining land degradation status and monitoring the changes (Le et al., 2015). Despite the large territory of Mongolia, very few studies estimated fractional vegetation cover and biomass using both field vegetation data and satellite imagery for land degradation assessment at national and regional levels in Mongolia (Otgonbayar et al., 2019). The reasons are that vegetation surveys with traditional sampling methods are very costly and time-consuming, especially for large, extended and remote areas as the Eastern Mongolian Steppe. Despite a few efforts, there is no study on fractional vegetation cover and above ground biomass, which combined in situ data as field reference with remotely sensed data providing a land degradation product in Mongolia.

To date, only few scientific studies mapped land degradation at regional to national levels in Mongolia. Of those, most of studies have mapped land degradation using only remote sensing products; especially these studies used spectral vegetation indices as proxy for land degradation mapping (Meng et al., 2021; Nasanbat et al., 2018; Wang et al., 2020, 2019; Wei et al., 2018). Furthermore, some of these studies have illustrated the dynamic changes of land cover types as proxy for land degradation mapping in Mongolia (Jamsran et al., 2019; Wang et al., 2022). To my knowledge, no scientific study has dealt with land degradation mapping through integrating field measurements, remote sensing products and land degradation proxies and drivers in Mongolia. In addition to the missing knowledge about the current land degradation status, drivers of land degradation changes are largely unknown because no integrative analysis of these drivers exists. The reasons are that most previous studies have focused on changes in land cover types and vegetation cover, only one study addressed the relationship between vegetation cover changes and their drivers in Mongolia (Xiaoyu et al., 2020). More specifically, this study investigated changes of the NDVI in response to variations in natural conditions and livestock number in Mongolia. Unfortunately, this study has a specific drawback for explaining impacts of human activities on vegetation cover change because they used only livestock number as single anthropogenic driver. Therefore, it is critically required to conduct an integrated assessment of drivers of land degradation at regional scale in order to understand interactions and relationships between land degradation proxies and drivers.

1.3 Conceptual framework

1.3.1 Research Questions and Objectives

The overall aim of this thesis is to gain a better understanding of the impacts of human drivers on ongoing steppe degradation and to assess and map the land degradation status of the grasslands on the Eastern Mongolian Steppe through performing estimates in the current vegetation cover condition and trend changes. To achieve this overall aim and filling the research gaps described in the previous chapter, the following three overarching research questions and associated objectives are fundamental for this thesis:

Research question 1: How did oil exploitation sites and associated infrastructure change in far eastern Mongolian steppe between 2005 and 2018? Can such relatively narrow linear infrastructure be detected from high/moderate resolution satellite time series data?

To answer these questions, the following four objectives were formulated:

Objective 1: Evaluate and test the suitability of machine learning based supervised object-oriented classification techniques and multiscale and multispectral remote sensing data to detect grasslands disturbed by dirt roads, road construction, oil exploitation field and other linear infrastructure.

Objective 2: Examine the predictive power of multispectral bands, spectral indices and segment properties provided by PlanetScope, RapidEye, and Landsat for linear object classification.

Objective 3: Quantify the uncertainty arising from the combination of data from different sensors in their spectral and spatial configurations.

Objective 4: Analyze the spatial and temporal changes in the land use/cover with respect to infrastructure in the far eastern Mongolian Steppe and identify their drivers.

Research question 2: What is the effect of infrastructure such as dirt road networks, transportation corridors on the ecology of the surrounding pristine steppe? Which effects have steppe fires on the surrounding ecosystem of eastern Mongolia steppe?

In the context of this question, a cost-effective model and procedure were developed and applied, which has been designed to effectively map the vegetation cover at plant functional group level using combined data from field-collected vegetation data, UAV imagery, and high-resolution PlanetScope satellite multi-temporal imagery. Three objectives were related to this research question as follows:

Objective 1: Develop a methodological approach that minimizes the scale issue in aggregating very high-resolution UAV data to low-resolution multispectral satellite data.

Objective 2: Produce maps of plant functional groups that are key to the assessment of the consequences of dirt road corridors and linear infrastructure on the surrounding steppes in Mongolia and their contribution to human-induced land degradation.

Objective 3: Investigate the effect of short-interval steppe fires on vegetation community shifts by comparing the vegetation in burned and unburned areas over several years.

Research question 3: What is the current condition of vegetation cover and land degradation in the eastern Mongolian steppe, and which are the drivers of land degradation?

To deal with this question, five objectives were included:

Objective 1: Estimate fractional vegetation cover and aboveground biomass using Random Forest modeling based on Sentinel-2 imagery and field measurements.

Objective 2: Perform a trend analysis to estimate the changes in the NDVI time series of Landsat.

Objective 3: Evaluate potential drivers of degradation for creating land degradation maps.

Objective 4: Map and quantify current land degradation status using a Random Forest model.

Objective 5: Perform a correlation analysis between AGB and all other potential drivers of land degradation.

1.3.2 Thesis outline and scientific publication

This cumulative thesis is comprised of three peer-reviewed scientific publications. Two of them have been published in peer-reviewed international journals; one paper has been submitted to the renowned peer-reviewed journal Remote Sensing of Environment and is currently under review. The general structure of this thesis is presented in Figure 5 below.

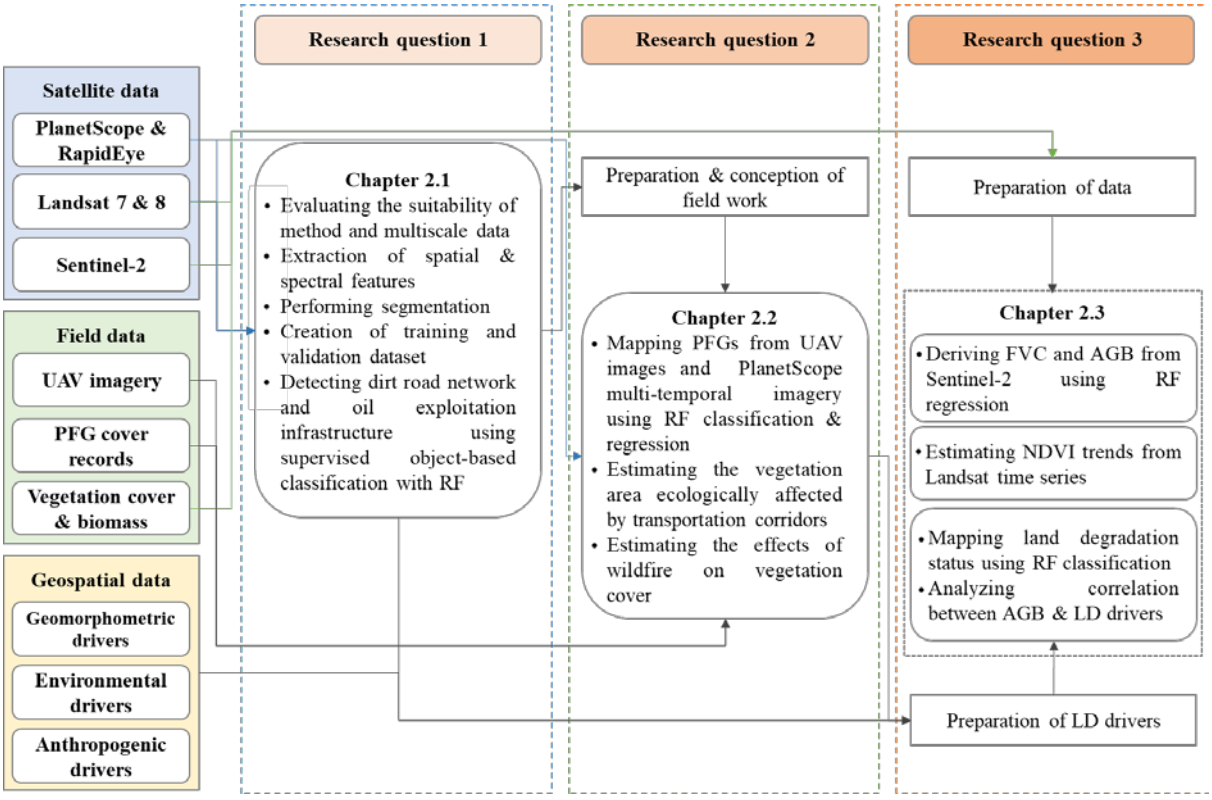

Figure 5. *Structure of the thesis*

In the following **Chapter 2,** the three peer-reviewed scientific articles are included which address each research question formulated above. **The first article** applies the spatiotemporal

analysis of multiscale and multispectral satellite data to assess changes in land cover/use due to oil exploitation and associated dirt roads and infrastructure in far eastern Mongolian steppe. In addition, the predictive power of different spatial and spectral resolution satellite data is evaluated with respect to their ability to detect dirt roads, linear infrastructure and narrow linear features. **The second article** evaluates the impacts of dirt roads, transportation corridors and steppe fires on surrounding steppe vegetation cover based on the changes in plant functional groups between transportation corridors and pristine steppe in far eastern Mongolian steppe. For fire effects on vegetation cover, a comparison analysis has been performed between burned and unburned areas in different years. This article also encompasses a model that has been developed and tested for integrating very high spatial resolution UAV data to coarser spatial resolution PlanetScope data with minimized scale effects using a pixel wise method. **The third article** addresses the evaluation of potential land degradation factors, and quantifies the changes in NDVI trend of Landsat time series. Finally, the fractional vegetation cover, above ground biomass and land degradation status is estimated using Random Forest in the eastern Mongolian steppe.

Finally, a conclusion and outlook chapter sums up the results of this thesis and gives an overview of the important contributions of the presented study to the scientific discussions of grassland degradation in Mongolian steppes (**Chapter 3**).

Chapter 2. Scientific publications

List of manuscripts

Paper I

Dashpurev, B.; Bendix, J.; Lehnert, L.W. Monitoring oil exploitation infrastructure and dirt roads with object-based image analysis and random forest in the Eastern Mongolian Steppe. *Remote Sensing.* **2020**, *12*, 144. https://doi.org/10.3390/rs12010144

Paper II

Dashpurev, B.; Wesche, K.; Jäschke, Y.; Oyundelger, K.; Phan, T.N.; Bendix, J.; Lehnert, L.W. A cost-effective method to monitor vegetation changes in steppes ecosystems: A case study on remote sensing of fire and infrastructure effects in eastern Mongolia. *Ecological Indicators*. **2021**, *132*, 108331. https://doi.org/10.1016/j.ecolind.2021.108331

Paper III

Dashpurev, B.; Phan, T.N.; Bendix, J.; Lehnert, L.W. Land degradation in the eastern Mongolian Steppe: Vegetation mapping, current trends and degradation modelling. This article is under review at *Remote sensing of Environment*. Submitted: 30 March 2022

2.1 Paper I:

Monitoring oil exploitation infrastructure and dirt roads with object-based image analysis and random forest in the Eastern Mongolian Steppe

Remote Sensing. 2020, 12, 144.

Dashpurev, B.; Bendix, J.; Lehnert, L.W.

Received: 21 November 2019; Revised: 14 December 2019; Accepted: 25 December 2019; Published: 1 January 2020

https://doi.org/10.3390/rs12010144

Impact Factor: 4.848

remote sensing

MDPI

Article

Monitoring Oil Exploitation Infrastructure and Dirt Roads with Object-Based Image Analysis and Random Forest in the Eastern Mongolian Steppe

Batnyambuu Dashpurev [1,2,*], Jörg Bendix [2] and Lukas W. Lehnert [1]

[1] Department of Geography, Ludwig-Maximilians-University Munich, 80333 Munich, Germany; lehnert.lu@lmu.de

[2] Faculty of Geography, Philipps-University of Marburg, 35032 Marburg, Germany; bendix@mailer.uni-marburg.de

* Correspondence: b.dashpurev@iggf.geo.uni-muenchen.de; Tel.: +49-(0)170-504-2338

Received: 21 November 2019; Accepted: 25 December 2019; Published: 1 January 2020

Abstract: Information on the spatial distribution of human disturbance is important for assessing and monitoring land degradation. In the Eastern Mongolian Steppe Ecosystem, one of the major driving factors of human-induced land degradation is the expansion of road networks mainly due to intensifications of oil exploration and exploitation. So far, neither the extents of road networks nor the extent of surrounding grasslands affected by the oil industry are monitored which is generally labor consuming. This causes that no information on the changes in the area which is affected by those disturbance drivers is available. Consequently, the study aim is to provide a cost-effective methodology to classify infrastructure and oil exploitation areas from remotely sensed images using object-based classifications with Random Forest. By combining satellite data with different spatial and spectral resolutions (PlanetScope, RapidEye, and Landsat ETM+), the product delivers data since 2005. For the classification variables, segmentation, spectral characteristics, and indices were extracted from all above mentioned imagery and used as predictors. Results show that overall accuracies of land use maps ranged 73%–93% mainly depending on satellites' spatial resolution. Since 2005, the area of grassland disturbed by dirt roads and oil exploitation infrastructure increased by 88% with its highest expansion by 47% in the period 2005–2010. Settlements and croplands remained relatively constant throughout the 13 years. Comparison of multiscale classification suggests that, although high spatial resolutions are clearly beneficial, all datasets were useful to delineate linear features such as roads. Consequently, the results of this study provide an effective evaluation for the potential of Random Forest for extracting relatively narrow linear features such as roads from multiscale satellite images and map products that are possible to use for detailed land degradation assessments.

Keywords: land degradation; anthropogenic drivers; land use change; Random Forest; PlanetScope; RapidEye; Landsat; remote sensing; Eastern Mongolian Steppe

1. Introduction

Land degradation is defined by Food and Agriculture Organization of the United Nations [1] as "a reduction in the capacity of the land to provide ecosystem goods and services over a period of time for its beneficiaries". Degradation is commonly caused by the mismanagement or over-exploitation of natural resources, such as vegetation clearance, nutrient deplete on, overgrazing, inappropriate irrigation, excessive use of agrochemicals, urban sprawl, pollution, or other direct impacts, such as mining, quarrying, trampling, or vehicle off-roading [2]. Consequently, the drivers of land degradation can be separated into those caused by nature (e.g., landslides, drought, floods) or by anthropogenic

activities (i.e., human-induced). In particular, the usage of all-terrain vehicles for off-road transportation as a consequence of mining and recreational activities is increasing worldwide, directly resulting in linear degradation pattern in landscapes [3]. The poor infrastructure in the Eastern Mongolian Steppe's rural areas fosters off-road vehicle travel and transport that consequently induces grassland degradation which is to date a big environmental challenge.

Recent studies report the negative environmental impacts of all forms of linear infrastructure required for natural resources extraction in Mongolia [4,5]. The expansion of dirt road networks as a main type of linear infrastructure has become more apparent in recent decades, mainly due to the rapid economic development [6]. At the same time, approximately 76.8% of the Mongolian countryside is affected by land degradation while 6.1% of the land is extremely degraded due to human activities [7,8]. Both developments are related: The usage of dirt roads accelerates the land degradation process in Mongolian grasslands through vehicle travel that causes the destruction of the surface vegetation, soil compaction, loss of soil aggregation, changes in soil texture, partial or complete removal of the top layer of soil, and loss of soil organisms [9]. Frequent and repeated usage of a track reduces the dirt road condition and leads to the generation of large ruts and corrugations [10]. As a consequence, drivers avoid the usage of bad conditioned old dirt roads and introduce new ones, which can increase the area affected by road transportation year by year. The adverse change of the abandoned roads mentioned above, however, prohibits a fast ecological rehabilitation of the area.

The detection of degradation due to dirt roads in extended and remote areas as the Eastern Mongolian Steppe is hardly possible with ground based surveys. The reasons are that GPS based land surveys are difficult in this remote area and dirt road networks may change rapidly across short time scales. Remote sensing, however, can provide powerful tools to derive accurate and timely information on the spatial distribution of land use/land cover changes over large areas across-scales and the related process of degradation [11,12], e.g., by means of change detection methods.

Assessing the possible environmental impact of dirt road usage by remote sensing is important for environmental conservation and land management in Mongolia. However, high resolution satellite data such as those acquired by WorldView are usually very expensive especially for developing countries [13]. Fortunately, there are several data sources which deliver satellite data free of charge. For regional scale, platforms such as Landsat and Sentinel provide increasing long-term records of continuous, consistent, and freely available imagery [14]. These satellite platforms are often complicated for mapping the dirt road and narrow linear features at local scale because their spatial resolution is coarser than the width of typical dirt roads. Recent studies combined high resolution PlanetScope and RapidEye data free of charge with other satellite imagery and achieved promising results for pixel-based classifications [15,16]. Therefore, such approaches could be straightforward and cost effective methods to detect linear features such as dirt roads and other infrastructure which have not been done so far. The disadvantage of such new satellite data sources is that data is only available for the recent years. Therefore, changes over longer time scales cannot be assessed. An alternative could be to combine high resolution data with data from long-term archives such as Landsat. Obviously, the classification results based on multi resolution remote sensing data have different accuracies which might depend on the spatial resolution of the satellite data [17].

The most common remote sensing classification techniques are pixel-based approaches. However, several studies showed that land-use classifications based on high spatial resolution data are challenging if the size of the target to classify is larger in comparison to the spatial resolution of the imagery [18]. As alternative, those studies suggest that object-oriented approaches may achieve highly accurate results [19]. Furthermore, modern machine learning techniques such as Random Forest now entered the field and have become popular within the remote sensing community due to the their good performance [20]. Recently, a comprehensive review summarized different methods to detect paved roads from high resolution imagery and found generally high accuracies for machine learning techniques [21]. The literature review confirmed that a few studies achieved to extract the oil exploitation infrastructures and dirt roads using different methods through Landsat ETM+ and RapidEye data [22–24]. To our

knowledge, there is no study on land cover classification of linear features which was conducted combining PlanetScope and RapidEye as high spatial resolution data with Landsat data providing a longer time series.

The major aim of the study is to provide a satellite based land-use classification monitoring product which is useful to detect land-use types such as infrastructure which are attributed to grassland degradation in the Eastern Mongolian Steppe Ecosystem. In this respect, we only use data which is free of charge in order to minimize the future monitoring costs. Specifically, this study aimed to (i) evaluate the suitability of machine learning based supervised object-oriented classification techniques and multiscale and multispectral remote sensing data to detect grasslands disturbed by dirt roads, road construction, oil extraction field and other infrastructure. (ii) The predictive power of multispectral bands, spectral indices and segment properties provided by PlanetScope, RapidEye, and Landsat were examined for linear object classification and (iii) the drivers of land degradation were assessed by analysing recent land use changes in the Eastern Mongolian Steppe. Special care is taken, to quantify the uncertainty arising from the combination of data from different sensors in their spectral and spatial configurations.

2. Materials and Methods

2.1. Study Area

The study was conducted in the Menen Steppe (Menengyn Tal) and the Khalkh river area (Khalkh Gol) which are part of the Eastern Mongolian Steppe in the Dornod province of Mongolia (Figure 1). The study area comprises approximately 20,000 km^2 between 46°33′N–48°02′N in latitude and 115°46′E–118°48′E in longitude. The steppe mainly consists of broad plains and rolling hills where the vegetation is dominated by Artemisia sp. and bunch grasses like Stipa sp. The area is characterized by an extremely continental climate. The average monthly temperature minimum reaches from −20 to −24 °C in January, the average maximum monthly temperature of 18–22 °C occurs in July. The average annual precipitation amounts to 200–300 mm, with monthly maxima mainly occurring in boreal summer.

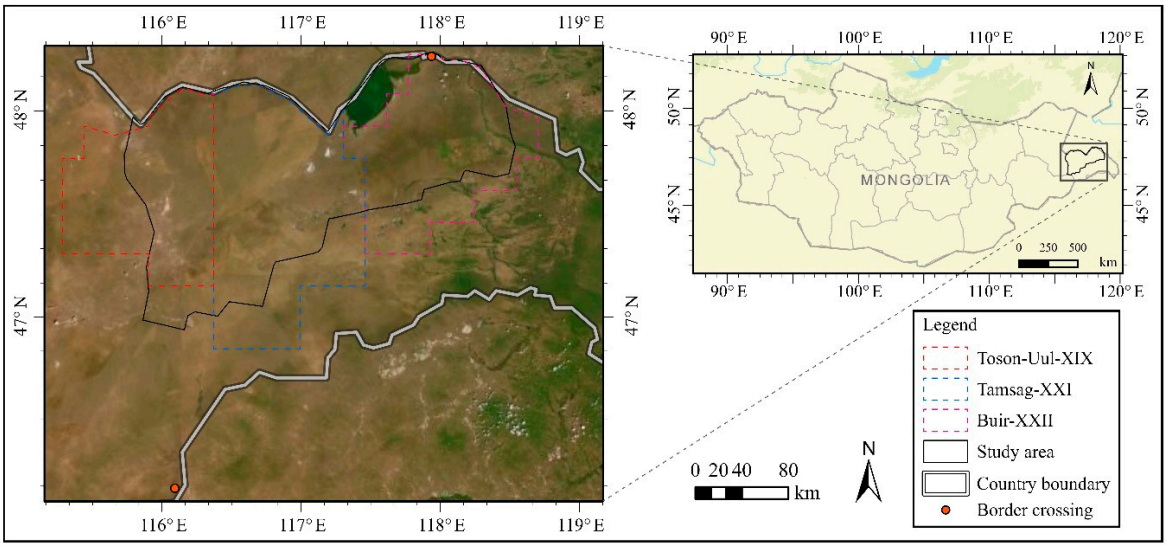

Figure 1. Study area map. The study area is a part of the Eastern Mongolian Steppe, which is one of the largest flat-steppes of Mongolia. The study area is registered in the World Heritage List of the UNESCO.

The major land use types in this area are rangelands, croplands, mines and a few permanent settlements [25,26]. The whole study area is covered by the oil exploration licenses divided into several blocks encompassing different areas granted in different years. For instance, block XIX, XXI, and XXII, were issued under the production sharing contract in 1993 and 1995 (Figure 1). In addition, two oil extraction sites were constructed in the Toson Uul XIX and Matad XXI in 2003 and 2005 [27,28].

2.2. Data Collection

The satellite data used for this study are depicted in Table 1. In order to estimate the recent change in transportation infrastructure, a set of 310 multispectral PlanetScope and RapidEye scenes were downloaded free-of-charge from the Planet Labs, Inc. as part of the Education and Research program website (www.planet.com) for the years 2010–2018 [29]. The imagery was selected according to its acquisition date, spatial resolution, and cloud coverage. To avoid major differences in phenology, all selected satellite scenes are acquired during summer and autumn. The satellite images were already georeferenced to the Universal Transverse Mercator (UTM) projection WGS84 zone 50 north.

Table 1. Satellite data used in this study. MS—multispectral, Pan—panchromatic.

Satellite Data	Data	Number of Bands	Ground Sample Distance (GSD)	Product Level	Number of Scenes
PlanetScope	29 October 2018 12 October 2018 8–26 September 2018 4 September 2018 23 August 2018 19 August 2018 18 August 2018 31 July 2018 13–16 September 2018	4	MS: 3 m	1B	200
RapidEye	22 August 2014 17 September 2014 10 October 2010 24 September 2010 02 September 2010 21 August 2010 19 August 2010 27 June 2010 16 October 2018	5	MS: 5 m	1B	124
Landsat ETM+	12 July 2008 14 July 2007 21 July 2007 15 August 2007 09 October 2007 9 August 2005 16 August 2005 25 August 2005 15 September 2005	8	MS: 30 m Pan: 15 m	1	10

The information about disturbed grassland change in the study area was obtained by examining a composite of cloud-free multispectral images acquired in 2005 and 2007 by Landsat Enhanced Thematic Mapper Plus (ETM+; bands 1–8). The data were downloaded free-of-charge from the United States Geological Survey's (USGS) website (https://earthexplorer.usgs.gov/) [30]. For each year, two Landsat scenes (path/row 124/27 and 125/27) covered the study area which were selected that cloud cover was below 10%. They have been merged to achieve one complete datasets.

Data Preparation and Pre-Processing

Since the area of investigation was covered by multiple scenes irrespective of the sensor, the top of atmosphere reflectance calibration was applied to all data in each year using sun elevation at the acquisition time, sensor gain and bias for each band and scene. Consequently, single scenes of the same satellite were merged into separate mosaics to achieve datasets covering the entire area of investigation. For Landsat ETM+ data, two additional steps were performed. (1) To fill missing data due to the scan line failure of Landsat ETM+, a global linear histogram matching technique (called SLC Gap-Filled

Products Phase One Methodology) was applied [31]. (2) Afterwards, the spatial resolution of the Landsat images was enhanced to 15 m applying the Gram-Schmidt spectral-sharpening algorithm which is a pansharpening technique to increase the spatial resolution of the multispectral images [32].

2.3. Supervised Classification Approach

To investigate the change in road networks in Eastern Mongolia during the last decade, supervised classification approaches were performed on all acquired imagery. In contrast to widely used pixel-based approaches, we performed an object-oriented classification to avoid the well-known "salt and pepper effect" if the size of the target to classify is larger in comparison to the spatial resolution of the imagery [18]. Recently, a comprehensive review summarized the supervised object-based land-cover image classification and found the development of the Random Forest (RF) in the supervised object-based framework is experiencing rapid advances and, which shows the best performance in land cover classification [19]. The following four land cover classes were distinguished because they represent the dominant land use categories of the study area: (1) dirt roads and petroleum extraction infrastructure sites, (2) croplands, (3) natural grasslands, and (4) settlement areas. The supervised classification approach involved five main steps (Figure 2): (i) the segmentation of the whole study area into objects, (ii) feature extraction on a segment basis to build a training samples database, (iii) using the training samples database to train Random Forest classifier models, (iv) classify each segment into dirt roads or other land-use, and (v) using Equalized Stratified Random and Cohen's Kappa scores to determine the accuracy of classified results.

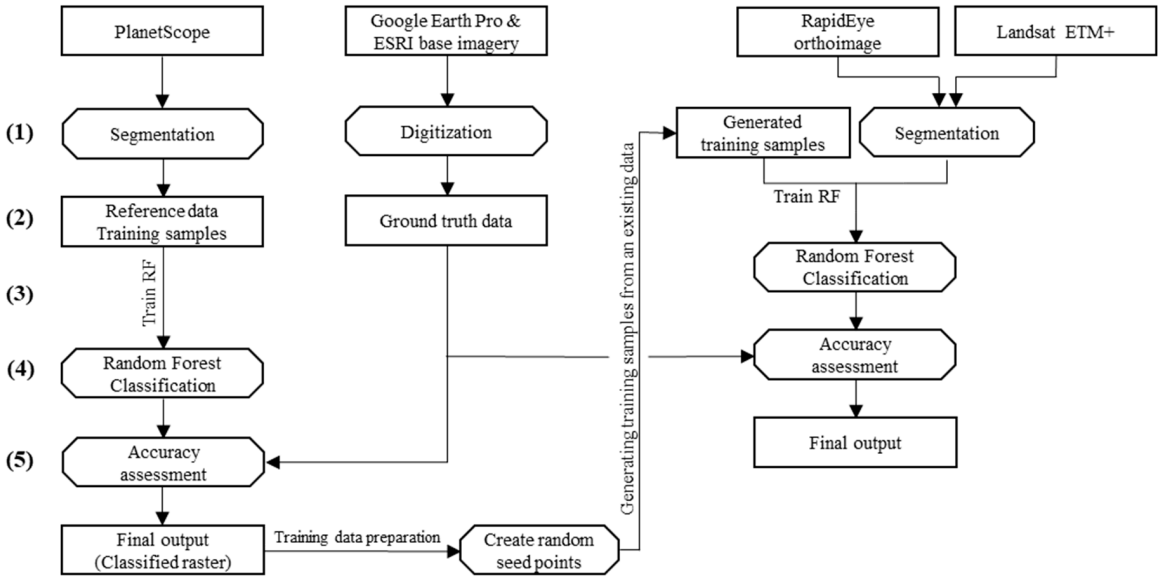

Figure 2. Workflow of supervised image classification.

The satellite data in this study feature different spatial resolutions which might have an effect on the accuracy of the classification results and could therefore distort the analysis of land-use changes over time. To quantify this uncertainty, the spatial resolutions of the PlanetScope (3 m) and RapidEye (5 m) images are reduced to 15 m to fit the resolution of Landsat. Those images are termed "spatially binned" datasets in the following. Afterward, the same analysis was performed with the images with artificially reduced spatial resolution and the results were compared to the classifications obtained from the data with original and high spatial resolutions. To save computational time, this was only conducted within a test area instead of the full Eastern Mongolian Steppe ecosystem.

2.3.1. Segmentation

Segmentation is key of any object-based classification workflow. This process groups neighboring pixels together into objects if pixels are similar in spectral and spatial characteristics. In our study, the images of PlanetScope, RapidEye, and Landsat ETM+ were segmented using the mean shift algorithm implemented in version 2.3 of the ArcGIS Pro software, which was developed by Fukunaga and Hostetler and generalized by Cheng [33,34]. After testing several band combinations for their suitability to segment roads in the images, a true color RGB composite was chosen as best option for segmentation based on visual interpretation of the results and expert knowledge. Mean shift is an iterative procedure that shifts each data point to the average of data points in its neighborhood. In this study, the segmentation process used a moving window within which average pixel values were calculated to decide which pixels are grouped into objects. As the window moves over the image, it iteratively re-computes a value to examine that each segment is concise. The characteristics of the image segments are determined by adjusting three parameters which are (i) spectral detail, (ii) spatial detail, and (iii) minimum segment size. In order to specify the spectral and spatial differences of features in each image, the values of segmentation parameters were adjusted on the basis of previous experience, visual analysis of different results and literature reviews. For instance, it is suggested that a higher value of spatial and spectral detail is appropriate in the case that the classified object is smaller than the spatial resolution of satellite image [35,36]. Therefore, values of spectral and spatial detail were set to 18 for all imagery (possible range: 1–20). The size of objects is defined by the parameter of minimum segment size, which merges segments smaller than this criterion with their best fitting neighboring segment. This parameter was adjusted to 30 pixels for PlanetScope, 20 pixels for RapidEye, and 10 pixels for Landsat ETM, which was determined by the minimum mapping unit as average width of linear features. As a result of the segmentation process, a set of attributes was generated for each segment within the input image. This set includes mean, standard deviation, segment size, active chromaticity color, rectangularity, and compactness. "Segment size" indirectly defines the scale of the segments, and rectangularity and compactness are defined by the degree to which a segment is compact or circular. Active chromaticity color is the average RGB color value that is derived from the input image. The segmentation quality was evaluated by means of visual inspection of the results and expert knowledge.

2.3.2. Training Samples

The feature samples were collected from segmented images of PlanetScope to build training datasets. Therefore, segments derived from PlanetScope data in 2018 were randomly and manually chosen and their boundary, homogeneity and heterogeneity values were included in the training dataset. The data of training samples was generated with 500 objects, which were assigned into dirt roads and oil extraction infrastructure (200), for natural grassland (100), cropland (100), and settlement area (100). The merging process was performed using the training tools available in ArcGIS Pro 2.3, which combined the training polygons of each of the four land use types with the selection of optimal object features and segmented layer. The training datasets for the classifications of previous years' RapidEye and Landsat images were generated from the classified data of PlanetScope images in 2018 (for further details on the classification see previous subsection, Figure 2). The selection of the training samples was repeated for each year using the classified results of the next year as reference. Fifty thousand randomly selected seed points were used to generate training data from an existing classified raster of PlanetScope imagery (Figure 2). In generating the training sample by seed points, the parameters of maximum sample radius and minimum sample area were needed to adjust. After testing several combinations of parameter values, the maximum sample radius was set to 50 meters, which defined the longest distance from any point within the training sample to its center seed point. The minimum sample area was set to 30 square meters. Furthermore, the spectral characteristics and indices were captured by a set of attributes extracted separately from the time series of multispectral images.

In particular several predictor variables were calculated from the four, five, and eight multispectral bands of PlanetScope, RapidEye and, Landsat ETM+ images, respectively. The multispectral bands were associated with polygons corresponding to the segmented image.

2.3.3. Random Forest Classifier

The random forest classification method [37] was applied to all satellite scenes of each year. It is an extension of the classification trees algorithm [38], belonging to the ensemble learning methods. The classification tree algorithm creates individual decision trees automatically based on tree-wise randomly chosen samples and subsets of the training data. For a random forest model, many classification trees are grown and the classification result is derived by a vote of each tree. Each classification tree is constructed separately by using an individual learning algorithm from a random sample of the training data set. At each node of classification trees, the best split is performed based on random subsets of the predictor variables. All trees are grown to the largest possible extent that is controlled by the node size set by the user. To run the random forest classification, it is necessary to define several important adjustable parameters. The primary parameters are the number of classification trees in the forest to run (ntree), number of randomly selected variables to use for building each tree (mtry) and depth of each tree in the forest. The predictor variables are listed in Table 2. Please note that the total number depended on the number of bands of the respective satellite.

Table 2. Description of the predictor variables used in random forest (RF) classification. Note that each variable has been calculated for each segment and image.

Variable	Description
	Data of single spectral bands
Mean value [1]	The average digital number (DN) of each band
Standard deviation [1]	Standard deviation of each bands
	Spectral indices
NDVI [2]	Mean value and standard deviation of the normalized difference vegetation index [3]: (NIR − Red)/(NIR + Red)
$NDVI_{Red\text{-}edge}$ [2]	Mean value and standard deviation of the normalized difference vegetation index [3]: (NIR – RE)/(NIR + RE)
PVI [2]	Mean value and standard deviation of the perpendicular vegetation index [3]: (NIR-a*Red-b)/(sqrt(1+a^2))
SAVI [2]	Mean value and standard deviation of the soil-adjusted vegetation index [3]: ((NIR − Red) / (NIR + Red + L)) × (1 + L)
	Segment
Average chromaticity color	The RGB color values of per-segment
Compactness	The degree to which a segment is compact or circular
Rectangularity	The degree to which a segment is rectangular
Count	The number of pixels comprising the segment

[1] Variables were calculated for each of the four multispectral bands of PlanetScope, the five multispectral bands of RapidEye and the 8 multispectral bands of Landsat. [2] The calculation of indices was performed on the multispectral bands of Landsat and RapidEye only. [3] The calculations are cited from References [39–42].

The importance of a certain variable to the overall model was calculated by the percentage of tree votes for the correct class in overall trees. In this study, the random forest algorithm [43] implemented in version 2.3 of the ArcGIS Pro software was used. The number of trees (ntree) was set to 2000 for each classification. Default values were used for the number of samples to be used for defining each class and the maximum depth of each tree in the forest. Classification of satellite imageries was performed separately using spectral and spatial variables and collection of training sample data which are delineated from the single date and multi-temporal imagery, respectively.

2.3.4. Accuracy Assessment and Validation

To assess the accuracy of the classification results, a stratified random sampling was applied to create a set of 500 random points independent from the training samples. Each point was manually assigned to its class based on the high-resolution satellite imagery and expert knowledge. The performance of the classifications was assessed by constructing confusion matrices and calculating overall accuracies, Cohen's Kappa scores, and quantity and allocation disagreement [44–48].

Two different sources for validation were used: (1) The base map images of ESRI (Environmental Systems Research Institute) and (2) Google Earth Pro images [49,50]. Both datasets differ in the temporal information and detail regarding the land use classes. The ground truth data for validation was generated using manual digitization. The objects were carefully selected by the basis of qualitative data of land use of Dornod provice in Mongolia [51]. The values of points were manually extracted and collected from high-resolution imagery of Google Earth Pro and ESRI (Figure 2).

3. Results

3.1. Classification Results and Accuracy

Supervised classification was performed using the random forest classification algorithm on each image to calculate the disturbed grassland due to dirt road and petroleum extraction infrastructure and other land uses for years 2005, 2007, 2010, 2014, and 2018. As a prerequisite to supervised classification, training samples were generated for all the land use classes mentioned above for each image. Three-meter spatial resolution images of PlanetScope enabled the generation of training samples and validation data for the classification. The training samples for RapidEye and Landsat ETM+ were created from an existing result of PlanetScope classification using seed points. The accuracy reports for each classified imagery included a confusion matrix and estimates of overall accuracy, kappa coefficient, user accuracy, producer accuracy, quantity, and allocation disagreement for each land use class. Summary of these metrics are shown in Table 1 for selected classification periods, with the full time series provided in Appendix A Tables A1 and A2.

For the classification of PlanetScope imagery, the basic information of dirt road and petroleum extraction infrastructure, and other land use classes were extracted from a 3-meter RGB-color mosaic which comprised 200 different PlanetScope scenes acquired in 2018 (Figure 3e). Accuracy assessment on the results revealed good overall classification accuracies and kappa coefficients between 0.85 and 0.91 for all classifications.

In the classification of RapidEye imagery, all land use classes were extracted from a 5-meter natural-color orthoimage that comprised 105 different scenes acquired in 2010 and 2014 (Figure 3c,d). Cohen's Kappa scores of RapidEye imagery classification were rated between 0.85 and 0.93. To obtain the land use change data in the period 2005 and 2007, the training samples for Landsat ETM+ raster prediction were generated from the classified maps based on PlanetScope acquired in year 2018. The land use classes were assigned to and predicted from a 15-meter mosaic which comprised 2 different Landsat ETM+ scenes acquired in 2007 and 2005 (Figure 3a,b). The Cohen's Kappa scores were rated 0.65 and 0.75. Some narrow dirt roads or linear features were detected which were not connected to the main network. Those features are most probably falsely classified as roads.

3.2. Comparison of Multiscale Classification by Satellite Images and Up-Scaling Images

The overall accuracies of native satellite imagery were 92.6% for PlanetScope, 87.2% for RapidEye, and 83.2% for Landsat ETM+. Regarding the overall accuracy of spatially binned satellite imagery was 81.8% for PlanetScope (15 m) and 84.6% for RapidEye (15 m). The comparison of original imageries shows that PlaneScope (3 m) has a higher accuracy than RapidEye (5 m) and Landsat (15 m). Comparing the original and spatially binned imagery of PlanetScope, the overall accuracy decreased by 10% as consequence of the reduced spatial resolution. The kappa value declined by 20% from original to spatially binned imagery. For the RapidEye classifications, both overall accuracy and kappa values

decreased by 3–5% if the spatial resolution was reduced from 5 m to 15 m (confusion matrices of the classification accuracy are shown in Table A2).

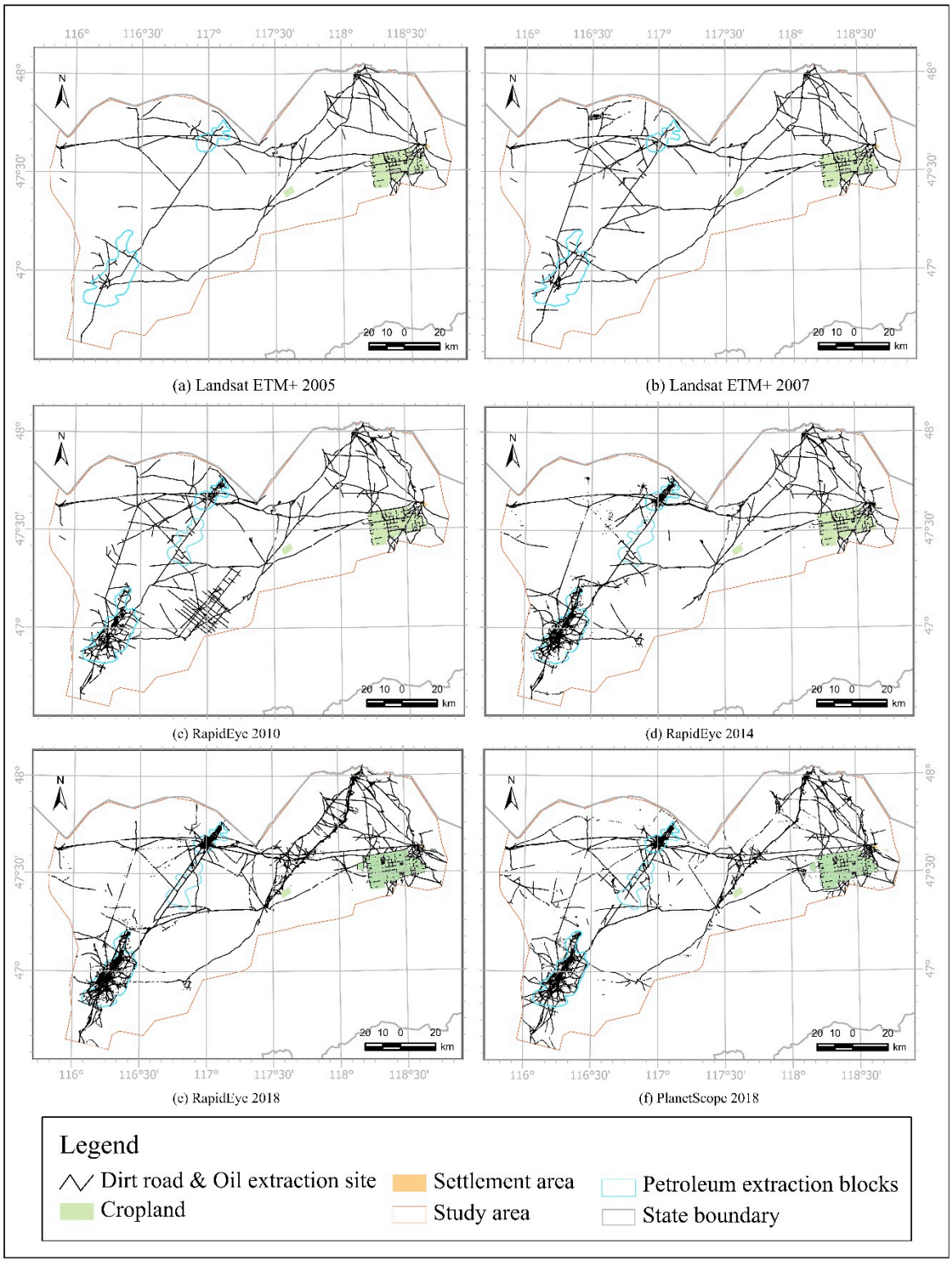

Figure 3. Classification results for expansion of dirt road and oil extraction infrastructure in 2005–2018: (**a**–**b**) Landsat ETM+ (15 m), (**c**–**e**) RapidEye (5 m), and (**f**) PlanetScope (3 m).

To analyze the dependence of the detection of linear features on spatial resolution, maps were compiled allowing a direct comparison. Figure 4 shows the classified result as dirt roads and oil extraction site, and grassland in the comparison plot of Menen Steppe in 2018. From the difference maps, minimum widths of feature were calculated which are required in relation to the spatial resolution in order to allow a reliable detection. For instance, PlanetScope (3 m) correctly detected linear features >6 m in width, while RapidEye (5 m) correctly detected >10 m wide. Landsat ETM+ (15 m) started to correctly detect linear features >25 m width as well as the spatially binned imagery of PlanetScope (15 m) and RapidEye (15 m). Consequently, a narrow linear feature of below 20 m in width was missed with Landsat ETM+ and all spatially binned imageries. Beside widths of features, their lengths also influenced the probability to be correctly classified. Consequently, narrow linear features below 20 m in widths were correctly classified based on Landsat 15 m data if they were long enough.

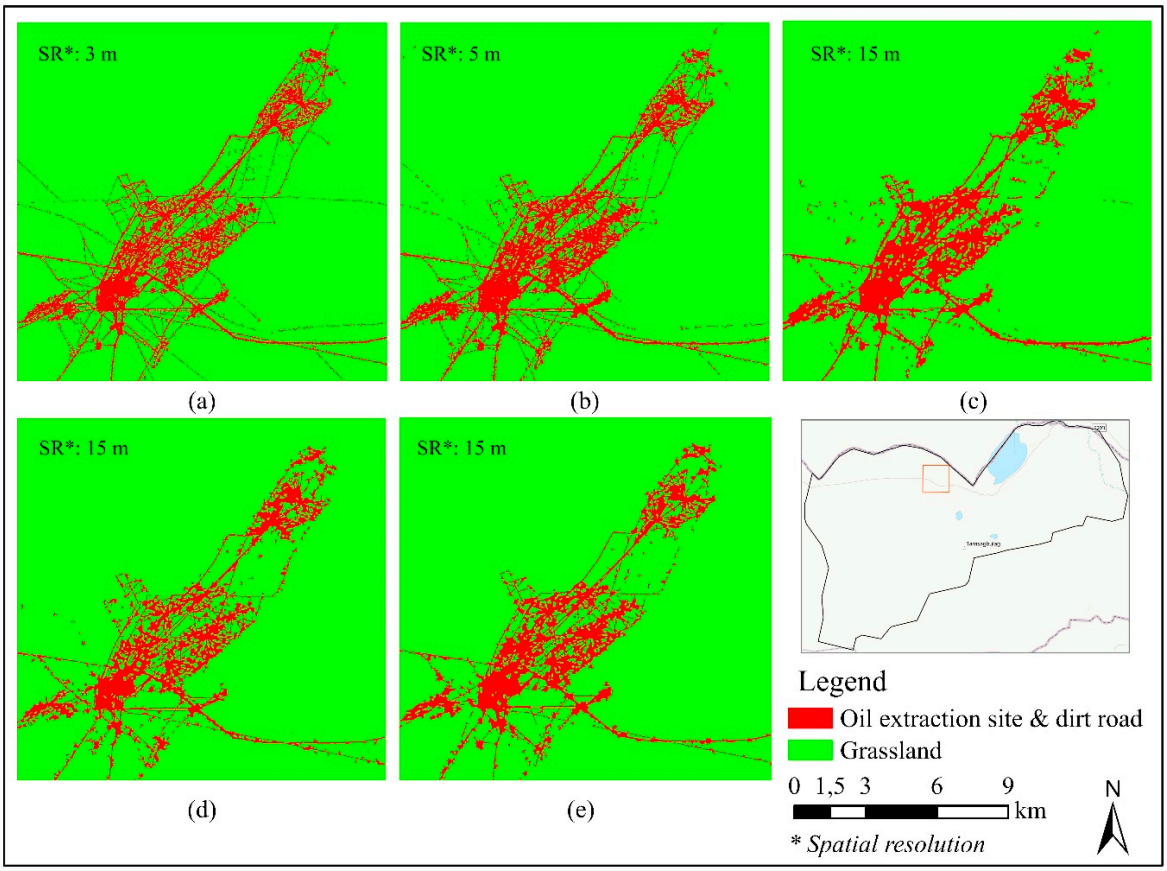

Figure 4. Comparison maps of the classification result: (**a**) PlanetScope imagery 3 m, (**b**) RapidEye imagery 5 m, (**c**) Landsat ETM+ imagery 15 m, (**d**) PlanetScope spatially binned imagery 15 m, (**e**) RapidEye spatially binned imagery 15 m. The location of the comparison area is shown in the lower right map.

Areas with high road densities such as those where multiple parallel dirt road lanes exist, are commonly classified as the linear features in classification of RapidEye (5 m), Landsat ETM+ (15 m), and spatially binned imageries. This overlapping leads to an increase in the size of classified area because pixels between then different lanes are not counted as grasslands. Table 3 provides the total area represented by the class. The result of linear feature class in all original finer resolution imageries was quite similar among the different image sources. For instance, the total area of dirt road and oil extraction infrastructure site was 2532 ha for PlanetScope (3 m) and 2602 ha for RapidEye (5 m), while lower resolution Landsat ETM+ (15 m) detected 2806 ha. Linear feature class in spatially binned imageries varied considerably if compared to original imagery results. As expected, the total area

of linear features decreased to 2393 ha for PlanetScope (15 m) and 2473 ha for RapidEye (15 m). Consequently, narrow linear features were missed.

Table 3. Comparison of classification performance by classes.

	Original Imagery			Upscaling Imagery	
	PlanetScope 3 m	RapidEye 5 m	Landsat ETM+ 15 m	PlanetScope 15 m	RapidEye 15 m
Dirt road and Oil extraction site (ha)	2532	2602	2806	2393	2473
Grassland (ha)	24,381	24,310	24,107	24,519	24,440

3.3. Analysis of Variable Importance

The variable importance was separately identified for all three different satellite data sources (Figure 5). Concerning PlanetScope data, the active chromaticity color of blue, green, and red were ranked as particularly important for classifying linear feature extraction. For RapidEye data, the variables derived from red edge and near-infrared channels stand out as the most important ones which had 2–3 times higher contributions than the other bands for predicting linear features. Furthermore, other spectral variables of above-mentioned satellite data were generally ranked as relatively important for classification and prediction.

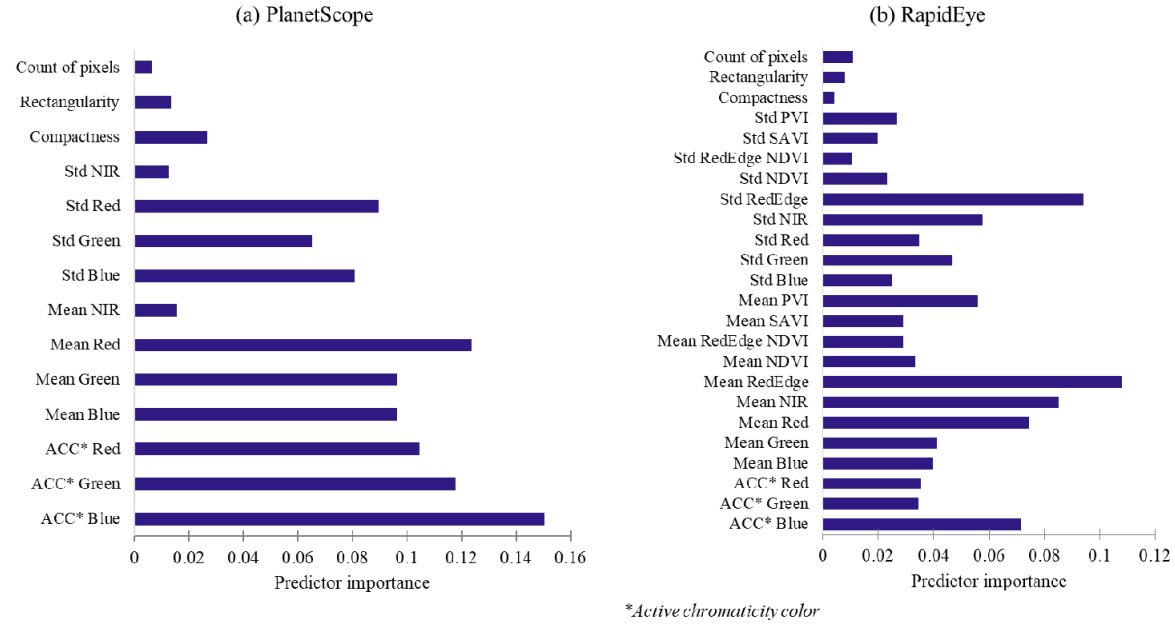

Figure 5. Variable importance for linear feature classification. (**a**) PlanetScope and (**b**) RapidEye.

Comparing variables importance in models based on RapidEye and PlanetScope, the mean and standard deviation value of near infrared was twice as high in the former compared to the latter. The largest difference was observed in the active chromaticity color of blue, green, and red, which was 3–4 times more important in models based on in PlanetScope compared to RapidEye.

For the Landsat imagery, the predictor variables derived from visible light and short-wave infrared-2 spectral bands of Landsat ETM+ were among the most important variables for linear feature extraction (Figure 6). In particular, the variables of the blue and short-wave infrared-2 (SWIR 2) band had high importances compared to all other predictors.

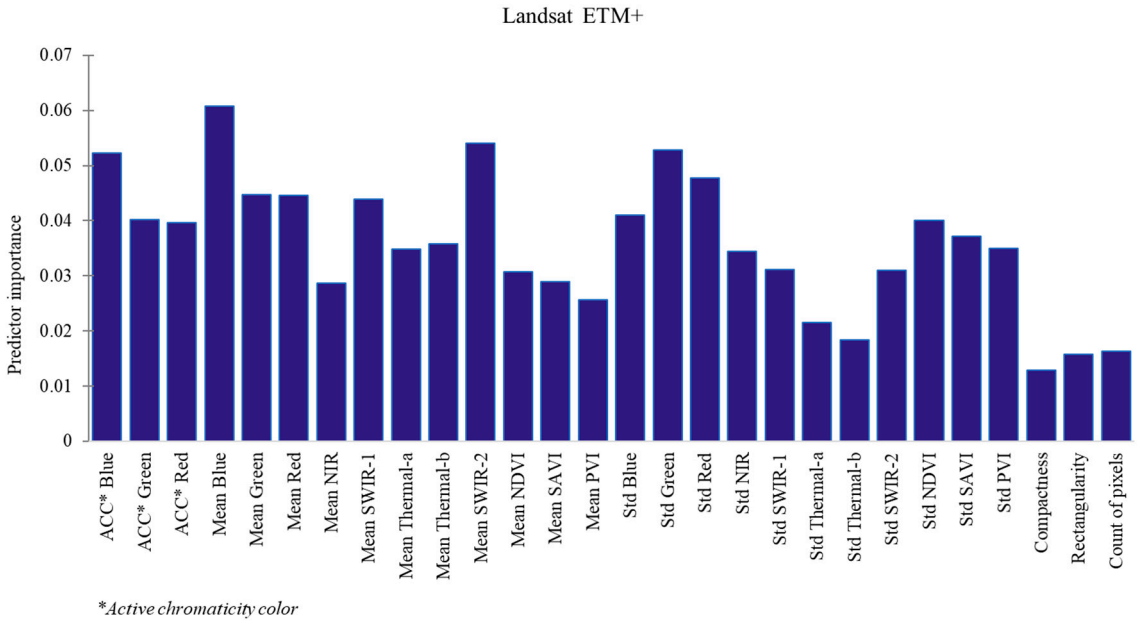

Figure 6. Variable importance for linear feature prediction in Landsat ETM+.

In general, the variables derived from NDVI, $NDVI_{red\text{-}edge}$, PVI, and SAVI spectral indices featured low importances compared to multi-spectral bands in both of RapidEye and Landsat ETM+. In the classification of PlanetScope, the variables of active chromaticity color in segmentation were more important than other spectral bands variables. In contrary, the variables of active chromaticity color in segmentation, spectral bands and indices in Landsat ETM+ were equally involved in the classification model.

3.4. Land Use Changes

As result of this research, the first time-series of land use data of dirt road network, oil extraction infrastructure, cropland and settlement area for Eastern Mongolia was derived from the satellite images. According to the data, the total disturbed grassland of dirt road and oil extraction infrastructure increased sharply from 7840 ha in 2005 to 14,730 ha in 2018. Detected linear features of less than 20 m in width accounted to 8 ha and 11 ha in 2005 and 2007, respectively. For the years 2010, 2015, and 2018, the dirt roads and oil extraction infrastructure with >20 m in width occupied areas of 287 ha, 302 ha, and 579 ha. To further examine these changes across the 13-year time period, the total areas expanded by all-above-mentioned land use types were shown in Figure 7.

In the study area, the dominant land use categories are dirt roads, oil exploitation sites and infrastructure, cropland and settlement. Areas of cropland increased from 48,546 ha in 2005 to 50,134 ha in 2018. Settlement area only marginally changed from 4557.4 ha in 2005 to 4648.1 ha in 2018 (Table 4).

Table 4. Total area change (hectare) observed by dominant land use categories in the study area in the period 2005–2018.

Dominant Land Use Types	2005	2007	2010	2014	2018	Change 2005–2010 (%)	Change 2010–2018 (%)
Dirt road and oil extraction infrastructure (ha)	7840	9940	11,487	11,506	14,730	47%	28%
Settlement area (ha)	4557	4557	4557	4642	4661	0%	2%
Cropland (ha)	48,546	48,546	48,546	48,546	50,134	0%	3%

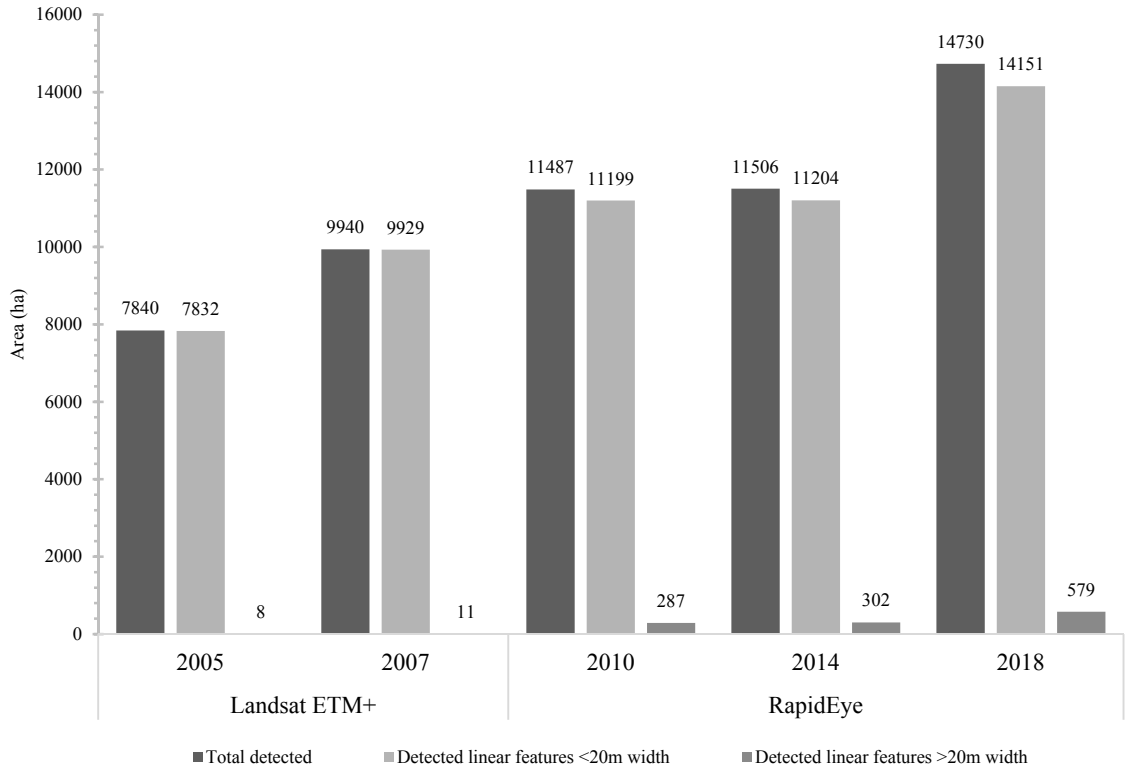

Figure 7. Bar graphs showing the dirt road and infrastructure expansion by width which are narrower/wider than 20 m. Each bar represents one of the classified 2–4 year interval time series imagery.

4. Discussion

4.1. Relevance of the Approach

The spatial distribution of land use change in the period 2005–2018 was extracted developing an object-based random forest classification method applied to long term multiscale and multi spectral remote sensing data. To detect changes in infrastructure in Eastern Mongolia since 2005, several images acquired by different satellite sensors were classified into "dirt road and oil extraction infrastructure site", "settlement area", "grassland", and "cropland". Since sensors differ in spatial and spectral resolutions, it is interesting to compare classification results among the different data sources. Highest overall accuracies between 87% and 93% were achieved using PlanetScope imagery, followed by RapidEye imagery with 85–91%. Classifications on Landsat ETM+ data yielded the lowest accuracies with 73–85%, respectively. Regardless of the spatial resolution of the satellite sensor, "cropland", "natural grassland", and "settlement area" classes were more accurately classified than the "dirt road and oil extraction infrastructure site" classes due to the relative homogeneity of the "cropland" "natural grassland", and "settlement" classes compared to the narrow disconnected linear "dirt road and infrastructure" classes.

For the extraction of linear features, the method was well-suited to identify dirt roads and infrastructure from PlanetScope and RapidEye imagery, which obtained accurate results and opened up possibilities to apply the methodology to other areas. Consequently, the classification model achieved affordable results with high accuracy by the basis of different satellite data, which is consistent with the findings of other studies [22–24,52]. However, as could be seen in the performance of the different classifications, the accuracies of the dirt road and linear infrastructure were strongly related to the spatial resolution of the images through the influence of boundary pixels and influence of finer spatial resolution that increases the spectral-radiometric variation of land cover types [53]. In contrast to previous studies applying object-based image analysis to detect roads, geometrical features only marginally contributed to the overall model [54]. One explanation could be that the homogeneous

undisturbed steppe ecosystems in Eastern Mongolia differed much more strongly in terms of spectral signatures from the infrastructure than it is the case in areas with more complex land-use as e.g., in cities. The segmentations were performed on images with different spatial resolution and same band composition. Previous studies suggested that, considering to set the high level on the parameters of spatial and spectral have given the opportunities to improve the segmentation results [35,55]. In the stage of experiments, the convenient adjustment was defined by the influence of spatial and spectral parameter on the segmentation in linear features. In this study, setting a high level of those parameters resulted in a decrease in homogeneity of objects. In other words, increasing the spatial and spectral parameter meant that a large number of small objects were obtained after segmentation. On the contrary, the lower level of those parameters made a homogeneity of objects increasing that failed to delimit linear features borders. Therefore, the selection of suitable parameters was paid much attention to the basis of those diverse in different spatial resolution.

The results of classification were validated using a ground truth dataset which were manually created by visual inspection of Google Earth Pro and ESRI base map images. Several studies showed that Google Earth imagery is a possible source of very high resolution imagery suitable to manually derive a reference dataset to assess the accuracy of remotely sensed image classifications [56,57]. In this study, the Google Earth and ESRI basemaps provided cost and time effective data sources especially from the point of view that this study covered an extremely large and remote area in Eastern Mongolia which is generally difficult to access. On the contrary, these sources have a scarcity of archived long time very-high-resolution imagery that cause difficulties in using the data in long-term image analysis. However, by selecting objects for reference data which have not been subject to change during the study period, both datasets were suitable to quantify the accuracy of the new product. The results obtained for Landsat ETM+ data were compared to original and spatially binned (15 m) multiscale imagery of PlanetSope and RapidEye to clarify the influence of different resolution on detecting linear features. Here, the comparison of different resolution image classification suggested that relatively wide dirt roads and linear infrastructures such as those featuring >20 m in width were easily classified from all types of images. Detection of 6–20 m wide narrow linear features from 3-meter resolution PlanetScope images and 5-meter resolution RapidEye revealed relatively high overall accuracies between 86% and 92%. In contrast, the detection of relatively narrow linear features such as roads featuring widths of 6–20 m was hardly possible from 15-meter spatial resolution data such as Landsat ETM+ and spatially binned images.

Differences in satellite imagery spectral significance for each random forest model are shown by calculation of variable importance. Generally, all variables derived from geometries of segments, multispectral channels and spectral indices were ranked as relatively important for classification and prediction. In general, the analysis of variable importance in all satellite imagery indicated that the variables of spectral channels and spectral indices are more important than geometrical variables. Comparing the variable importance, classification accuracy, and spatial resolution, the results suggested that the finer spatial resolution and lower spectral resolution of PlanetScope imagery yielded the highest overall accuracy (93.2%) and its most important variables were derived from active chromaticity color in segments and visible bands. Concerning the set of 5-meter spatial resolution, 5 spectral bands and 4 spectral indices composites in RapidEye data source, the variables of red, red edge and near-infrared channels, and active chromaticity color in blue were important to distinguish dirt road and infrastructure from all other surfaces with higher overall accuracy (87.3%). In the classification of RapidEye, red-edge and near-infrared channels had 2–3 times higher contributions than the other bands. According to the spectral reflectance, a typical bare soil and unvegetated surface such as dirt roads have a high reflectance in the near-infrared and shortwave infrared bands [58]. For the coarser spatial resolution and higher spectral resolution imagery of Landsat ETM+, generally, all variables derived from the geometry of segments, spectral bands, and spectral indices were equally involved. Considering individual variables, the results suggested that the visible and SWIR-2 bands proved to the most important variable for predicting and classifying linear features with 73.1% overall accuracy.

Conceptually, the result of this analysis suggest that finer spatial resolution data is preferable to coarser spatial resolution data when a land use/land cover object is small and linear. Furthermore, the higher-spectral resolution data could not provide the possibilities to deal effectively with the detection of smaller and linear feature than their spatial resolution.

4.2. Land Use Analysis

Remote sensing technologies play an important role in continually delivering the quantitative information needed to analyze the nature, dynamic, and spatial distribution of land degradation processes. Diverse assessment approaches are used to monitor the scope and consequences of land degradation. According to several studies [59–61], the infrastructure development, especially, construction and extension of oil extraction infrastructure can foster land degradation processes. The main interest of this study is to estimate the land use change such as dirt road, oil extraction infrastructure, and site that can be determined by multiscale remote sensing imagery and RF classification. The land use change in the study area was determined by a combination of supervised classification methods and long-term multiscale earth observation data. In the research area, there are several man-made factors contributing to land degradation distinguished by the manners and types.

The land use change analysis of Menen steppe and Khalkh river area indicates significant shifts in dirt road and infrastructure over the last 13 years. The most pronounced change detected in this study was the expansion of dirt roads and infrastructure due to growth of oil exploitation, exploration and transportation. Over the observed 13 years, the total area occupied by dirt roads and oil exploitation infrastructure expanded by 75% or 14,730 ha. Regarding their change over space, the dirt roads and infrastructure expanded over the whole territory of the study area. Cropland slightly increased by 3% to approximately 50,134 ha. Concerning the land usage, the cropland area is relatively concentrated at a few locations; one of those was built in 1972 with approximately 40,000 ha. The slight growth was related to additional extension of main cropland in 2015–2018 and its further extension is purposed to establish 72,000 ha in 2020 [62]. Settlement area did not change during the last 13 years.

The analysis recorded some declination or some artificial changes, particularly, several temporal expansion of dirt roads were detected in the period 2007–2010, and their detection was decreased or disappeared from satellite images in 2014–2018. In this case, for the short period, dirt roads were visibly recovered by pioneering plants shortly after the roads were abandoned. However, it has to be questioned if the successional stages of the vegetation are structurally and functionally equivalent to the native vegetation cover before creation of the dirt roads [5,63].

Several studies (e.g., [4,64]) have indicated that dirt roads are a major anthropogenic driver for land degradation in Mongolia. Therein contrast much less studies analyzed anthropogenic drivers of grassland degradation in Mongolia [63]. However, no detailed study of dirt road impact on land degradation has been done yet. Intensive growth of dirt road in broad territory of Mongolia challenges the detection and registration of the short-term dirt roads into official data base. In addition, temporal dirt roads due to oil exploitation in the study area have never taken into account in official databases, because dirt roads are abandoned shortly after they have been created. These difficulties preclude a detailed analysis of dirt road impact on land degradation at regional scales. In this study, the permanent and temporal dirt roads due to exploitation were detected from an analysis of PlanetScope, RapidEye and Landsat ETM+ in 2005–2018.

5. Conclusions

Extensive land utilization for oil exploitation and dirt roads are major drivers of land degradation in the steppe ecosystem of eastern Mongolia. This research highlighted the potential usage of multi-resolution and multi-spectral remote sensing images and Random Forest classification to investigate the extraction of linear features and their change in extent over time. The performance of segmentation shows that adjusting high level of spatial and spectral detail provided the largest

number of objects that were characterized by boundary, homogeneity, and heterogeneity, and thus, contained useful information for the linear features detection.

Understanding the driving factors such as the extent of land use change is particularly important for policies to develop sustainable land management practices, counteracting land degradation processes and fostering environmental conservation in the country. We tested and applied the method to data from 13 years to analyze spatio-temporal changes in land use for an area of more than 20,000 km^2 in the Menen Steppe and Khalkh River area. The classified results of 13 years of satellite data indicate that the land usage for dirt road and oil extraction infrastructure in the Eastern Mongolian Steppe is increasing due to the active oil exploitation and exploration. Within the study area over the observed 13 years, the total area occupied by dirt roads and oil exploitation infrastructure expanded by 75% to occupy an additional area of approximately 14,730 ha. For the spatial distribution, the dirt roads and infrastructure were expanded over the whole territory of the study area. In future, the results of this study will serve as data source to quantify the impact of human and climate induced disturbances on steppe ecosystems in Eastern Mongolia. This knowledge is key to preserve the unique open steppe ecosystems under global change.

Author Contributions: B.D. prepared the raw and validation data of PlanetScope, RapidEye, and Landsat, and performed the formal analysis including classification and spatial analyses, and wrote the original draft manuscript. B.D. developed the methodology and ideas with contribution from L.W.L. and J.B. L.W.L. and J.B. contributed to the methodology and review, and supervised the study. Finally, all authors (B.D., L.W.L., and J.B.) participated in additional editing of the original draft. All authors have read and agreed to the published version of the manuscript.

Funding: This research was funded by the German Academic Exchange Service (DAAD), Research Grants—Doctoral Programmes in Germany (57381412), Grant reference number 91691130 for Batnyambuu Dashpurev and the More Step project funded by the German Ministry for Education and Research (BMBF), grant number 01LC1820B.

Acknowledgments: We are grateful to the Education and Research Program of Planet Labs Inc. for providing access to Planet's imagery and archive.

Conflicts of Interest: The authors declare no conflict of interest.

Appendix A

Table A1. Summary of confusion matrices for the multi-resolution and multi-spectral satellite image classification in 2005–2018.

a. Landsat ETM+ 2005 and 2007			**Reference Data**		
Classification result	Dirt road and Oil extraction site	Grassland	Cropland	Settlement area	User Accuracy
Dirt road and Oil extraction site	89	9	2	9	81.6%
Grassland	19	105	3	7	78.3%
Cropland	12	5	120	0	87.5%
Settlement area	5	6	0	109	90.8%
Producer Accuracy	71.2%	84.2%	96.1%	87.2%	
Overall accuracy = 84.6%, kappa statistic = 71.9%, Quantity disagreement = 0.084 and Allocation disagreement = 0.186					
b. RapidEye 2010, 2014, and 2018			**Reference Data**		
Classification result	Dirt road and Oil extraction site	Grassland	Cropland	Settlement area	User Accuracy
Dirt road and Oil extraction site	95	6	3	14	80.5%

Table A1. *Cont.*

Grassland	13	119	13	4	79.8%
Cropland	5	0	109	0	95.6%
Settlement area	4	0	0	107	96.3%
Producer Accuracy	81.1%	95.2%	87.2%	85.6%	
Overall accuracy = 87.3%, kappa statistic = 74.6% Quantity disagreement = 0.0508 and Allocation disagreement = 0.0752					
c. PlanetScope 2018		**Reference Data**			
Classification result	Dirt road and Oil extraction site	Grassland	Cropland	Settlement area	User Accuracy
Dirt road and Oil extraction site	111	7	2	4	89.5%
Grassland	5	118	1	6	90.7%
Cropland	6	0	122	0	95.3%
Settlement area	3	0	0	115	97.4%
Producer Accuracy	88.8%	94.4%	97.6%	92%	
Overall accuracy = 93.2%, kappa statistic = 87.1% Quantity disagreement = 0.016 and Allocation disagreement = 0.052					

Table A2. Confusion matrices for the comparison of multi-spatial resolution images in 2018.

a. PlanetScope (Original)	**Reference Data**		
Classification result	Dirt road and Oil extraction site	Grassland	User Accuracy
Dirt road and Oil extraction site	226	13	94.5%
Grassland	24	237	90.8%
Producer Accuracy	90.4%	94.8%	
Overall accuracy = 92.6%, kappa statistic = 85.2% Quantity disagreement = 0.022 and Allocation disagreement = 0.052			
b. PlanetScope (15 m)	**Reference Data**		
Classification result	Dirt road and Oil extraction site	Grassland	User Accuracy
Dirt road and Oil extraction site	165	6	96.4%
Grassland	85	244	74.1%
Producer Accuracy	66.1%	97.6%	
Overall accuracy = 81.8%, kappa statistic = 63.6% Quantity disagreement = 0.158 and Allocation disagreement = 0.024			
c. RapidEye (Original)	**Reference Data**		
Classification result	Dirt road and Oil extraction site	Grassland	User Accuracy
Dirt road and Oil extraction site	198	12	94.2%
Grassland	52	238	82.1%
Producer Accuracy	79.2%	95.2%	
Overall accuracy = 87.2%, kappa statistic = 74.4% Quantity disagreement = 0.08 and Allocation disagreement = 0.048			

Table A2. *Cont.*

d. RapidEye (15 m)	**Reference Data**		
Classification result	Dirt road and Oil extraction site	Grassland	User Accuracy
Dirt road and Oil extraction site	176	3	98.3%
Grassland	74	247	76.9%
Producer Accuracy	70.4%	98.8%	
Overall accuracy = 84.6%, kappa statistic = 69.2% Quantity disagreement = 0.142 and Allocation disagreement = 0.012			
e. Landsat ETM+ (Original)	**Reference Data**		
Classification result	Dirt road and Oil extraction site	Grassland	User Accuracy
Dirt road and Oil extraction site	199	19	91.2%
Grassland	51	231	81.9%
Producer Accuracy	79.2%	92.4%	
Overall accuracy = 86.1%, kappa statistic = 72% Quantity disagreement = 0.116 and Allocation disagreement = 0.052			

References

1. Biancalani, R.; Nachtergaele, F.; Petri, M.; Bunning, S. *Land Degradation Assessment in Drylands Methodology and Results*; Food and Agriculture Organization: Rome, Italy, 2013.
2. Dudley, N.; Alexander, S.; Johnson, I. Secretariat of the United Nations Convention to Combat Desertification Drivers of Change. In *The Global Land Outlook*; United Nations Convention to Combat Desertification: Bonn, Germany, 2017; pp. 40–51. ISBN 9789295110472.
3. Duniway, M.C.; Herrick, J.E.; Pyke, D.A.; Toledo, P.D. Assessing transportation infrastructure impacts on rangelands: Test of a standard rangeland assessment protocol. *Rangel. Ecol. Manag.* **2010**, *63*, 524–536. [CrossRef]
4. Batkhishig, O. Human Impact and Land Degradation in Mongolia. In *Dryland East Asia: Land Dynamics amid Social and Climate Change*; The Higher Education Press: Beijing, China, 2013; ISBN 978-3-11-028791-2.
5. Cane, I.; Schleger, A.; Ali, S.; Kemp, D.; McIntyre, N.; McKenna, P.; Lechner, A.; Dalaibuyan, B.; Lahiri-Dutt, K.; Bulovic, N. *Responsible Mining in Mongolia: Enhancing Positive Engagement*; Sustainable Minerals Institute, The University of Queensland: St Lucia, Australia, 2015.
6. Wingard, J. *CMS Convention on Migratory Species: Guidelines for Addressing the Impact of Linear Infrastructure on Large Migratory Mammals in Central Asia*; UNEP/CMS Secretariat, Wildlife Conservation Society: Quito, Ecuador, 2014.
7. Ministry of Environment and Tourism of Mongolia. *Mongolian Environmental Report*; Ministry of Environment and Tourism of Mongolia: Ulaanbaatar, Mongolia, 2018.
8. Nasanbat, E.; Sharav, S.; Sanjaa, T.; Lkhamjav, O.; Magsar, E.; Tuvdendorj, B. Frequency analysis of MODIS NDVI time series for determining hotspot of land degradation in Mongolia. In Proceedings of the International Archives of the Photogrammetry, Remote Sensing and Spatial Information Sciences—ISPRS TC III Mid-Term Symposium "Developments, Technologies and Applications in Remote Sensing", Beijing, China, 7–10 May 2018; pp. 1299–1304.
9. Li, S.G.; Tsujimura, M.; Sugimoto, A.; Davaa, G.; Sugita, M. Natural recovery of steppe vegetation on vehicle tracks in central Mongolia. *J. Biosci.* **2006**, *31*, 85–93. [CrossRef] [PubMed]
10. Keshkamat, S.S.; Tsendbazar, N.E.; Zuidgeest, M.H.P.; Van Der Veen, A.; De Leeuw, J. The environmental impact of not having paved roads in arid regions: An example from Mongolia. *Ambio* **2012**, *41*, 202–205. [CrossRef] [PubMed]
11. Gibbs, H.K.; Salmon, J.M. Mapping the world's degraded lands. *Appl. Geogr.* **2015**, *57*, 12–21. [CrossRef]
12. Baynard, C.W. Remote Sensing Applications: Beyond Land-Use and Land-Cover Change. *Adv. Remote Sens.* **2013**, *2*, 228–241. [CrossRef]
13. United Nations Office for Outer Space Affairs. *UNOOSA's Annual Reports*; UNOOSA: Vienna, Austria, 2018.

14. Claverie, M.; Ju, J.; Masek, J.G.; Dungan, J.L.; Vermote, E.F.; Roger, J.C.; Skakun, S.V.; Justice, C. The Harmonized Landsat and Sentinel-2 surface reflectance data set. *Remote Sens. Environ.* **2018**, *219*, 145–161. [CrossRef]
15. Dobrinic, D. Horizontal Accuracy Assessment of PlanetScope, RapidEye and WorldView-2 Satellite Imagery. In Proceedings of the 18th International Multidisciplinary Scientific GeoConference SGEM2018, Informatics, Geoinformatics and Remote Sensing, Albena, Bulgaria, 30 June–9 July 2018.
16. Cooley, S.W.; Smith, L.C.; Stepan, L.; Mascaro, J. Tracking dynamic northern surface water changes with high-frequency planet CubeSat imagery. *Remote Sens.* **2017**, *9*, 1306. [CrossRef]
17. Toure, S.I.; Stow, D.A.; Shih, H.C.; Weeks, J.; Lopez-Carr, D. Land cover and land use change analysis using multi-spatial resolution data and object-based image analysis. *Remote Sens. Environ.* **2018**, *210*, 259–268. [CrossRef]
18. Blaschke, T. Object based image analysis for remote sensing. *ISPRS J. Photogramm. Remote Sens.* **2010**, *65*, 2–16. [CrossRef]
19. Ma, L.; Li, M.; Ma, X.; Cheng, L.; Du, P.; Liu, Y. A review of supervised object-based land-cover image classification. *ISPRS J. Photogramm. Remote Sens.* **2017**, *130*, 277–293. [CrossRef]
20. Lu, D.; Weng, Q. A survey of image classification methods and techniques for improving classification performance. *Int. J. Remote Sens.* **2007**, *28*, 823–870. [CrossRef]
21. Wang, W.; Yang, N.; Zhang, Y.; Wang, F.; Cao, T.; Eklund, P. A review of road extraction from remote sensing images. *J. Traffic Transp. Eng. (English Ed.)* **2016**, *3*, 271–282. [CrossRef]
22. Mjachina, K.; Hu, Z.; Chibilyev, A. Detection of damaged areas caused by the oil extraction in a steppe region using winter landsat imagery. *J. Appl. Remote Sens.* **2018**, *12*, 1. [CrossRef]
23. Plank, S.; Mager, A.; Schoepfer, E. Monitoring of oil exploitation infrastructure by combining unsupervised pixel-based classification of polarimetric SAR and object-based image analysis. *Remote Sens.* **2014**, *6*, 11977–12004. [CrossRef]
24. Zhang, Y.; Lantz, N.; Guindon, B.; Jiao, X. Spectral-analysis-based extraction of land disturbances arising from oil and gas development in diverse landscapes. *J. Appl. Remote Sens.* **2017**, *11*, 015026. [CrossRef]
25. Pfeiffer, M.; Dulamsuren, C.; Jäschke, Y.; Wesche, K. Grasslands of China and Mongolia: Spatial Extent, Land Use and Conservation. In *Grasslands of the World: Diversity, Management and Conservation*; CRC Press: Boca Raton, FL, USA, 2018; pp. 168–196. ISBN 9781498796262.
26. National Statistics Office of Mongolia Environment. *Mongolian Statistical Yearbook*; National Statistics Office of Mongolia Environment: Ulaanbaatar, Mongolia, 2017; pp. 224–227. ISBN 978-99978-758-0-8.
27. Mineral Resources and Petroleum Authority of Mongolia Petroleum Exploitation and Production. Available online: https://www.mrpam.gov.mn/ (accessed on 26 June 2019).
28. Mongolia Extractive Industries Transparency Initiative EITI-Extractive Industries Transparency Initiative. Available online: http://www.eitimongolia.mn/en (accessed on 26 June 2019).
29. Planet Team Planet Application Program Interface: In Space for Life on Earth. Available online: https://api.planet.com/ (accessed on 10 December 2018).
30. U.S. Geological Survey Landsat Image Courtesy of the U.S. Geological Survey. Available online: https://earthexplorer.usgs.gov/ (accessed on 1 October 2018).
31. Scaramuzza, P.; Esad Micijevic, G.C. SLC Gap-Fill Methodology. Available online: https://landsat.usgs.gov/sites/default/files/documents/SLC_Gap_Fill_Methodology.pdf (accessed on 13 December 2019).
32. Amro, I.; Mateos, J.; Vega, M.; Molina, R.; Katsaggelos, A.K. A survey of classical methods and new trends in pansharpening of multispectral images. *EURASIP J. Adv. Signal Process.* **2011**, *2011*, 79. [CrossRef]
33. Fukunaga, K.; Hostetler, L.D. The Estimation of the Gradient of a Density Function, with Applications in Pattern Recognition. *IEEE Trans. Inf. Theory* **1975**, *21*, 32–40. [CrossRef]
34. Cheng, Y. Mean Shift, Mode Seeking, and Clustering. *IEEE Trans. Pattern Anal. Mach. Intell.* **1995**, *17*, 790–799. [CrossRef]
35. Mesner, N.; Oštir, K. Investigating the impact of spatial and spectral resolution of satellite images on segmentation quality. *J. Appl. Remote Sens.* **2014**, *8*, 083696. [CrossRef]
36. El-naggar, A.M. Determination of optimum segmentation parameter values for extracting building from remote sensing images. *Alex. Eng. J.* **2018**, *57*, 3089–3097. [CrossRef]
37. Breiman, L. Random Forests LEO. *Mach. Learn.* **2001**, *45*, 5–32. [CrossRef]

38. Breiman, L.; Friedman, J.H.; Jerome, H.; Olshen, R.A.; Stone, C.J. *Classification and Regression Trees*; Taylor & Francis: Monterey, CA, USA, 1984; ISBN 9781138469525.
39. Tucker, C.J. Red and photographic infrared linear combinations for monitoring vegetation. *Remote Sens. Environ.* **1979**, *8*, 127–150. [CrossRef]
40. Gitelson, A.; Merzlyak, M.N. Spectral Reflectance Changes Associated with Autumn Senescence of *Aesculus hippocastanum* L. and *Acer platanoides* L. Leaves. Spectral Features and Relation to Chlorophyll Estimation. *J. Plant Physiol.* **1994**, *143*, 286–292. [CrossRef]
41. Richardson, A.J.; Wiegand, C.L. Distinguishing vegetation from soil background information. [by gray mapping of Landsat MSS data]. *Photogramm. Eng. Remote Sensing* **1977**, *43*, 1541–1552.
42. Huete, A.R. A soil-adjusted vegetation index (SAVI). *Remote Sens. Environ.* **1988**, *25*, 295–309. [CrossRef]
43. Breiman, L.; Cutler, A. Random Forests. Available online: https://www.stat.berkeley.edu/~{}breiman/RandomForests/cc_home.htm#home (accessed on 15 October 2018).
44. Rosenfield, G.H.; Fitzpatrick-Lins, K. A coefficient of agreement as a measure of thematic classification accuracy. *Photogramm. Eng. Remote Sensing* **1986**, *52*, 223–227.
45. Cohen, J. A Coefficient of Agreement for Nominal Scales. *Educ. Psychol. Meas.* **1960**, *20*, 37–46. [CrossRef]
46. Russell, G.C. A review of assessing the accuracy of classifications of remotely sensed data. *Remote Sens. Environ.* **1991**, *37*, 35–46.
47. Pontius, R.G.; Millones, M. Death to Kappa: Birth of quantity disagreement and allocation disagreement for accuracy assessment. *Int. J. Remote Sens.* **2011**, *32*, 4407–4429. [CrossRef]
48. Pickard, B.; Gray, J.; Meentemeyer, R. Comparing quantity, allocation and configuration accuracy of multiple land change models. *Land* **2017**, *6*, 52. [CrossRef]
49. ESRI World Imagery [basemap]. Available online: http://www.arcgis.com/home/item.html?id=10df2279f9684e4a9f6a7f08febac2a9 (accessed on 1 December 2018).
50. Google LLC. Google Earth Pro. Available online: https://www.google.com/earth/versions/#earth-pro (accessed on 1 December 2018).
51. Mongolian National Land Information System of Land Administration and Management, Geodesy and Cartography. Available online: http://www.egazar.gov.mn (accessed on 1 March 2019).
52. Salehi, B.; Chen, Z.; Jefferies, W.; Adlakha, P.; Bobby, P.; Power, D. Well site extraction from Landsat-5 TM imagery using an object- and pixel-based image analysis method. *Int. J. Remote Sens.* **2014**, *35*, 7941–7958. [CrossRef]
53. Markham, B.L.; Townshend, J.R.G. Land cover classification accuracy as a function of sensor spatial resolution. In Proceedings of the the 15th International Symposium on Remote Sensing of Environment, Ann Arbor, MI, USA, 11–15 May 1981; pp. 1075–1090.
54. Nobrega, R.A.A.; O'Hara, C.G.; Quintanilha, J.A. An object-based approach to detect road features for informal settlements near Sao Paulo, Brazil. In *Object-Based Image Analysis*; Lecture Notes in Geoinformation and Cartography; Springer: Berlin/Heidelberg, Germany, 2008; pp. 589–607.
55. Schultz, B.; Immitzer, M.; Formaggio, A.; Sanches, I.; Luiz, A.; Atzberger, C. Self-Guided Segmentation and Classification of Multi-Temporal Landsat 8 Images for Crop Type Mapping in Southeastern Brazil. *Remote Sens.* **2015**, *7*, 14482–14508. [CrossRef]
56. Wu, W.; De Pauw, E.; Helldén, U. Assessing woody biomass in African tropical savannahs by multiscale remote sensing. *Int. J. Remote Sens.* **2013**, *34*, 4525–4549. [CrossRef]
57. Dimobe, K.; Ouédraogo, A.; Soma, S.; Goetze, D.; Porembski, S.; Thiombiano, A. Identification of driving factors of land degradation and deforestation in the Wildlife Reserve of Bontioli (Burkina Faso, West Africa). *Glob. Ecol. Conserv.* **2015**, *4*, 559–571. [CrossRef]
58. Bowker, D.E.; Davis, R.E.; Myrick, D.L.; Stacy, K.; Jones, W.T. *Spectral Reflectances of Natural Targets for Use in Remote Sensing Studies*; NASA Langley Research Center: Hampton, VA, USA, 1985.
59. Ngene, S.; Tota-Maharaj, K.; Eke, P.; Hills, C. Environmental and Economic Impacts of Crude Oil and Natural Gas Production in Developing Countries. *Int. J. Econ. Energy Environ.* **2016**, *1*, 64–73.
60. Chijioke, B.; Onuoha, B.; Bassey, I.; Ufomba, H. The Impact of Oil Exploration and Environmental Degradation in the Niger Delta Region of Nigeria: A Study of Oil Producing Communities in Akwa Ibom State. *Glob. J. Hum. Soc. Sci. Polit. Sci.* **2018**, *18*, 55–70.
61. Forman, R.T.T.; Alexander, L.E. Roads and their major ecological effects. *Annu. Rev. Ecol. Syst.* **1998**, *29*, 207–231. [CrossRef]

62. Khalkh Gol Project. Available online: http://khalkhgol.mofa.gov.mn/ (accessed on 15 June 2019).
63. John, R.; Chen, J.; Kim, Y.; Ou-yang, Z.T.; Xiao, J.; Park, H.; Shao, C.; Zhang, Y.; Amarjargal, A.; Batkhshig, O.; et al. Differentiating anthropogenic modification and precipitation-driven change on vegetation productivity on the Mongolian Plateau. *Landsc. Ecol.* **2016**, *31*, 547–566. [CrossRef]
64. Nyamtseren, M. The land degradation and desertification process in Mongolia. In *Mongolia Second Assessment Report on Climate Change*; The Ministry of Environment and Green Development of Mongolia: Ulaanbaatar, Mongolia, 2014; pp. 132–139.

2.2 Paper II:

A cost-effective method to monitor vegetation changes in steppes ecosystems: A case study on remote sensing of fire and infrastructure effects in eastern Mongolia.

Ecological Indicators. 2021, 132, 108331.

Dashpurev, B.; Wesche, K.; Jäschke, Y.; Oyundelger, K.; Phan, T.N.; Bendix, J.; Lehnert, L.W.

Received: 20 October 2020; Received in revised form 22 October 2021; Accepted 25 October 2021; Available online 29 October 2021

https://doi.org/10.1016/j.ecolind.2021.108331

Impact Factor: 4.958

Ecological Indicators 132 (2021) 108331

Contents lists available at ScienceDirect

Ecological Indicators

journal homepage: www.elsevier.com/locate/ecolind

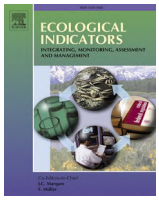

Original Articles

A cost-effective method to monitor vegetation changes in steppes ecosystems: A case study on remote sensing of fire and infrastructure effects in eastern Mongolia

Batnyambuu Dashpurev [a,*], Karsten Wesche [b,c,d], Yun Jäschke [b], Khurelpurev Oyundelger [b], Thanh Noi Phan [a], Jörg Bendix [e], Lukas W. Lehnert [a]

[a] Department of Geography, Ludwig-Maximilians-University Munich, 80333 Munich, Germany
[b] Department of Botany, Senckenberg Museum of Natural History, 02826 Görlitz, Germany
[c] German Centre for Integrative Biodiversity Research (iDiv), Halle-Jena-Leipzig, Deutscher Platz 5e, 04103 Leipzig, Germany
[d] International Institute Zittau, Technische Universität Dresden, Markt 23, 02763 D-Zittau, Germany
[e] Faculty of Geography, Philipps-University of Marburg, 35032 Marburg, Germany

ARTICLE INFO

Keywords:
PlanetScope
Unmanned aerial vehicle
Steppe fire
Plant functional group
Land degradation
Remote sensing
Random forest

ABSTRACT

Land degradation is a major environmental and social issue in temperate steppes. It is commonly determined from vegetation cover using remote sensing techniques. Steppes in eastern Mongolia are subject to resource extraction activities, such as mining and oil extraction, which affect land degradation. Recent technological progress in remote sensing has facilitated the acquirement of high-resolution data by, for example, the CubeSat satellite or unmanned aerial vehicles (UAV), providing data for detailed maps of vegetation cover and plant functional groups (PFGs). Traditional methods for monitoring vegetation cover often face typical scale issues, such as the upscaling of vegetation parameters if plot-scale field measurements are integrated to satellite data. Here, we studied the spatial distribution of PFG using machine learning and a combination of field measurements, UAV imagery (spatial resolution: 2 cm), and PlanetScope multi-temporal imagery. We provide two products at two spatial resolutions: one for UAV data, which is restricted to comparatively small areas around field measurements, and one for PlanetScope, which covers large parts of northeastern Mongolia. The results showed that the overall accuracies of UAV classification were 91–95%, whereas those of PlanetScope were 78–95%. In integrating the classified UAV data to the PlaneScope data, our proposed model minimized the scale issue that often impedes classification. Importantly, our findings revealed that the ecological effects of dirt road and railroad extended up to 60–120 m into the adjacent, otherwise less degraded steppe vegetation. A comparison between burned and unburned areas in different years indicates that wildfires affect the composition of PFG in reducing the fractional cover of graminoids and forbs, and that increasing cover of bare ground leads to a distinct and patchy mosaic of different vegetation types.

1. Introduction

The temperate steppes of Mongolia provide valuable socioeconomic and ecosystem resources on which human communities and native wildlife are dependent (ADB, 2014; Reading et al., 2010). In recent decades, Mongolian steppes have been intensively used owing to the rapid growth of natural resource extraction, including mining and oil extraction, as the extractive sector has become a major part of the economy of Mongolia (Mongolia EITI, 2018; Reading et al., 2006). Extractive industry leads to land degradation and other anthropogenic stressors that made an increase in the ecological vulnerability of Mongolian steppes (Batkhishig, 2013; Liu et al., 2013; Wang et al., 2019a). The extractive industries trigger the development of extended dirt road networks and other supporting infrastructure in the eastern Mongolian steppe (Dashpurev et al., 2020), which hosts some of the world's largest and most intact steppe regions (Batsaikhan et al., 2014). A recent

Abbreviations: PFG, Plant functional group; UAV, Unmanned aerial vehicles; RF, Random forest; GLCM, Grey level co-occurrence matrix; OBIA, Object-based image analysis; VARI, Visible atmospherically resistant index; ACC, Active chromaticity color; MAUP, Modifiable Areal Unit Problem.

* Corresponding author.
E-mail address: B.Dashpurev@iggf.geo.uni-muenchen.de (B. Dashpurev).

https://doi.org/10.1016/j.ecolind.2021.108331
Received 20 October 2020; Received in revised form 22 October 2021; Accepted 25 October 2021
Available online 29 October 2021

spatiotemporal analysis of the eastern Mongolian steppe indicated that the total area occupied by dirt roads as well as oil exploration and exploitation infrastructure expanded by 75% in the past decade (Dashpurev et al., 2020). Nevertheless, the impact of dirt roads and infrastructure expansion on the surrounding ecosystems is unclear in the eastern Mongolian steppe, although this knowledge is key for safeguarding ecosystem services, the conservation of the steppe, and the assessment of future developments in the area. Besides land use change, the livestock grazing pressure largely influences land degradation in Mongolia (Batkhishig, 2013; Na et al., 2018; Tuvshintogtokh and Ariungerel, 2013). Continuous growth of livestock numbers causes pasturelands to vastly exceed their carrying capacities (Tumur et al., 2020). A recent assessment estimates that 75% of the total pastureland in Mongolia have exceeded their carrying capacities, of which over 50% show moderate to heavy signals of overgrazing (Coslet et al., 2017). For instance, overgrazing was mostly observed around permanent locations of herders and administration centers, as well as near urbanized areas in central Mongolia (Coslet et al., 2017; Densambuu et al., n.d.). However, a recent assessment of livestock-caused land degradation showed that the grazing pressure in the eastern Mongolian steppe has been consistently low compared to that in other parts of Mongolia (Jamsranjav et al., 2018). Another cause for land degradation is wildfires, which are caused by both human activities and climate (Nasanbat and Lkhamjav, 2016; Rihan et al., 2019). Indeed, according to wildfire statistics in Mongolia, approximately 95% of steppe and forest fires are caused by human activities (Erdenetuya, 2012). The statistical data show that eastern Mongolia has experienced multiple, massive steppe fires over the past decades (FARUKH et al., 2009; National Statistics Office of Mongolia, 2020). According to the official statistics, 193 wildfires occurred between 2004 and 2018 in Dornod Province, and there were 16 wildfires in Choibalsan District. Consequently, approximately 3 million ha of steppe were burned within over 14 years in Dornod Province, and approximately 119.3 thousand ha of lands were repeatedly burned in Choibalsan District (Environmental Information Center, 2021). Furthermore, Nasanbat et al. (2018) and Nasanbat and Lkhamjav (2016) developed a wildfire risk map for Mongolia and found a very high wildfire risk in eastern Mongolia. Steppe fires are known to alter plant community composition and thus may lead to land degradation, together with other drivers, such as excessive grazing intensities (Indree and Magsar, 2007; Stavi, 2019; Tuvshintogtokh, 2014; Yoshihara et al., 2015). Because of the vast extent of steppes in Mongolia, remote sensing-based analyses are advantageous to gain knowledge of land degradation along infrastructure and recovery patterns. However, no studies have been conducted to analyze the impacts of steppe fire on vegetation cover and post-fire vegetation recovery in eastern Mongolia using remote sensing data of sufficiently high spatial resolution to detect the small-scale effects of degradation on plant community composition.

In degradation studies based on vegetation cover, approaches based on plant functional groups (PFGs) have been increasingly used in the past decades and have shown that time-series studies can effectively determine the trends of PFG (Luo et al., 2018). Plant species are grouped into PFG using an *a priori* scheme that considers growth form, life history, and other morphological characteristics (Gitay and Noble, 1997; Thomas et al., 2019; Wright et al., 2006). Usually, plants in Mongolian steppe communities are classified by functional similarity based on the growth form (shrub, grass and forbs), life forms and broader taxonomic groups (e.g. graminoids), and plant lifespan (annual and perennial), depending on the purpose and scale of the research (Cowles et al., 2018; Jamiyansharav et al., 2018; Liu et al., 2013; Narantsetseg et al., 2018). In the present study, the functional groups included graminoids, true shrubs, dwarf shrubs, perennial forbs, and annual forbs. In addition, we consider litter and bare ground. We adopted these groups because they allow comparison across different taxonomical groups; for example, several species of true shrubs and dwarf shrubs occurring in Eastern Mongolia are indicators for land degradation (Tuvshintogtokh and Ariungerel, 2013). In several previous studies, degradation indicator plants in Mongolian steppes were summarized (Danzhalova et al., 2012; Tuvshintogtokh, 2014; Tuvshintogtokh and Ariungerel, 2013), and their classification showed that true shrubs and dwarf shrubs of genera *Caragana*, *Artemisia,* and *Ephedra*, and annual forbs could be indicator plants for land degradation. For instance, the dwarf shrub *Artemisia frigida* showed increased abundance along abandoned tracks and spread into the surrounding, formerly intact vegetation (Bazha et al., 2012; Li et al., 2006). Furthermore, the dominance of the dwarf shrubs *A. frigida* and *Ephedra sinica* as well as the true shrubs *Caragana microphylla* and *Caragana pygmaea* indicate degradation in Mongolian steppe ecosystems (Bazha et al., 2012; Gunin et al., 2012); (Densambuu et al., n.d.). Hence, considering the function of PFG in this study, the distribution of shrubs and annual forbs suggests a degraded land, whereas species of other taxonomic groups indicate a healthy steppe.

Surveying plant communities with traditional vegetation sampling methods is costly and time-consuming, especially for larger areas. Alternatively, in the past decade, imagery taken by an unmanned aerial vehicle (UAV) has emerged as a cost-effective method to successfully identify species of PFG (Kaneko and Nohara, 2014). Small-size UAVs are typically equipped with sensors sensitive to the visible spectrum, providing red, green, and blue (RGB) image bands (Hassanalian and Abdelkefi, 2017). Recently, several studies have successfully tested vegetation mapping using UAV-based high-resolution RGB images and vegetation indices (Silver et al., 2019; Themistocleous, 2019). To extract vegetation information from RGB data, the visible atmospherically resistant index (VARI) was developed, and the data can be used to construct models capable of accurately estimating fractional vegetation cover (A. A. Gitelson et al., 2002; Zhang et al., 2019). In addition to this vegetation index, a widely used method for vegetation identification is texture metrics derived from RGB imagery, which can correctly detect species or PFGs, as shown in previous studies (Haralick et al., 1973; Li et al., 2019; Wang et al., 2018).

Hernandez-Santin et al. (Hernandez-Santin et al., 2019) reviewed and summarized the power of UAV data to identify plant species and revealed the high potential of UAV data for measuring and monitoring vegetation cover at the micro to local scale. The most recent review noted that UAVs greatly contribute to the mapping and monitoring of vegetation cover in various areas (de Castro et al., 2021). UAVs are equipped to acquire very high spatial resolution imagery, thereby allowing the analysis of small parts of vegetation cover. In numerous studies, UAVs have been used to map plant communities (Kattenborn et al., 2019; Lu and He, 2017; Villoslada et al., 2020), individual species (Hamylton et al., 2020; Sankey et al., 2019; Wijesingha et al., 2020), and PFG (Nelson et al., 2017; Zhao et al., 2021b). However, in Mongolia, relatively few studies have applied UAV-based remote sensing for vegetation cover estimation. Some studies have shown that UAVs can be an effective method to map shrub biomass and structure in the steppe and desert steppe regions of the Mongolian plateau (Dong et al., 2019; Zhao et al., 2021a; Zhou et al., 2021). For small-size drones, the range of capturing images usually depends on flight distance, height, and available time. The flight range of small-size drones is 5–7 km, and its flight time is 15–30 min (Cano et al., 2017). Nevertheless, as small-size UAVs are usually employed for surveying small areas, the data need to be integrated with other sources of remotely sensed satellite data that allow the estimation of vegetation cover at the local to regional scales.

Earth observation satellite data have a range of spectral, spatial, and multi-temporal characteristics, and thus are suitable for different purposes of vegetation mapping, especially over large areas (Xie et al.,

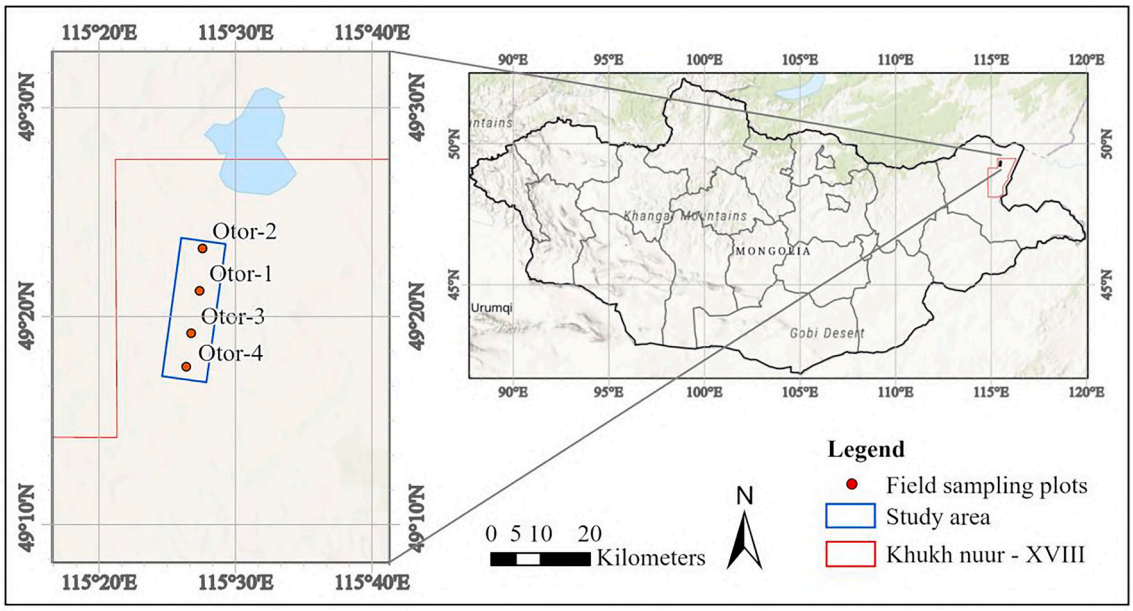

Fig. 1. Study area map.

2008). Remotely sensed data have been extensively used to estimate vegetation cover in Mongolian steppes, yet most studies are based on medium or coarse spatial resolution satellite data, such as Landsat and MODIS (Hilker et al., 2014; Kim et al., 2020; Otgonbayar et al., 2019; von Wehrden et al., 2009). These types of satellite data are usually capable of mapping vegetation at the community level and in different land cover types (Xie et al., 2008). Novel satellites of PlanetScope CubeSat (also named doves) capture a four-band multispectral dataset at 3-m resolution, opening new possibilities for surveying vegetation at the species level. Currently, more than 130 satellites of PlanetScope are operated by Planet Labs (www.planet.com); they provide a near-real time imagery of the global land surface (Cooley et al., 2017; Planet Team, 2017). Such data increasingly allow the recording of vegetation phenology with a high precision from time-series satellite images (Kimball, 2014; Vrieling et al., 2018; Zhang et al., 2009). The satellites of PlanetScope acquire data on a daily basis with a high spatial resolution; this high observation frequency allows the creation of very high multi-temporal resolution datasets over different vegetation periods across large areas. As far as we know, no previous study has investigated the possibilities of using PlanetScope satellite data to map vegetation in Mongolia. In addition to sensor technology, analysis techniques play is important to derive reliable vegetation data at the local to regional scales. Modern machine learning techniques, such as Random Forest (RF) classification and regression, have widely been used in previous remote sensing studies for high-accuracy vegetation mapping (Belgiu and Drăgu, 2016; Maxwell et al., 2018).

Consequently, this study aimed to unravel the current impacts of anthropogenic drivers on land degradation, such as intensive utilization of dirt roads, and their influence on the surrounding steppes. To achieve this, we firstly addressed the potential utilization of combined data from field-collected vegetation data, UAV imagery, and high-resolution satellite multi-temporal imagery to provide details on the spatial distribution of dominant and indicator species (such as shrubs) of PFGs based on changes in their spectral characteristics during the vegetation period. Therefore, in this study, we developed a model that merged the remote sensing methods for analyzing field-collected vegetation data and remotely sensed data. The second objective was to produce maps of fractional cover of PFGs that are key to the assessment of the consequences of dirt road networks and infrastructure construction on the surrounding steppes in Mongolia and their contribution to human-induced land degradation. Lastly, this study examined the effect of short-interval steppe fires on vegetation community shifts by comparing the vegetation in burned and unburned areas over several years.

2. Materials and method

2.1. Study area

The study was conducted in the inter-province reserve pasture ("Otor") area of Choibalsan, which is part of the eastern Mongolian steppe in Dornod Province, Mongolia (Fig. 1). The study area comprises approximately 109.5 km^2 between 49°14′9″N–49°24′28″N in latitude and 115°25′1″E–115°31′57″E in longitude. The steppe mainly consists of broad plains and rolling hills where the vegetation is dominated by bunch grasses such as *Stipa krylovii* and *Cleistogenes squarrosa* (Hilbig, 2016). The area is characterized by an extremely continental climate. According to long-term climate data, the average minimum monthly temperature reaches − 20 to − 22 °C in January, and the average maximum monthly temperatures of 19–21 °C occur in July. The average annual precipitation amounts to 200–300 mm, with the monthly maximum mainly occurring in summer (Martin Pfeiffer, Choimaa Dulamsuren, 2018; National Statistics Office of Mongolia, 2018). The major land use types in this area are rangelands and mines with only one settlement (National Statistics Office of Mongolia, 2020). Approximately 70% of the total land in eastern Mongolia is rangelands used for traditional livestock herding. Dornod Province possessed approximately 3.7 million sheep equivalent units at the end of November 2017 (Coslet et al., 2017). For the remote area of eastern Mongolian steppes, it is estimated that the livestock carrying capacity is not exceeded (Coslet et al., 2017; Jamsranjav et al., 2018) and there are several inter-province and inter-district reserve pasture areas in eastern Mongolia steppes, such as the reserve pasture area of Choibalsan. Reserve pastures are land for special needs (emergency grazing areas) and established for emergency use in severe climatic conditions during winter and spring (ADB, 2014).

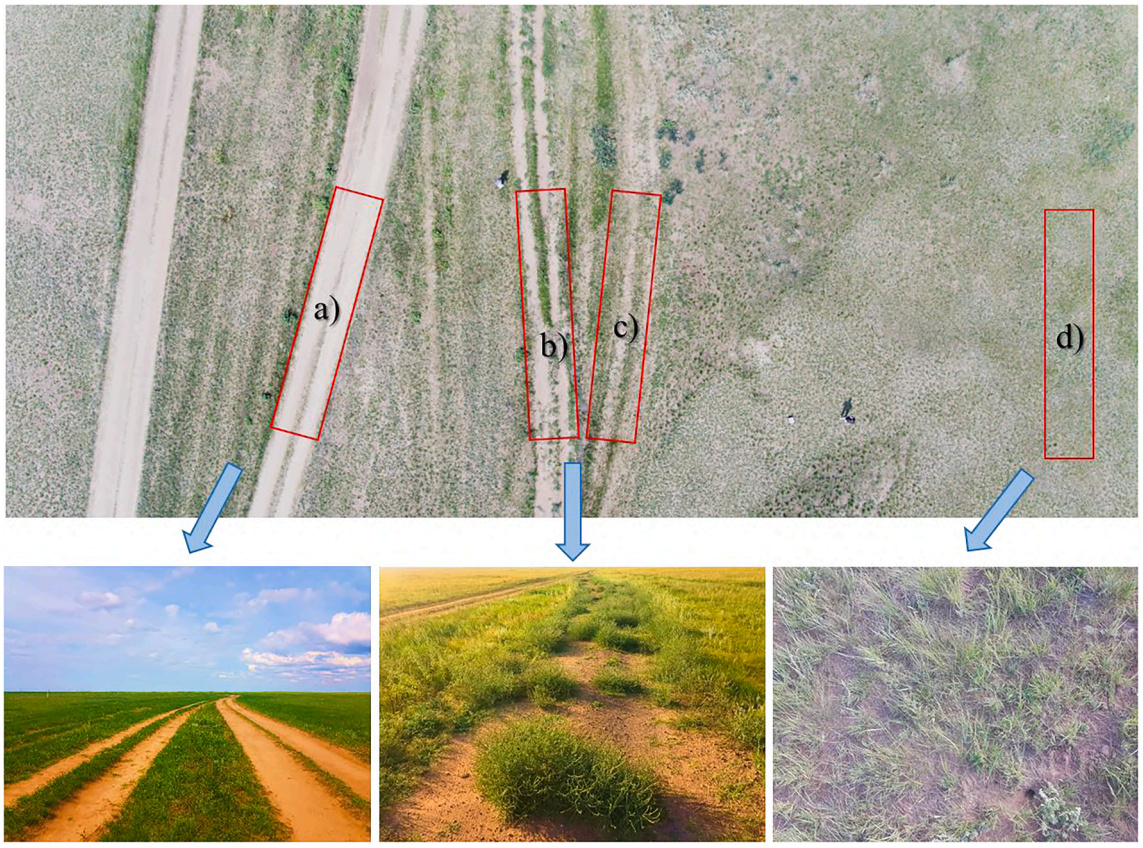

Fig. 2. Field data collection in one of the sampling sites (Otor 2, represented by the northernmost red dot in Fig. 1). a) Active track. b-c) Abandoned tracks where dwarf shrubs (Artemisia frigida) dominated. d) Reference plot where the vegetation was dominated by a mixture of graminoids and forbs. (For interpretation of the references to color in this figure legend, the reader is referred to the web version of this article.)

The whole study area is subject to an oil exploration license. For instance, the Khukh nuur XVIII block was issued under a production sharing contract in 2009 and 2017 (Mongolia EITI, 2020).

2.2. Datasets and processing

2.2.1. UAV image data

UAV image data were collected in August 2019 by a DJI Phantom 4 UAV drone flown at an average height of 50 m above ground level. The UAV images were captured at four vegetation survey sites, which covered all vegetation sampling plots. The UAV was equipped with a DJI FC300 camera, which was used to collect visible wavelength RGB bands in the DNG format. The camera has a resolution of 12.4 megapixels with a ground resolution of approximately 2 cm/pixel at 50 m flight altitude. The images were taken during manual flight using the DJI GO 4.0 smartphone application provided by DJI.

2.2.2. Satellite data

Multi-temporal remote sensing data from April to September in 2018 and 2019 were downloaded free-of-charge from the PlanetScope image archive of Planet Lab Inc. as part of the Education and Research program website (www.planet.com) (Planet Team, 2017). All images were selected according to their acquisition dates and cloud coverage. To capture as much phenological stages as possible, images from all months during the vegetation growth season were selected (Table A1). The multi-temporal images were already georeferenced to the Universal Transverse Mercator projection WGS84 zone 50 north.

2.2.3. Field data collection

In August 2019, vegetation field surveys were conducted on a total of 16 random and non-permanent rectangular plots of 25 × 4 m at four sites along the main dirt roads of Choilbalsan soum to Ereentsav border crossing (Fig. 2). The sites were 5 km apart from each other. Regarding the location, two sites were selected in non-disturbed steppes, and another two sites were in burned steppes. At each site, one plot was established on the active track where non-vegetation cover types, including bare ground, soil, and stone dominate (a). In addition, two rectangular plots (b and c) were established on two abandoned tracks that were parallel and adjacent to the active track. A reference plot (d) (roadside vegetation) was selected in the surrounding steppe close to the dirt roads (Fig. 2). The average distance of plots within each site was 2–5 m in tracks and 15–20 m in reference. The total vegetation cover and cover for each functional group at each rectangular plot were visually estimated by experts. Plant species were grouped into a functional classification scheme that considered the growth form, common plant species, plant lifespan, and study purpose. The scheme is comprised of graminoids, true shrubs (*Caragana*), dwarf shrubs (*A. frigida* and *Ephedra*), perennial forbs, annual forbs, litter (dead plant material), and bare ground. At each plot, 10 points were measured, and the values were then averaged. A GPS was used to determine the location of each plot.

2.2.4. Image preprocessing for UAV data

The raw UAV data were processed using the Esri ArcGIS Pro 2.4 software to produce the photogrammetrically corrected orthomosaic images. For subsequent supervised image classification and processing, a series of image 'preprocessing' steps were carried out:

1. **Photogrammetric calibration and orthorectification** – removal of geometric distortion in the collected image data using a block adjustment technique based on the computation of the photogrammetric relationships between overlapping images, ground control points, the camera model, and terrain variability.

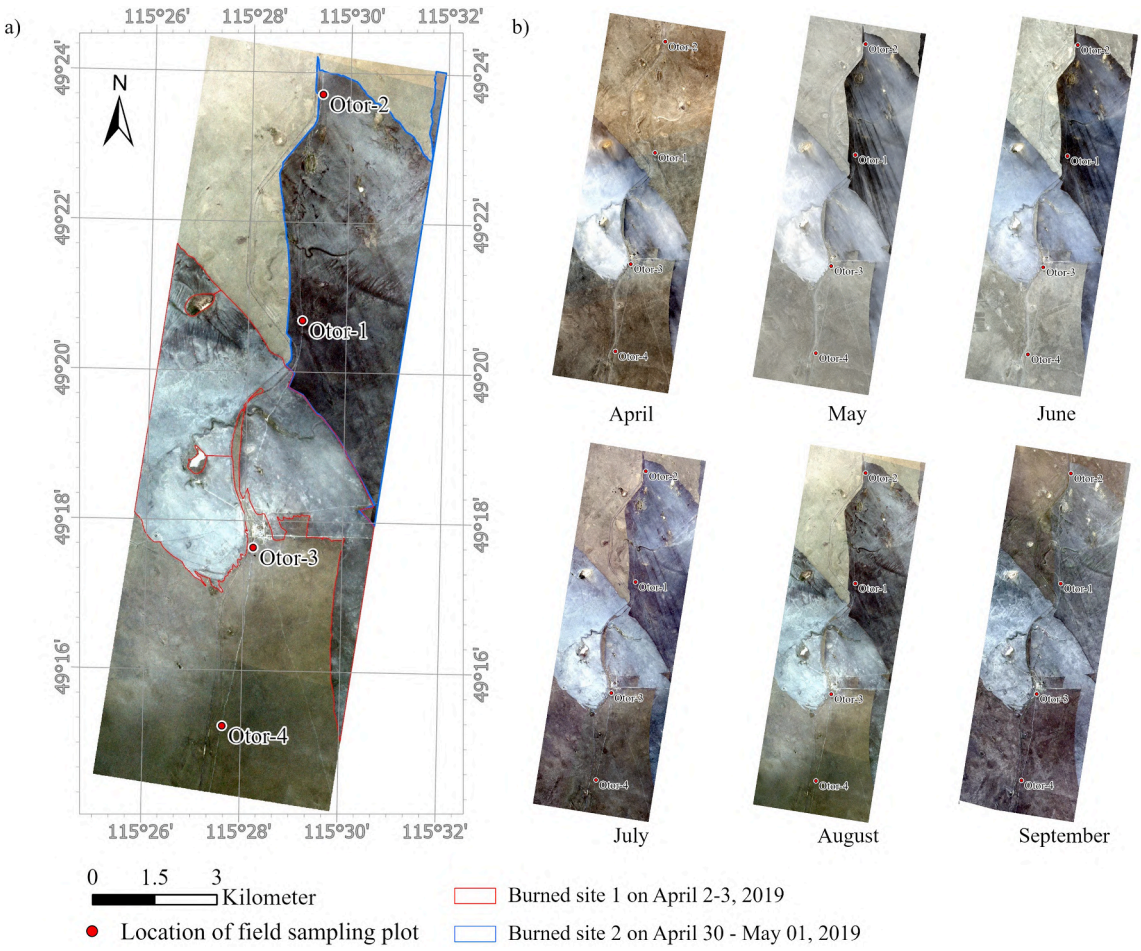

Fig. 3. Collection of orthomosaic imagery from PlanetScope. a) The daily mosaic data from PlanetScope acquired on the 16th August 2019; b) the monthly mosaic data illustrating the temporal changes in land cover in the vegetation growth season from April to September 2019.

2. **Mosaicking, seamlines, and color-balancing** – creation of a single seamless image from adequately color balanced UAV image collection.

Consequently, a set of orthomosaic UAV images data was created and subsequently used to perform an object-based image classification (Fig. A1).

2.2.5. Image preprocessing for remote sensing data of PlanetScope

The 3B level product of PlanetScope comprises raw analytic images as digital numbers, as well as images with radiometrically calibrated and surface reflectance data (SR). In this study, the SR images were selected for further analysis, which were already processed to convert top of atmosphere reflectance (TOA) into surface reflectance (Planet Labs Inc., 2019).

Each daily orthomosaic image was created from three scenes and subjected to color matching via the blending method (Pan et al., 2016). Monthly mosaic images were created to manually check for monthly land cover changes and steppe fire occurrences between 2018 and 2019 (Fig. 3 and Fig. A3). Before the images were used in the classification algorithm, they were clipped to the area of interest, and then the near infrared band was separated for further processing. In our study area, steppe wildfire events occurred twice in spring 2019, and were recorded in the archive of PlanetScope daily images. The first wildfire occurred on April 2–3, 2019, and the second wildfire took place on April 30–May 01, 2019.

2.3. Workflow for image analysis of UAV data and PlanetScope multi-temporal data

Two techniques of classification and regression (Liu et al., 2011) were separately applied to UAV imagery and PlanetScope multi-temporal data, each using the RF algorithm (Fig. 4) (Breiman, L., Cutler, 2018; Breiman, 2001; Breiman et al., 1984). UAV images were classified by RF in the ArcGIS Pro 2.4 software, and estimation of multi-temporal PlanetScope data was carried out by a RF model using a framework of the Scikit-Learn 0.21.3 package in Python 3.4.7 (Pedregosa et al., 2011).

2.3.1. UAV image classification workflow and accuracy assessment

An object-based supervised classification method was developed to classify the orthomosaic images of UAV. In this way, segmentation was performed to create pixels based on their spectral and spatial similarities. We applied a moving window approach that merges similar neighboring pixels based on color and shape. The segmented image contained the following types of predictors: (1) spectral, (2) textural, and (3) geometric features of segments (see Table A6 for details of predictors). For the spectral features, means and standard deviations of

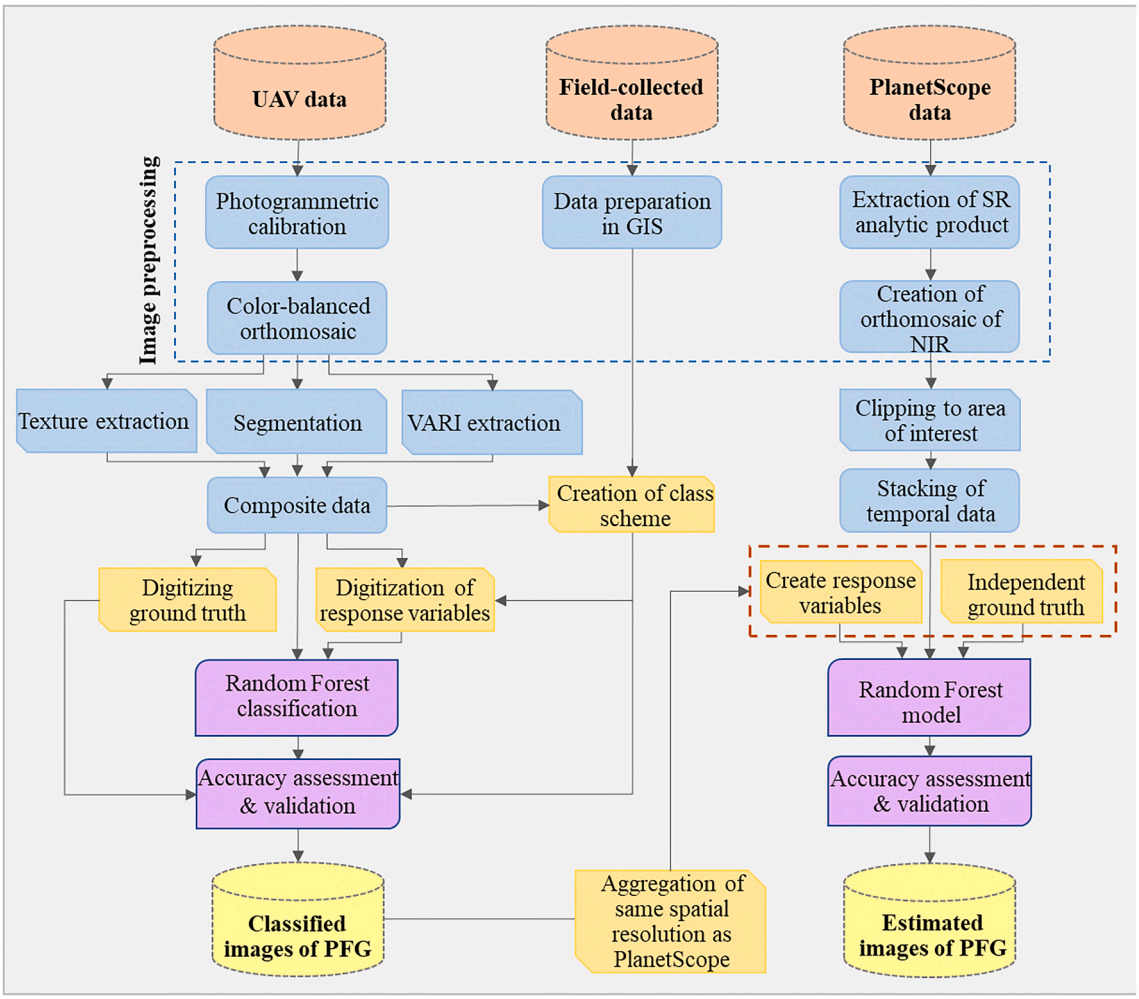

Fig. 4. Image analysis workflow. The colors indicate that the same image analysis process was applied to the three different data sources.

Table 1
Summary of degradation indicator classes discriminated in the field and in remote sensing products. A class scheme for image classification (2) was applied to both UAV and PlanetScope imagery.

1) A scheme for field sampling	2) A class scheme for image classification	
	Class name	A function of class
Graminoids Perennial forbs Annual forbs	Graminoids and forbs-dominated mixed PFG	The spatial distribution of PFGs indicates healthy or undisturbed land
True shrubs Dwarf shrubs	Shrubs	The spatial distribution of shrubs indicates ecologically affected or degraded land
Bare soil Litter Stone	Bare ground (non-vegetation)	The spatial distribution of this class indicates non-vegetation area, bare soil/ground, or disturbed land
–	Man-made objects	Detected railroad and building

RGB color (chromaticity) were calculated from each band. Regarding the textural features, texture metrics were extracted from the red band of the UAV images, as spectral differences between and within PFGs were higher than in any other band based on visual interpretation. The calculation of texture metrics was carried out in the Envi software (Version 5.3, Harris Geospatial Solutions, Inc.). For the calculation, a 3 × 3 processing window was used to construct a grey level co-occurrence matrix (GLCM) (Haralick et al., 1973; Zhang, 2001), which was the basis for deriving several textural indexes, such as mean, variance, homogeneity, contrast, dissimilarity, entropy, second moment, and correlation. Those texture metrics were used as additional predictors in the object-based classification. The geometric attributes of features refer to the shape characteristics of segments derived from drone imagery. Three basic metrics of shape characteristics were computed in the segmentation process, namely the number of pixels per segment, compactness, and rectangularity. VARI was calculated from the RGB bands of the images and used as an additional predictor (Anatoly A. Gitelson et al., 2002). The index is a quantitative proxy for the fractional cover of vegetation.

The classification scheme for remotely sensed data was created by

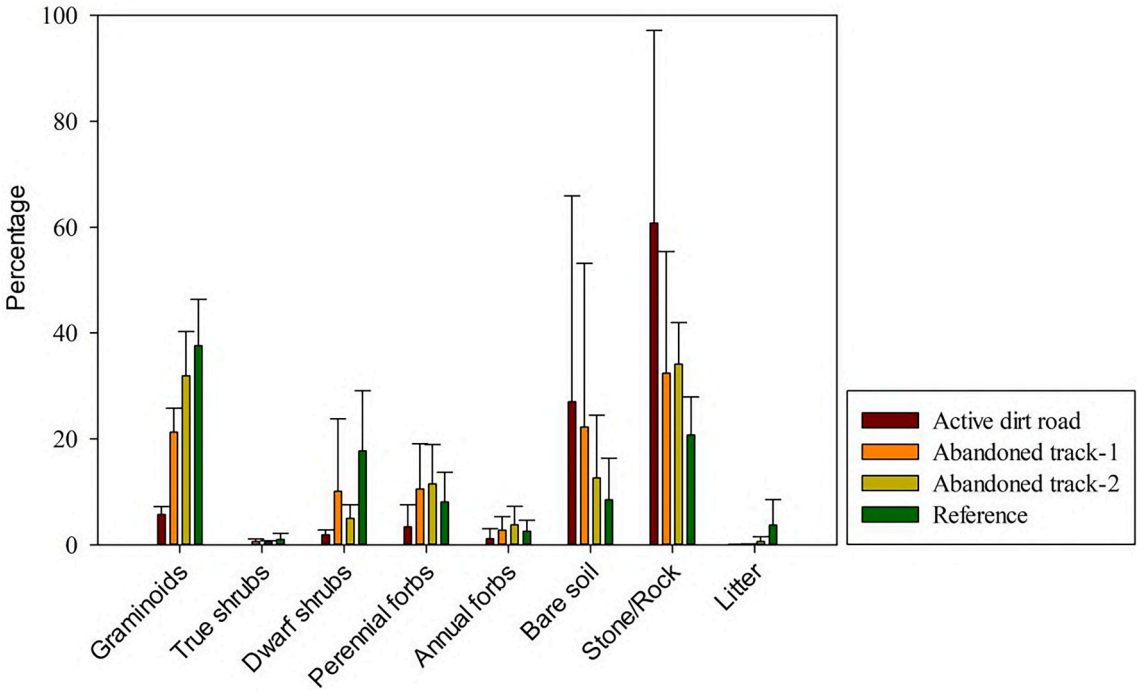

Fig. 5. The composition of functional groups along dirt roads to reference transects. In the figure, the composition illustrates the average proportion of all four sites and error bars (standard deviation).

summarizing the dominant PFGs in field campaigns and by detecting man-made objects on UAV images (Table A2). The classification scheme applied in the field (e.g., individual functional groups or mixtures of functional groups) was modified based on how well species of functional groups can be realistically discriminated in the drone images (Table 1). Thus, the classes in the scheme were characterized as graminoids and forbs, shrubs, bare ground, and man-made objects based on the comparison in Section 3.1. To prepare a set of response variables (digitized), selected classes were manually digitized throughout the orthomosaic images of UAV with the objective to capture representative samples of classes. A total of 160 sample points were collected and distributed throughout the whole study plots. Subsequently, the RF classification algorithm was used to classify all orthomosaic images of UAV.

Classification accuracy was assessed using equalized stratified random sampling from the mosaic images of UAV. A confusion matrix with errors of omission and commission, a kappa index, and an overall accuracy were used to examine the accuracy of the classification (Cohen, 1960; Rosenfield and Fitzpatrick-Lins, 1986; Russell, 1991). Additionally, the existing classified images were compared to field-collected vegetation cover data using a cross-validation to evaluate classification accuracy. Data for comparison were extracted from the classified images using the spatial information of field sampling plots.

2.3.2. *PlanetScope image classification and accuracy assessment*

To investigate the impacts of dirt roads, other infrastructures, and wildfire events on the surrounding steppe, map products of PFG were created by RF based on multi-temporal PlanetScope satellite imagery. In the classification and regression analysis of PlanetScope data, a pixel-based approach was employed to estimate the fractional cover of PFG from the temporal images. The response variables of the RF model were generated from the existing data of UAV classified images. All classified UAV images were used for generating the dataset of response variables, which covers all four field sampling sites. To apply the RF to the different sources of data, the resolution of all UAV map products (0.02 m) must be spatially aggregated to the same resolution as the PlanetScope data (3 m), as this integration process faces a typical scale effect (Dark and Bram, 2007). According to Wu et al. (Wu and Li, 2009), there is no universal scaling method to solve this issue. For each PFG and bare ground, cover is calculated in a pixel-wise manner by counting the number of collocated pixels classified into the respective class in the drone image classification. In the second step, the count values were converted into proportion (fractional cover) of PFGs and bare ground by dividing them by the total number of pixels in the high spatial resolution images covered by each pixel at the lower resolution. The fractional cover was calculated for grid cell by using the Zonal histogram tool in ArcGIS Pro. Consequently, each aggregated pixel contained the fractional (percentage) cover in each class. Subsequently, estimations of PFGs and bare ground were performed by the RF classification and regression in the multi-temporal PlanetScope images. Performance of RF models can be computed during the calculation of the out-of-bag error, which is calculated from the remaining training data (approximately one-thirds) not used to build the actual tree. Finally, the classification output was assessed for the overall, producer, and user accuracies in error matrices (Rosenfield and Fitzpatrick-Lins, 1986; Russell, 1991). For predicting a categorical variable, both sensitivity and accuracy are calculated to evaluate the performances of classification using a confusion matrix. For the regression results, model performance was examined using 10% of the reference data excluded for validation (10-fold cross-validation). From each class, validation sample sets of approximately 1500 pixels (no overlap) were extracted. In the prediction of continuous variable, the accuracy metric of R-square was used to assess the performances of uncategorized features in the RF model. We calculated the root mean square error (RMSE) to evaluate the error propagation of the RF regression model.

To estimate the effects of dirt roads and railroads on the surrounding steppe, the fractional cover of PFGs was extracted from the final maps

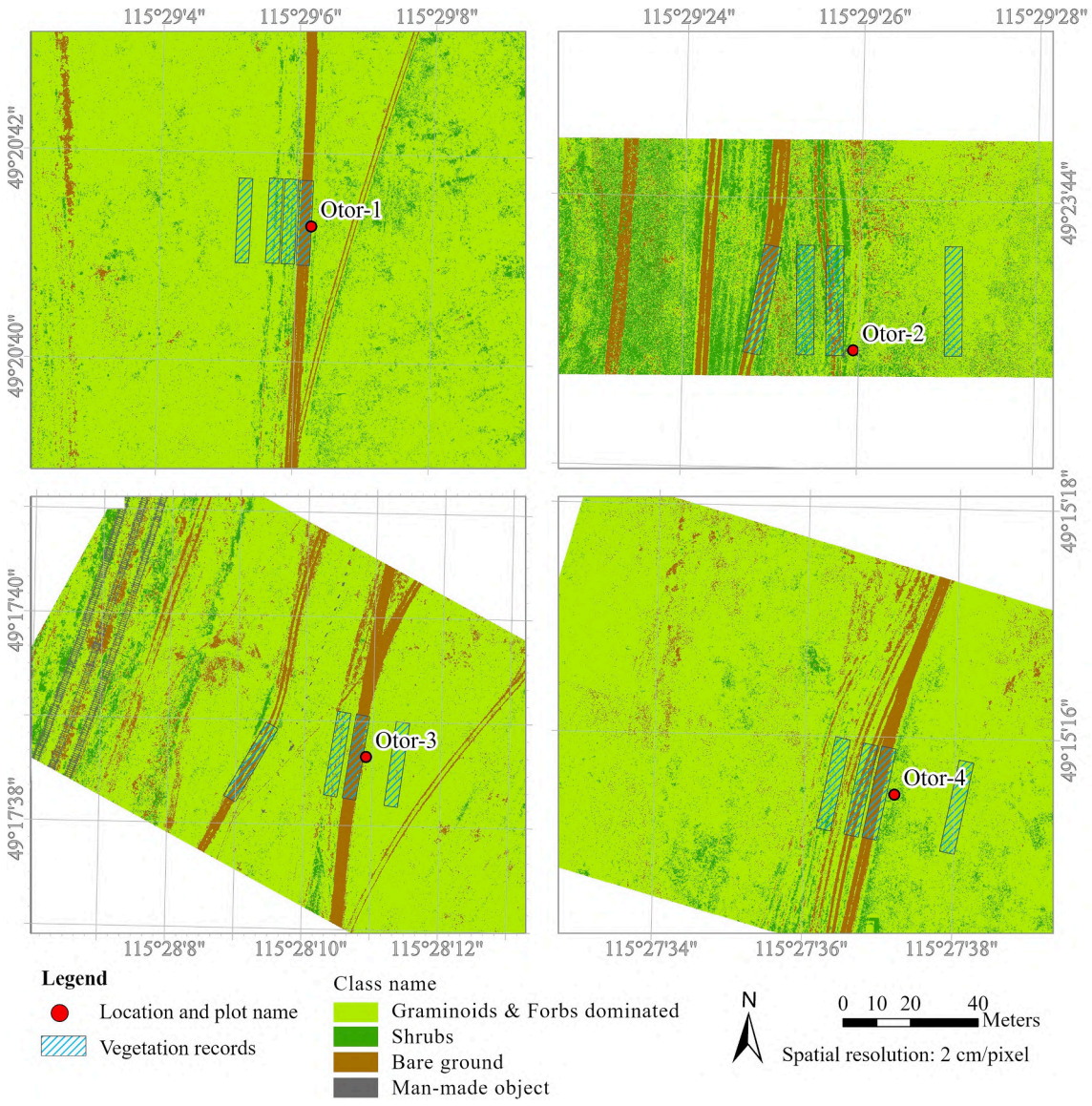

Fig. 6. Classified images of UAV data.

within multiple buffer rectangles at different distances to the roads/railroads using the zonal histogram function in ArcGIS Pro. At 15 random locations, transects of 300 m in length were established in both sides of the roads/railroads (for further details on the buffer locations, see figure in Section 3.4). The transects were 100 m in width. At an interval of 20 m, the PFGs were extracted from the 100 m long stripes. The extracted data were averaged, and the results were summarized into two categories including dirt roads and railroads. Regression analysis (McIntosh et al., 2010) was applied to estimate the relationships between distance and PFGs. Regarding the effects of wildfire on steppes, the fractional cover of PFGs was extracted from the final maps and linked to the polygons of burned areas using the zonal histogram function. The polygon was manually drawn from the mosaic imagery of PlanetScope in 2019 (Fig. 3).

3. Result

3.1. Plant functional groups detectable within UAV imagery

In the study area, a total of nine PFGs and cover types were determined in field sampling (Table A2). At the plot level, the composition of the PFGs was strongly affected by distance to active dirt roads (Fig. 5). For instance, the reference plots had higher vegetation cover than those on active tracks and abandoned tracks. There was a higher richness of functional groups in reference plots, and their dominant groups were graminoids (36%), dwarf shrubs (17%), and perennial forbs (8%). In contrast, the number of functional groups in active dirt road plots were lower, with a total vegetated cover of only 10–15%.

Furthermore, the dominant groups in naturally recovered vegetation in abandoned tracks were graminoids, followed by dwarf shrubs and annual forbs, altogether covering 42–46% of the total area. The cover of bare soil and stone was 29% in the reference plot, 46–55% in abandoned tracks, and 87% in active dirt roads. The proportion of functional groups also differed between sites (Table A2). At site Otor-1, the overall low vegetation cover was dominated by graminoids, and litter was missing at this site. At the other sites, the vegetation composition was more heterogeneous. In non-disturbed steppes, graminoids cover 40%, whereas the proportion of perennial and annual forbs is 5% and 10%, respectively, and dwarf shrubs covered 13–28% of the roadside vegetation (Otor-3&4). In burned steppes, graminoids and dwarf shrubs were equally dominant, accounting for 25–26% of the roadside vegetation cover of Otor-2. However, the abovementioned functional groups

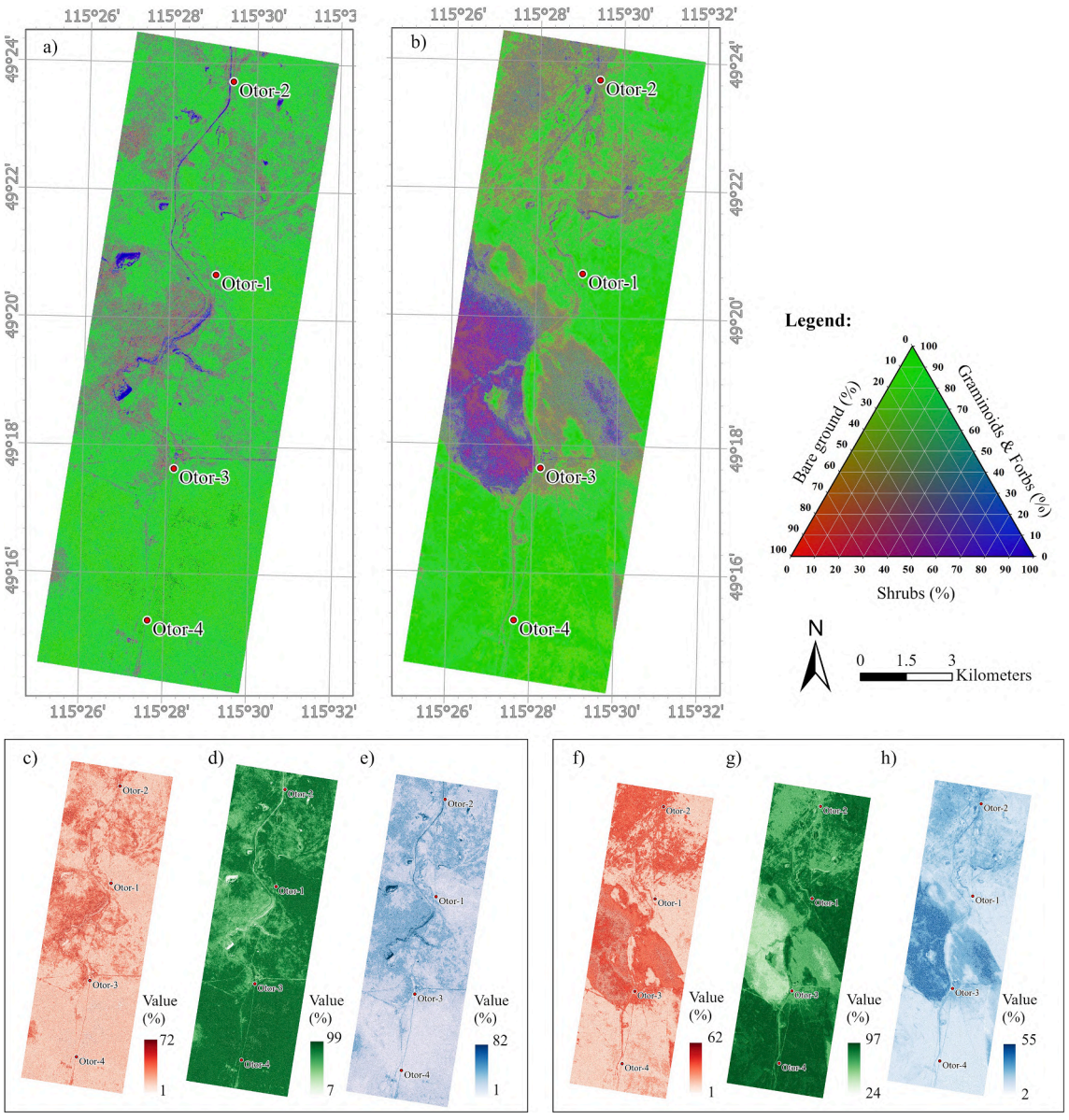

Fig. 7. a & b) RGB composite image illustrating the subset of PFGs and bare ground in 2018 and 2019. In the composite, the following color code order was used: red, green, and blue are shrubs, graminoids/forbs, and bare ground, respectively. Maps of each fractional cover are shown in c & f) bare ground, d & g) graminoids/forbs, and e & h) shrubs. Map coverages of c-e and f-h are shown as the distribution of each class in 2018 and 2019. The inset legend is a color triangle that shows the RGB composite that contains a subset of image a and b. (For interpretation of the references to color in this figure legend, the reader is referred to the web version of this article.)

(graminoids, perennial forbs, annual forbs, true shrubs, stone/rock and litter) in Table 1-1 and Fig. 5 could not be detected by UAV imagery; therefore, we summarized these functional groups into three major groups (graminoids and forbs, shrubs and bare ground) to achieve a reasonable accuracy.

3.2. UAV image classification of PFGs and accuracy assessment

The orthomosaic products of UAV at four sites were classified using the RF model. Fig. 6 shows the classified images at different sites. The overall accuracies of the classifications were 92.1% in Otor-1, 92.6% in Otor-2, 91.5% in Otor-3, and 94.5% in Otor-4 (Table A3). Variable importance metrics were derived from the internal calculation of the RF model (Fig. A2). Generally, spectral variables, such as the active chromaticity of RGB, were revealed to be of high importance. Furthermore, all spectral bands of imagery and VARI were rated as highly important. Regarding the texture variables, the mean metric was considered of high importance. All other texture metrics were only marginally important, with importance values of 15–20 times lower than those of the mean metric. The least important ones were geometric variables, such as the number of pixels per segment, compactness, and rectangularity.

The frequency of classified pixels was calculated for each individual land cover category. According to the data, the classified imagery of Otor-1 and Otor-4 on average contained 5–7% of shrubs, 88–90% of

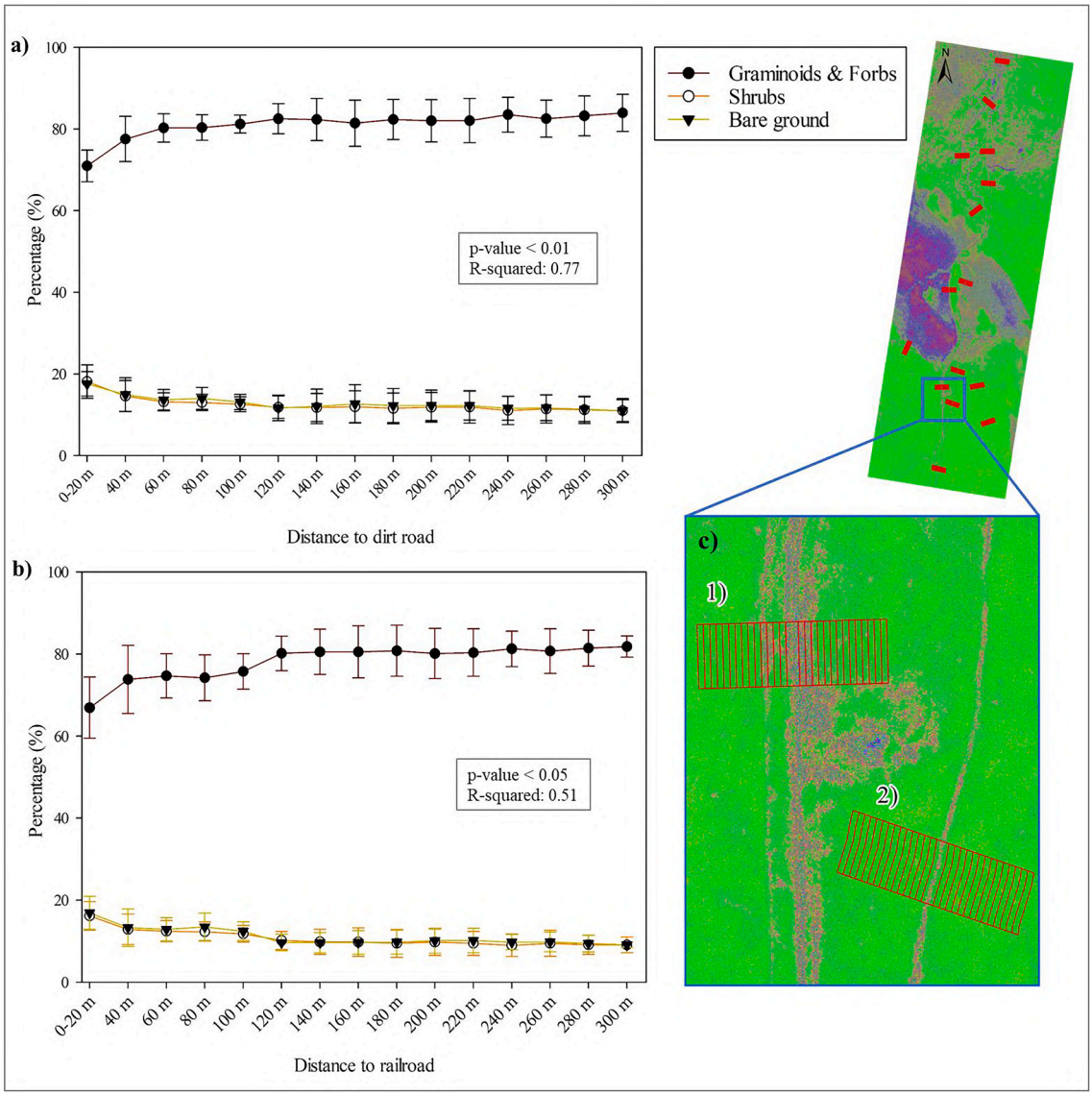

Fig. 8. The covers of the main PFGs and bare ground along the distance to a) dirt roads and b) railways. Points are mean values, and error bars denote standard deviations of estimates considering all transects. The location of buffers are shown in c. Here, the example of multi-buffer rectangles is illustrated in 1) railroads and 2) dirt roads.

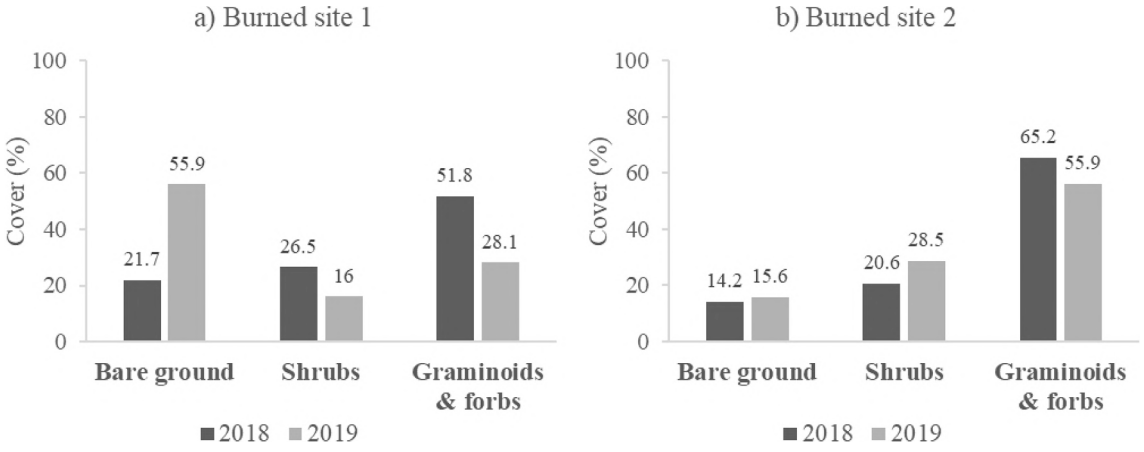

Fig. 9. The comparison of PFG covers at two burned sites between the year of the fire (2019) and the year before (2018). The bar graph in Figure a & b indicates shifts in the proportion of PFGs.

graminoids and forbs, and 3–7% of bare ground. Regarding the results of Otor-2 and Otor-3, the average pixels of land cover classes were 4% and 20% in shrubs, 66% and 80% in graminoids and forbs, 13–14% in bare ground, and 1–2% in man-made objects, respectively.

3.3. Classification of PlanetScope multi-temporal imagery and accuracy assessment

Through our model, we obtained two different outputs that illustrated the proportion of land cover types/PFGs. Fractional covers of PFGs and bare ground were estimated separately from PlanetScope data in 2018 and 2019, and those classes were subsequently used to create a single RGB composite image (Fig. 7a and b). In the RF regression, the output for each pixel contained a percent value for each single class that ranged theoretically between 0% and 100% (Fig. 7c-h). For the estimation of graminoids and forbs, the RF model produced an output map that ranged from 7% to 97%, whereas the estimated shrub coverage ranged from 1% to 82%. The fractional cover of bare ground was estimated to range between 1% and 72%. Accuracy evaluation was performed using a 10-fold cross-validation. The results showed that the RF regression model performed well with R^2 values of 0.82 in graminoids and forbs, 0.61 in shrubs, and 0.94 in bare ground class. The validation results of the RF model revealed RMSE values of 6.891% in graminoids and forbs, 8.202% in shrubs, and 4.449% in bare ground (Table A4). Regarding the RF classification, the land cover types were classified using the PlanetScope data from April to September 2019 with overall accuracy of 88% (Fig. A4). In the accuracy report, the overall accuracy of graminoids and forbs was 78%, whereas shrubs achieved 88% accuracy. Regarding the bare ground class, the overall accuracy was 91%. The overall accuracy of man-made objects was estimated to be 95% (Table A5). According to the map products, graminoids and forbs covered large areas of the southern part of the study region in 2018 and 2019, whereas a mixture of shrubs, graminoids, and forbs dominated the northern part. The middle parts were dominated by shrubs and bare ground in 2019. The proportion of each class was calculated from the final classified map. Graminoids and forbs covered 72% of the total pixels, whereas bare ground accounted for 20% of the total coverage. Shrubs and man-made objects accounted for 3% and 5%, respectively.

3.4. Estimation of the vegetation area ecologically affected by transportation corridors

The final map product of RF classification was used to extract information on changes in vegetation composition from dirt roads and railroads to the pristine steppe using a transect approach. The results are shown in Fig. 8, where the average distance of altered vegetation was determined by the change in dominated PFGs and bare ground using sharp transitions. In general, Fig. 8a and b show that the average proportion of graminoids and forbs increased with distance to dirt roads and railroads (distance up to 60–120 m), whereas the average proportion of shrubs and bare ground both decreased with distance.

Focusing on dirt roads, Fig. 8a clearly shows that the average proportion of graminoids and forbs increased from 72% in 0–20 m to 82% in 60–100 m, and hereafter the proportion ranged between 81 and 83% (p-value < 0.01). In shrubs and bare ground, the average proportions decreased from 15 to 16% in 0–20 m to 9–10% at 60–100 m, respectively, beyond which the proportions remained constant. The linear plot shows that the lowest standard deviation of graminoids and forbs was in 80–100 m, whereas shrubs and bare ground were in 100 m. These changes imply that the effects of dirt roads on the surrounding vegetation extend up to 60–100 m.

Fig. 8b indicates a significant effect of railroads on vegetation cover (p-value = 0.04). The average share of graminoids and forbs increased from 65% in 0–20 m to 82% in 120 m, beyond which the average proportion remained constant at 83–84% as distance increased. For shrubs and bare ground, the average cover share decreased from 15 to 16% in 0–20 m to 8–9% in 120 m, beyond which no further changes occurred up to 300 m and onwards. This suggests that vegetation located up to 120 m from a railroad is affected.

3.5. The effects of wildfire on vegetation cover

We estimated the spatial distribution of PFGs and bare ground using daily PlanetScope imagery from 2018 and 2019 (Fig. 7a and b). According to the archive, there was no wildfire event in 2018 (Fig. A3). In 2019, wildfire occurred twice in the study area; the locations of the burned area are shown in Fig. 3. The first wildfire occurred around a small settlement area (Burned site 1) on April 2–3, 2019, and the second wildfire occurred in a remote and native steppe (Burned site 2) on April 30–May 01, 2019. For the estimation of burned year (2019), we used temporal PlanetScope data that included imagery of the site both during (April 2019) and after wildfire (May to September 2019). The comparison of PFG distribution at the two wildfire sites in the year of the fire (2019) and the year before (2018) showed that there were shifts in the proportion of PFGs (Fig. 9).

At burned site 1, the amount of bare ground doubled in the year of the fire (Fig. 9a). On the contrary, shrubs cover declined by 10%, whereas the graminoids and forbs-dominated group declined by 23% in 2019. For burned site 2, the values of bare ground and shrub cover increased by 1.4% and 8%, respectively, in the year of the fire (Fig. 9b). The cover of the graminoids and forbs-dominated group decreased by 10% in 2019. Overall, the changes in PFG covers between the year of the fire and the year before indicated that the steppe fire led to increased bare ground cover and decreased graminoid and forb cover at both sites of wildfire. Shrub cover did not show a clear trend because it decreased at burned site 1, but increased at burned site 2. Likewise, the field-sampling data of burned and unburned sites showed that the proportion of dwarf shrub cover at burned plot Otor-2 was the same as that of graminoid cover, but was relatively low at burned plot Otor-1. Furthermore, the PFG richness in burned plots was lower than that in unburned plots (Table A2).

4. Discussion

4.1. Estimation of PFG from remotely sensed data

We evaluated the efficacy of UAV imagery and high-resolution PlanetScope multi-temporal data combined with RF analysis for mapping PFG and bare ground cover to assess land degradation. The results revealed that the spatial distribution of indicator and dominant PFGs can be accurately estimated at both the micro and local scales. For mapping vegetation cover at the local scale, high-resolution UAV imagery yielded accurate results. However, the suitable spatial resolution depends on the research purposes, instrument capacity, and target vegetation types, among other factors. Some studies suggested that 0.02–0.03 m spatial resolution is appropriate in vegetation cover classification in a small area (Hamylton et al., 2020; Liu et al., 2020; Räsänen and Virtanen, 2019). Based on our field observation, we chose 0.02 m resolution for the present study.

Recent studies showed that utilization of texture information significantly improves classification performance (Kwak and Park, 2019; Popescu and Ichim, 2015). However, in our study, texture metrics

showed mixed contributions to classification performance, which is consistent with previous findings (Kupidura, 2019; Wang et al., 2018). The mean metric of textures contributed much more to classification than other texture features. Among spectral indices, we found that VARI had high efficiency to distinguish between shrubs and bare ground. Applied to UAV imagery, the highest values were obtained for shrubs, and the lowest value for bare ground. This indicated that the prediction of shrubs was highly sensitive to VARI. This is consistent with the finding of Lin et al. (Lin et al., 2015) that combining visible spectrum images and VARI resulted in a significant improvement in performance of object-based image analysis (OBIA). Zhang et al. (Zhang et al., 2019) also proposed that measures such as VARI extracted from high-resolution UAV imagery allow for accurate estimates of vegetation cover.

High classification accuracy values of 91–94% were obtained using UAV data. This is consistent with the findings of other studies at different locations (Gray et al., 2018; Wang et al., 2018). Regarding the satellite data, the overall accuracy of four classes ranged between 78 and 95% in multi-temporal PlanetScope data analysis. For the Mongolian steppe, few studies have been conducted to estimate the vegetation communities using RF. For example, Nanette et al. (Nanette Reece, Ganchimeg Wingard, Bayart Mandakh, 2019) applied RF classifier to identify steppe vegetation communities using single-date Landsat OLI data. The study showed the classification of six different vegetation communities with an overall accuracy of 85.3%.

4.2. Map products for land degradation monitoring

The latest thematic report of the United Nations on the Northeast Asia land outlook stated that "…countries in Northeast Asia face the growing threats of desertification, land degradation and drought. In Mongolia, it is estimated that land degradation occurred to some extent on about 77.8 percent of total land" (United Nations, 2019). According to several studies, the joint effect of climate change and human activities resulted in land degradation (Batunacun et al., 2018; Wang et al., 2019b; Zhang et al., 2021). For instance, in a study conducted in the Eurasian steppe, it was found that land degradation in Mongolia was mainly caused by human activities (Zhang et al., 2021). Further, there have been numerous studies demonstrating that overgrazing, mining development and infrastructure construction largely influence land degradation in the Mongolian plateau (Batkhishig, 2013; Darbalaeva et al., 2020; Dashpurev et al., 2020; Hu and Nacun, 2018; Na et al., 2018; Su et al., 2017; Suzuki, 2013; Tuvshintogtokh and Ariungerel, 2013; Wang et al., 2019b). With human-induced land degradation representing a serious environmental problem in Mongolia, this study sought to estimate the consequences of dirt road networks and infrastructure construction in eastern Mongolia on the surrounding steppe.

Land degradation is generally defined as a reduction or loss in vegetative biomass in steppe ecosystems (Dudley et al., 2017; Wick et al., 2016). Many previous studies indicated that remote sensing is an applicable method for monitoring vegetation cover as a main evaluation indicator for degraded land in large and remote areas (Akiyama and Kawamura, 2007; Gao et al., 2006; Lehnert et al., 2015). Similarly, our result indicates that high-accuracy maps of PFGs and bare ground can be obtained using PlanetScope multi-temporal images. The changes in PFG covers imply that the effects of dirt roads extend for 60–100 m into the neighboring vegetation, but this distance can increase depending on dirt road condition. For instance, frequent and repeated usage of a track reduces the dirt road condition and leads to the generation of large ruts and corrugations (Keshkamat et al., 2012). Consequently, drivers avoid the usage of bad conditioned old dirt roads and introduce new ones, which can increase the area affected by dirt road transportation. For railroads, the effects even extend up to distances of 120 m, but the impact distances may differ depending on all the structures, power lines, and dirt roads to support rail lines. According to Forman et al. (Forman, 2000; Forman and Alexander, 1998), the effects of secondary roads commonly extend to 200 m. Railroads can negatively affect vegetation cover similarly as roads (Dorsey et al., 2015; Lucas et al., 2017; Pollock et al., 2017). This distance, however, modified other major and minor determinants, such as road characteristics, density, landscape, and vegetation (Seiler, 2001). Besides that, our result shows that the effects of dirt roads and railroads extended differently into the surrounding vegetation cover. Most likely, the reason is that railroads are more complex and have a wider structure than dirt roads, as the former include regular maintenance dirt tracks and fire-prevention strips.

In disturbed sites, the plant community composition commonly changes, and even non-native plants may become dominant (Road ecology: science and solutions, 2003; Spellerberg, 1998). Our field-collected data showed that the proportion of PFGs depends on the local conditions. The cover of PFGs differed strongly among active dirt roads, abandoned tracks, and roadside plots, and was influenced by distance from the main dirt road. Focusing on the change in shrubs in non-disturbed and burned steppes, the dirt road and railroad affected roadside vegetation cover differently, depending on the additional factor of wildfire. Consequently, our comparison suggested that the extent of vegetation degradation can be determined by shifts in dominant functional groups. The dominance of graminoids and forbs indicates less degraded vegetation (Densambuu et al., n.d.; Jamiyansharav et al., 2018; Tuvshintogtokh, 2014). On the contrary, the dominance of shrubs indicates degraded vegetation. Previous studies in Mongolian steppes also found that changes in the proportions of graminoids, forbs, and shrubs are indicative of land degradation (Jamsranjav et al., 2018; Lkhagva et al., 2013; Otgontuya et al., 2019). Potential indicator plant species for degradation are shrubs of genera *Artemisia*, *Ephedra*, and *Caragana* (Bazha et al., 2012; Gunin et al., 2012; Kinugasa et al., 2019).

Recent estimations of wildfire risk indicated that the eastern Mongolia steppe tends to be at a very high risk for wildfire, and with increasing frequency of fires in the past decades (Nasanbat and Lkhamjav, 2016; Rihan et al., 2019). An increase in the frequency of fires may affect vegetation composition and structure (Cheng et al., 2013). Overall, the impacts of fire on vegetation community mainly depend on the combination of site conditions and fire frequency (Stavi, 2019). Some studies showed that wildfires have a neutral to positive effect on vegetation community by fostering plant species diversity (Lü et al., 2012; Pereira et al., 2013; Weir et al., 2013). For instance, in a study conducted in Southern High Plains, USA, it was shown that fire increased plant species diversity and evenness in the short term; however, burned sites had similar species richness as non-burned sites 3 years after a fire (Wester et al., 2014). After wildfire events, plant species react differently depending on their regeneration capabilities, and changes in the composition of dominating plants often occur (Byambasuren et al., n.d.). Some detailed studies indicated that vegetation recovery starts between 17 and 31 days after grassland (steppe) fires, and that the vegetation fully recovers 1 year after the fire (Li and Guo, 2018; Pereira et al., 2016, 2013). At our sites, fires occurred twice in April 2019. However, we conducted field surveys 4 months after the steppe fires, and the results showed that the effects of the fires remained on the vegetation cover. Bare ground is more extensive in the burned area according to the two map products from 2019, whereas shrubs responded differently between the two burned sites. Fire disturbance can differently affect species of shrubs, depending on their roots, regeneration structures, and seeds. For instance, dwarf shrub *A. frigida* has been reported to be frequently killed by fire, but its species abundances

recovered in approximately 3 years, as shown by the seeds (Wasser and Shoemaker, 1982). In a study conducted in the Xilingol steppe of Inner Mongolia, the aboveground net primary productivity of true shrub *C. microphylla* was reduced by 27–66% after repeated fires (Lin et al., 2010). The effects of fire on dwarf shrub *E. sinica* is unclear in Mongolian steppes. However, some species of *Ephedra* have been reported as being relatively highly fire-resistant, as they provide only little fuel (Wasser and Shoemaker, 1982). After fire disturbance, *Ephedra* communities successfully recovered, sprouting vigorously from the roots or woody root crown (Young and Evans, 1978, 1974) and rapidly producing aboveground biomass from surviving meristematic tissue (Everett, 1987). Besides the effects of fire on vegetation cover, experimental studies revealed that fire increases the proportion of bare ground by removing dead plant materials and litter (Bock and Bock, 1991; Fuhlendorf and Engle, 2004; Pollak and Kan, 1998; Wilson and Shay, 1990). The amount of bare ground generally declined with time since fire owing to vegetation recovery and litter layer accumulation (Wohlgemuth et al., 2008). Yet, until the pre-fire site condition is restored, bare ground has a high erosion risk owing to surface runoff as well as water and wind erosions (Larsen et al., 2009; Santín and Doerr, 2016; Wang et al., 2020), depending on the properties of the fire site (Mataix-Solera et al., 2011). For the monitoring of wildfire impacts (Archer et al., 2017; Heisler et al., 2003; Lett and Knapp, 2005, 2003; McCarron and Knapp, 2003; Peng et al., 2013), comparison between the proportion of PFGs in the year of the fire and the year before indicates that our model can evaluate the response of PFGs pre- and post-fire. This evaluation on the level of PFGs is an important measure of the effect of fire on landscapes and ecosystems. In their review of the applications of remote sensing in fire ecology, Szpakowski et al. (Szpakowski and Jensen, 2019) indicate that spectral vegetation indices are commonly used to assess the influence of fire on vegetation cover and post-fire vegetation recovery.

Relatively few studies have examined the responses of vegetation composition to fire in Mongolian steppes. Studies of the effects of fire on steppe plants have shown that fire suppresses forb species and improves grass productivity in Mongolian steppes (Yoshihara et al., 2015). Several researchers (Allred et al., 2011; Indree and Magsar, 2007; Noy-Meir, 1995; Valone et al., 2002) noted that fire has a significant effect on PFG species in steppes, which negatively effects post-fire recovery, but this effect may vary depending on grazing pressure. Additionally, increased grazing loads tends to lead to the dominance of shrubs in PFGs (Bazha et al., 2012; Tuvshintogtokh, 2014). In a study conducted in the semiarid grasslands (Huang et al., 2018) indicate that the interactive effects of fire and grazing reduces species diversity in steppes.

5. Conclusion

This study showed that extent of indicator and dominant PFGs can be measured with high accuracy using information on the vegetation along dirt roads and other infrastructures in Choibalsan soum, which is obtained from UAV imagery and multi-temporal PlanetScope data. We also demonstrated an effective approach for future integrations of UAV and satellite imagery data in studies of land degradation. Maps of indicator and dominant PFGs are particularly essential for land degradation assessment, environmental conservation, and decision making in future development. Based on the results, we reached the following key findings and conclusions:

(i) VARI contributed significantly to some stages of RGB image classification in the OBIA of UAV-collected data.
(ii) The proposed approach for integrating data with different resolutions minimizes the classic scale issue in aggregating UAV data to low-resolution multispectral satellite data.
(iii) Dirt roads ecologically affects up to 60–100 m of roadside vegetation cover, whereas railroads affect up to 120 m distance in eastern Mongolian steppes.
(iv) The degradation rate of affected roadside vegetation area can be determined according to shifts in the dominance of graminoids, forbs, and shrubs.
(v) The estimation of PFGs in the years where a fire occurred and did not occur indicates that the map products can be used to monitor the effects of wildfire on steppes by analyzing the shifts in the proportion of PFG composition.
(vi) The cover of bare ground was largely increased due to the wildfires in burned sites.

Declaration of Competing Interest

The authors declare that they have no known competing financial interests or personal relationships that could have appeared to influence the work reported in this paper.

Acknowledgments

The authors acknowledge financial support from the German Academic Exchange Service (DAAD), Research Grants—Doctoral Programmes in Germany (57381412) for Batnyambuu Dashpurev (grant reference number 91691130), and the More Step project funded by the German Ministry for Education and Research (BMBF) (grant number 01LC1820B). We are thankful to all cooperating scientists who provided assistance with and supported the coordination and organization of the fieldwork. The authors thank Munkhzul Oyunbileg, Institute of General and Experimental Biology, Mongolian Academy of Sciences, for organizing the field work. We also thank Amarbat Galsantsevel who helped and provided professional guidance for operating drone in the field. We are grateful to the Education and Research Program of Planet Labs Inc. (www.planet.com) for providing access to Planet's imagery and archive.

Authors' contribution

Batnyambuu Dashpurev prepared the raw and validation data of UAV and PlanetScope, performed the formal analyses (including classification, estimation, and vegetation) and spatial analyses, and wrote the original draft of the manuscript. Karsten Wesche, Yun Jäschke and Thanh Noi Phan designed the field vegetation study and supervised the field observation. Oyundelger Khurelpurev collected vegetation data in the field and provided support in species determination. Lukas W. Lehnert designed and contributed to the methodology and review, and supervised both of the field and laboratory studies. Jörg Bendix and Lukas W. Lehnert contributed to the design and conceptualization of the study, and supervised the whole study. Finally, all authors participated in additional editing of the original draft. All authors have read and agreed to the published version of the manuscript.

Appendix A

Table A1
Product specifications of the PlanetScope sensor operated by Planet.

Product Attribute	Description
Number of active satellites	+130 Doves
Bands	Four (Blue, Green, Red, and Near Infrared)
Ground Sample Distance	3.7 m
Temporal resolution	Daily
Product type	Ortho Scene–Analytic
Product Level	3B–SR
Acquisition dates	**2018** May 03, 18, 30 June 16, 23 July 15, 23 August 05, 17, 30 September 13, 25 **2019** April 23, 27 May 06, 17, 27 June 04, 15, 22 July 05, 13, 22, 28 August 04, 13, 29 September 05, 15, 23
Cloud cover	<10%
Total number of Scenes	101

Table A2
Field-collected data of plant functional groups using random and non-permanent rectangular plots of 25 × 4 m in the inter-province reserve pasture ("Otor") area of Choibalsan soum, Dornod Province, Mongolia, complemented by soil compaction.

		Graminoids	True shrubs	Dwarf shrubs	Perennial forbs	Annual forbs	Bare soil	Stone/ Rock	Litter	Canopy height	Soil compaction
		%								cm	kg/cm^2
Otor-1	Active dirt road	5		2		0.2	85	8		10	*
	Abandoned track 1	20	1	0.5		0.5	68	10		20	*
	Abandoned track 2	35	0.8	4	1	2.2	30	27		25	3.3
	Reference	40	2	4	2.5	3.5	18	30		25	2.3
Otor-2	Active dirt road	8		2.5	9.5		15	65		20	*
	Abandoned track 1	25.5	0.5	8	17	5	15	30		40	*
	Abandoned track 2	35.09	0.5	6	18	0.01	10	30		25	3.6
	Reference	25	0.02	26	15	0.2	12	22		15	2.6
Otor-3	Active dirt road	5		2.5	2	0.5	5	85		2	*
	Abandoned track 1	24.2		30	18	0.5	2	25	0.3	5	*
	Abandoned track 2	35.3	0.1	2	12	8	5	34.4	0.5	15	4.4
	Reference	40.5		28	5	1.5	2	18	5	15	3
Otor-4	Active dirt road	5	0.01	0.5	2	4	3.3	85	0.2	3	*
	Abandoned track 1	15.5	1	2	7	5	5	64.5		5	*
	Abandoned track 2	19.5	0.5	8	15	5	5	45	2	20	2.6
	Reference	45	2	13	10	5	2	13	10	50	3.1

In Table A-2, * means above the measurement limit.

Table A3
Summary of confusion matrices for UAV orthomosaic image classification.

a. Otor-1				Reference data	
Classification result	Graminoids and forbs	Shrubs	Bare ground	Total	User Accuracy
Graminoids and forbs	458	56	21	535	85.6%
Shrubs	37	439	0	476	92.2%
Bare ground	5	0	479	484	98.9%
Total	500	495	500	1495	
Producer Accuracy	91.6%	88.6%	95.8%		92.1%
	Overall accuracy = 92.1% , kappa statistic = 88.5%				

b. Otor-2			Reference data			
Classification result	Graminoids and forbs	Shrubs	Bare ground	Man-made object	Total	User Accuracy
Graminoids and forbs	453	43	9	14	519	87.2%
Shrubs	25	456	0	5	486	93.8%
Bare ground	14	0	489	25	528	92.6%
Man-made object	8	1	2	452	463	97.6%
Total	500	500	500	496	1996	
Producer Accuracy	90.6%	91.2%	97.8%	91.1		92.6%
	Overall accuracy = 92.6% , kappa statistic = 90.2%					
c. Otor-3			Reference data			
Classification result	Graminoids and forbs	Shrubs	Bare ground	Man-made object	Total	User Accuracy
Graminoids and forbs	435	61	8	6	510	85.2%
Shrubs	2	414	1	1	418	99%
Bare ground	54	12	491	23	580	84.6%
Man-made object	0	0	0	470	470	99%
Total	491	487	500	500	1978	
Producer Accuracy	88.5%	85%	98.2%	94%		91.5%
	Overall accuracy = 91.5%, kappa statistic = 88.6%					
d. Otor-4			Reference data			
Classification result	Graminoids and forbs	Shrubs	Bare ground	Total	User Accuracy	
Graminoids and forbs	489	56	15	560	87.3%	
Shrubs	7	444	0	451	98.4%	
Bare ground	4	0	485	489	99%	
Total	500	500	500	1500		
Producer Accuracy	97.8%	88.8%	97%			94.5%
	Overall accuracy = 94.5% , kappa statistic = 91.8%					

Table A4
Evaluation of RF regression performance for PlanetScope multi-temporal data. In performance, 10% of the reference data were excluded for validation.

Land cover types	Out-of-bag errors				Validation data for regression		
	Number of Trees	Mean squared error (MSE)	Percentage of variation explained	Root mean square error (RMSE)	R-Squared	p-value	Standard Error
Estimation of graminoids and forbs	100	174.79	83.11	6.891	0.83	0.00	0.01
Estimation of shrubs	100	80.89	63.30	8.202	0.61	0.00	0.01
Estimation of bare ground	100	115.85	53.68	4.449	0.94	0.00	0.01

Table A5
Evaluation of RF classification performance for PlanetScope multi-temporal data. In performance, 10% of the reference data were excluded for validation.

Land cover types	Out-of-bag errors			Validation data for classification			
	Number of Trees	Mean squared error (MSE)		F1-Score	MCC	Sensitivity	Accuracy
Graminoids and forbs	100	24.528	85.9	0.86	0.36	0.92	0.78
Shrubs			90.14	0.19	0.14	0.15	0.88
Bare ground			29.25	0.13	0.11	0.10	0.91
Man-made objects			7.40	0.72	0.70	0.66	0.95

Table A6
Description of the predictor variables used in RF classification. Note that each variable has been calculated for each segment and image.

Variable	Description
Spectral variable	
Average chromaticity color	RGB color values per segment
Mean value	The average digital number of each band
Standard deviation	Standard deviation of each band
VARI[1]	Visible atmospherically resistant index (Green - Red)/ (Green + Red - Blue)
Textural variable[1]	
Mean	Mean of texture values
Variance	The local variance of texture values
Homogeneity	The closeness of the distribution of the image texture element
Contrast	The depth and smoothness of the image texture structure
Dissimilarity	Similar to Contrast. In Dissimilarity, weights increase linearly
Entropy	The complexity of the texture distribution
Second moment	The regularity and uniformity of the image distribution
Correlation	The similarity of the image texture in a horizontal or vertical direction
Geometric variable	
Compactness	The degree to which a segment is compact or circular
Rectangularity	The degree to which a segment is rectangular
Count	The number of pixels comprising the segment

Predictor variables were calculated based on UAV images only. [1] The calculations were cited from References (Anatoly A. Gitelson et al., 2002; Haralick et al., 1973; Zhang et al., 2017; Zhang, 2001).

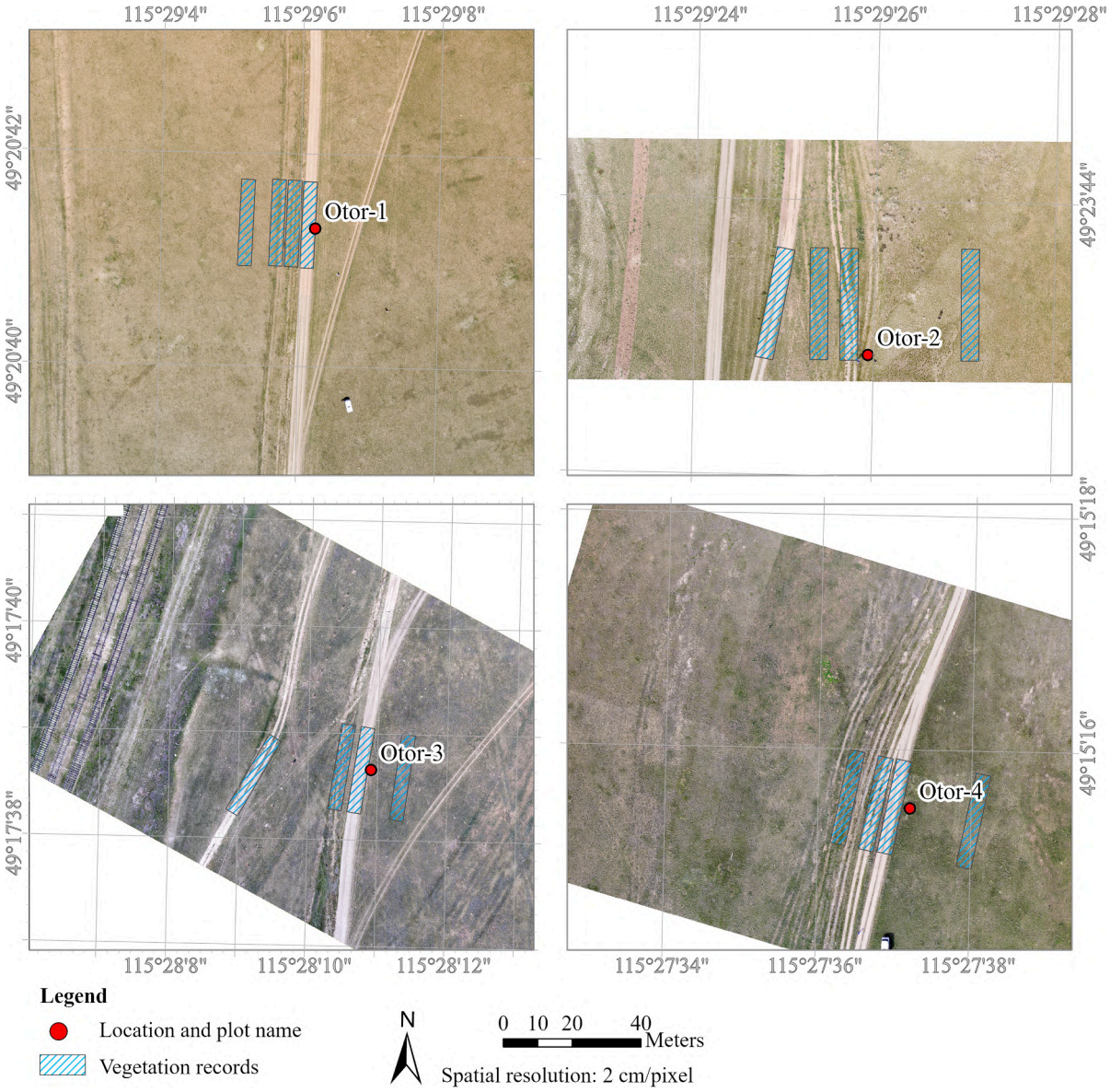

Fig. A1. An orthomosaic of collected UAV images taken in four locations.

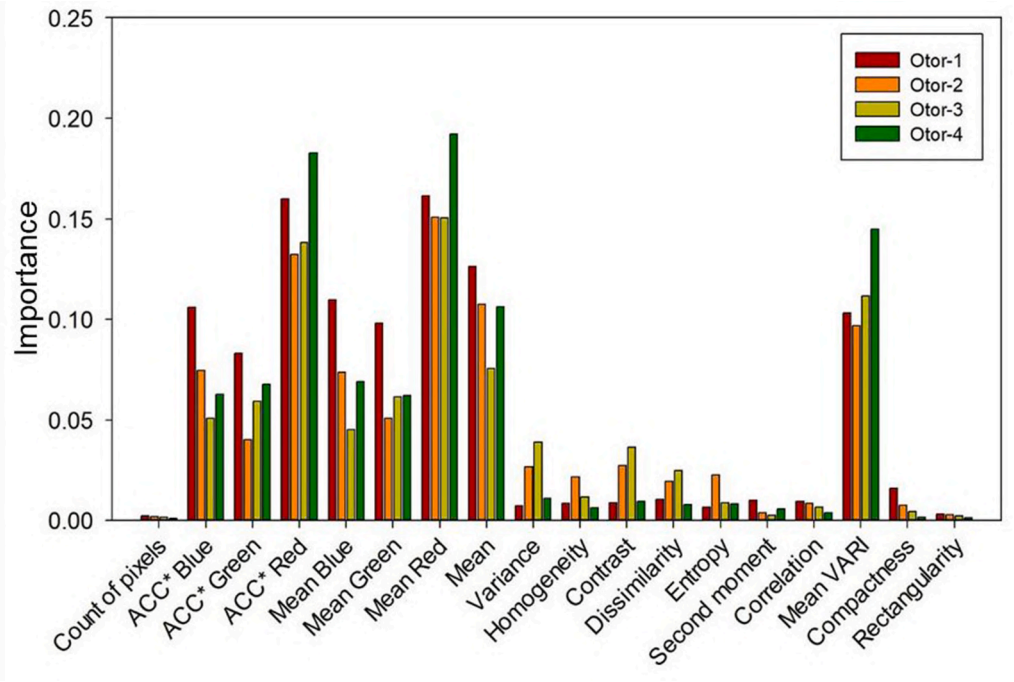

Fig. A2. Summary of variable importance for UAV imagery classification (ACC = active chromaticity color). The max values in panels are the maximum predicted values.

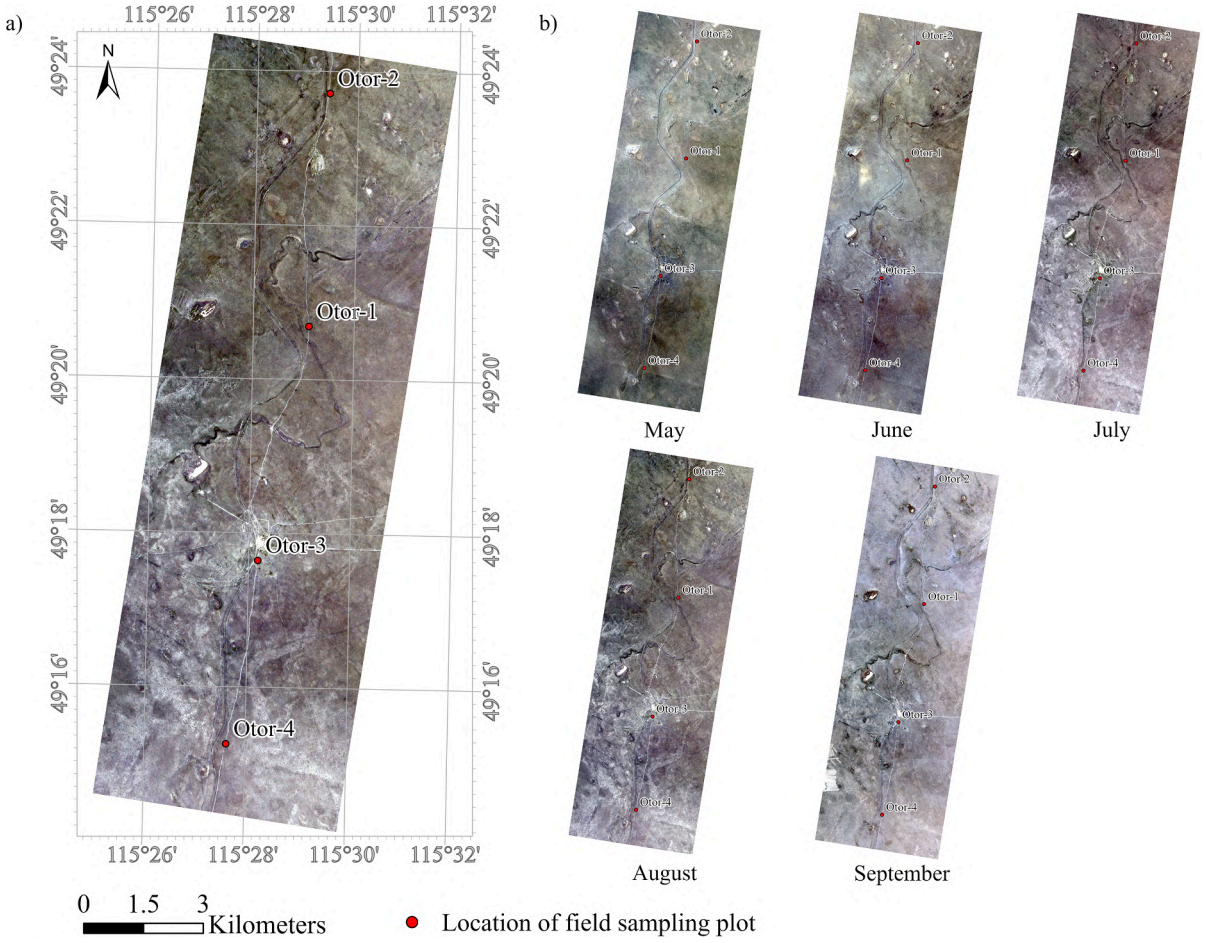

Fig. A3. Collection of orthomosaic imagery of PlanetScope in 2018. a) The daily mosaic of PlanetScope acquired in August 30, 2018 and b) the monthly mosaic data illustrating the temporal changes in land cover in warm season from May to September 2018.

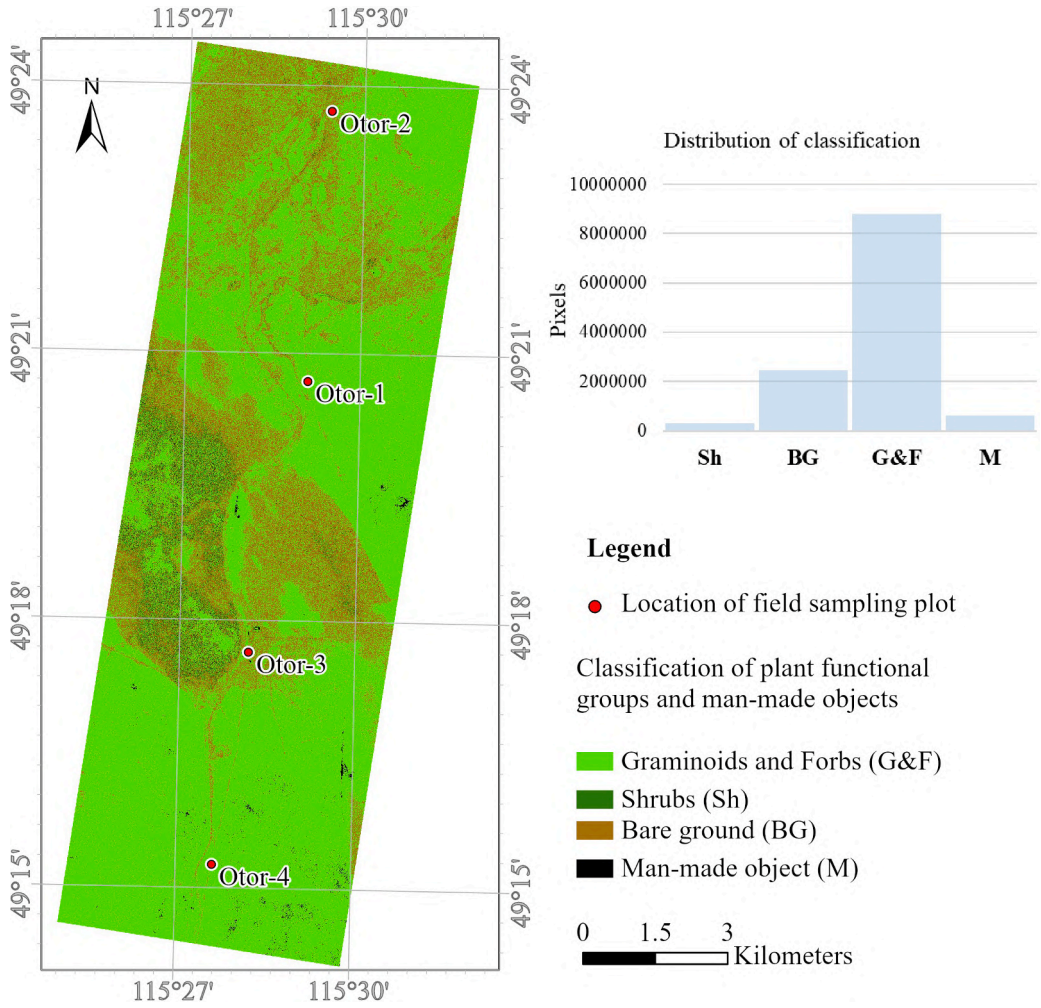

Fig. A4. Classified land cover types using multi-temporal NIR bands of PlanetScope in 2019. In the figure, the bar chart illustrates the distribution of classes by the number of pixels.

References

ADB, 2014. Making Grasslands Sustainable in Mongolia International Experiences with Payments for Environmental Services in Grazing Lands and Other Rangelands.

Akiyama, T., Kawamura, K., 2007. Grassland degradation in China: Methods of monitoring, management and restoration. Grassl. Sci. 53, 1–17. https://doi.org/10.1111/j.1744-697x.2007.00073.x.

Allred, B.W., Fuhlendorf, S.D., Engle, D.M., Elmore, R.D., 2011. Ungulate preference for burned patches reveals strength: Of fire-grazing interaction. Ecol. Evol. 1, 132–144. https://doi.org/10.1002/ece3.12.

Archer, S.R., Andersen, E.M., Predick, K.I., Schwinning, S., Steidl, R.J., Woods, S.R., 2017. Woody Plant Encroachment: Causes and Consequences. Springer, Cham, pp. 25–84. https://doi.org/10.1007/978-3-319-46709-2_2.

Batkhishig, O., 2013. Human Impact and Land Degradation in Mongolia, in: Dryland East Asia: Land Dynamics amid Social and Climate Change. The Higher Education Press. https://doi.org/10.1515/9783110287912.

Batsaikhan, N., Buuveibaatar, B., Chimed, B., Enkhtuya, O., Galbrakh, D., Ganbaatar, O., Lkhagvasuren, B., Nandintsetseg, D., Berger, J., Calabrese, J.M., Edwards, A.E., Fagan, W.F., Fuller, T.K., Heiner, M., Ito, T.Y., Kaczensky, P., Leimgruber, P., Lushchekina, A., Milner-Gulland, E.J., Mueller, T., Murray, M.G., Olson, K.A., Reading, R., Schaller, G.B., Stubbe, A., Stubbe, M., Walzer, C., Von Wehrden, H., Whitten, T., 2014. Conserving the world's finest grassland amidst ambitious national development. Conserv. Biol. 28, 1736–1739. https://doi.org/10.1111/cobi.12297.

Batunacun, Nendel, C., Hu, Y., Lakes, T., 2018. Land-use change and land degradation on the Mongolian Plateau from 1975 to 2015—A case study from Xilingol. China. L. Degrad. Dev. 29, 1595–1606. https://doi.org/10.1002/ldr.2948.

Bazha, S.N., Gunin, P.D., Danzhalova, E. V., Drobyshev, Y.I., Prishcepa, A. V., 2012. Pastoral Degradation of Steppe Ecosystems in Central Mongolia. Springer, Dordrecht, pp. 289–319. https://doi.org/10.1007/978-94-007-3886-7_10.

Belgiu, M., Drăgu, L., 2016. Random forest in remote sensing: A review of applications and future directions. ISPRS J. Photogramm. Remote Sens. https://doi.org/10.1016/j.isprsjprs.2016.01.011.

Bock, C.E., Bock, J.H., 1991. Response of Grasshoppers (Orthoptera: Acrididae) to Wildfire in a Southeastern Arizona Grassland. Am. Midl. Nat. 125, 162. https://doi.org/10.2307/2426379.

Breiman, L., Cutler, A., 2018. Random Forests [WWW Document]. Univ, California, Berkeley.

Breiman, L., 2001. Random Forests LEO. Mach. Learn. 45, 5–32. https://doi.org/10.1023/A:1010933404324.

Breiman, L., Friedman, J.H., Jerome, H., Olshen, R.A., Stone, C.J., 1984. Classification and regression trees. Taylor & Francis, Monterey, CA.

Byambasuren, O., Myers, R.L., Babler, M., n.d. Technical report for Fire Management Assessment of the Eastern Steppe, Mongolia.

Cano, E., Horton, R., Liljegren, C., Bulanon, D.M., 2017. Comparison of small unmanned aerial vehicles performance using image processing. J. Imaging 3, 4. https://doi.org/10.3390/jimaging3010004.

Cheng, C.H., Chen, Y.S., Huang, Y.H., Chiou, C.R., Lin, C.C., Menyailo, O.V., 2013. Effects of repeated fires on ecosystem C and N stocks along a fire induced forest/grassland gradient. J. Geophys. Res. Biogeosciences 118, 215–225. https://doi.org/10.1002/jgrg.20019.

Cohen, J., 1960. A coefficient of agreement for nominal scales. Educ. Psychol. Meas. 20, 37–46. https://doi.org/10.1177/001316446002000104.

Cooley, S.W., Smith, L.C., Stepan, L., Mascaro, J., 2017. Tracking dynamic northern surface water changes with high-frequency planet CubeSat imagery. Remote Sens. 9, 1306. https://doi.org/10.3390/rs9121306.

Coslet, Cristina, Palmeri, etc., 2017. Special report FAO/WFP crop and livestock assessment mission to Mongilia. Rome.

Cowles, J., Boldgiv, B., Liancourt, P., Petraitis, P.S., Casper, B.B., 2018. Effects of increased temperature on plant communities depend on landscape location and precipitation. Ecol. Evol. 8, 5267–5278. https://doi.org/10.1002/ece3.3995.

Danzhalova, E.V., Bazha, S.N., Gunin, P.D., Drobyshev, Y.I., Kazantseva, T.I., Prischepa, A.V., Slemnev, N.N., Ariunbold, E., 2012. Indicators of pasture digression in steppe ecosystems of mongolia. Erforsch. Biol. Ressourcen der Mongolei / Explor. into Biol. Resour. Mong. 12, 297–306.

Darbalaeva, D., Mikheeva, A., Zhamyanova, Y., 2020. The socio-economic consequences of the desertification processes in Mongolia, in: E3S Web of Conferences. EDP Sciences, p. 11001. https://doi.org/10.1051/e3sconf/202016411001.
Dark, S.J., Bram, D., 2007. The modifiable areal unit problem (MAUP) in physical geography. Prog. Phys. Geogr. 31, 471–479. https://doi.org/10.1177/0309133307083294.
Dashpurev, B., Bendix, J., Lehnert, L., 2020. Monitoring Oil Exploitation Infrastructure and Dirt Roads with Object-Based Image Analysis and Random Forest in the Eastern Mongolian Steppe. Remote Sens. 12, 144. https://doi.org/10.3390/rs12010144.
de Castro, A.I., Shi, Y., Maja, J.M., Peña, J.M., 2021. Uavs for vegetation monitoring: Overview and recent scientific contributions. Remote Sens. https://doi.org/10.3390/rs13112139.
Densambuu, B., Sainnemekh, S., Bestelmeyer, B., Ulambayar, B., Batjargal, E., n.d. National report on the rangeland health of Mongolia: Second Assessment.
Dong, Y., Yan, H., Wang, N., Huang, M., Hu, Y., 2019. Automatic Identification of Shrub-Encroached Grassland in the Mongolian Plateau Based on UAS Remote Sensing. Remote Sens. 11, 1623. https://doi.org/10.3390/rs11131623.
Dorsey, B., Olsson, M., Rew, L.J., 2015. Ecological Effects of Railways on Wildlife, in: Handbook of Road Ecology. John Wiley & Sons, Ltd, Chichester, UK, pp. 219–227. https://doi.org/10.1002/9781118568170.ch26.
Dudley, N.; Alexander, S.; Johnson, I., 2017. The Global Land Outlook, first edition. United Nations Convention to Combat Desertification: Bonn, Germany, Bonn. https://doi.org/ISBN: 978-92-95110-48-9.
Environmental Information Center, 2021. Database on forest and steppe fire [WWW Document]. Nature, Environ. Tour, Mong https://www.eic.mn (accessed 7.22.21).
Erdenetuya, M., 2012. Fire occurrence and burning biomass statistics in Mongolia, in: 33rd Asian Conference on Remote Sensing 2012, ACRS 2012. pp. 118–125.
Everett, R.L., 1987. Plant response to fire in the pinyon-juniper zone, in: Proceedings, Pinyon-Juniper Conference. pp. 152-157 ST-Plant response to fire in the pinyon.
Farukh, M.A., Hayasaka, H., Mishigdorj, O., 2009. Recent Tendency of Mongolian Wildland Fire Incidence: Analysis Using MODIS Hotspot and Weather Data. J. Nat. Disaster Sci. 31, 23–33. https://doi.org/10.2328/jnds.31.23.
Forman, R.T.T., 2000. Estimate of the area affected ecologically by the road system in the United States. Conserv. Biol. 14, 31–35. https://doi.org/10.1046/j.1523-1739.2000.99299.x.
Forman, R.T.T., Alexander, L.E., 1998. Roads and their major ecological effects. Annu. Rev. Ecol. Syst. 29, 207–231. https://doi.org/10.1146/annurev.ecolsys.29.1.207.
Fuhlendorf, S.D., Engle, D.M., 2004. Application of the fire-grazing interaction to restore a shifting mosaic on tallgrass prairie. J. Appl. Ecol. 41, 604–614. https://doi.org/10.1111/j.0021-8901.2004.00937.x.
Gao, Q., Li, Y., Wan, Y., Lin, E., Xiong, W., Jiangcun, W., Wang, B., Li, W., 2006. Grassland degradation in Northern Tibet based on remote sensing data. J. Geogr. Sci. 16, 165–173. https://doi.org/10.1007/s11442-006-0204-1.
Gitay, H., Noble, I.R., 1997. What are functional types and how should we seek them?, in: Plant Functional Types: Their Relevance to Ecosystem Properties and Global Change. Cambridge ; New York : Cambridge Unversity Press, 1997., pp. 3–19.
Gitelson, Anatoly A., Kaufman, Y.J., Stark, R., Rundquist, D., 2002a. Novel algorithms for remote estimation of vegetation fraction. Remote Sens. Environ. 80, 76–87. https://doi.org/10.1016/S0034-4257(01)00289-9.
Gitelson, A.A., Stark, R., Grits, U., Rundquist, D., Kaufman, Y., Derry, D., 2002b. Vegetation and soil lines in visible spectral space: A concept and technique for remote estimation of vegetation fraction. Int. J. Remote Sens. 23, 2537–2562. https://doi.org/10.1080/01431160110107806.
Gray, P., Ridge, J., Poulin, S., Seymour, A., Schwantes, A., Swenson, J., Johnston, D., 2018. Integrating Drone Imagery into High Resolution Satellite Remote Sensing Assessments of Estuarine Environments. Remote Sens. 10, 1257. https://doi.org/10.3390/rs10081257.
Gunin, P.D., Bazha, S.N., Danzhalova, E.V., Dmitriev, I.A., Drobyshev, Y.I., Kazantseva, T.I., Miklyaeva, I.M., Ogureeva, G.N., Slemnev, N.N., Titova, S.V., Ariunbold, E., Battseren, C., Jargalsaikhan, L., 2012. Expansion of Ephedra sinica Stapf. in the arid steppe ecosystems of Eastern and Central Mongolia. Arid Ecosyst. 2, 18–33. https://doi.org/10.1134/S2079096112010052.
Hamylton, S.M., Morris, R.H., Carvalho, R.C., Roder, N., Barlow, P., Mills, K., Wang, L., 2020. Evaluating techniques for mapping island vegetation from unmanned aerial vehicle (UAV) images: Pixel classification, visual interpretation and machine learning approaches. Int. J. Appl. Earth Obs. Geoinf. 89, 102085 https://doi.org/10.1016/j.jag.2020.102085.
Haralick, R.M., Dinstein, I., Shanmugam, K., 1973. Textural Features for Image Classification. IEEE Trans. Syst. Man Cybern. SMC-3, 610–621. https://doi.org/10.1109/TSMC.1973.4309314.
Hassanalian, M., Abdelkefi, A., 2017. Classifications, applications, and design challenges of drones: A review. Prog. Aerosp. Sci. https://doi.org/10.1016/j.paerosci.2017.04.003.
Heisler, J.L., Briggs, J.M., Knapp, A.K., 2003. Long-term patterns of shrub expansion in a C4-dominated grassland: Fire frequency and the dynamics of shrub cover and abundance. Am. J. Bot. 90, 423–428. https://doi.org/10.3732/ajb.90.3.423.
Hernandez-Santin, L., Rudge, M.L., Bartolo, R.E., Erskine, P.D., 2019. Identifying Species and Monitoring Understorey from UAS-Derived Data: A Literature Review and Future Directions. Drones 3, 9. https://doi.org/10.3390/drones3010009.
Hilbig, W., 2016. Plant Communities in Eastern Mongolia.
Hilker, T., Natsagdorj, E., Waring, R.H., Lyapustin, A., Wang, Y., 2014. Satellite observed widespread decline in Mongolian grasslands largely due to overgrazing. Glob. Chang. Biol. 20, 418–428. https://doi.org/10.1111/gcb.12365.
Hu, Y., Nacun, B., 2018. An analysis of land-use change and grassland degradation from a policy perspective in Inner Mongolia, China, 1990–2015. Sustain. 10 https://doi.org/10.3390/su10114048.
Huang, Y., Wang, K., Deng, B., Sun, X., Zeng, D.-H., 2018. Effects of fire and grazing on above-ground biomass and species diversity in recovering grasslands in northeast China. J. Veg. Sci. 29, 629–639. https://doi.org/10.1111/jvs.12641.
Indree, T., Magsar, U., 2007. Fire effects on productivity and community dynamics of Mongolian grasslands. Int. For, Fire News.
Jamiyansharav, K., Fernández-Giménez, M.E., Angerer, J.P., Yadamsuren, B., Dash, Z., 2018. Plant community change in three Mongolian steppe ecosystems 1994–2013: applications to state-and-transition models. Ecosphere 9, e02145. https://doi.org/10.1002/ecs2.2145.
Jamsranjav, C., Reid, R.S., Fernández-Giménez, M.E., Tsevlee, A., Yadamsuren, B., Heiner, M., 2018. Applying a dryland degradation framework for rangelands: the case of Mongolia. Ecol. Appl. 28, 622–642. https://doi.org/10.1002/eap.1684.
Kaneko, K., Nohara, S., 2014. Review of Effective Vegetation Mapping Using the UAV (Unmanned Aerial Vehicle) Method. J. Geogr. Inf. Syst. 06, 733–742. https://doi.org/10.4236/jgis.2014.66060.
Kattenborn, T., Eichel, J., Fassnacht, F.E., 2019. Convolutional Neural Networks enable efficient, accurate and fine-grained segmentation of plant species and communities from high-resolution UAV imagery. Sci. Rep. 9, 1–9. https://doi.org/10.1038/s41598-019-53797-9.
Keshkamat, S.S., Tsendbazar, N.E., Zuidgeest, M.H.P., Van Der Veen, A., De Leeuw, J., 2012. The environmental impact of not having paved roads in arid regions: An example from Mongolia. Ambio 41, 202–205. https://doi.org/10.1007/s13280-011-0155-3.
Kim, J., Kang, S., Seo, B., Narantsetseg, A., Han, Y., 2020. Estimating fractional green vegetation cover of Mongolian grasslands using digital camera images and MODIS satellite vegetation indices. GIScience Remote Sens. 57, 49–59. https://doi.org/10.1080/15481603.2019.1662166.
Kimball, J., 2014. Vegetation phenology, in: Encyclopedia of Earth Sciences Series. Springer Netherlands, pp. 886–890. https://doi.org/10.1007/978-0-387-36699-9_188.
Kinugasa, T., Ishibashi, K., Miyawaki, M., Gantsetseg, B., 2019. Germination characteristics and phytotoxic inhibition of germination in Artemisia adamsii, a low-palatability weed in the Mongolian steppe. Seed Sci. Res. 29, 197–203. https://doi.org/10.1017/S0960258519000163.
Kupidura, P., 2019. The comparison of different methods of texture analysis for their efficacy for land use classification in satellite imagery. Remote Sens. 11, 1233. https://doi.org/10.3390/rs11101233.
Kwak, G.H., Park, N.W., 2019. Impact of texture information on crop classification with machine learning and UAV images. Appl. Sci. 9, 643. https://doi.org/10.3390/app9040643.
Larsen, I.J., MacDonald, L.H., Brown, E., Rough, D., Welsh, M.J., Pietraszek, J.H., Libohova, Z., Dios Benavides-Solorio, J., Schaffrath, K., 2009. Causes of Post-Fire Runoff and Erosion: Water Repellency, Cover, or Soil Sealing? Soil Sci. Soc. Am. J. 73, 1393–1407. https://doi.org/10.2136/sssaj2007.0432.
Lehnert, L.W., Meyer, H., Wang, Y., Miehe, G., Thies, B., Reudenbach, C., Bendix, J., 2015. Retrieval of grassland plant coverage on the Tibetan Plateau based on a multi-scale, multi-sensor and multi-method approach. Remote Sens. Environ. 164, 197–207. https://doi.org/10.1016/j.rse.2015.04.020.
Lett, M.S., Knapp, A.K., 2005. Woody plant encroachment and removal in mesic grassland: Production and composition responses of herbaceous vegetation. Am. Midl. Nat. 153, 217–231. https://doi.org/10.1674/0003-0031(2005)153[0217:WPEARI]2.0.CO;2.
Lett, M.S., Knapp, A.K., 2003. Consequences of shrub expansion in mesic grassland: Resource alterations and graminoid responses. J. Veg. Sci. 14, 487–496. https://doi.org/10.1111/j.1654-1103.2003.tb02175.x.
Li, M., Guo, X., 2018. Evaluating Post-Fire Vegetation Recovery in North American Mixed Prairie Using Remote Sensing Approaches. Open J. Ecol. 08, 646–680. https://doi.org/10.4236/oje.2018.812038.
Li, S., Yuan, F., Ata-UI-Karim, S.T., Zheng, H., Cheng, T., Liu, X., Tian, Y., Zhu, Y., Cao, W., Cao, Q., 2019. Combining color indices and textures of UAV-based digital imagery for rice LAI estimation. Remote Sens. 11, 1763. https://doi.org/10.3390/rs11151763.
Li, S.G., Tsujimura, M., Sugimoto, A., Davaa, G., Sugita, M., 2006. Natural recovery of steppe vegetation on vehicle tracks in central Mongolia. J. Biosci. 31, 85–93. https://doi.org/10.1007/BF02705239.
Lin, C., Popescu, S.C., Thomson, G., Tsogt, K., Chang, C.I., 2015. Classification of tree species in overstorey canopy of subtropical forest using QuickBird images. PLoS One 10, e0125554. https://doi.org/10.1371/journal.pone.0125554.
Lin, Y., Bai, Y., 2010. Responses of aboveground net primary production and population structure of Caragana microphylla to prescribed burning in a typical steppe of Inner Mongolia. Acta Prataculturae Sin. 19, 170–178.
Liu, G., Xie, X., Ye, D., Ye, X., Tuvshintogtokh, I., Mandakh, B., Huang, Z., Dong, M., 2013a. Plant Functional Diversity and Species Diversity in the Mongolian Steppe. PLoS One 8, e77565. https://doi.org/10.1371/journal.pone.0077565.
Liu, M., Yu, T., Gu, X., Sun, Z., Yang, J., Zhang, Z., Mi, X., Cao, W., Li, J., 2020. The impact of spatial resolution on the classification of vegetation types in highly fragmented planting areas based on unmanned aerial vehicle hyperspectral images. Remote Sens. 12 https://doi.org/10.3390/RS12010146.
Liu, Y., Zhang, H.H., Wu, Y., 2011. Hard or soft classification? large-margin unified machines. J. Am. Stat. Assoc. 106, 166–177. https://doi.org/10.1198/jasa.2011.tm10319.
Liu, Y.Y., Evans, J.P., McCabe, M.F., de Jeu, R.A.M., van Dijk, A.I.J.M., Dolman, A.J., Saizen, I., 2013b. Changing Climate and Overgrazing Are Decimating Mongolian Steppes. PLoS One 8, e57599. https://doi.org/10.1371/journal.pone.0057599.
Lkhagva, A., Boldgiv, B., Goulden, C.E., Yadamsuren, O., Lauenroth, W.K., 2013. Effects of grazing on plant community structure and aboveground net primary production of

semiarid boreal steppe of northern Mongolia. Grassl. Sci. 59, 135–145. https://doi.org/10.1111/grs.12022.
Lu, B., He, Y., 2017. Species classification using Unmanned Aerial Vehicle (UAV)-acquired high spatial resolution imagery in a heterogeneous grassland. ISPRS J. Photogramm. Remote Sens. 128, 73–85. https://doi.org/10.1016/j.isprsjprs.2017.03.011.
Lü, X.T., Lü, F.M., Zhou, L.S., Han, X., Han, X.G., 2012. Stoichiometric response of dominant grasses to fire and mowing in a semi-arid grassland. J. Arid Environ. 78, 154–160. https://doi.org/10.1016/j.jaridenv.2011.11.008.
Lucas, P.S., de Carvalho, R.G., Grilo, C., 2017. Railway disturbances on wildlife: Types, effects, and mitigation measures, in: Railway Ecology. Springer International Publishing, pp. 81–99. https://doi.org/10.1007/978-3-319-57496-7_6.
Luo, J., Liu, X., Yang, J., Liu, Y., Zhou, J., 2018. Variation in plant functional groups indicates land degradation on the Tibetan Plateau. Sci. Rep. 8, 1–9. https://doi.org/10.1038/s41598-018-36028-5.
Martin Pfeiffer, Choimaa Dulamsuren, Y.J. and K.W., 2018. Grasslands of China and Mongolia: Spatial Extent, Land Use and Conservation, in: Grasslands of the World : Diversity, Management and Conservation. CRC Press, Boca Raton, US, pp. 168–196.
Mataix-Solera, J., Cerdà, A., Arcenegui, V., Jordán, A., Zavala, L.M., 2011. Fire effects on soil aggregation: A review. Earth-Science Rev. https://doi.org/10.1016/j.earscirev.2011.08.002.
Maxwell, A.E., Warner, T.A., Fang, F., 2018. Implementation of machine-learning classification in remote sensing: An applied review. Int. J. Remote Sens. https://doi.org/10.1080/01431161.2018.1433343.
McCarron, J.K., Knapp, A.K., 2003. C3 shrub expansion in a C4 grassland: Positive post-fire responses in resources and shoot growth. Am. J. Bot. 90, 1496–1501. https://doi.org/10.3732/ajb.90.10.1496.
McIntosh, A.M., Sharpe, M., Lawrie, S.M., 2010. Research methods, statistics and evidence-based practice, in: Companion to Psychiatric Studies. Elsevier, pp. 157–198. https://doi.org/10.1016/b978-0-7020-3137-3.00009-7.
Mongolia EITI, 2020. EITI-Extractive industries transparency initiative [WWW Document].
Mongolia EITI, 2018. Mongolia 2017 EITI Report: Extractive Industries Transparency Initiative. Ulaanbaatar.
Na, Y., Li, J., Hoshino, B., Bao, S., Qin, F., Myagmartseren, P., 2018. Effects of different grazing systems on aboveground biomass and plant species dominance in typical Chinese and Mongolian steppes. Sustain. 10, 4753. https://doi.org/10.3390/su10124753.
Reece, Nanette, Wingard, Ganchimeg, Bayart Mandakh, R.P.R., 2019. Using Random Forest to Classify Vegetation Communities in the Southern Area of Ikh Nart Nature Reserve in Mongolia. Mong. J. Biol. Sci. 17, 31–39.
Narantsetseg, A., Kang, S., Ko, D., 2018. Livestock grazing and trampling effects on plant functional composition at three wells in the desert steppe of Mongolia. J. Ecol. Environ. 42, 1–8. https://doi.org/10.1186/s41610-018-0075-2.
Nasanbat, E., Lkhamjav, O., 2016. WIld fire risk map in the eastern steppe of Mongolia using spatial multi-criteria analysis. International Archives of the Photogrammetry, Remote Sensing and Spatial Information Sciences - ISPRS Archives. 469–473. https://doi.org/10.5194/isprsarchives-XLI-B1-469-2016.
Nasanbat, E., Lkhamjav, O., Balkhai, A., Tsevee-Oirov, C., Purev, A., Dorjsuren, M., 2018. A spatial distributionmap of the wildfire risk in Mongolia using decision support system, in: International Archives of the Photogrammetry. In: Remote Sensing and Spatial Information Sciences - ISPRS Archives. International Society for Photogrammetry and Remote Sensing, pp. 357–362. https://doi.org/10.5194/isprs-archives-XLII-3-W4-357-2018.
National Statistics Office of Mongolia Mongolian statistical information service [WWW Document] http://1212.mn/default.aspx 2020 accessed 7.26.20.
National Statistics Office of Mongolia, 2018. Environment. Mongolian Statistical Yearbook. Ulaanbaatar 243–259.
Nelson, P., Paradis, D.P., Nelson, P., Paradis, D.P., 2017. Evaluating rapid ground sampling and scaling estimated plant cover using UAV imagery up to Landsat for mapping arctic vegetation. AGUFM 2017, B21F–B2016.
Noy-Meir, I., 1995. Interactive effects of fire and grazing on structure and diversity of Mediterranean grasslands. J. Veg. Sci. 6, 701–710. https://doi.org/10.2307/3236441.
Otgonbayar, M., Atzberger, C., Chambers, J., Damdinsuren, A., 2019. Mapping pasture biomass in Mongolia using Partial Least Squares, Random Forest regression and Landsat 8 imagery. Int. J. Remote Sens. 40, 3204–3226. https://doi.org/10.1080/01431161.2018.1541110.
Otgontuya, L., Elmarsdottir, A., Lkhagvajav, N., Munkhbat, C., 2019. Influence of different grazing intensity on above-ground biomass in Mongolian rangeland. Proc. Mong. Acad. Sci. 29–38 https://doi.org/10.5564/pmas.v59i3.1244.
Pan, J., Wang, M., Cao, X., Chen, S., Hu, F., 2016. A multi-resolution blending considering changed regions for orthoimage mosaicking. Remote Sens. 8, 842. https://doi.org/10.3390/rs8100842.
Pedregosa, F., Varoquaux, G., Gramfort, A., Michel, V., Thirion, B., Grisel, O., Blondel, M., Prettenhofer, P., Weiss, R., Dubourg, V., Vanderplas, J., Passos, A., Cournapeau, D., Brucher, M., Perrot, M., Duchesnay, É., 2011. Scikit-learn: Machine learning in Python. J. Mach. Learn. Res. 12, 2825–2830.
Peng, H.Y., Li, X.Y., Li, G.Y., Zhang, Z.H., Zhang, S.Y., Li, L., Zhao, G.Q., Jiang, Z.Y., Ma, Y.J., 2013. Shrub encroachment with increasing anthropogenic disturbance in the semiarid Inner Mongolian grasslands of China. Catena 109, 39–48. https://doi.org/10.1016/j.catena.2013.05.008.
Pereira, P., Cerda, A., Jordan, A., Bolutiene, V., Pranskevicius, M., Ubeda, X., Mataix-Solera, J., 2013. Spatio-temporal Vegetation Recuperation after a Grassland Fire in Lithuania. Procedia Environ. Sci. 19, 856–864. https://doi.org/10.1016/j.proenv.2013.06.095.
Pereira, P., Cerdà, A., Lopez, A.J., Zavala, L.M., Mataix-Solera, J., Arcenegui, V., Misiune, I., Keesstra, S., Novara, A., 2016. Short-Term Vegetation Recovery after a Grassland Fire in Lithuania: The Effects of Fire Severity, Slope Position and Aspect. L. Degrad. Dev. 27, 1523–1534. https://doi.org/10.1002/ldr.2498.
Planet Labs Inc., 2019. Planet imagery product specifications.
Planet Team Planet Application Program Interface Space for Life on Earth [WWW Document] 2017 San Fr. CA.
Pollak, O., Kan, T., 1998. The Use of Prescribed Fire to Control Invasive Exotic Weeds at Jepson Prairie Preserve. Ecol. Conserv. Manag. Vernal Pool Ecosyst. – Proc. from a 1996 Conf. 94105, 241–249.
Pollock, S.Z., Nielsen, S.E., St. Clair, C.C., 2017. A railway increases the abundance and accelerates the phenology of bear-attracting plants in a forested, mountain park. Ecosphere 8, e01985. https://doi.org/10.1002/ecs2.1985.
Popescu, D., Ichim, L., 2015. Image recognition in UAV application based on texture analysis. In: Lecture Notes in Computer Science (Including Subseries Lecture Notes in Artificial Intelligence and Lecture Notes in Bioinformatics). Springer Verlag, pp. 693–704. https://doi.org/10.1007/978-3-319-25903-1_60.
Räsänen, A., Virtanen, T., 2019. Data and resolution requirements in mapping vegetation in spatially heterogeneous landscapes. Remote Sens. Environ. 230, 111207 https://doi.org/10.1016/j.rse.2019.05.026.
Reading, R.P., Bedunah, D., Amgalanbaatar, S., 2010. Conserving mongolia's grasslands, with challenges, opportunities, and lessons for north america's great plains. Gt. Plains Res. 20, 85–107.
Reading, R.P., Bedunah, D.J., Amgalanbaatar, S., 2006. Conserving biodiversity on Mongolian rangelands: implications for protected area development and pastoral uses. Rangelands Cent. Asia Proc. Conf. Transform. Issues, Futur. Challenges 1–17.
Rihan, W., Zhao, J., Zhang, H., Guo, X., Ying, H., Deng, G., Li, H., 2019. Wildfires on the Mongolian Plateau: Identifying drivers and spatial distributions to predict wildfire probability. Remote Sens. 11, 2361. https://doi.org/10.3390/rs11202361.
Road ecology: science and solutions, 2003. , Choice Reviews Online. https://doi.org/10.5860/choice.40-6438.
Rosenfield, G.H., Fitzpatrick-Lins, K., 1986. A coefficient of agreement as a measure of thematic classification accuracy. Photogramm. Eng. Remote Sensing 52, 223–227.
Russell, G.C., 1991. A review of assessing the accuracy of classifications of remotely sensed data. Remote Sens. Environ. 37, 35–46. https://doi.org/10.1016/0034-4257(91)90048-b.
Sankey, T.T., Leonard, J.M., Moore, M.M., 2019. Unmanned Aerial Vehicle – Based Rangeland Monitoring: Examining a Century of Vegetation Changes. Rangel. Ecol. Manag. 72, 858–863. https://doi.org/10.1016/j.rama.2019.04.002.
Santín, C., Doerr, S.H., 2016. Fire effects on soils: The human dimension. Philos. Trans. R. Soc. B Biol. Sci. https://doi.org/10.1098/rstb.2015.0171.
Seiler, A., 2001. Ecological effects of roads: a review. Introd. Res. essay 9, 1–40.
Silver, M., Tiwari, A., Karnieli, A., 2019. Identifying vegetation in arid regions using object-based image analysis with RGB-only aerial imagery. Remote Sens. 11, 2308. https://doi.org/10.3390/rs11192308.
Spellerberg, I.F., 1998. Ecological Effects of Roads and Traffic: A Literature Review. Glob. Ecol. Biogeogr. Lett. 7, 317. https://doi.org/10.2307/2997681.
Stavi, I., 2019. Wildfires in grasslands and shrublands: A review of impacts on vegetation, soil, hydrology, and geomorphology. Water (Switzerland). https://doi.org/10.3390/w11051042.
Su, R., Cheng, J., Chen, D., Bai, Y., Jin, H., Chao, L., Wang, Z., Li, J., 2017. Effects of grazing on spatiotemporal variations in community structure and ecosystem function on the grasslands of Inner Mongolia. China. Sci. Rep. 7, 1–10. https://doi.org/10.1038/s41598-017-00105-y.
Suzuki, Y., 2013. Conflict Between Mining Development and Nomadism in Mongolia. Springer, Tokyo, pp. 269–294. https://doi.org/10.1007/978-4-431-54052-6_20.
Szpakowski, D.M., Jensen, J.L.R., 2019. A review of the applications of remote sensing in fire ecology. Remote Sens. https://doi.org/10.3390/rs11222638.
Themistocleous, K., 2019. DEM modeling using RGB-based vegetation indices from UAV images. In: Papadavid, G., Themistocleous, K., Michaelides, S., Ambrosia, V., Hadjimitsis, D.G. (Eds.), Seventh International Conference on Remote Sensing and Geoinformation of the Environment (RSCy2019). SPIE, p. 21. https://doi.org/10.1117/12.2532748.
Thomas, H.J.D., Myers-Smith, I.H., Bjorkman, A.D., Elmendorf, S.C., Blok, D., Cornelissen, J.H.C., Forbes, B.C., Hollister, R.D., Normand, S., Prevéy, J.S., Rixen, C., Schaepman-Strub, G., Wilmking, M., Wipf, S., Cornwell, W.K., Kattge, J., Goetz, S.J., Guay, K.C., Alatalo, J.M., Anadon-Rosell, A., Angers-Blondin, S., Berner, L.T., Björk, R.G., Buchwal, A., Buras, A., Carbognani, M., Christie, K., Siegwart Collier, L., Cooper, E.J., Eskelinen, A., Frei, E.R., Grau, O., Grogan, P., Hallinger, M., Heijmans, M.M.P.D., Hermanutz, L., Hudson, J.M.G., Hülber, K., Iturrate-Garcia, M., Iversen, C.M., Jaroszynska, F., Johnstone, J.F., Kaarlejärvi, E., Kulonen, A., Lamarque, L.J., Lévesque, E., Little, C.J., Michelsen, A., Milbau, A., Nabe-Nielsen, J., Nielsen, S.S., Ninot, J.M., Oberbauer, S.F., Olofsson, J., Onipchenko, V.G., Petraglia, A., Rumpf, S.B., Semenchuk, P.R., Soudzilovskaia, N.A., Spasojevic, M.J., Speed, J.D.M., Tape, K.D., te Beest, M., Tomaselli, M., Trant, A., Treier, U.A., Venn, S., Vowles, T., Weijers, S., Zamin, T., Atkin, O.K., Bahn, M., Blonder, B., Campetella, G., Cerabolini, B.E.L., Chapin, F.S., Dainese, M., de Vries, F.T., Díaz, S., Green, W., Jackson, R.B., Manning, P., Niinemets, Ozinga, W.A., Peñuelas, J., Reich, P.B., Schamp, B., Sheremetev, S., van Bodegom, P.M.,, 2019. Traditional plant functional groups explain variation in economic but not size-related traits across the tundra biome. Glob. Ecol. Biogeogr. 28, 78–95. https://doi.org/10.1111/geb.12783.
Tumur, E., Heijman, W., Gurjav, E.-A., Agipar, B., Heerink, N., 2020. Options for Increasing Mongolia's Livestock Sector Exports - A Revealed Comparative Advantage Analysis. Mong. J. Agric. Sci. 30, 38–50. https://doi.org/10.5564/mjas.v30i2.1490.

Tuvshintogtokh, I., 2014. Grassland in Mongolia and their degradation indicator plants, in: International Symposium on the East Asia Environmental Problems. Kyushu University, Fukuoka.
Tuvshintogtokh, I., Ariungerel, D., 2013. Degradation of Mongolian Grassland Vegetation Under Overgrazing by Livestock and Its Recovery by Protection from Livestock Grazing. In: Ecological Research Monographs. Springer, Tokyo, pp. 115–130. https://doi.org/10.1007/978-4-431-54052-6_10.
United Nations, 2019. Global Land Outlook Northeast Asia Thematic Report: Partnerships to Achieve Land Degradation Neutrality.
Valone, T.J., Nordell, S.E., Ernest, S.K.M., 2002. Effects of fire and grazing on an arid grassland ecosystem. Southwest. Nat. 47, 557–565. https://doi.org/10.2307/3672659.
Villoslada, M., Bergamo, T.F., Ward, R.D., Burnside, N.G., Joyce, C.B., Bunce, R.G.H., Sepp, K., 2020. Fine scale plant community assessment in coastal meadows using UAV based multispectral data. Ecol. Indic. 111, 1–13. https://doi.org/10.1016/j.ecolind.2019.105979.
von Wehrden, H., Zimmermann, H., Hanspach, J., Ronnenberg, K., Wesche, K., 2009. Predictive mapping of plant species and communities using GIS and Landsat data in a southern Mongolian mountain range. Folia Geobot. 44, 211–225. https://doi.org/10.1007/s12224-009-9042-0.
Vrieling, A., Meroni, M., Darvishzadeh, R., Skidmore, A.K., Wang, T., Zurita-Milla, R., Oosterbeek, K., O'Connor, B., Paganini, M., 2018. Vegetation phenology from Sentinel-2 and field cameras for a Dutch barrier island. Remote Sens. Environ. 215, 517–529. https://doi.org/10.1016/j.rse.2018.03.014.
Wang, J., Cheng, K., Liu, Q., Zhu, J., Ochir, A., Davaasuren, D., Li, G., Wei, H., Chonokhuu, S., Namsrai, O., Bat-Erdene, A., 2019a. Land cover patterns in Mongolia and their spatiotemporal changes from 1990 to 2010. Arab. J. Geosci. 12, 1–13. https://doi.org/10.1007/s12517-019-4893-z.
Wang, J., Stern, M.A., King, V.M., Alpers, C.N., Quinn, N.W.T., Flint, A.L., Flint, L.E., 2020. PFHydro: A New Watershed-Scale Model for Post-Fire Runoff Simulation. Environ. Model. Softw. 123 https://doi.org/10.1016/j.envsoft.2019.104555.
Wang, J., Wei, H., Cheng, K., Li, G., Ochir, A., Bian, L., Davaasuren, D., Chonokhuu, S., Nasanbat, E., 2019b. Spatio-temporal pattern of land degradation along the China-Mongolia Railway (Mongolia). Sustain. 11, 2705. https://doi.org/10.3390/su11092705.
Wang, M., Fei, X., Zhang, Y., Chen, Z., Wang, X., Tsou, J.Y., Liu, D., Lu, X., 2018. Assessing texture features to classify coastal wetland vegetation from high spatial resolution imagery using Completed Local Binary Patterns (CLBP). Remote Sens. 10, 778. https://doi.org/10.3390/rs10050778.
Wasser, C.H.C.H.C.H.C.H., Shoemaker, J.W., 1982. Ecology and culture of selected species useful in revegetating disturbed lands in the West.
Weir, J.R., Fuhlendorf, S.D., Engle, D.M., Bidwell, T.G., Cummings, D.C., Elmore, D., Limb, R.F., Allred, B.W., Scasta, J.D., Winter, S.L., 2013. Patch Burning : Integrating Fire and Grazing. Publ, US Fish Wildl.
Wester, D.B., Rideout-Hanzak, S., Britton, C.M., Whitlaw, H., 2014. Plant community response to the East Amarillo Complex wildfires in the Southern High Plains, USA. Community Ecol. 15, 222–234. https://doi.org/10.1556/ComEc.15.2014.2.11.
Wick, A.F., Geaumont, B.A., Sedivec, K.K., Hendrickson, J.R., 2016. Grassland Degradation, in: Biological and Environmental Hazards, Risks, and Disasters. Elsevier Inc., pp. 257–276. https://doi.org/10.1016/B978-0-12-394847-2.00016-4.
Wijesingha, J., Astor, T., Schulze-Brüninghoff, D., Wachendorf, M., 2020. Mapping Invasive Lupinus polyphyllus Lindl. in Semi-natural Grasslands Using Object-Based Image Analysis of UAV-borne Images. PFG -. J. Photogramm. Remote Sens. Geoinf. Sci. 88, 391–406. https://doi.org/10.1007/s41064-020-00121-0.
Wilson, S.D., Shay, J.M., 1990. Competition, fire, and nutrients in a mixed-grass prairie. Ecology 71, 1959–1967. https://doi.org/10.2307/1937604.
Wohlgemuth, P.M., Hubbert, K.R., Beyers, J.L., Narog, M.G., 2008. Post-Fire Watershed Response at the Wildland-Urban Interface, Southern California. Third Interag. Conf. Res. Watersheds, 8-11 Sept. 2008, Estes Park. CO 8–11.
Wright, J.P., Naeem, S., Hector, A., Lehman, C., Reich, P.B., Schmid, B., Tilman, D., 2006. Conventional functional classification schemes underestimate the relationship with ecosystem functioning. Ecol. Lett. 9, 111–120. https://doi.org/10.1111/j.1461-0248.2005.00850.x.
Wu, H., Li, Z.L., 2009. Scale issues in remote sensing: A review on analysis, processing and modeling. Sensors. https://doi.org/10.3390/s90301768.
Xie, Y., Sha, Z., Yu, M., 2008. Remote sensing imagery in vegetation mapping: a review. J. Plant Ecol. 1, 9–23. https://doi.org/10.1093/jpe/rtm005.
Yoshihara, Y., Koyama, A., Undarmaa, J., Okuro, T., 2015. Prescribed burning experiments for restoration of degraded semiarid Mongolian steppe. Plant Ecol. 216, 1649–1658. https://doi.org/10.1007/s11258-015-0548-7.
Young, J.A., Evans, R.A., 1978. Population Dynamics after Wildfires in Sagebrush Grasslands. J. Range Manag. 31, 283. https://doi.org/10.2307/3897603.
Young, J.A., Evans, R.A., 1974. Population Dynamics of Green Rabbitbrush in Disturbed Big Sagebrush Communities. J. Range Manag. 27, 127. https://doi.org/10.2307/3896748.
Zhang, J., Virk, S., Porter, W., Kenworthy, K., Sullivan, D., Schwartz, B., 2019. Applications of unmanned aerial vehicle based imagery in turfgrass field trials. Front. Plant Sci. 10 https://doi.org/10.3389/fpls.2019.00279.
Zhang, X., Cui, J., Wang, W., Lin, C., 2017. A study for texture feature extraction of high-resolution satellite images based on a direction measure and gray level co-occurrence matrix fusion algorithm. Sensors (Switzerland) 17, 1474. https://doi.org/10.3390/s17071474.
Zhang, X., Friedl, M.A., Schaaf, C.B., 2009. Sensitivity of vegetation phenology detection to the temporal resolution of satellite data. Int. J. Remote Sens. 30, 2061–2074. https://doi.org/10.1080/01431160802549237.
Zhang, Y., 2001. Texture-integrated classification of urban treed areas in high-resolution color-infrared imagery. Photogramm. Eng, Remote Sensing.
Zhang, Y., Wang, Q., Wang, Z., Li, J., Xu, Z., 2021. Dynamics and drivers of grasslands in the eurasian steppe during 2000–2014. Sustain. 13, 5887. https://doi.org/10.3390/su13115887.
Zhao, Y., Liu, X., Wang, Y., Zheng, Z., Zheng, S., Zhao, D., Bai, Y., 2021a. UAV-based individual shrub aboveground biomass estimation calibrated against terrestrial LiDAR in a shrub-encroached grassland. Int. J. Appl. Earth Obs. Geoinf. 101, 102358 https://doi.org/10.1016/j.jag.2021.102358.
Zhao, Yujin, Sun, Y., Chen, W., Zhao, Yanping, Liu, X., Bai, Y., 2021b. The Potential of Mapping Grassland Plant Diversity with the Links among Spectral Diversity, Functional Trait Diversity, and Species Diversity. Remote Sens. 13, 3034. https://doi.org/10.3390/rs13153034.
Zhou, H., Fu, L., Sharma, R.P., Lei, Y., Guo, J., 2021. A hybrid approach of combining random forest with texture analysis and vdvi for desert vegetation mapping based on uav rgb data. Remote Sens. 13, 1891. https://doi.org/10.3390/rs13101891.

2.3 Paper III:

Mapping vegetation cover, aboveground biomass and land degradation in the vast eastern Mongolian steppe from remote sensing and multi-source geospatial data using random forest

This paper is currently under review at Remote sensing of Environment.

Submitted: 29.03.2022

Dashpurev, B.; Munkhtsetseg, D.; Phan, T.N.; Bendix, J.; Lehnert, L.W.

Mapping vegetation cover, aboveground biomass and land degradation in the vast eastern Mongolian steppe from remote sensing and multi-source geospatial data using random forest

Batnyambuu Dashpurev[1]*, Munkhtsetseg Dorj[2], Thanh Noi Phan[1], Jörg Bendix[3] and Lukas W. Lehnert[1]

[1] Department of Geography, Ludwig-Maximilians-University Munich, 80333 Munich, Germany

[2] Agency of Land Administration and Management, Geodesy and Cartography, Government building XII, Barilgachidiin square, Chingeltei district, 4th khoroo, Ulaanbaatar, Mongolia, Mongolia

[3] Faculty of Geography, Philipps-University of Marburg, 35032 Marburg, Germany

*Correspondence: B.Dashpurev@iggf.geo.uni-muenchen.de; Tel.: +49-(0)170-504-2338

Abstract

Land degradation (LD) poses many serious challenges to ecosystems and sustainable livelihoods in Mongolia. Particularly, in eastern Mongolian steppe, an increase of human pressure caused e.g., by the growth of extractive industries and overgrazing combined with climate variability contribute to increasing LD. Main purpose of this study was to develop a quantitative model of current LD status using remote sensing and machine learning techniques. To map LD, we determined 20 potential driver and proxy variables based on a literature review and derived them using remote sensing and Geographical Information System (GIS) techniques. In this context, proxy variables are those which change as a consequence of LD and, thus, allow to monitor and observe LD. Key proxies for LD mapping are fractional vegetation cover (FVC) and aboveground biomass (AGB); therefore, we derived both variables from Sentinel-2 imagery using 256 field vegetation measurements in the vast eastern Mongolian steppe as reference for Random forest (RF) models (R^2_{FVC}=0.76, R^2_{AGB} = 0.81). In addition, we tested for temporal trends in the vegetation using NDVI time series data and Mann-Kendall trend test. This revealed that in 7.3% of the area the NDVI significantly increased while in 58% a significant decrease has been observed. For LD mapping, we trained a separate random forest classification model using all potential explanatory variables and field measurements of degradation rates as response variable (n = 200). The classification model obtained a reasonable overall accuracy of 73%. Amongst the 20 potential explanatory variables, annual soil loss, slope, soil erodibility and AGB were the most important ones for the estimation of current LD status. The obtained results revealed that most of study area is generally affected by some degree of degradation partitioning into an area of 2,472 km^2 (2%) for severely degraded, 7,416 km^2 (6%) for heavily degraded, 35,843 km^2 (29%) for moderately degraded and 71,687 km^2 (58%) for slightly degraded. No degradation was observed in an area of 6180 km^2 (5%).

Keywords: Eastern Mongolian steppe, Fractional vegetation cover, Aboveground biomass, Normalized difference vegetation index (NDVI), Landsat NDVI time series, Land degradation map, Random forest, Remote sensing

1. Introduction

Land degradation in drylands is one of the critical global environmental and social issues, and thus pose serious challenges for sustainable development (FAO, 2013; Stavi and Lal, 2015;

Zambon et al., 2017). The latest report of the United Nations (UN) on the global land outlined that approximately one third of global drylands are at least moderately degraded. (UNCCD, 2017). Various socio-economic and climatic factors contribute to land degradation, but the relationship between these factors varies among regions (UNCCD, 2017). For Mongolia, it is estimated that 77.8% of the total land area is degraded to some extent, resulting in substantial negative impacts on sustainable livelihoods and environment, especially in areas covered by grasses (Asian Development Bank, 2013; Cowie et al., 2018; United Nations, 2019; Wang et al., 2020). There have been several efforts to assess land degradation based on satellite data at national and regional scales in Mongolia (Eckert et al., 2015; Lee et al., 2019; Tian et al., 2014; Wang et al., 2020). However, despite these efforts, the existing land degradation assessments in Mongolia do not consider any anthropogenic drivers. Therefore, the identification of land degradation status, as well as the consideration of anthropogenic drivers is crucial for national and regional efforts toward a sustainable use of Mongolia's grassland resources.

To assess degradation, many previous studies used estimates of vegetation cover and biomass as proxies for land degradation (Bai et al., 2008; Higginbottom and Symeonakis, 2014; Le et al., 2015). For instance, approaches based on vegetation cover have been increasingly used in the past decades and have shown that results of the studies effectively indicate the status and process of land degradation (Dubovyk, 2017; Easdale et al., 2019; Wessels et al., 2008). In this context, remotely sensed data have been extensively used to estimate vegetation cover (Hilker et al., 2014; Jaebeom Kim et al., 2020; von Wehrden et al., 2009; Wang et al., 2020); however, to our knowledge only one study estimated AGB using both field vegetation data and satellite imagery in Mongolia (Otgonbayar et al., 2019). Unfortunately, this study was not based on any field sample in the Eastern Mongolian Steppe area. The reasons for the low number of studies are that vegetation surveys with traditional sampling method are very costly and time-consuming, especially for large, extended and remote areas as the Eastern Mongolian Steppe. Fortunately, continuous development of the rangeland health monitoring systems in Mongolia resulted in extensive databases that provide free-of-charge reference data about vegetation cover and AGB (Densambuu et al., 2018). To our knowledge, there is no study on FVC and AGB which was conducted combining in situ data of this rangeland health monitoring databases as field reference with remotely sensed data providing a land degradation product in Mongolia. In addition, many studies have proven that changes in satellite-derived Normalized Difference Vegetation Index (NDVI) time-series have a potential to serve as a proxy for land degradation assessment (Bai et al., 2008; Huang et al., 2021; Yengoh et al., 2015). Because the NDVI correlates directly with vegetation productivity (Tucker and Sellers, 1986), this index is easily calculated from spectral bands with long time series. On the other hand, the rapid advancements in remote sensing technology and application are making the use of NDVI more popular for vegetation cover assessments (Huang et al., 2021; Yengoh et al., 2015)

There are numerous drivers that lead to land degradation, but the combination and role of drivers depend on the regions (GEIST and LAMBIN, 2004). Generally, the drivers of land degradation are summarized into two categories: proximate and underlying causes. Proximate or direct drivers are human activities and natural conditions that directly affect the terrestrial ecosystems. Underlying or indirect drivers are complex interactions of social, economic, political drivers etc. that indirectly affect the proximate cause of land degradation (Nkonya et

al., 2015, 2012). Literature on mapping land degradation confirmed that proximate drivers such as topography, climate, and soil conditions are useful to estimate the land degradation status (Gibbs and Salmon, 2015; Mirzabaev et al., 2015). Furthermore, analysis of soil properties, erosion and erodibility are the most commonly applied drivers of land degradation (Borrelli et al., 2017a; Saygın et al., 2011; Song et al., 2005). Underlying socioeconomic drivers indirectly affect the proximate drivers (von Braun et al., 2013). For instance, anthropogenic factors of land degradation relate to human activities that directly or indirectly impact the health and productivity of land (UNCCD, 2017). For Mongolian steppes, there are numerous natural and anthropogenic forces, which causes land degradation. The major cause of land degradation in Mongolian grassland steppes was widely discussed by several studies. Overall, these previous studies suggested that major drivers of land degradation are an increase of human pressure (Batkhishig, 2013; Pfeiffer et al., 2020), land use change due to mining and oil exploitation (Batkhishig, 2013; Dashpurev et al., 2020; Elbegjargal et al., 2014; Han et al., 2021; Ma et al., 2021; Juanle Wang et al., 2019), an expansion of dirt roads (Batkhishig, 2013; Dashpurev et al., 2021, 2020; Keshkamat et al., 2013; Kinugasa et al., 2015; Juanle Wang et al., 2019), overgrazing (Lkhagva et al., 2013; Munkhzul et al., 2021; Pfeiffer et al., 2020; Sainnemekh et al., 2022), climate variability (Elbegjargal et al., 2014; Han et al., 2021; Liu et al., 2013; Nandintsetseg et al., 2021; Pfeiffer et al., 2020), soil erosion (Batkhishig, 2013; Han et al., 2021; Jugder et al., 2018; Jungrack Kim et al., 2020) and topography (Meng et al., 2021, 2020).

The modeling of land degradation is a process that typically involves potential drivers and proxies of land degradation, field measurements and remote sensing products (Albalawi and Kumar, 2013; Caspari et al., 2015). Spatially explicit land degradation models have an enormous advantage for the prediction of current degraded land and potential land degradation locations in an optimal and evaluable manner. Recent comprehensive and systematic reviews summarized the existing global assessments on land degradation and noted that modern machine learning algorithms have been widely used to model land degradation condition (Aynekulu et al., 2017; Belgiu and Drăgu, 2016; David and Mathew, 2020; Padarian et al., 2020; Vågen et al., 2014; Youssef et al., 2020). To estimate land degradation, machine learning approaches were successfully used to analyze degraded areas using field measurements and the processing of potential variables through the application of geographic information system (GIS) and remote sensing techniques (AbdelRahman et al., 2019; Nzuza et al., 2020; Sarparast et al., 2018). Regarding existing literature, most previous studies modeling land degradation condition have used various variables of environmental conditions, spatiotemporal patterns of land cover change and socioeconomic variables (AbdelRahman et al., 2019; Grinand et al., 2020; Perović et al., 2021; Salvati et al., 2008; Torabi Haghighi et al., 2021).

The eastern Mongolian steppes have been intensively used due to the rapid growth of natural resource extraction including mining and oil extraction, where the extractive sector became a major part of the economy of Mongolia (Mongolia EITI, 2018). The extractive industries trigger extensions of dirt road networks and other supporting infrastructure in the eastern Mongolian steppe, which hosts some of the world's largest and most intact grassland regions (Batsaikhan et al., 2014). In particular, a recent spatiotemporal study of the eastern Mongolian steppe indicated that the total area occupied by dirt roads, oil exploration and exploitation infrastructure expanded by 75% in the past decade (Dashpurev et al., 2020).

Gradually, effects of transportation corridors could ecologically extent up to distance of 60-120 m in the neighboring vegetated steppes in eastern Mongolia (Dashpurev et al., 2021). Likewise, due to other factors such as climate change, environment (e.g., water erosion), landforms (e.g., slope), land use change (e.g., centralization and development of the local infrastructures), as well as the other anthropogenic stressors (e.g., overexploitation of the vegetative cover for domestic use), the steppes in Mongolia that made one of the global hotspots for biomass reduction (Batkhishig, 2013; Darbalaeva et al., 2020; Khishigbayar et al., 2015; Liu et al., 2013; Noi Phan et al., 2020). Based on this problem definition, this study seeks to answer the following research questions: What is the current condition of vegetation cover and land degradation at the regional level? Which variables drive land degradation? To deal with those questions, the present study aims to: (1) estimate FVC and AGB using RF based on Sentinel-2 imagery and field measurements of vegetation; (2) perform a trend analysis to estimate the changes of vegetation over time; (3) evaluate and prepare explanatory variables for creating potential LD map; and (4) map and quantify current land degradation status based on the RF model.

2. Materials and methods

2.1. Study area

Dornod aimag (or province) is the study area which is located in the easternmost part of Mongolia, bordering with Russia to the north and China to the eastward and southward (Fig. 1). It comprises approximately 124,000 km^2 between 50°28'N–46°25'N in latitude and 112°05'E–119°56'E in longitude. The study area has three distinct ecoregions: the Mongolian Daurian (or Mongol Daguur) forest steppe, the Eastern Mongolian steppe and the Numrug forest steppe. The Mongolian Daurian forest steppe in the northern part of study area covers marginal branches of the Khentii Mountain Range and plains.

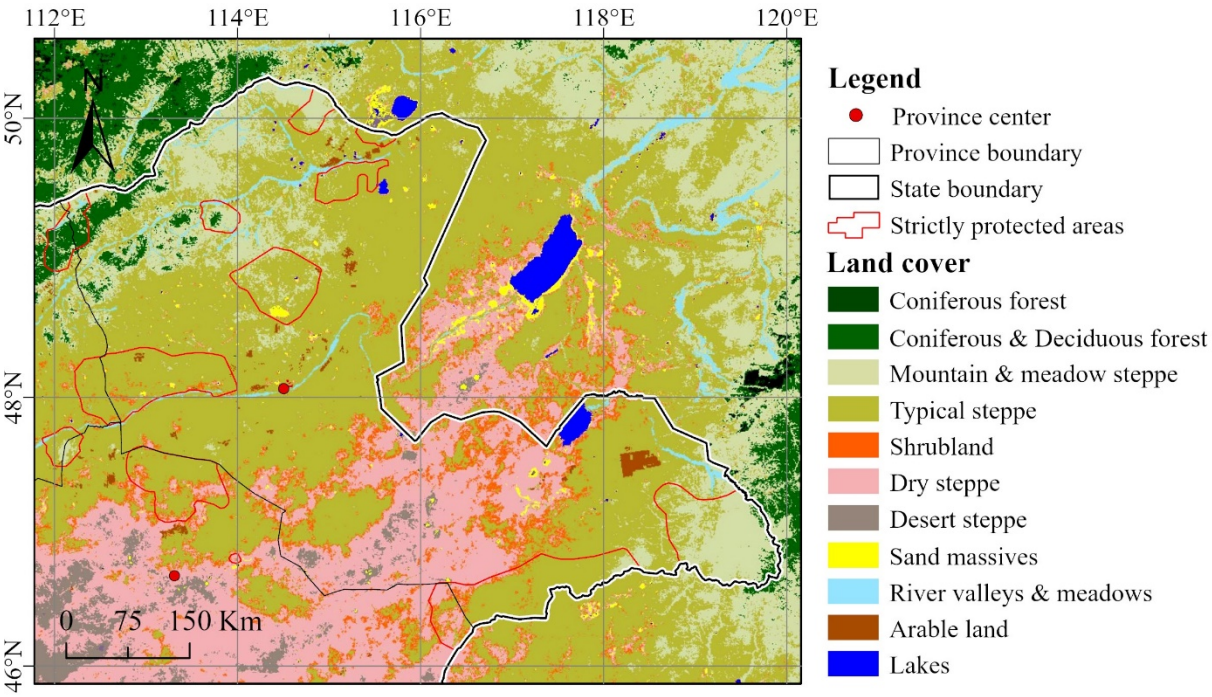

***Figure 1**. Location of study area and pasture photo-monitoring data. Source: Environmental Information center Mongolia.*

The eastern Mongolian steppe, the main part of study area, mainly consists of broad plains and rolling hills where the vegetation is dominated by bunch grasses like *Stipa krylovii* and *Cleistogenes squarrosa*. The Numrug forest steppe, the far eastern part of study area, comprises marginal branches of the Greater Khingan Mountains, foothills and plains. The study area is characterized by an extremely continental climate. The average monthly temperature minimum reaches −20 to −26 °C in January; the average maximum monthly temperature of 21 °C occurs in July. Average annual precipitation amounts to 300-350 mm in Mongolian Daurian forest steppe and 200–300 mm in Eastern Mongolian steppe and Numrug forest steppe, with monthly maxima mainly occurring in summer (Girvetz et al., 2014; Martin Pfeiffer, Choimaa Dulamsuren, 2018; Shukherdorj et al., 2019; Yembuu, 2021a). In the study area, there are three strictly protected areas (SPA) and three nature reserves (NR). Traditionally, land use has been associated with livestock pastoralism, but mining and oil extraction related activities are becoming more and more important. Other land use types in this area includes settlements, agriculture and infrastructure (Tsedev, 2021).

2.2. Remote sensing of grassland degradation

2.2.1 Data for FVC, AGB estimation and trend analysis

Remote sensing data

Multispectral imagery of Sentinel-2 were used to estimate the FVC and AGB encompassing 13 spectral bands in the visible, near infrared and short-wave infrared regions of the spectrum with 10-60 m spatial resolution. The level L1C images were downloaded free-of-charge from the United States Geological Survey's (USGS) website (https://earthexplorer.usgs.gov/). A set of 54 images with low cloud cover (twenty five tiles) of Sentinel-2 data acquired on 7-17 July 2020 were used in this study (Fig. 1). These images were atmospherically corrected and clouds were masked using Sentinel Application Platform (SNAP) of the European Space Agency. Afterward, single scenes of Sentinel-2 were merged into mosaic to achieve dataset covering the entire area of investigation. Finally, spectral indices were calculated from the spectral bands of the Sentinel-2 imagery and used as an additional predictor for FVC and AGB estimation. The spectral indices and their description are listed in Table 1 below.

Table 1. Description of the spectral indices used in RF regression models for FVC and AGB.

Spectral indices	Abbreviation	Formula	Reference
Normalized difference vegetation index	NDVI	(NIR − Red)/(NIR + Red)	(Tucker, 1979)
Red-Edge Normalized Difference Vegetation Index	$NDVI_{Red-edge}$	(NIR – RE)/(NIR + RE)	(Gitelson and Merzlyak, 1994)
Green Normalized Difference Vegetation Index	$NDVI_{Green}$	(NIR - Green)/(NIR + Green)	(Gitelson et al., 1996)
Simple Ratio	SR_{value}	NIR / Red	(Jordan, 1969)
Red-Edge Simple Ratio	$SR_{Red-Edge}$	NIR / RedEdge	(Gitelson et al., 2002)
Green Chlorophyll Index	CL_{Green}	(NIR / Green)-1	(Gitelson et al., 2003)

Red-Edge Chlorophyll Index	$CL_{Red-Edge}$	(NIR / RedEdge) - 1	(Gitelson et al., 2005)
Red-Edge Triangulated Vegetation Index	$RTVI_{Core}$	(100*(NIR - RedEdge) - 10*(NIR - Green))	(Haboudane et al., 2004)

For the trend analysis of vegetation cover, we used the atmospherically corrected surface reflectance collections from the Landsat 5 ETM and Landsat 8 OLI sensors in the Google Earth Engine platform. In these dataset, all satellite imagery are atmospherically corrected using the LEDAPS algorithms for Landsat 5 (Sayler, 2020) and the LaSRC algorithms for Landsat 8 (USGS, 2020) (USGS Landsat Surface Refectance Tier 1). For all images acquired between 1st of June and 31st of August in years 2010-2020 we employed the CFMask algorithm to identify and mask clouds and cloud shadows (Foga et al., 2017). Afterward, the NDVI was calculated based on the red and near infrared band. Finally, annual NDVI mosaics were produced by calculating the median NDVI value of all available images for the indicated time-period within a year.

Photo-monitoring data

Photo-monitoring data were downloaded free-of-charge from the Agency for Land Administration and Management, Geodesy and Cartography in Mongolia (https://egazar.gov.mn). The database contains FVC and AGB with corresponding land cover photos over 256 plots in Eastern Mongolia (Fig. 1). Each sampling plot in the photo-monitoring database internally consists of nine photos taken in nadir with a footprint of approx. 0.9 m². Each image is 5 meter apart from the next one. So all images line-up along a 50 m transect. Cover values for each sampling plot are mean values of the nine different image-locations. Photo-monitoring images were collected annually at 5 meter intervals along two parallel 50 meter long tapes by authorities for land management. Field data was collected during the vegetation-growing season in August 2020. Analysis is performed using Sample Point software that facilitates manual, pixel-based, image analysis from nadir digital images of any scale, and automatically records data to a spreadsheet (Cagney et al., 2011). The photo monitoring network was established and developed for grazing management and to report vegetation trends in Mongolian pasturelands.

2.2.2 RF regression and classification

Two techniques of regression and classification were separately applied to Sentinel-2 data and LD model, each using the Random Forest (RF) algorithm (Breiman, 2001). We used RF ensemble models for the prediction of FVC, AGB and LD status. RF, which is a representative of the so called “ensemble learning” methods (Saini and Ghosh, 2017), is widely used for regression and classification tasks in remote sensing. In the estimation of vegetation cover, two RF regression models were trained to estimate FVC and AGB. As predictors, the spectral bands and indices of Sentinel-2 data were used (Fig. 2). Training and validation data for both RF regression models were selected from Mongolian pasture photo-monitoring data. The models were validated and their accuracies were estimated using a 10-fold cross-validation. From the independent estimates, R-square values were calculated to evaluate the performances of the RF regression models (Belgiu and Drăgu, 2016; Sheykhmousa et al., 2020). For estimation of LD status, RF classification model was trained to predict LD status. LD driving factors including ecological, geomorphometric, environmental and anthropogenic were used as predictor variables. The training and

validation data for the RF classification were generated from field degradation estimates of Mongolian pasture photo-monitoring database. Performance of RF classification can be computed during the calculation of the out-of-bag error, which is calculated from the remaining training data not used to build the actual tree. Finally, the classification output was assessed for the overall, producer, and user accuracies in error matrices (Congalton, 1991; Rosenfield and Fitzpatrick-Lins, 1986)

2.2.3 Mann-Kendall trend test

A Mann-Kendall trend test and a Sen's Slope test were applied for each pixel in the time series to analyze NDVI trends for significance and slope of change, respectively. The Mann-Kendall test determines whether there is a monotonic trend (upward or downward) in the multidimensional time series data of NDVI. It performs the comparison between two sets of ranks given by the same datasets. The trend values range between -1 (negative trend) and +1 (positive trend). The slope of the trend for each pixel was calculated by the non-parametric coefficient developed by Sen (Sen, 1968). The Sen's slope test detects the magnitude of the slope based on the assumption of a linear trend (significance levels of 0.01 (high), 0.05 (medium) and 0.1 (low)).

2.2.4 Statistical analyses

Spearman's rank correlation analysis (Dodge, 2008) was used to examine the relationship between rankings of aboveground biomass and potential driving factors except FVC. Separate correlation models between aboveground biomass and each potential driving factor have been fit within moving windows of 500 x 500 pixels. The moving window approach ensures that local importance of driving factors could be detected even if the respective driving factor is relatively unimportant in the entire study area.

2.2.5 Land degradation model and its components

The conceptual framework of model and factors

Modeling the driving factors behind degraded land is important for understanding the land degradation process. Therefore, we test a set of potential variables to explain degradation status using a RF classification (Fig. 2). Our concept is focused on the values and changes of vegetation cover as a proxy for land degradation, therefore, we selected potential variables of land degradation based on how they contribute to the estimation of land degradation in other similar studies and literature reviews. In our study area, we identified 20 potential driver variables based on literature findings of land degradation in this region and categorized them into four groups: ecological, geomorphometric, environmental and anthropogenic variable (Description of variables are presented in Appendix A Figure A-1, A-2 and A-3).

Ecological variables

Ecological variables as the basic indicator of land degradation comprise FVC, AGB and NDVI trends. Previous reviews on methods for land degradation modeling reported that FVC, AGB and NDVI are the most powerful variables to map the land degradation at different scales, from local to a global scale (Aynekulu et al., 2017; T. S. Kapalanga, 2008; Turner et al., 2015). Consequently, FVC and AGB were included as proxies of degradation status in model for the current land degradation status. Furthermore, to incorporate temporal changes of vegetation in the study area, we included Sen's values of the trend analysis of Landsat NDVI time series.

Geomorphometric variables

Geomorphometric variables such as altitude, slope, aspect, terrain ruggedness index, and compound topographic index are widely used in land degradation modeling studies, and have been reported as the important variables (Abuzaid et al., 2021; Nzuza et al., 2020; Perović et al., 2021; Torabi Haghighi et al., 2021). Geomorphometric variables, also known as topographic variables, were obtained from ASTER Global Digital Elevation Model (ASTER-GDEM 30 m) data. All primary geomorphometric parameters such as altitude, slope and aspect were derived directly from ASTER-DEM data in the raster format using ArcGIS Pro Surface parameters tools, which implement specific algorithms with a moving window analysis (Fig. A-1 a-c). Terrain ruggedness index was derived from ASTER-DEM data using ArcGIS Pro Arc Hydro functions, while the topographic wetness index was generated based on multiple calculation of flow direction, flow accumulation and slope (Fig. A-1 d and e).

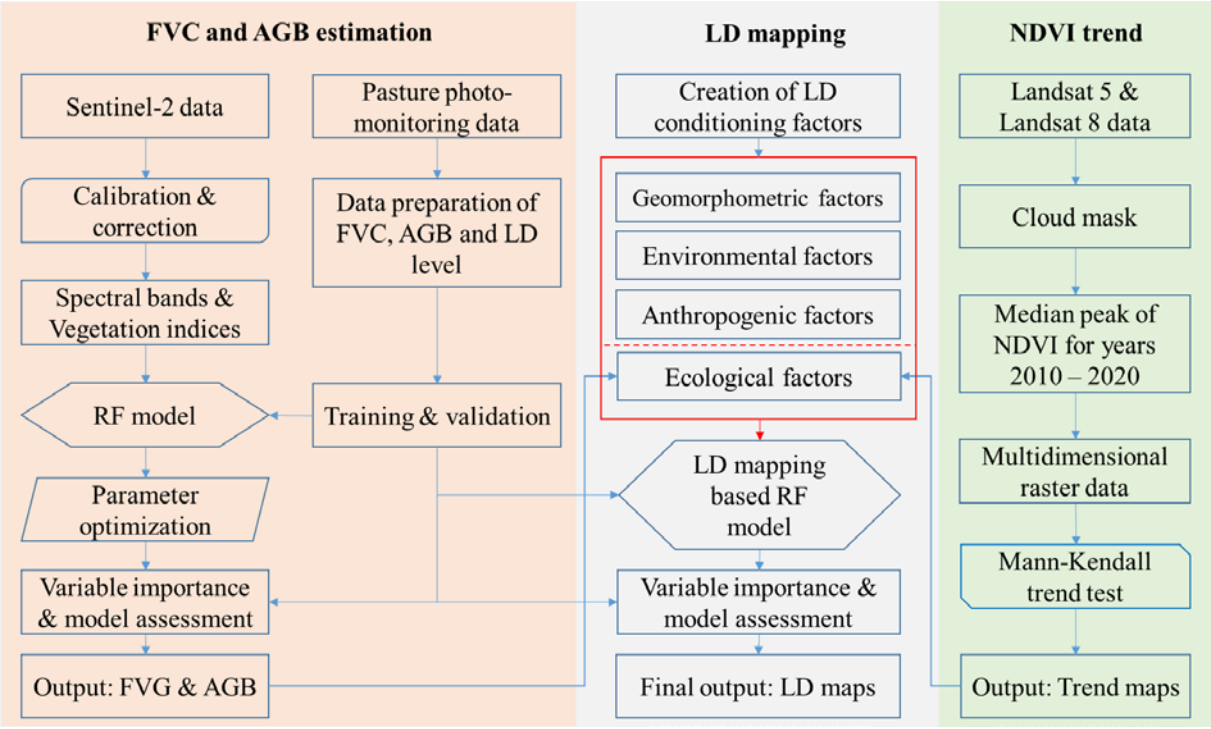

***Figure 2**. Workflow for the estimation of FVG and AGB, NDVI trend analysis and LD mapping*

Environmental factors

Distance to water body is a potential determinant for land degradation mapping (Fig. A-2 a). In dry lands, distance from river and lakes influences vegetation cover and species composition (Tsheboeng, 2018; Wang et al., 2021). In this study, the distance to water body was calculated in ArcGIS Pro using the distance tool.

Precipitation data of eastern Mongolian steppe recorded at four weather stations in 2010-2020 were used (Fig. A-2 b). We interpolated average annual precipitation with a resolution of 30 m using the simple Kriging method in ArcGIS pro.

Temperature trend of eastern Mongolian steppe estimated using long term (Fig. A-2 c).

Precipitation change of eastern Mongolian steppe estimated using long term precipitation (Fig. A-2 d).

Soil erodibility is a measure of the inherent resistance of soils to erosion (Wischmeier et al., 1971) (Fig. A-2 e). Soil erodibility was calculated based on soil properties (sand, silt, clay and organic matter) using data of ISRIC – World Soil Information at 250 m spatial resolution (Hengl et al., 2017), and then, the spatial resolution of result was downscaled to a resolution of 30 using a nearest neighbor technique.

Annual soil loss was calculated by the Universal Soil Loss Equation (USLE) (Wischmeier and Smith, 1978) which is widely used to assess the land degradation through soil related measures (Borrelli et al., 2017b) (Fig. A-2 f). This is done through performing the raster calculation with a resolution of 30 m.

Soil type is mutually associated to the formation of vegetation cover, which can affect vegetation structure and plant diversity (Hironaka et al., 1991; Rodrigues et al., 2018). Soils in eastern Mongolian steppe are characterized into 46 local soil types (Fig. A-2 g shown a group of local sol types). In this study, we used soil data of Mongolian soil monitoring database at Environmental database of Mongolia (National agency for meteorology and the environmental monitoring., 2021).

Anthropogenic factors

Distance to road is directly related with human disturbance. In other word, if the distance to road network is large, there is less human disturbance, less infrastructure development and less land use changes (Spellerberg, 2002). We created the road network map of eastern Mongolia merging the road detection result of our previous study (Dashpurev et al., 2020) and Mongolian open database for road network at Environmental database of Mongolia (National agency for meteorology and the environmental monitoring., 2021) (Fig. A-3 a). In this study, the distance to road was calculated in ArcGIS Pro using the distance tool.

Effect distance of road network refers to the cumulative ecological effect of the roads on the surrounding land (Forman and Alexander, 1998). Our previous study estimated that the ecological effects of road system extended up to 60–120 m into the adjacent steppe vegetation in eastern Mongolia. We created multiple buffer rectangles at 60 m and 120 m distances to the roads (Fig. A-3 b).

Population density can contribute to land degradation as high population densities cause increasing pressure due to human activities (Mortimore, 1993). Therefore, we created a population density map at the smallest administrative units of Dornod province using demographic statistics of Mongolia (National Statistics Office of Mongolia, 2020) (Fig. A-3 c).

The license area of mining and oil extraction shows the location of permitted area to extract any mineral, coal and oil (Fig. A-3 d). Around or on site of license area indicates that there are disturbed lands due to exploration activities and operation of mining and oil extraction. In this study, we used data of mining and oil extraction license from environmental database of Mongolia (National agency for meteorology and the environmental monitoring., 2021).

The pasture livestock carrying capacity is defined as the number of livestock units that can graze for a specific time period within a certain area (Ungar, 2019). In other words, carrying capacity refers to the maximum number of livestock not detrimental to the sustainability of pastureland or ecosystem (Hartvigsen, 2017). Approximately 70% of the total land in eastern Mongolia is rangeland used for traditional livestock herding. Dornod Province possessed

approximately 6.1 million sheep equivalent units at the end of 2020 (National Statistics Office of Mongolia, 2020). In this study, we used the pasture carrying capacity data provided by environmental database of Mongolia (National agency for meteorology and the environmental monitoring., 2021) (Fig. A-3 e).

Field measurements of land degradation

We used field degradation estimates of the pasture photo-monitoring database (data source is explained in Section 2.2.2). Here, degradation levels were determined in the field based on key criteria encompassing species composition, total species number, bare soil cover, the proportion of degradation indicator species, litter accumulation, and AGB (Densambuu et al., 2018). Degradation levels are explained in Table 2. A total of 256 degradation point samples were used (for location and distribution of the data, see Fig. 1).

Table 2. *Description of degradation levels* (Densambuu et al., 2018).

Degradation level	Description
Not degraded	All dominant species are present
Slightly degraded	Key dominant species are still dominating, some grazing sensitive forbs are in decline and abundance of grazing resistant species are in increase.
Moderately degraded	Key dominant species are in decline and replaced by other subdominants, number of species drops down.
Heavily degraded	Remnants of key species are thinned-out, and abundance of degradation indicator species increases.
Severely degraded	Total vegetation cover is reduced or dominated by very few degradation indicator species

3. Results

3.1 Estimation of vegetation cover and NDVI trend

Fractional vegetation cover and aboveground biomass

RF regression model was applied on the spectral bands and indices of Sentinel-2 data in order to estimate FVC and AGB in eastern Mongolian steppe in 2020 (Fig. 3 a and b). The training and validation data for RF model were prepared from Mongolian pasture photo-monitoring data. The validation results show that the RF regression models performed well at R-squared values of 0.81 for FVC and 0.76 for AGB.

Supplementary Fig. A-4 shows the variable importance values for the RF models. According to the ranks, the important variables of the FVC and AGB regressions were similar. To estimate FVC, the most important variables were the spectral vegetation indices, including the simple ratio (SR and SR red-edge) vegetation index and red-edge chlorophyll Index (Cl red-edge), and NDVI. For the spectral bands, red and vegetation red-edge bands were considered also very important for the model performance. For AGB, the most important predictor variables were NDVI, simple ratio (SR and SR red-edge) vegetation index, red-edge

chlorophyll Index (Cl red-edge), NDVI red-edge, red band and SWIR band, respectively, and the spectral vegetation indices were generally dominated to promote the performance of model.

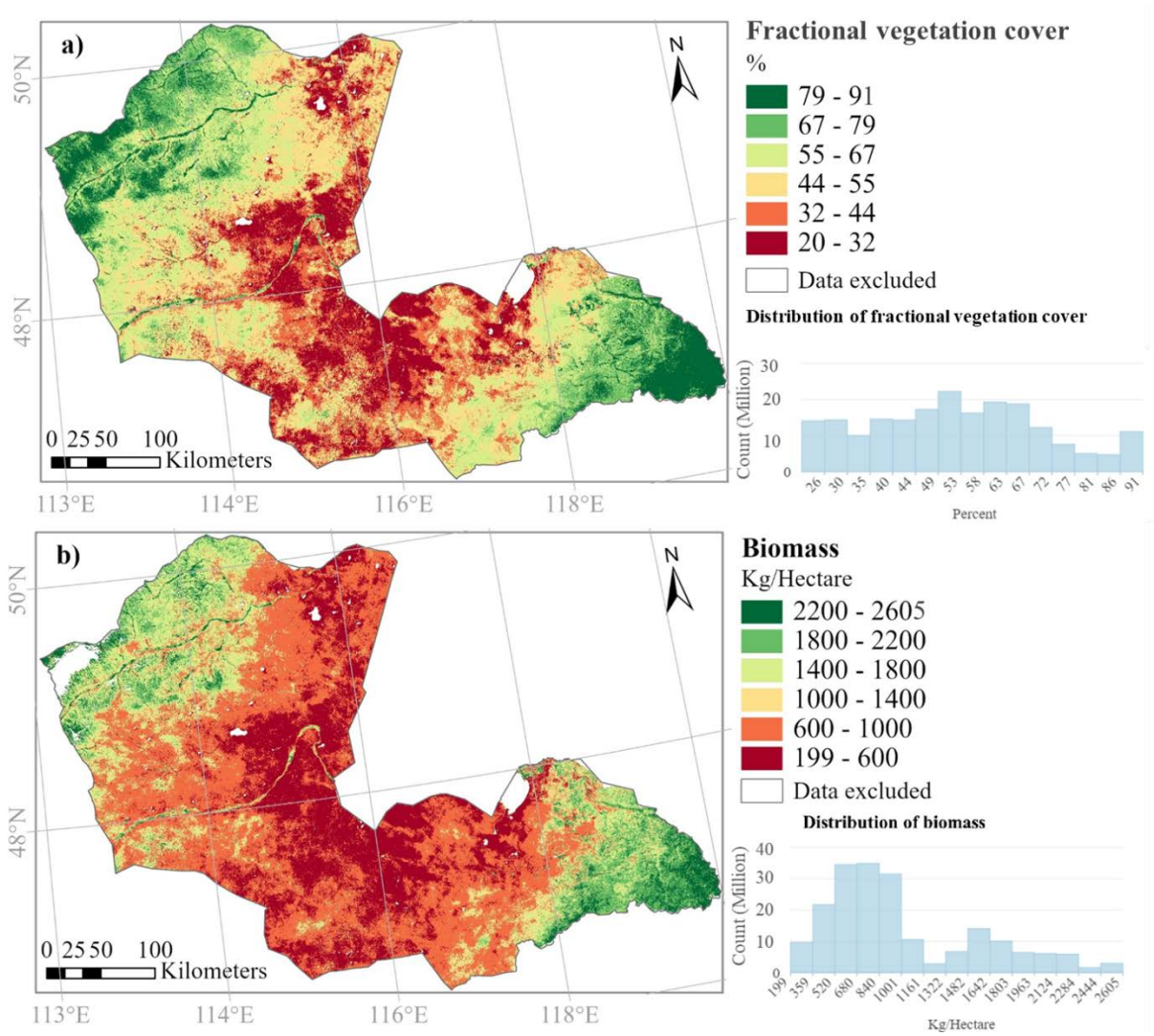

Figure 3. *Maps of FVC (a) and AGB (b) for year 2020 using Sentinel-2 data in Eastern Mongolian Steppe. Water surface was excluded for FVC while water surface and forest area were excluded for AGB.*

As shown in Figure 3, the FVC and AGB had a similar spatial distribution. Large values of both maps were concentrated in the northwestern and far eastern parts, where FVC ranged 67-90%, while AGB ranged 1800-2604 kg/ha. Those areas are covered by mountain and meadow steppes. According to the histogram charts in Fig. 3, the larger value of FVC occupied 20% of total area, while AGB was 11% of total area. The intermediate values of both maps, 44-67% and 1000-1800 kg/ha, were located in the transition zone of high and low fraction of vegetation value, which occupied 47% of total area in FVC, while AGB was 22% of total area. The low values of both maps, 20-44% and 198-1000 kg/ha, were clustered in the central and northeastern parts of study area, where lands are composed of moderately dry steppe and dry steppe. The histogram charts of both maps show that the low values of FVC occupied 33% of study area, while AGB was dominated as 67% of study area.

The result of Mann-Kendall trend test

The Mann-Kendall trend test statistics were obtained from the median NDVI value of Landsat time series during the vegetation period of 2010-2020 at a spatial resolution of 30 m. Based on Sen's slope, positive and negative NDVI trends were observed in different ecological regions, which are presented in Figure 4. According to the trend magnitude of Mann-Kendall analysis, NDVI values in 29% of all pixels in the study area were increasing (Fig. 5).

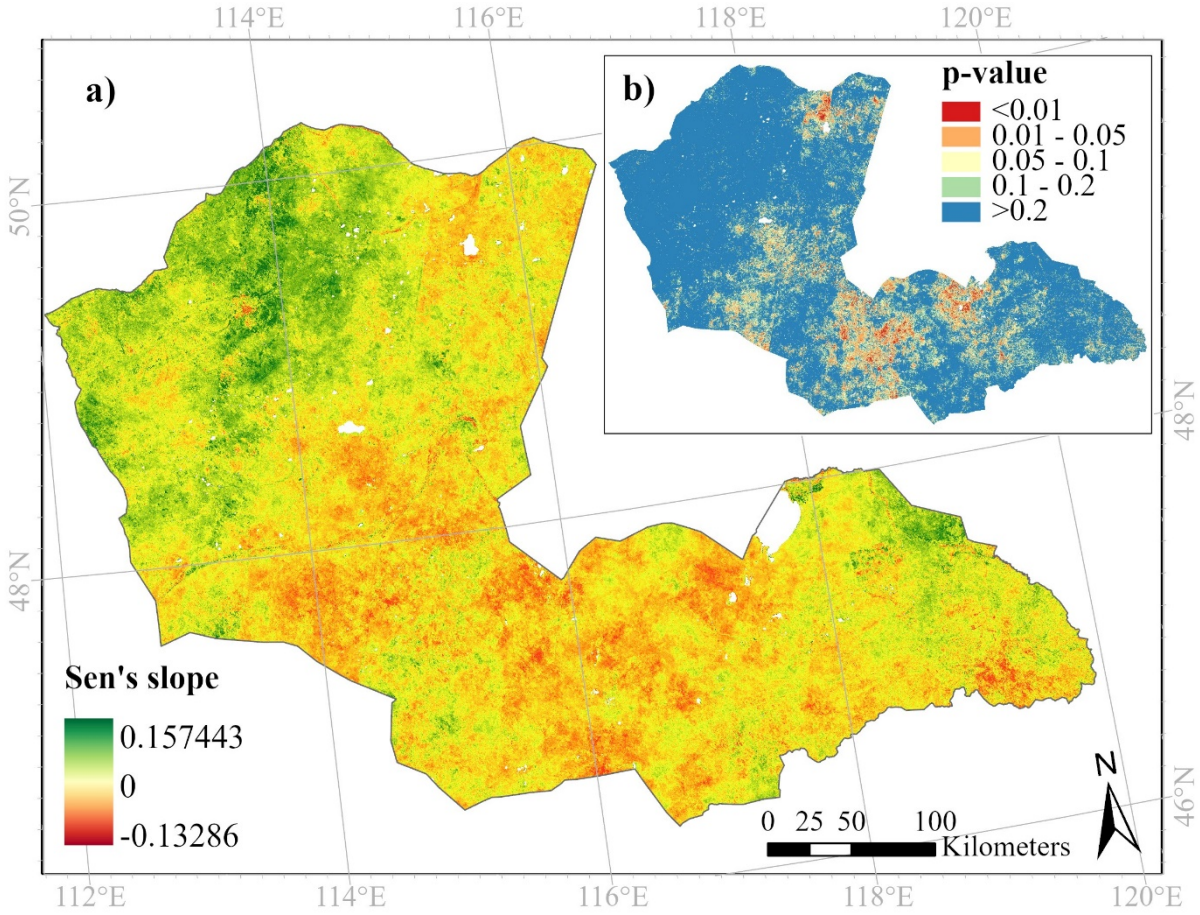

Figure 4. *Mann-Kendall trend test results of NDVI time series 2010-2020. Magnitude of trend is shown in a b represents significant levels.Water surface was excluded.*

Regarding the spatial distribution, these areas tended to be clustered along the northern and far eastern part of study area, where landscape mainly consists of forest steppe. Of those, only 25% gained a statistically significant trend, with a maximum magnitude of 0.15. In other words, 7.3% of total study area experienced positive statistically significant trends. Contrarily, the NDVI in 71% of the study area showed a decreasing trend. Of those, 84% had a statistically significant trend that is most concentrated in the middle-eastern, central part and along the northeastern boundary of study area. These areas are composed of moderately dry steppe and dry steppe. Fig. 4b shows that significantly decreasing trends were located in areas that are mostly used for oil exploration and exploitation around the middle-eastern cluster, the center of the province and areas along the northeastern country borders.

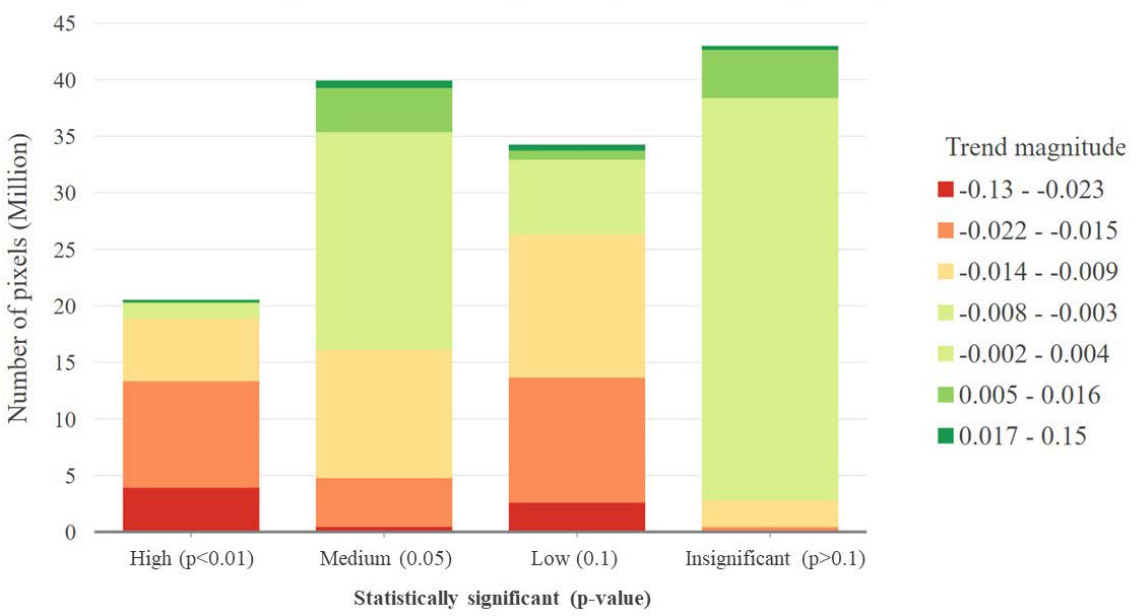

Figure 5. *Comparison of Sen's slope and significance level (p-value).*

3.2 Estimation of current land degradation condition

The RF classification model was applied on a field measurment data set and twenty land degradation explanatory variables including ecological variables (3), geomorphometric variables (5), environmental variables (7) and anthropogenic variables (5) in order to determine the map of land degradation in the eastern Mongolian steppe. The spatially explicit degradation rates were successfully estimated using field measurement of land degradation rates as response variables and validation for RF model. To consider potential uncertainties due to the repeated usage of vegetation cover and AGB as predictors for LD modeling, we obtained two different outputs: one estimated LD with all potential variables (Fig. 6a) and the second without FVC and AGB (Fig. 6b). Results showed that both outputs were in reasonalbe agreement with the reference data (overall accuracy of 73% if all potantial variables were included and 75.5% if FVC and AGB were excluded) (Appindix Table. A-1). Importance values of most of the predictor variables were similar except some anthropogenic variables (ecologically effect distance of roads and petroleum and mining license area). In the estimation with all potential variables, annual soil loss, slope, AGB, elevation and distance to roads were identified as top five important variables (Fig. A-5a). For the estimation without FVC and AGB, the most important predictor variables were compound topographic index, distance to road, annual soil loss, soil type, elevation and soil erodibility (Fig. A-5b). According to classification scheme based on field measurements, the land degradation rates are divided into five classes: not degraded, slightly degraded, moderately degraded, heavily degraded and severely degraded. The spatial distribution of degradation and their percentage values is shown in the pie charts of Fig. 6. Consequently, percent distribution for each class is similar in both of LD maps. Furthermore, our results confirmed that most parts of the steppe were affected by some degree of degradation, with more than 36% of the area falling into moderate and severe degradation classes. Overall, only 5-7% of the area were not degraded steppes, whereas slightly degraded steppes occupied 57-58%, moderately degraded 29-30%, heavily degraded 5-6% and severely degraded 1-2%, respectively.

Generally, all degradation classes are similarly discriminated in the both of LD maps. A comparison between the two LD maps clearly shows that not degraded area was largely detected around the lakes and along the river and floodplain vegetation areas in the LD map with all variables (Fig. 6a) while this area was detected only along the river and floodplain vegetation areas in the LD map excluded FVC and AGB (Fig. 6b). Heavily and severely degraded classes were detected as patches in central part of LD map using all variables. For LD estimated without FVC and AGB, heavily degraded areas were similar while severely degraded areas were less pronounced compared to the estimates based on all variables.

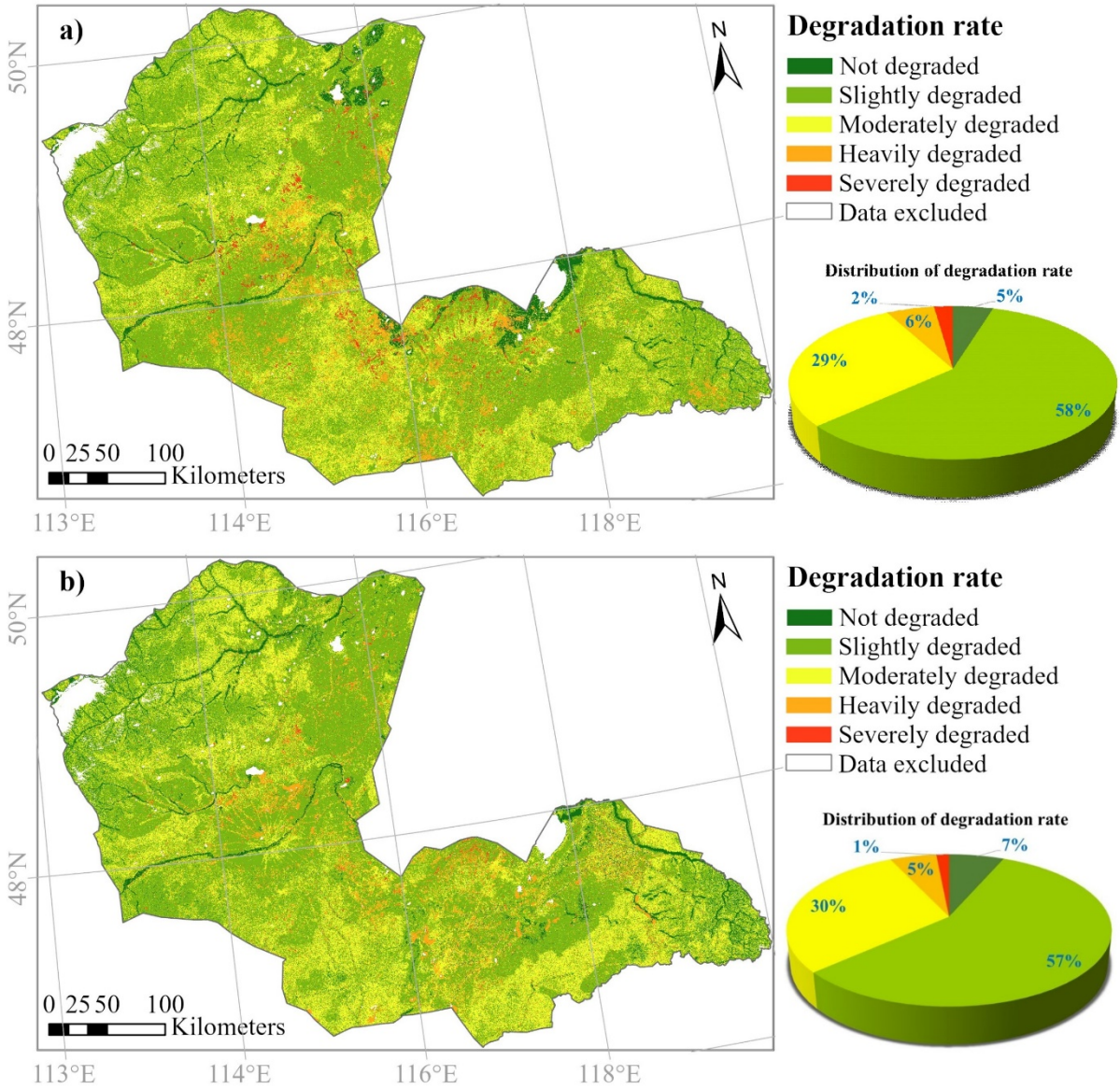

Figure 6. *Land degradation maps: a) all explanatory variables were used for the estimation of LD and b) FVC and AGB were excluded as predictors in the model. Displayed is spatial distribution of degradation rates and their percentage. Water surface and forest area were excluded.*

Regarding the spatial configuration of degradation, not degraded areas were spatially distributed around the meadow steppe, lowland steppe, along the river and floodplain vegetation areas and remote mountain steppe in the far eastern and northern part of study area

(See example in Fig. 7a). Slightly degraded area dominated all over the study area. Areas along the roadside and province center were detected as moderately and heavily degraded (Fig. 7b). The moderately and severely degraded land was spatially concentrated in the central parts of the study area where moderate dry steppe and dry steppe occur. Those areas are generally close to settlements, agriculture, mining and oil exploitation areas (Fig. 7b and c).

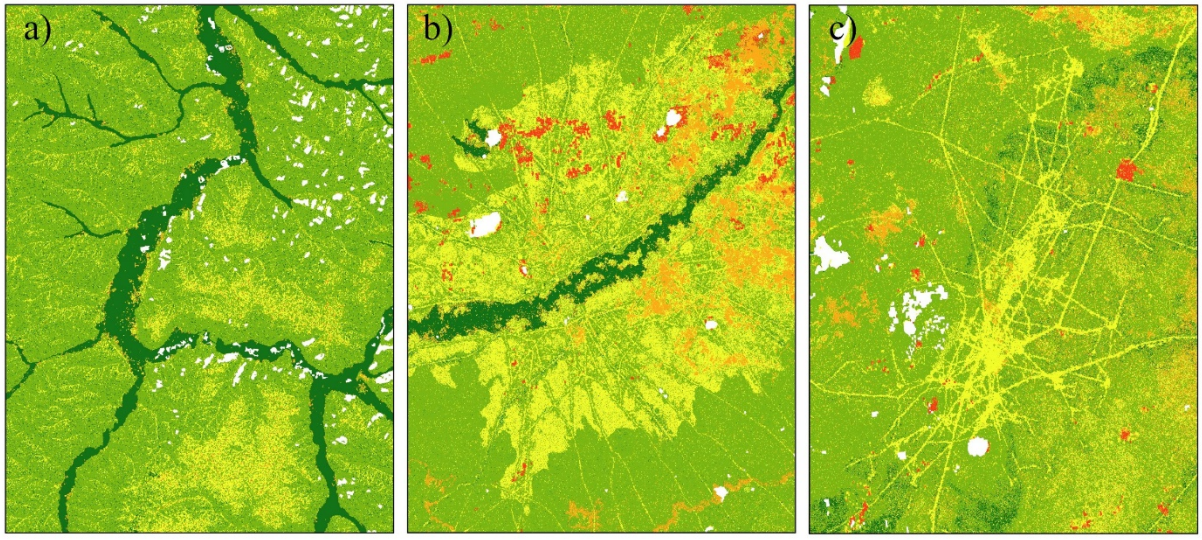

Figure 7. Illustration of land degradation showing mountain steppe and river basin (a), the area around the province center and coal mining (b) and oil exploitation area (c). The color order assigned same as previous Figure 6.

To understand factors driving biomass in Eastern Mongolia, relationships between AGB and all other LD drivers except FVC were examined using Spearman correlation analysis in a running moving window of 500 x 500 pixels in size. Results indicate that no strong relationship between AGB and other LD drivers could be found for any of the individual features over the entire study area. Overall, the correlation analysis suggests that AGB is weakly positively correlated with distance to road, distance to water body, distance to mining and oil exploitation sites, elevation, NDVI trend, precipitation and soil erodibility (for further details on the correlation results, see histograms Fig. A-6 in appendix). Furthermore, AGB is weakly negatively correlated with annual soil loss, aspect, slope and livestock carrying capacity. Regarding the spatial configuration of correlation ranks, AGB has weak to moderate positive relation with distance to roads, distance to water bodies, distance to mining and oil exploitation sites, soil erodibility and soil type in the areas of moderate dry steppe and dry steppe (for further details on the spatial distribution of correlation, see maps Fig. A-7 in appendix). In contrast to the overall results, strong correlations have been detected at local scales indicating that the driving forces are not constant over the entire study area (Fig. 8). In areas for oil exploitation (area 1), AGB is positively correlated with elevation, NDVI trends, distance to mining and oil exploitation sites, distance to road network, while precipitation and road corridors negatively correlate with AGB. More to the south in area 2, AGB is either negatively or positively correlated with distance to water and precipitation sums while it is negatively correlated with precipitation change. In contrast to area 1, distance to mining areas has a negative effect on AGB in area 2. In the province center (area 3), AGB is either negatively or positively correlated with soil types, elevation, distance to water body and distance to road network. In mountain steppes (areas 4 and 5), AGB is positively correlated

with elevation. Precipitation sums affect AGB positively in the northern part, while correlation coefficients were dominantly negative in the southern part.

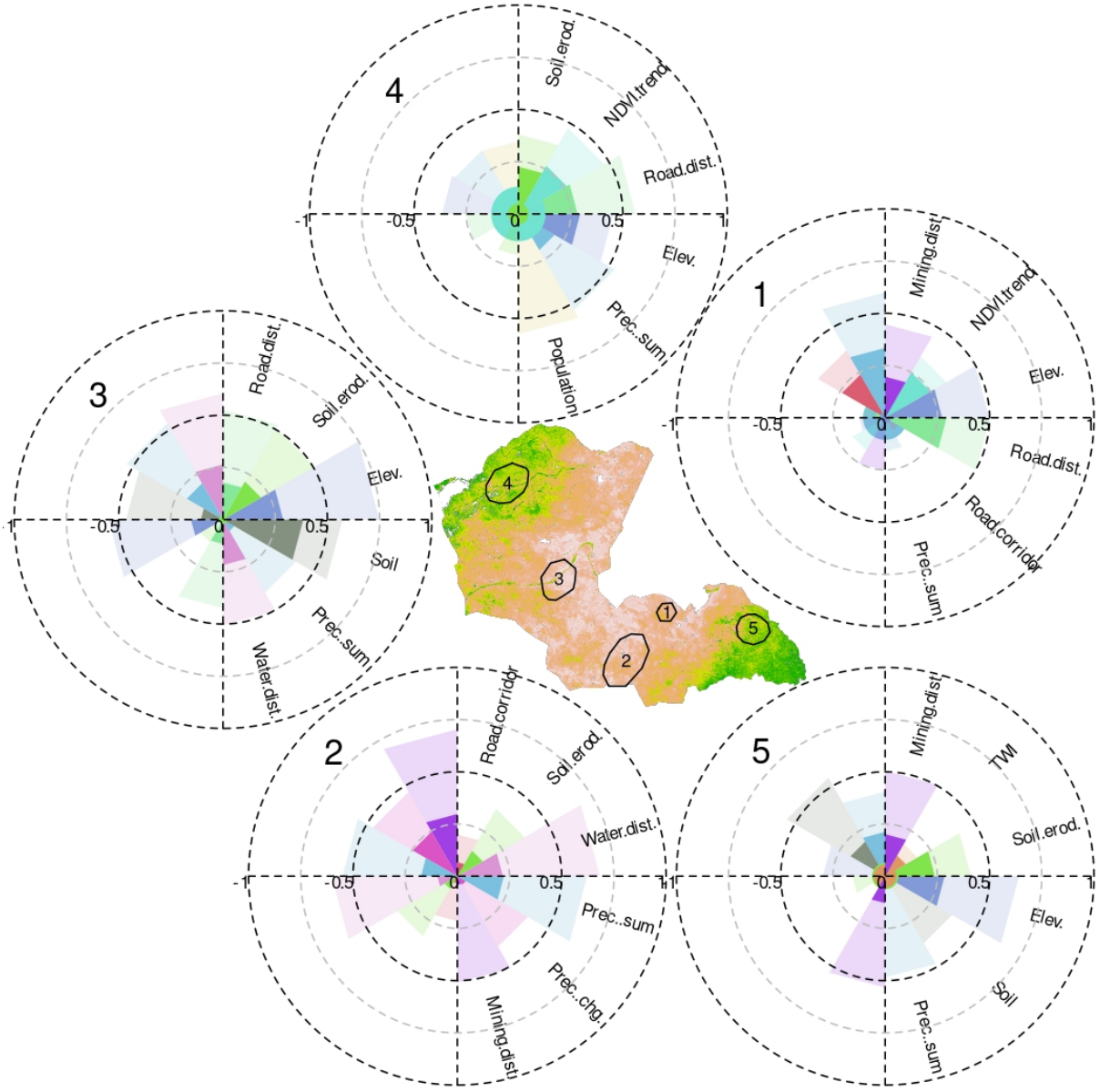

Figure 8. Summary of spearman rank correlation between AGB and potentially important LD drivers in five different areas indicated by numbers 1-5 in the map. Each circle shows a subset of the most important driving factors. The dark coloured parts in the right half of each cicle indicate the 75% quantile of all significant spearman correlation coefficients in the respective area (significance level = 0.001). The light coloured segments indicate the maximum spearman correlation coefficient. The left half of the circles indicate the 25% quantile (solid colour) and the minimum (light colour) of the spearman correlation coefficient. Driving factors were selected for the figure based on the two most important positive and negative factors. In addition, the two factors with the largest interquartile difference were selected.

4. Discussion

4.1 Relevance of the vegetation cover estimation and NDVI trends

One objective of this study is to produce FVC and AGB maps that have been estimated based on Mongolian pasture photo-monitoring data and Sentinel 2 satellite imagery using RF algorithms. The results of FVC and AGB estimation models provide the following new contributions compared to the existing literature. First, the pasture photo-monitoring system in Mongolia is newly developed; however, its platform has already accumulated a unprecedented amount of vegetation data over Mongolia. Nevertheless, no studies have carried out maps of vegetation cover using this above mentioned large vegetation cover data over Mongolia and our study region as well. Therefore, our models and their results provide an effective manner to use this pasture photo-monitoring data for producing vegetation maps over Mongolia and eastern Mongolian steppe regions as well. Next, very few studies have been conducted to map the FVC and AGB over Mongolia and steppe region (Nyamsuren et al., 2019; Yamamoto et al., 2000), however, those studies used very limited field measurement data. For instance, Munkhdulam et.al (Otgonbayar et al., 2019) recently mapped AGB using also an RF model and Landsat imagery over Mongolia that used 553 field measurement sites as training data of RF model for over 1.56 million km^2 area. For this study, we used 256 field measurement sites as training and validation data of RF model for 123.5 thousand km^2 area. Third, our results showed that the spectral indices and characteristics of Sentinal-2 data enable to derive maps of vegetation cover with a spatial resolution of 20 m in Mongolian grasslands. The Sentinel-2 imagery is the one of most widely used remote sensing data for vegetation cover mapping worldwide (Bareth and Waldhoff, 2017; Phiri et al., 2020); however, no study has so far been conducted to derive FVC and AGB from Sentinel-2 data in Mongolian grasslands except forest AGB estimation at small spatial scales (Norovsuren et al., 2019). As expected, the spectral vegetation indices and the spectral channels ranging from the visible red to the near-infrared were the most influential variables in RF models. Especially, NDVI and the Rededge-NIR channels were ranked as most important for the estimation of FVC and AGB, which confirms findings of other studies (Wang et al., 2018; Jie Wang et al., 2019). Regarding the map products, comparison between the higher and lower vegetation values show that the spatial distribution of FVC and AGB perfectly related to the landscapes and ecoregions. The northwestern and far eastern parts are at higher altitudes, high vegetation coverage, and less human interference, while the conditions in the central and northeast area are the opposite.

The majority of similar studies for NDVI trend analysis usually considered that the significantly increasing trends could be a proxy for vegetation cover restoration while significantly decreasing trends are interpreted as ongoing degradation. Thus, NDVI trends have been commonly used for detecting the area of ecological vulnerability (Deng et al., 2020; Easdale et al., 2019; Lamchin et al., 2019; Ma et al., 2020). Likewise, the result of Mann-Kendall trend test showed that both vegetation cover restoration and degradation spatially varied over study area. Focusing on statistically significant parts, a large cluster of decreasing NDVI trends was observed in the central part of the study area over past decades. This observation is generally similar to those found by Wang et al. and Meng et al. (Meng et al., 2021; Wang et al., 2020), who used classification methods on the same NDVI dataset in different year period (1990-2015 and 1990-2020) to estimate the vegetation cover trends over Mongolia. Besides that, Nasanbat et al. (Nasanbat et al., 2018) found that the moderate dry

and dry steppes of Eastern Mongolia experienced decreasing NDVI trends in 2000-2016 based on the Mann-Kendall trend analysis through NDVI time series. Decreasing trends were especially observed for the months June and July during the same period. The significant decreasing trends can be related to the increase of human activities. For instance, the central part of study area is being under high human pressure which is mostly related to oil exploration, exploitation fields and mining. In this area, our previous spatio-temporal analysis showed that the land use for dirt roads, oil exploration and exploitation infrastructure increased by 75% in the past decade (Dashpurev et al., 2020). Besides land use change, several studies confirmed that the aridity of semi-arid ecosystem is one of the driving forces behind land degradation potentially accelerating the degradation process due the climate change in Mongolian grasslands (Miao et al., 2017; Nandintsetseg et al., 2021; Yembuu, 2021b). For instance, air temperatures have increased about 1.4–2.4 °C in Mongolia since 1960s, while the warm season precipitation rapidly declined in the central and eastern parts of Mongolia (Yembuu, 2021b). In addition, our literature review confirmed that livestock grazing pressure largely influences land degradation in Mongolia (Batkhishig, 2013; Na et al., 2018; Tuvshintogtokh and Ariungerel, 2013). However, a recent livestock-caused land degradation assessment showed that Eastern Mongolian steppe grazing has been consistently low compared to other parts of Mongolia (Jamsranjav et al., 2018).

4.2 Relevance of the land degradation mapping

Typical machine learning models were recently applied in the spatial mapping of land degradation (Ghorbanzadeh et al., 2020; Perović et al., 2021; Torabi Haghighi et al., 2021; Yousefi et al., 2021). Several previous studies reported that random forest-based models are applicable for mapping land degradation with reasonable accuracy (Achour et al., 2021; Cheng et al., 2018; Grinand et al., 2020; Nzuza et al., 2020; Sarparast et al., 2018). However, the selection of driver variables was different, which depended on study location and purpose (Mirzabaev et al., 2015). In previous studies, land degradation mapping was generally performed using geomorphometric, geo-environmental, proximity and anthropogenic variables (Grinand et al., 2020; Perović et al., 2021; Sarparast et al., 2018; Torabi Haghighi et al., 2021). In the present study, our model highly depended on ecological variables such as FVC, AGB and MK trend of NDVI. The latter can be interpreted as loss of vegetation cover as a consequence of land degradation. This is consistent with the findings of other studies that used the vegetation cover change as the proxy for land degradation mapping (Higginbottom and Symeonakis, 2014; Kirui et al., 2021; Le et al., 2015). In addition, distance to road, annual soil loss, and soil erodibility were repeatedly ranked as highly important (Fig. A-5a and b). This clearly indicates that those variables can play a major role in the occurrence of land degradation. In the meantime, many studies have stated the impact of soil erodibility and annual soil loss on land degradation in terrestrial ecosystems (Borrelli et al., 2020, 2017b; Zhu et al., 2009). In addition, the result of present study shows that most parts of the steppe were affected by some degree of degradation, with more than 36% of the area falling at least into the moderate degradation class. This result is consistent with the estimate of other studies that used remote sensing and machine learning. For instance, in the most recent study conducted to map land degradation over Mongolia, it was shown that the extensive area of slightly degraded land in eastern Mongolian steppe transformed to moderately degraded land in the year between 1990 and 2020 (Meng et al., 2021).

Conclusion

This research mapped the current land degradation that involved the estimation of FVC, AGB and NDVI trend. In this study, we used 256 field vegetation measurement sites as training and validation data for 124,000 km^2 area. As a result, we obtained maps of FVC and AGB with good accuracy (R^2=0.76-0.81). We additionally found that a statistically significant decreasing trend in NDVI occurred on 59% of the whole study area, which was mostly clustered around the central, middle-eastern and northeastern parts. Finally, we integrated those estimated maps with driving variables of geomorphometric, environment and anthropogenic in order to map the current land degradation using RF model in eastern Mongolia. Results demonstrated current land degradation status with reasonable accuracy based on 256 land degradation field samples. Additionally, correlation analysis showed that no strong relationship could be found over the entire study area; however, strong correlations have been detected at local scales. In other word, results suggested that the land degradation driving forces are not constant over the entire study area. These results are particularly important for policy makers to support counteracting land degradation and improve land management. Furthermore, our models and results show the best practice to use Mongolian pasture photo-monitoring data for producing land degradation and vegetation maps at regional to country-wide scales.

Acknowledgments

The authors acknowledge financial support from the German Academic Exchange Service (DAAD), Research Grants—Doctoral Programmes in Germany (57381412) for Batnyambuu Dashpurev (grant reference number 91691130), and the More Step project (Mobility at risk: Sustaining the Mongolian Steppe Ecosystem) funded by the German Ministry for Education and Research (BMBF) (grant number 01LC1820B). We are thankful to the Agency for Land Administration and Management, Geodesy and Cartography in Mongolia (https://egazar.gov.mn) for providing open access to pasture photo-monitoring data and archive.

Authors' contribution

Batnyambuu Dashpurev: Conceptualization, Methodology, Software, Data preparation, Formal analysis, Investigation, Visualization, Writing- Original draft preparation and Editing. **Munkhtsetseg Dorj:** Field data preparation. **Thanh Noi Phan:** Methodology and Reviewing. **Jörg Bendix:** Conceptualization, Methodology, Supervision and Reviewing. **Lukas W. Lehnert:** Conceptualization, Methodology, Software, Statistical analysis, Supervision, Writing- Reviewing and Editing.

Abbreviations

The following abbreviations are used in this manuscript:

LD	Land degradation
FVC	Fractional vegetation cover
AGB	Aboveground biomass
RF	Random forest
NDVI	Normalized difference vegetation index
MK	"Mann-Kendall" trend test

Appendix A

Figure A-1. *Maps of geomorphometric variables used to estimate the current land degradation condition (a) altitude, b) slope, c) aspect-slope, d) terrain ruggedness index, and e) compound topographic index). Water surface and forest area were excluded.*

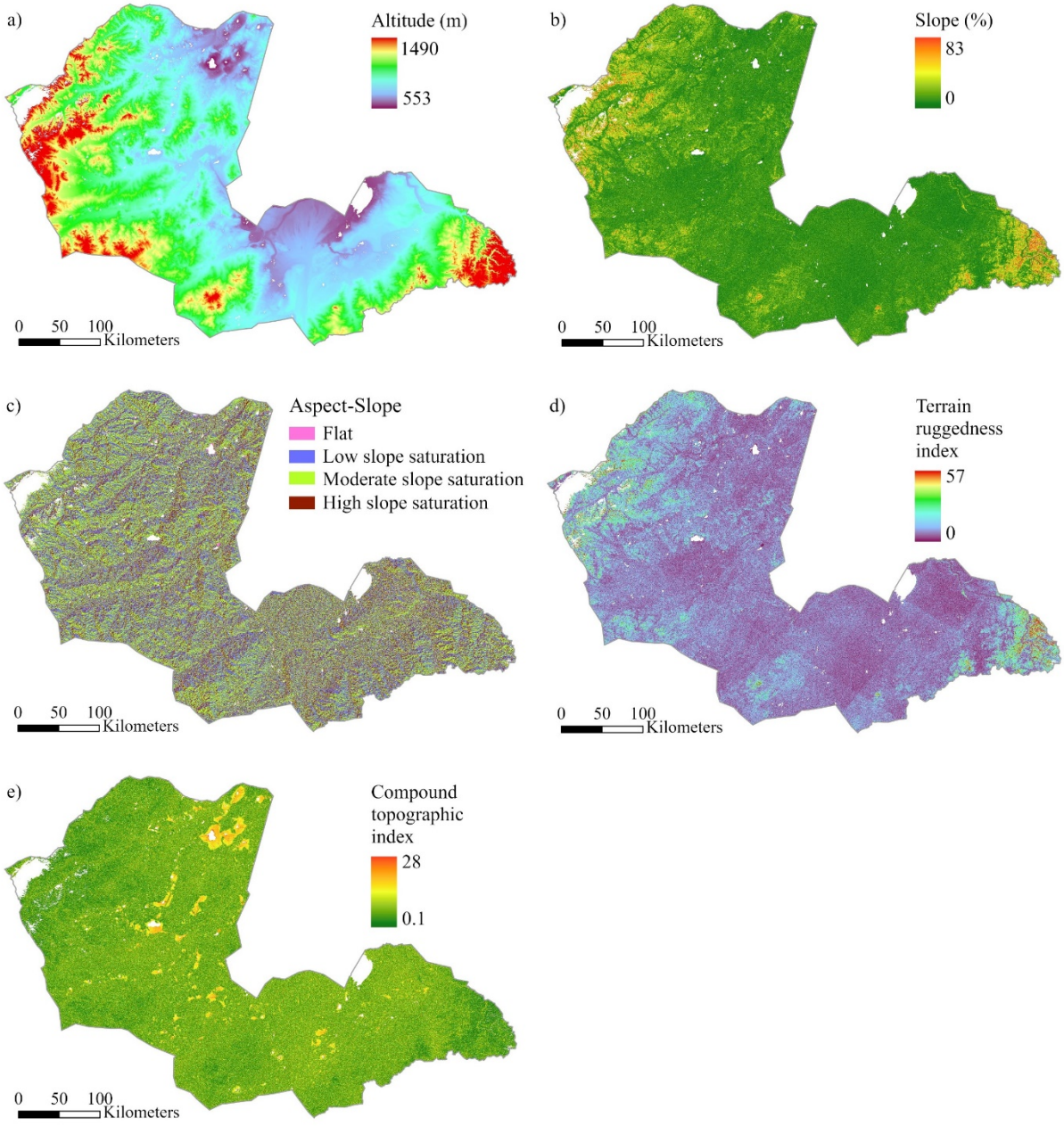

Figure A-2. *Illustration of environmental variables used to estimate the current land degradation condition (a) distance to water body, b) precipitation, c) temperature trend, d) precipitation change, e) soil erodibility, f) annual soil loss, and g) soil type). Water surface and forest area were excluded.*

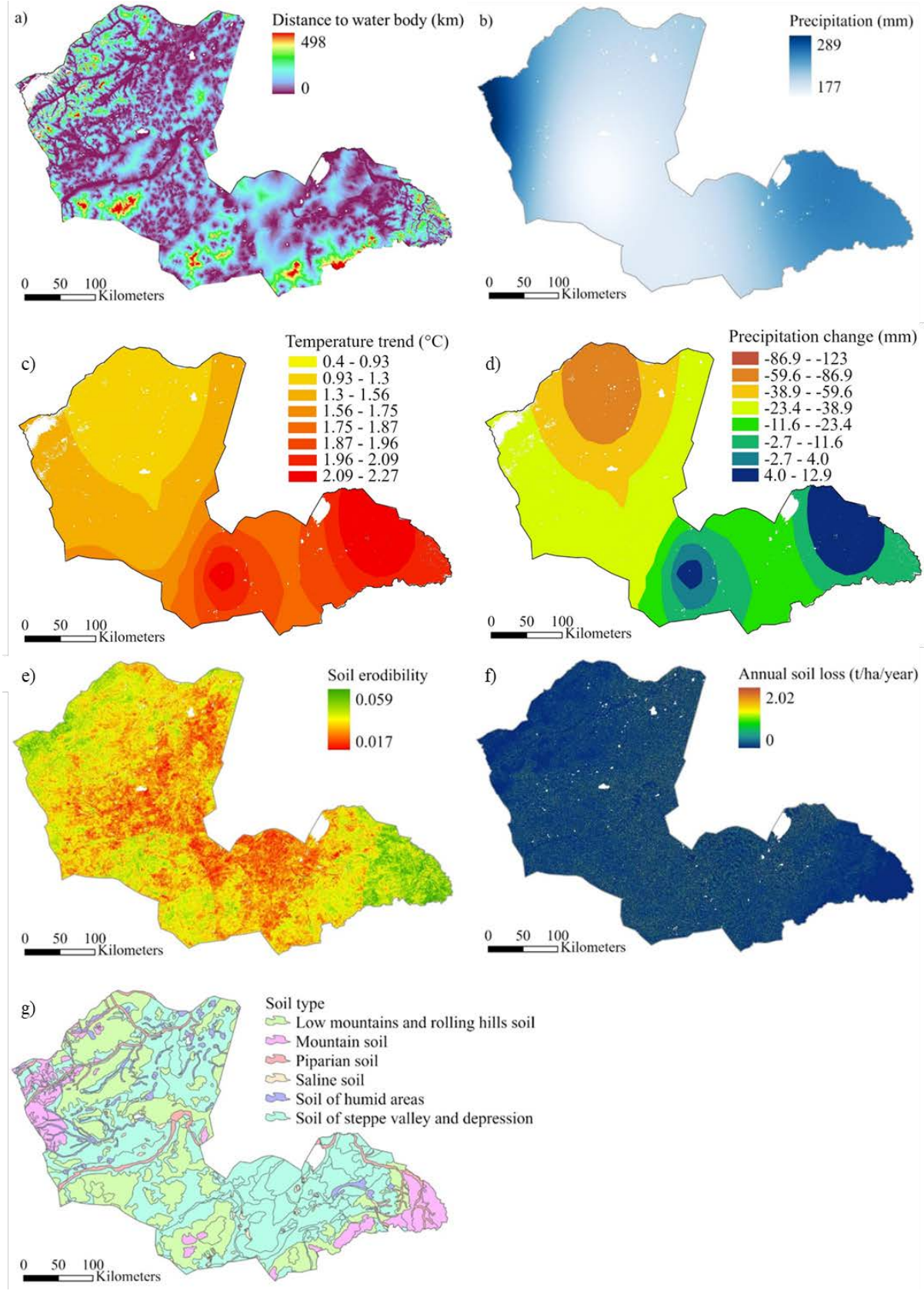

Figure A-3. *Illustration of anthropogenic variables used to estimate the current land degradation condition (a) distance to road, b) effect distance of road network, c) population density, d) mining and oil extraction license area, and e) pasture carrying capacity). Water surface and forest area were excluded.*

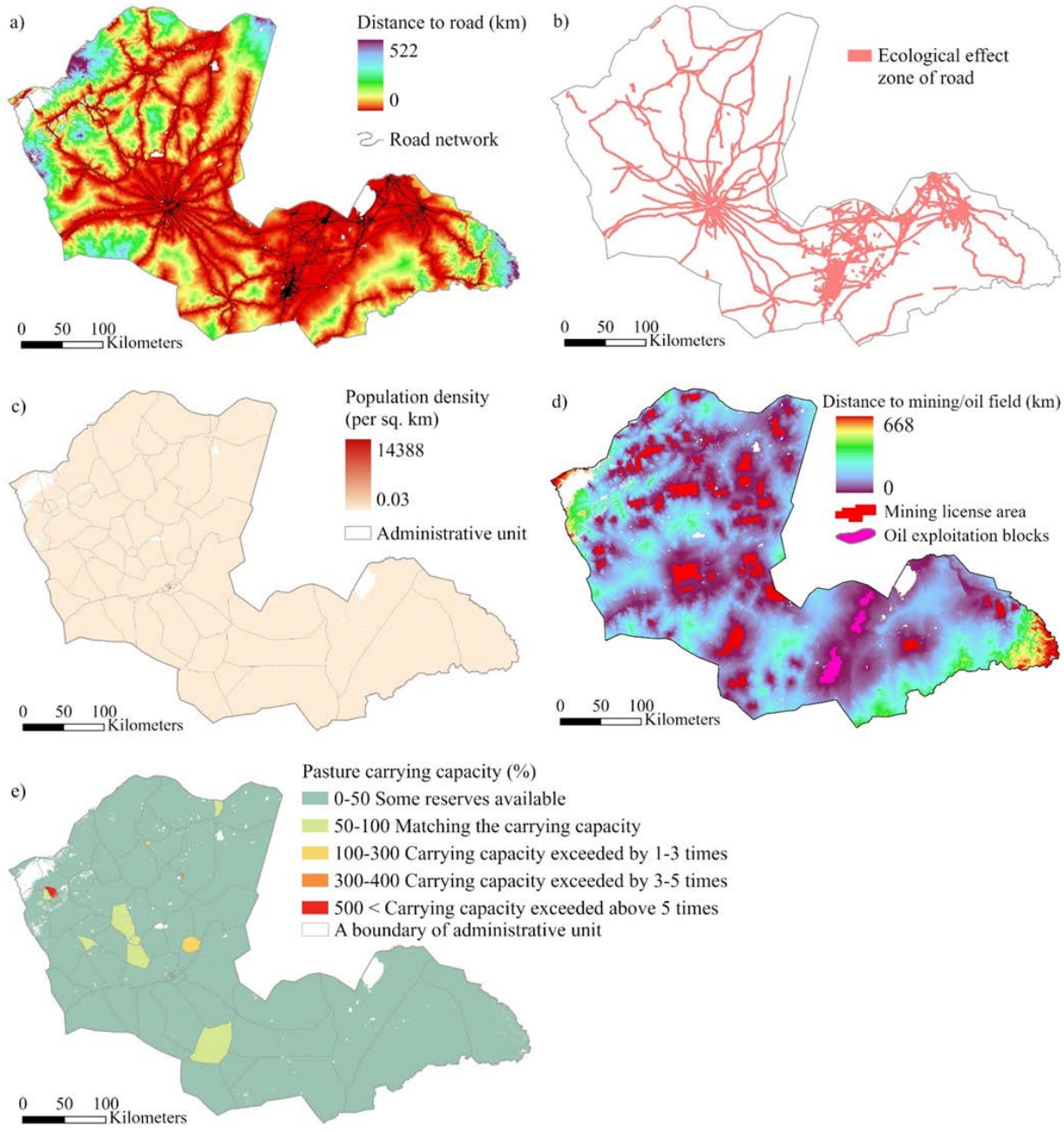

Table A-1. *Evaluation of RF regression performance for Sentinal-2 data. In performance, 10% of reference data excluded for validation.*

Land cover types	Out of Bag (OOB) Errors		Validation data for regression		
	Number of Trees	Percentage of variation explained	R-Squared	p-value	Standard Error
Fractional vegetation cover	250	57.85	0.81	< 0.01	0.12
Aboveground biomass	250	50.9	0.76	< 0.01	0.11

Table A-2. *Evaluation of RF classification performance for twenty land degradation explanatory variables. In performance, 10% of reference data excluded for validation.*

Classes	Out of Bag (OOB) Errors		Validation data for classification			
	Number of Trees	Mean Squared Error (MSE)	F1-Score	MCC	Sensitivity	Accuracy
Not degraded	200	41.58	2.12	0.25	0.31	1.00	0.68
Slightly degraded			50.31	0.17	0.18	0.12	0.67
Moderately degraded			50.20	0.25	0.14	0.17	0.71
Heavily degraded			16.00	0.29	0.13	0.33	0.74
Severely degraded			0.85	0.67	0.69	1.00	0.85

Figure A-4*. Variable importance of FVC (a) and AGB estimation (b).*

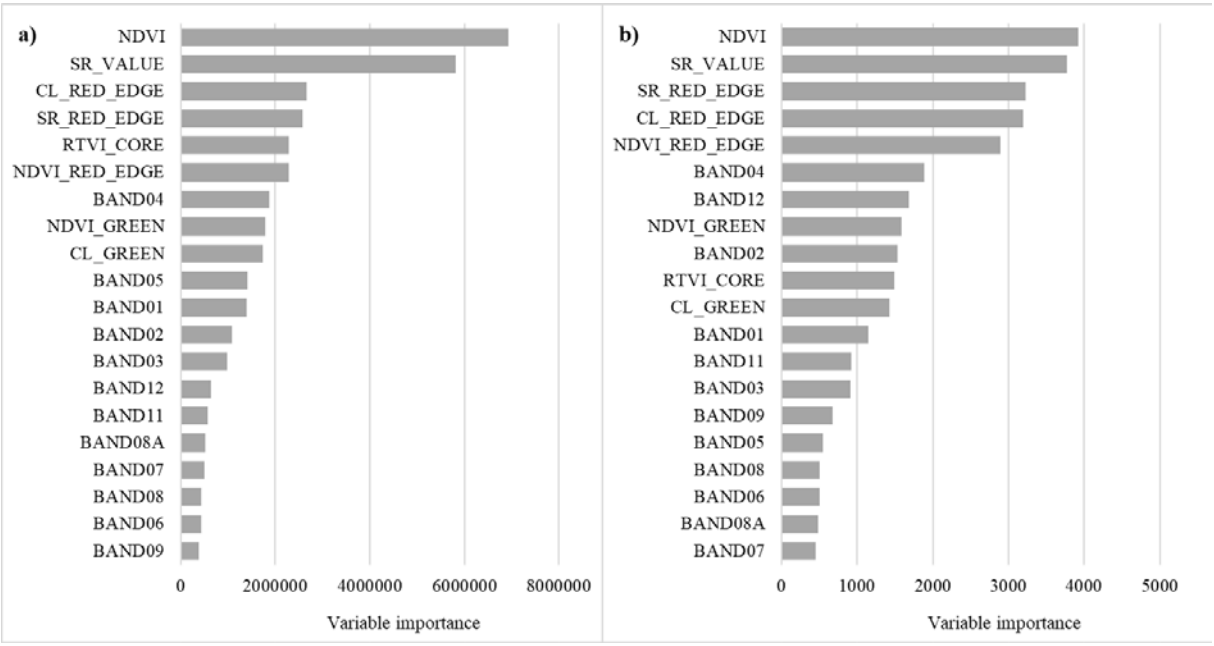

Figure A-5. *Variable importance of land degradation mapping: a) all explanatory variables were used in estimation and b) FVC and AGB were excluded in estimation.*

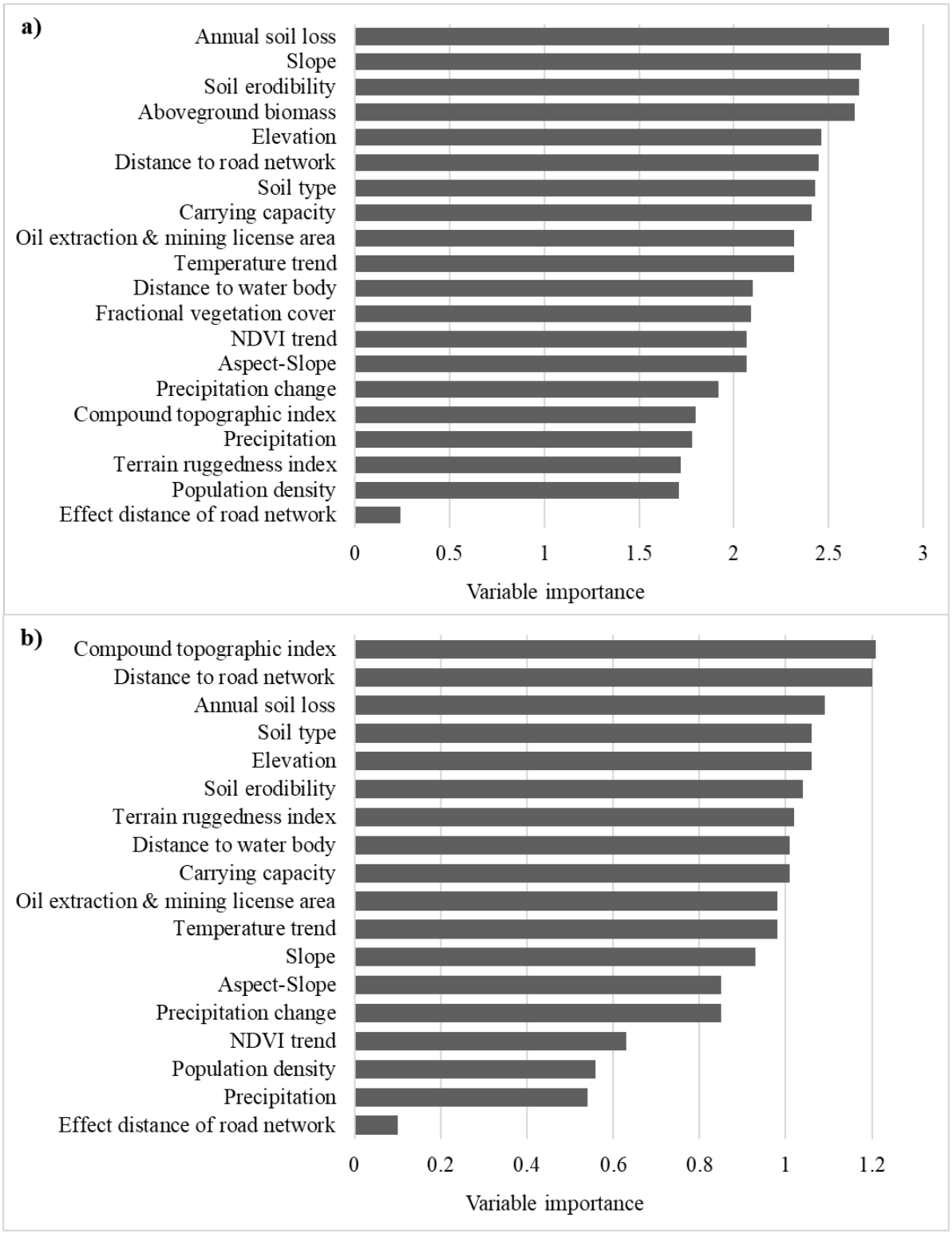

Figure A-6. Spearman rank correlation between biomass and all other land degradation drivers except FVC ($p < 0.05$).

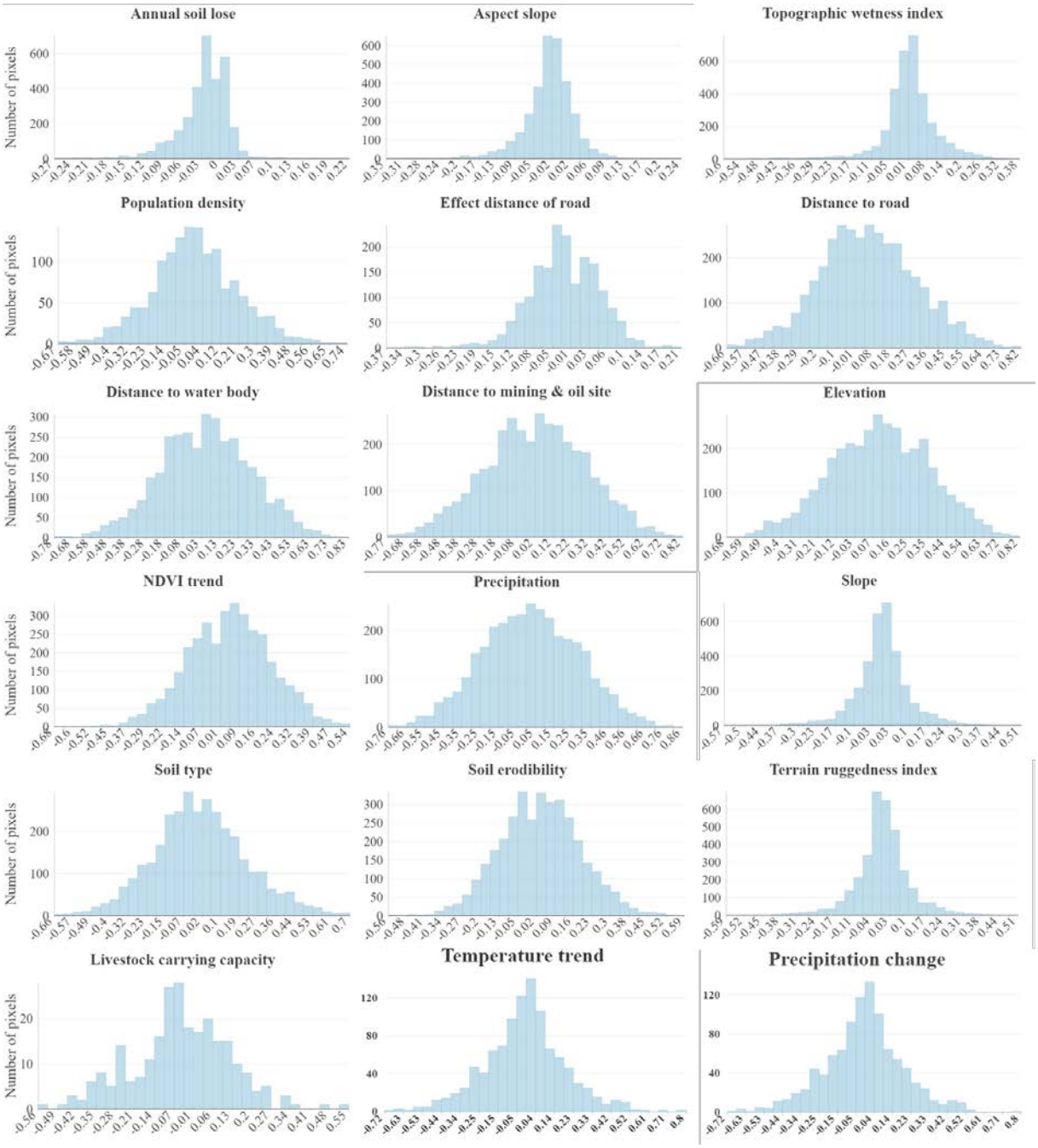

Figure A-7. Spatial distribution of Spearman rank correlation coefficient ($p < 0.05$).

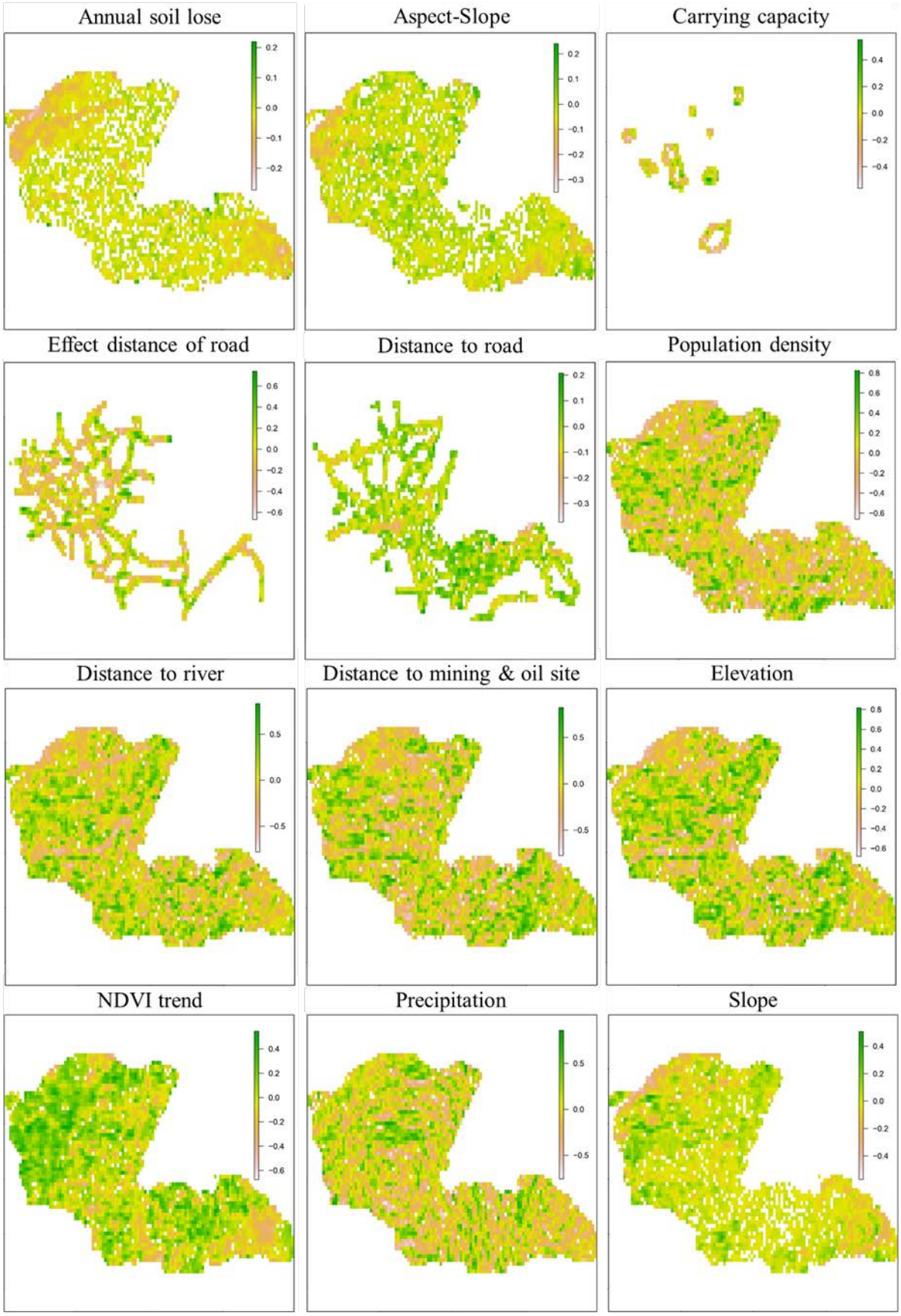

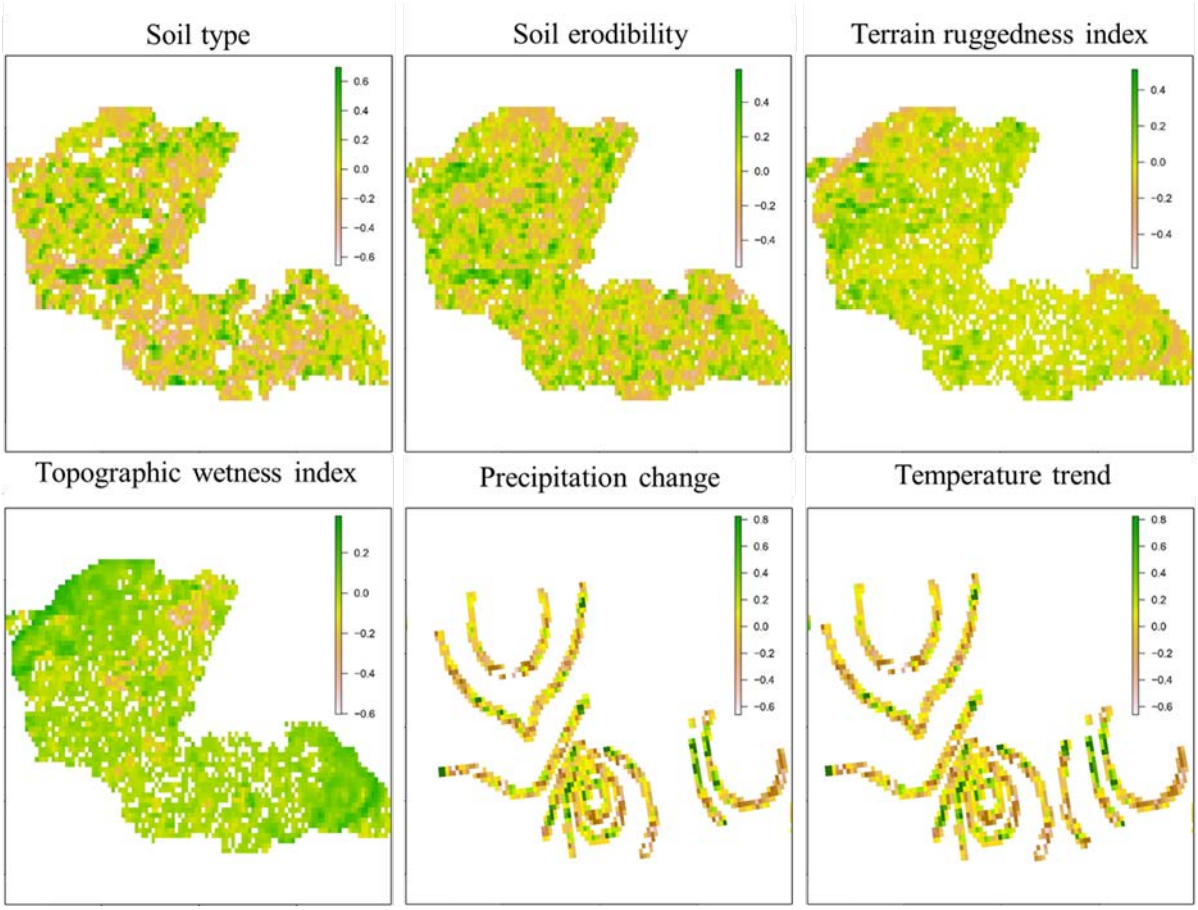
Soil type
Soil erodibility
Terrain ruggedness index
Topographic wetness index
Precipitation change
Temperature trend

References

AbdelRahman, M.A.E., Natarajan, A., Hegde, R., Prakash, S.S., 2019. Assessment of land degradation using comprehensive geostatistical approach and remote sensing data in GIS-model builder. Egypt. J. Remote Sens. Sp. Sci. 22, 323–334. https://doi.org/10.1016/j.ejrs.2018.03.002

Abuzaid, A.S., Abdelrahman, M.A.E., Fadl, M.E., Scopa, A., 2021. Land degradation vulnerability mapping in a newly-reclaimed desert oasis in a hyper-arid agro-ecosystem using ahp and geospatial techniques. Agronomy 11, 1426. https://doi.org/10.3390/agronomy11071426

Achour, Y., Saidani, Z., Touati, R., Pham, Q.B., Pal, S.C., Mustafa, F., Balik Sanli, F., 2021. Assessing landslide susceptibility using a machine learning-based approach to achieving land degradation neutrality. Environ. Earth Sci. 80. https://doi.org/10.1007/s12665-021-09889-9

Albalawi, E.K., Kumar, L., 2013. Using remote sensing technology to detect, model and map desertification: A review. J. Food, Agric. Environ. 11, 791–797.

Asian Development Bank, 2013. Making Grasslands Sustainable in Mongolia Adapting to climate and encironmental change.

Aynekulu, E., Lohbeck, M., Nijbroek, R., Ordoñez, J.C., Turner, K., Vågen, T.-G., Winowiecki, L., 2017. Review of Methodologies for Land Degradation Neutrality Baselines 58.

Bai, Z.G., Dent, D.L., Olsson, L., Schaepman, M.E., 2008. Proxy global assessment of land degradation. Soil Use Manag. https://doi.org/10.1111/j.1475-2743.2008.00169.x

Bareth, G., Waldhoff, G., 2017. GIS for Mapping Vegetation, in: Comprehensive Geographic Information Systems. Elsevier Inc., pp. 1–27. https://doi.org/10.1016/B978-0-12-409548-9.09636-6

Batkhishig, O., 2013. Chapter 12. Human Impact and Land Degradation in Mongolia, in: Dryland East Asia: Land Dynamics amid Social and Climate Change. DE GRUYTER. https://doi.org/10.1515/9783110287912.265

Batsaikhan, N., Buuveibaatar, B., Chimed, B., Enkhtuya, O., Galbrakh, D., Ganbaatar, O., Lkhagvasuren, B., Nandintsetseg, D., Berger, J., Calabrese, J.M., Edwards, A.E., Fagan, W.F., Fuller, T.K., Heiner, M., Ito, T.Y., Kaczensky, P., Leimgruber, P., Lushchekina, A., Milner-Gulland, E.J., Mueller, T., Murray, M.G., Olson, K.A., Reading, R., Schaller, G.B., Stubbe, A., Stubbe, M., Walzer, C., Von Wehrden, H., Whitten, T., 2014. Conserving the World's Finest Grassland Amidst Ambitious National Development. Conserv. Biol. 28, 1736–1739. https://doi.org/10.1111/cobi.12297

Belgiu, M., Drăgu, L., 2016. Random forest in remote sensing: A review of applications and future directions. ISPRS J. Photogramm. Remote Sens. https://doi.org/10.1016/j.isprsjprs.2016.01.011

Borrelli, P., Robinson, D.A., Fleischer, L.R., Lugato, E., Ballabio, C., Alewell, C., Meusburger, K., Modugno, S., Schütt, B., Ferro, V., Bagarello, V., Oost, K. Van, Montanarella, L., Panagos, P., 2017a. An assessment of the global impact of 21st century land use change on soil erosion. Nat. Commun. 8, 1–13. https://doi.org/10.1038/s41467-017-02142-7

Borrelli, P., Robinson, D.A., Fleischer, L.R., Lugato, E., Ballabio, C., Alewell, C., Meusburger, K., Modugno, S., Schütt, B., Ferro, V., Bagarello, V., Oost, K. Van, Montanarella, L., Panagos, P., 2017b. An assessment of the global impact of 21st century land use change on soil erosion. Nat. Commun. 8, 1–13. https://doi.org/10.1038/s41467-017-02142-7

Borrelli, P., Robinson, D.A., Panagos, P., Lugato, E., Yang, J.E., Alewell, C., Wuepper, D., Montanarella, L., Ballabio, C., 2020. Land use and climate change impacts on global soil erosion by water (2015-2070). Proc. Natl. Acad. Sci. U. S. A. 117, 21994–22001. https://doi.org/10.1073/pnas.2001403117

Breiman, L., 2001. Random forests. Mach. Learn. 45, 5–32. https://doi.org/10.1023/A:1010933404324

Cagney, J., Cox, S.E., Booth, D.T., 2011. Comparison of point intercept and image analysis for monitoring rangeland transects. Rangel. Ecol. Manag. 64, 309–315. https://doi.org/10.2111/REM-D-10-00090.1

Caspari, T., van Lynden, G., Bai, Z., Databases, D. not cite information about, 2015. Land Degradation Neutrality: An Evaluation of Methods 57 p.

Cheng, Z., Lu, D., Li, G., Huang, J., Sinha, N., Zhi, J., Li, S., 2018. A random forest-based approach to map soil erosion risk distribution in hickory plantations in Western Zhejiang Province, China. Remote Sens. 10, 1899. https://doi.org/10.3390/rs10121899

Congalton, R.G., 1991. A review of assessing the accuracy of classifications of remotely sensed data. Remote Sens. Environ. 37, 35–46. https://doi.org/10.1016/0034-4257(91)90048-B

Cowie, A.L., Orr, B.J., Castillo Sanchez, V.M., Chasek, P., Crossman, N.D., Erlewein, A., Louwagie, G., Maron, M., Metternicht, G.I., Minelli, S., Tengberg, A.E., Walter, S., Welton, S., 2018. Land in balance: The scientific conceptual framework for Land Degradation Neutrality. Environ. Sci. Policy 79, 25–35. https://doi.org/10.1016/j.envsci.2017.10.011

Darbalaeva, D., Mikheeva, A., Zhamyanova, Y., 2020. The socio-economic consequences of the desertification processes in Mongolia, in: E3S Web of Conferences. https://doi.org/10.1051/e3sconf/202016411001

Dashpurev, B., Bendix, J., Lehnert, L.W., 2020. Monitoring oil exploitation infrastructure and dirt roads with object-based image analysis and random forest in the Eastern Mongolian Steppe. Remote Sens. 12, 144. https://doi.org/10.3390/RS12010144

Dashpurev, B., Wesche, K., Jäschke, Y., Oyundelger, K., Phan, T.N., Bendix, J., Lehnert, L.W., 2021. A cost-effective method to monitor vegetation changes in steppes ecosystems: A case study on remote sensing of fire and infrastructure effects in eastern Mongolia. Ecol. Indic. 132, 108331. https://doi.org/10.1016/j.ecolind.2021.108331

David, N., Mathew, R., 2020. Review of Machine Learning in Geosciences and Remote Sensing, in: Lecture Notes on Data Engineering and Communications Technologies. Springer Science and Business Media Deutschland GmbH, pp. 195–204. https://doi.org/10.1007/978-3-030-43192-1_22

Deng, H., Yin, Y., Han, X., 2020. Vulnerability of vegetation activities to drought in Central Asia. Environ. Res. Lett. 15, 084005. https://doi.org/10.1088/1748-9326/ab93fa

Densambuu, B., Sainnemekh, S., Bestelmeyer, B., Ulambayar, B., Batjargal, E., 2018. National report on the rangeland health of Mongolia: Second Assessment. Ulaanbaatar.

Dodge, Y., 2008. Spearman Rank Correlation Coefficient, in: The Concise Encyclopedia of Statistics. Springer New York LLC, New York, pp. 502–505. https://doi.org/10.1007/978-0-387-32833-1

Dubovyk, O., 2017. The role of Remote Sensing in land degradation assessments: opportunities and challenges. Eur. J. Remote Sens. https://doi.org/10.1080/22797254.2017.1378926

Easdale, M.H., Fariña, C., Hara, S., Pérez León, N., Umaña, F., Tittonell, P., Bruzzone, O., 2019. Trend-cycles of vegetation dynamics as a tool for land degradation assessment and monitoring. Ecol. Indic. 107, 105545. https://doi.org/10.1016/j.ecolind.2019.105545

Eckert, S., Hüsler, F., Liniger, H., Hodel, E., 2015. Trend analysis of MODIS NDVI time series for detecting land degradation and regeneration in Mongolia. J. Arid Environ. 113, 16–28. https://doi.org/10.1016/j.jaridenv.2014.09.001

Elbegjargal, N., Khudulmur, S., Tsogtbaatar, J., Dash, D., Mandakh, N., 2014. Desertification Atlas of Mongolia, Institute of Geoecology, Mongolian Academy of Sciences.

FAO, 2013. The state of the world's land and water resources for food and agriculture: Managing systems at risk, FAO. https://doi.org/10.4324/9780203142837

Foga, S., Scaramuzza, P.L., Guo, S., Zhu, Z., Dilley, R.D., Beckmann, T., Schmidt, G.L., Dwyer, J.L., Joseph Hughes, M., Laue, B., 2017. Cloud detection algorithm comparison and validation for operational Landsat data products. Remote Sens. Environ. 194, 379–390. https://doi.org/10.1016/j.rse.2017.03.026

Forman, R.T.T., Alexander, L.E., 1998. Roads and their major ecological effects. Annu. Rev. Ecol. Syst. 29, 207–231. https://doi.org/10.1146/annurev.ecolsys.29.1.207

GEIST, H.J., LAMBIN, E.F., 2004. Dynamic Causal Patterns of Desertification. Bioscience 54, 817. https://doi.org/10.1641/0006-3568(2004)054[0817:dcpod]2.0.co;2

Ghorbanzadeh, O., Shahabi, H., Mirchooli, F., Valizadeh Kamran, K., Lim, S., Aryal, J., Jarihani, B., Blaschke, T., 2020. Gully erosion susceptibility mapping (GESM) using machine learning methods optimized by the multi-collinearity analysis and K-fold cross-validation. Geomatics, Nat. Hazards Risk 11, 1653–1678. https://doi.org/10.1080/19475705.2020.1810138

Gibbs, H.K., Salmon, J.M., 2015. Mapping the world's degraded lands. Appl. Geogr. https://doi.org/10.1016/j.apgeog.2014.11.024

Girvetz, E.H., McDonald, R., Heiner, M., Kiesecker, J., Davaa, G., Pague, C., Durnin, M., Oidov, E., 2014. Eastern mongolian grassland steppe, in: Climate and Conservation: Landscape and Seascape Science, Planning, and Action. Island Press-Center for Resource Economics, pp. 92–103. https://doi.org/10.5822/978-1-61091-203-7_8

Gitelson, A., Merzlyak, M.N., 1994. Spectral Reflectance Changes Associated with Autumn Senescence of Aesculus hippocastanum L. and Acer platanoides L. Leaves. Spectral Features and Relation to Chlorophyll Estimation. J. Plant Physiol. 143, 286–292. https://doi.org/10.1016/S0176-1617(11)81633-0

Gitelson, A.A., Gritz, Y., Merzlyak, M.N., 2003. Relationships between leaf chlorophyll

content and spectral reflectance and algorithms for non-destructive chlorophyll assessment in higher plant leaves. J. Plant Physiol. 160, 271–282. https://doi.org/10.1078/0176-1617-00887

Gitelson, A.A., Kaufman, Y.J., Merzlyak, M.N., 1996. Use of a green channel in remote sensing of global vegetation from EOS- MODIS. Remote Sens. Environ. 58, 289–298. https://doi.org/10.1016/S0034-4257(96)00072-7

Gitelson, A.A., Kaufman, Y.J., Stark, R., Rundquist, D., 2002. Novel algorithms for remote estimation of vegetation fraction. Remote Sens. Environ. 80, 76–87. https://doi.org/10.1016/S0034-4257(01)00289-9

Gitelson, A.A., Viña, A., Ciganda, V., Rundquist, D.C., Arkebauer, T.J., 2005. Remote estimation of canopy chlorophyll content in crops. Geophys. Res. Lett. 32, 1–4. https://doi.org/10.1029/2005GL022688

Grinand, C., Vieilledent, G., Razafimbelo, T., Rakotoarijaona, J.R., Nourtier, M., Bernoux, M., 2020. Landscape-scale spatial modelling of deforestation, land degradation, and regeneration using machine learning tools. L. Degrad. Dev. 31, 1699–1712. https://doi.org/10.1002/ldr.3526

Haboudane, D., Miller, J.R., Pattey, E., Zarco-Tejada, P.J., Strachan, I.B., 2004. Hyperspectral vegetation indices and novel algorithms for predicting green LAI of crop canopies: Modeling and validation in the context of precision agriculture. Remote Sens. Environ. 90, 337–352. https://doi.org/10.1016/j.rse.2003.12.013

Han, J., Dai, H., Gu, Z., 2021. Sandstorms and desertification in Mongolia, an example of future climate events: a review. Environ. Chem. Lett. https://doi.org/10.1007/s10311-021-01285-w

Hartvigsen, G., 2017. Carrying Capacity, Concept of ☆, in: Reference Module in Life Sciences. Elsevier. https://doi.org/10.1016/b978-0-12-809633-8.02393-1

Hengl, T., De Jesus, J.M., Heuvelink, G.B.M., Gonzalez, M.R., Kilibarda, M., Blagotić, A., Shangguan, W., Wright, M.N., Geng, X., Bauer-Marschallinger, B., Guevara, M.A., Vargas, R., MacMillan, R.A., Batjes, N.H., Leenaars, J.G.B., Ribeiro, E., Wheeler, I., Mantel, S., Kempen, B., 2017. SoilGrids250m: Global gridded soil information based on machine learning. PLoS One 12, e0169748. https://doi.org/10.1371/journal.pone.0169748

Higginbottom, T.P., Symeonakis, E., 2014. Assessing land degradation and desertification using vegetation index data: Current frameworks and future directions. Remote Sens. https://doi.org/10.3390/rs6109552

Hilker, T., Natsagdorj, E., Waring, R.H., Lyapustin, A., Wang, Y., 2014. Satellite observed widespread decline in Mongolian grasslands largely due to overgrazing. Glob. Chang. Biol. 20, 418–428. https://doi.org/10.1111/gcb.12365

Hironaka, M., Fosberg, M.A., Kenneth E. Neiman, J., 1991. The Relationship Between Soils and Vegetation. Proc. - Manag. Product. West. For. soils, Boise, April 1990 280, 29–31.

Huang, S., Tang, L., Hupy, J.P., Wang, Y., Shao, G., 2021. A commentary review on the use of normalized difference vegetation index (NDVI) in the era of popular remote sensing. J. For. Res. https://doi.org/10.1007/S11676-020-01155-1/FIGURES/2

Jamsranjav, C., Reid, R.S., Fernández-Giménez, M.E., Tsevlee, A., Yadamsuren, B., Heiner, M., 2018. Applying a dryland degradation framework for rangelands: the case of Mongolia. Ecol. Appl. 28, 622–642. https://doi.org/10.1002/eap.1684

Jordan, C.F., 1969. Derivation of Leaf-Area Index from Quality of Light on the Forest Floor. Ecology 50, 663–666. https://doi.org/10.2307/1936256

Jugder, D., Gantsetseg, B., Davaanyam, E., Shinoda, M., 2018. Developing a soil erodibility map across Mongolia. Nat. Hazards 92, 71–94. https://doi.org/10.1007/s11069-018-3409-6

Keshkamat, S.S., Tsendbazar, N.E., Zuidgeest, M.H.P., Shiirev-Adiya, S., van der Veen, A., van Maarseveen, M.F.A.M., 2013. Understanding transportation-caused rangeland damage in Mongolia. J. Environ. Manage. 114, 433–444. https://doi.org/10.1016/j.jenvman.2012.10.043

Khishigbayar, J., Fernández-Giménez, M.E., Angerer, J.P., Reid, R.S., Chantsallkham, J., Baasandorj, Y., Zumberelmaa, D., 2015. Mongolian rangelands at a tipping point? Biomass and cover are stable but composition shifts and richness declines after 20years of grazing and increasing temperatures. J. Arid Environ. 115, 100–112. https://doi.org/10.1016/j.jaridenv.2015.01.007

Kim, Jungrack, Dorjsuren, M., Choi, Y., Purevjav, G., 2020. Reconstructed Aeolian Surface Erosion in Southern Mongolia by Multi-Temporal InSAR Phase Coherence Analyses. Front. Earth Sci. 8, 458. https://doi.org/10.3389/feart.2020.531104

Kim, Jaebeom, Kang, S., Seo, B., Narantsetseg, A., Han, Y., 2020. Estimating fractional green vegetation cover of Mongolian grasslands using digital camera images and MODIS satellite vegetation indices. GIScience Remote Sens. 57, 49–59. https://doi.org/10.1080/15481603.2019.1662166

Kinugasa, T., Suzuyama, Y., Tsuchihashi, N., Nachinshonhor, G.U., 2015. Colonization and expansion of grassland species after abandonment of dirt roads in the Mongolian steppe. Landsc. Ecol. Eng. 11, 19–27. https://doi.org/10.1007/s11355-013-0230-y

Kirui, O.K., Mirzabaev, A., von Braun, J., 2021. Assessment of land degradation ‘on the ground’ and from ‘above.’ SN Appl. Sci. 3, 1–13. https://doi.org/10.1007/s42452-021-04314-z

Lamchin, M., Lee, W.K., Jeon, S.W., Wang, S.W., Lim, C.H., Song, C., Sung, M., 2019. Corrigendum to “Mann-Kendall Monotonic Trend Test and Correlation Analysis using Spatio-temporal Dataset: the case of Asia using vegetation greenness and climate factors” (MethodsX (2018) 5 (803–807), (S2215016118301134), (10.1016/j.mex.2018.07.006)). MethodsX. https://doi.org/10.1016/j.mex.2019.05.030

Le, Q.B., Nkonya, E., Mirzabaev, A., 2015. Biomass productivity-based mapping of global land degradation hotspots, in: Economics of Land Degradation and Improvement - A Global Assessment for Sustainable Development. Springer International Publishing, pp. 55–84. https://doi.org/10.1007/978-3-319-19168-3_4

Lee, E.J., Piao, D., Song, C., Kim, J., Lim, C.H., Kim, E., Moon, J., Kafatos, M., Lamchin, M., Jeon, S.W., Lee, W.K., 2019. Assessing environmentally sensitive land to desertification using MEDALUS method in Mongolia. Forest Sci. Technol. 15, 210–220. https://doi.org/10.1080/21580103.2019.1667880

Liu, Y.Y., Evans, J.P., McCabe, M.F., de Jeu, R.A.M., van Dijk, A.I.J.M., Dolman, A.J., Saizen, I., 2013. Changing Climate and Overgrazing Are Decimating Mongolian Steppes. PLoS One 8, 57599. https://doi.org/10.1371/journal.pone.0057599

Lkhagva, A., Boldgiv, B., Goulden, C.E., Yadamsuren, O., Lauenroth, W.K., 2013. Effects of grazing on plant community structure and aboveground net primary production of semiarid boreal steppe of northern Mongolia. Grassl. Sci. 59, 135–145. https://doi.org/10.1111/grs.12022

Ma, J., Zhang, C., Guo, H., Chen, W., Yun, W., Gao, L., Wang, H., 2020. Analyzing ecological vulnerability and vegetation phenology response using NDVI time series data and the BFAST algorithm. Remote Sens. 12, 1–21. https://doi.org/10.3390/rs12203371

Ma, Q., Wu, J., He, C., Fang, X., 2021. The speed, scale, and environmental and economic impacts of surface coal mining in the Mongolian Plateau. Resour. Conserv. Recycl. 173, 105730. https://doi.org/10.1016/j.resconrec.2021.105730

Martin Pfeiffer, Choimaa Dulamsuren, Y.J. and K.W., 2018. Grasslands of China and Mongolia: Spatial Extent, Land Use and Conservation, in: Grasslands of the World : Diversity, Management and Conservation. pp. 168–196.

Meng, X., Gao, X., Li, S., Lei, J., 2020. Spatial and Temporal Characteristics of Vegetation NDVI Changes and the Driving Forces in Mongolia during 1982–2015. Remote Sens. 2020, Vol. 12, Page 603 12, 603. https://doi.org/10.3390/RS12040603

Meng, X., Gao, X., Li, Sen, Li, Shengyu, Lei, J., 2021. Monitoring desertification in Mongolia based on Landsat images and Google Earth Engine from 1990 to 2020. Ecol. Indic. 129, 107908. https://doi.org/10.1016/j.ecolind.2021.107908

Miao, L., Müller, D., Cui, X., Ma, M., 2017. Changes in vegetation phenology on the Mongolian Plateau and their climatic determinants. PLoS One 12. https://doi.org/10.1371/journal.pone.0190313

Mirzabaev, A., Nkonya, E., Goedecke, J., Johnson, T., Anderson, W., 2015. Global drivers of land degradation and improvement, in: Economics of Land Degradation and Improvement - A Global Assessment for Sustainable Development. Springer International Publishing, pp. 167–195. https://doi.org/10.1007/978-3-319-19168-3_7

Mongolia EITI, 2018. Mongolia 2017 EITI Report: Extractive Industries Transparency Initiative. Ulaanbaatar.

Mortimore, M., 1993. Population growth and land degradation. GeoJournal 31, 15–21. https://doi.org/10.1007/BF00815897

Munkhzul, O., Oyundelger, K., Narantuya, N., Tuvshintogtokh, I., Oyuntsetseg, B., Wesche, K., Jäschke, Y., 2021. Grazing Effects on Mongolian Steppe Vegetation—A Systematic Review of Local Literature. Front. Ecol. Evol. 9, 719. https://doi.org/10.3389/FEVO.2021.703220/BIBTEX

Na, Y., Li, J., Hoshino, B., Bao, S., Qin, F., Myagmartseren, P., 2018. Effects of different grazing systems on aboveground biomass and plant species dominance in typical Chinese and Mongolian steppes. Sustain. 10, 4753. https://doi.org/10.3390/su10124753

Nandintsetseg, B., Boldgiv, B., Chang, J., Ciais, P., Davaanyam, E., Batbold, A., Bat-Oyun, T., Stenseth, N.C., 2021. Risk and vulnerability of Mongolian grasslands under climate

change. Environ. Res. Lett. 16, 034035. https://doi.org/10.1088/1748-9326/abdb5b

Nasanbat, E., Sharav, S., Sanjaa, T., Lkhamjav, O., Magsar, E., Tuvdendorj, B., 2018. Frequency analysis of MODIS NDVI time series for determining hotspot of land degradation in Mongolia, in: International Archives of the Photogrammetry, Remote Sensing and Spatial Information Sciences - ISPRS Archives. International Society for Photogrammetry and Remote Sensing, pp. 1299–1304. https://doi.org/10.5194/isprs-archives-XLII-3-1299-2018

National agency for meteorology and the environmental monitoring., 2021. Environmental database of Mongolia [WWW Document]. URL https://www.eic.mn/ (accessed 9.28.21).

National Statistics Office of Mongolia, 2020. Mongolian statistical information service [WWW Document]. URL http://1212.mn/default.aspx (accessed 7.26.20).

Nkonya, E., Gerber, N., Baumgartner, P., von Braun, J., De Pinto, A., Graw, V., Kato, E., Kloos, J., Walter, T., 2012. The Economics of Desertification, Land Degradation, and Drought Toward an Integrated Global Assessment. SSRN Electron. J. https://doi.org/10.2139/ssrn.1890668

Nkonya, E., Von Braun, J., Mirzabaev, A., Le, Q.B., Kwon, H.Y., Kirui, O., 2015. Concepts and methods of global assessment of the economics of land degradation and improvement, in: Economics of Land Degradation and Improvement - A Global Assessment for Sustainable Development. Springer International Publishing, pp. 15–32. https://doi.org/10.1007/978-3-319-19168-3_2

Noi Phan, T., Kuch, V., Lehnert, L.W., 2020. Land cover classification using google earth engine and random forest classifier-the role of image composition. Remote Sens. 12, 2411. https://doi.org/10.3390/RS12152411

Norovsuren, B., Tseveen, B., Batomunkuev, V., Renchin, T., 2019. Estimation for forest biomass and coverage using Satellite data in small scale area, Mongolia, in: IOP Conference Series: Earth and Environmental Science. https://doi.org/10.1088/1755-1315/320/1/012019

Nyamsuren, B., Nasahara, K.N., Kubota, T., Masaki, T., 2019. Vegetation mapping by using GPM/DPR over the mongolian land. Remote Sens. 11, 2386. https://doi.org/10.3390/rs11202386

Nzuza, P., Ramoelo, A., Odindi, J., Kahinda, J.M., Madonsela, S., 2020. Predicting land degradation using Sentinel-2 and environmental variables in the Lepellane catchment of the Greater Sekhukhune District, South Africa. Phys. Chem. Earth 102931. https://doi.org/10.1016/j.pce.2020.102931

Otgonbayar, M., Atzberger, C., Chambers, J., Damdinsuren, A., 2019. Mapping pasture biomass in Mongolia using Partial Least Squares, Random Forest regression and Landsat 8 imagery. Int. J. Remote Sens. 40, 3204–3226. https://doi.org/10.1080/01431161.2018.1541110

Padarian, J., Minasny, B., McBratney, A.B., 2020. Machine learning and soil sciences: A review aided by machine learning tools. SOIL. https://doi.org/10.5194/soil-6-35-2020

Perović, V., Kadović, R., Đurđević, V., Pavlović, D., Pavlović, M., Čakmak, D., Mitrović, M., Pavlović, P., 2021. Major drivers of land degradation risk in Western Serbia: Current trends and future scenarios. Ecol. Indic. 123, 107377.

https://doi.org/10.1016/j.ecolind.2021.107377

Pfeiffer, M., Dulamsuren, C., Wesche, K., 2020. Grasslands and Shrublands of Mongolia, in: Encyclopedia of the World's Biomes. Elsevier, pp. 759–772. https://doi.org/10.1016/B978-0-12-409548-9.12057-3

Phiri, D., Simwanda, M., Salekin, S., Nyirenda, V.R., Murayama, Y., Ranagalage, M., 2020. Sentinel-2 data for land cover/use mapping: A review. Remote Sens. https://doi.org/10.3390/rs12142291

Rodrigues, P.M.S., Schaefer, C.E.G.R., De Oliveira Silva, J., Ferreira, W.G., Dos Santos, R.M., Neri, A.V., 2018. The influence of soil on vegetation structure and plant diversity in different tropical savannic and forest habitats. J. Plant Ecol. 11, 226–236. https://doi.org/10.1093/jpe/rtw135

Rosenfield, G.H., Fitzpatrick-Lins, K., 1986. A coefficient of agreement as a measure of thematic classification accuracy. Photogramm. Eng. Remote Sens. 52, 223–227.

Saini, R., Ghosh, S.K., 2017. Ensemble classifiers in remote sensing: A review, in: Proceeding - IEEE International Conference on Computing, Communication and Automation, ICCCA 2017. Institute of Electrical and Electronics Engineers Inc., pp. 1148–1152. https://doi.org/10.1109/CCAA.2017.8229969

Sainnemekh, S., Barrio, I.C., Densambuu, B., Bestelmeyer, B., Aradóttir, Á.L., 2022. Rangeland degradation in Mongolia: A systematic review of the evidence. J. Arid Environ. https://doi.org/10.1016/j.jaridenv.2021.104654

Salvati, L., Zitti, M., Ceccarelli, T., 2008. Integrating economic and environmental indicators in the assessment of desertification risk: A case study. Appl. Ecol. Environ. Res. 6, 129–138. https://doi.org/10.15666/aeer/0601_129138

Sarparast, M., Ownegh, M., Najafinejad, A., Sepehr, A., 2018. An applied statistical method to identify desertification indicators in northeastern Iran. Geoenvironmental Disasters 5, 1–10. https://doi.org/10.1186/s40677-018-0095-3

Saygın, S.D., Basaran, M., Ozcan, A.U., Dolarslan, M., Timur, O.B., Yilman, F.E., Erpul, G., 2011. Land degradation assessment by geo-spatially modeling different soil erodibility equations in a semi-arid catchment. Environ. Monit. Assess. 180, 201–215. https://doi.org/10.1007/s10661-010-1782-z

Sayler, K., 2020. Landsat 4-7 Collection 1 (C1) Surface Reflectance (LEDAPS). Product Guide. Version 3.0.

Sen, P.K., 1968. Estimates of the Regression Coefficient Based on Kendall's Tau. J. Am. Stat. Assoc. 63, 1379–1389. https://doi.org/10.1080/01621459.1968.10480934

Sheykhmousa, M., Mahdianpari, M., Ghanbari, H., Mohammadimanesh, F., Ghamisi, P., Homayouni, S., 2020. Support Vector Machine Versus Random Forest for Remote Sensing Image Classification: A Meta-Analysis and Systematic Review. IEEE J. Sel. Top. Appl. Earth Obs. Remote Sens. https://doi.org/10.1109/JSTARS.2020.3026724

Shukherdorj, B., Shiga, T., Batlai, O., Wesche, K., Ritz, C.M., Khurelbaatar, K., Kim, J.Y., Jo, H.J., Nyam-Osor, B., Chung, G.Y., Choi, H.J., 2019. Contribution to the knowledge on the flora of Numrug Strictly Protected Area and some parts of East Mongolia. J. Asia-Pacific Biodivers. 12, 284–301. https://doi.org/10.1016/j.japb.2019.01.005

Song, Y., Liu, L., Yan, P., Cao, T., 2005. A review of soil erodibility in water and wind erosion research. J. Geogr. Sci. 15, 167–176. https://doi.org/10.1007/bf02872682

Spellerberg, I.F., 2002. Ecological Effects of Roads, Ecological Effects of Roads. https://doi.org/10.1201/9781482279931

Stavi, I., Lal, R., 2015. Achieving Zero Net Land Degradation: Challenges and opportunities. J. Arid Environ. 112, 44–51. https://doi.org/10.1016/j.jaridenv.2014.01.016

T. S. Kapalanga, Ó.A., 2008. A Review of Land Degradation Assessment Methods. undefined 17–68.

Tian, F., Herzschuh, U., Mischke, S., Schlütz, F., 2014. What drives the recent intensified vegetation degradation in Mongolia – Climate change or human activity? Holocene 24, 1206–1215. https://doi.org/10.1177/0959683614540958

Torabi Haghighi, A., Darabi, H., Karimidastenaei, Z., Davudirad, A.A., Rouzbeh, S., Rahmati, O., Sajedi-Hosseini, F., Klöve, B., 2021. Land degradation risk mapping using topographic, human-induced, and geo-environmental variables and machine learning algorithms, for the Pole-Doab watershed, Iran. Environ. Earth Sci. 80, 1. https://doi.org/10.1007/s12665-020-09327-2

Tsedev, B.-E., 2021. Land Use and Nature Conservation in Mongolia, in: The Physical Geography of Mongolia. Springer, Cham, pp. 195–211. https://doi.org/10.1007/978-3-030-61434-8_11

Tsheboeng, G., 2018. Spatial variation of the influence of distance from surface water on riparian plant communities in the Okavango Delta, Botswana. Ecol. Process. 2018 71 7, 1–12. https://doi.org/10.1186/S13717-018-0140-X

Tucker, C.J., 1979. Red and photographic infrared linear combinations for monitoring vegetation. Remote Sens. Environ. 8, 127–150. https://doi.org/10.1016/0034-4257(79)90013-0

Tucker, C.J., Sellers, P.J., 1986. Satellite remote sensing of primary production. Int. J. Remote Sens. 7, 1395–1416. https://doi.org/10.1080/01431168608948944

Turner, K.G., Anderson, S., Gonzales-Chang, M., Costanza, R., Courville, S., Dalgaard, T., Dominati, E., Kubiszewski, I., Ogilvy, S., Porfirio, L., Ratna, N., Sandhu, H., Sutton, P.C., Svenning, J.C., Turner, G.M., Varennes, Y.D., Voinov, A., Wratten, S., 2015. A review of methods, data, and models to assess changes in the value of ecosystem services from land degradation and restoration. Ecol. Modell. https://doi.org/10.1016/j.ecolmodel.2015.07.017

Tuvshintogtokh, I., Ariungerel, D., 2013. Degradation of Mongolian Grassland Vegetation Under Overgrazing by Livestock and Its Recovery by Protection from Livestock Grazing, in: The Mongolian Ecosystem Network. Springer, Tokyo, pp. 115–130. https://doi.org/10.1007/978-4-431-54052-6_10

UNCCD, 2017. The Global Land Outlook, first edition., UNCCD.

Ungar, E.D., 2019. Perspectives on the concept of rangeland carrying capacity, and their exploration by means of Noy-Meir's two-function model. Agric. Syst. 173, 403–413. https://doi.org/10.1016/j.agsy.2019.03.023

United Nations, 2019. Global Land Outlook Northeast Asia Thematic Report: Partnerships to

Achieve Land Degradation Neutrality.

USGS, 2020. Landsat 8 Collection 1 (C1) Land Surface Reflectance Code (LaSRC) Product Guide, Lsds-1368.

Vågen, T.G., Winowiecki, L.A., Tondoh, J.E., Desta, L.T., Gumbricht, T., 2014. Mapping of soil properties and land degradation risk in Africa using MODIS reflectance. Geoderma 263, 216–225. https://doi.org/10.1016/j.geoderma.2015.06.023

von Braun, J., Gerber, N., Mirzabaev, A., Nkonya, E., 2013. The Economics of Land Degradation. SSRN Electron. J. https://doi.org/10.2139/ssrn.2237977

von Wehrden, H., Zimmermann, H., Hanspach, J., Ronnenberg, K., Wesche, K., 2009. Predictive mapping of plant species and communities using GIS and Landsat data in a southern Mongolian mountain range. Folia Geobot. 44, 211–225. https://doi.org/10.1007/s12224-009-9042-0

Wang, B., Jia, K., Liang, S., Xie, X., Wei, X., Zhao, X., Yao, Y., Zhang, X., 2018. Assessment of Sentinel-2 MSI spectral band reflectances for estimating fractional vegetation cover. Remote Sens. 10, 1927. https://doi.org/10.3390/rs10121927

Wang, Juanle, Wei, H., Cheng, K., Li, G., Ochir, A., Bian, L., Davaasuren, D., Chonokhuu, S., Nasanbat, E., 2019. Spatio-temporal pattern of land degradation along the China-Mongolia Railway (Mongolia). Sustain. 11, 2705. https://doi.org/10.3390/su11092705

Wang, J., Wei, H., Cheng, K., Ochir, A., Davaasuren, D., Li, P., Shun Chan, F.K., Nasanbat, E., 2020. Spatio-Temporal Pattern of Land Degradation from 1990 to 2015 in Mongolia. Environ. Dev. 34, 100497. https://doi.org/10.1016/j.envdev.2020.100497

Wang, Jie, Xiao, X., Bajgain, R., Starks, P., Steiner, J., Doughty, R.B., Chang, Q., 2019. Estimating leaf area index and aboveground biomass of grazing pastures using Sentinel-1, Sentinel-2 and Landsat images. ISPRS J. Photogramm. Remote Sens. 154, 189–201. https://doi.org/10.1016/j.isprsjprs.2019.06.007

Wang, Z., Wang, W., Zhang, Z., Hou, X., Ma, Z., Chen, B., 2021. River-groundwater interaction affected species composition and diversity perpendicular to a regulated river in an arid riparian zone. Glob. Ecol. Conserv. 27, e01595. https://doi.org/10.1016/j.gecco.2021.e01595

Wessels, K.J., Prince, S.D., Reshef, I., 2008. Mapping land degradation by comparison of vegetation production to spatially derived estimates of potential production. J. Arid Environ. 72, 1940–1949. https://doi.org/10.1016/j.jaridenv.2008.05.011

Wischmeier, W.H., Johnson, C.B., Cross, B. V, 1971. A soil erodibility nomograph for farmland and construction sites. J. Soil Water Conserv. 26, 189–193.

Wischmeier, W.H., Smith, D.D., 1978. Predicting rainfall erosion losses. Agric. Handb. no. 537 285–291.

Yamamoto, H., Kajiwara, K., Honda, Y., 2000. The study on biomass estimation in Mongolian grassland using satellite data and field measurement data.

Yembuu, B., 2021a. General Geographical Characteristics of Mongolia, in: The Physical Geography of Mongolia. pp. 1–8. https://doi.org/10.1007/978-3-030-61434-8_1

Yembuu, B., 2021b. Climate and Climate Change of Mongolia, in: The Physical Geography

of Mongolia. Springer, Cham, pp. 51–76. https://doi.org/10.1007/978-3-030-61434-8_4

Yengoh, G.T., Dent, D., Olsson, L., Tengberg, A.E., Tucker, C.J., 2015. Key Issues in the Use of NDVI for Land Degradation Assessment, in: Use of the Normalized Difference Vegetation Index (NDVI) to Assess Land Degradation at Multiple Scales. Springer, Cham, pp. 31–35. https://doi.org/10.1007/978-3-319-24112-8_5

Yousefi, S., Pourghasemi, H.R., Avand, M., Janizadeh, S., Tavangar, S., Santosh, M., 2021. Assessment of land degradation using machine-learning techniques: A case of declining rangelands. L. Degrad. Dev. 32, 1452–1466. https://doi.org/10.1002/ldr.3794

Youssef, R., Aniss, M., Jamal, C., 2020. Machine Learning and Deep Learning in Remote Sensing and Urban Application: A Systematic Review and Meta-Analysis, in: ACM International Conference Proceeding Series. Association for Computing Machinery. https://doi.org/10.1145/3399205.3399224

Zambon, I., Colantoni, A., Carlucci, M., Morrow, N., Sateriano, A., Salvati, L., 2017. Land quality, sustainable development and environmental degradation in agricultural districts: A computational approach based on entropy indexes. Environ. Impact Assess. Rev. https://doi.org/10.1016/j.eiar.2017.01.003

Zhu, B., Li, Z., Li, P., Shen, Z., Lu, J., 2009. Dynamic changes of soil erodibility during process of land degradation and restoration. Nongye Gongcheng Xuebao/Transactions Chinese Soc. Agric. Eng. 25, 56–61. https://doi.org/10.3969/j.issn.1002-6819.2009.2.010

Chapter 3. Conclusion and outlook

This thesis focused on the detailed assessment of current land degradation status and its anthropogenic drivers in grasslands of the eastern Mongolian steppe. Therefore, the overall aim of this thesis is to gain a better understanding of the impacts of human induced drivers on ongoing steppe degradation and to assess and map the land degradation status of the grasslands on the Eastern Mongolian Steppe through performing estimates in the current vegetation cover condition and trend changes. The study shows that large parts of the eastern Mongolia steppe were rapidly transformed from pristine steppe into anthropogenic land cover types and experienced at least some degree of degradation. Furthermore, this study provides a detailed assessment of ecological effects of steppe fire and transportation corridors including railroad and dirt roads on surrounding ecosystem of the eastern Mongolia steppe. Then, the land degradation map of vast Eastern Mongolian steppe were derived through estimating vegetation cover and aboveground biomass, evaluating potential land degradation drivers and analyzing relationship between land degrading proxy and potential drivers. The main findings of this thesis are presented in the following conclusion together with the corresponding questions outlined in section 1.3.

Research question 1: How did oil exploitation sites and associated infrastructure change in far eastern Mongolian steppe between 2005 and 2018, and can the relatively narrow linear infrastructure such as dirt road be detected from high/moderate resolution satellite time series data?

In **chapter 2.1**, the Random Forest algorithm in the supervised object-oriented framework has been successfully applied to time series of remote sensed data with different spatial and spectral resolutions. Consequently, land use changes due to oil exploitation and associated linear infrastructure and dirt roads network development have been detected. High overall accuracies between 73% and 93% were achieved. Differences in accuracy mainly depended on satellites' spatial resolution, where high spatial resolutions are clearly beneficial. However, it should be empathized that all datasets were useful to delineate linear features such as roads. For the methodology, Random Forest with object-oriented supervised classification has high potential for extracting relatively narrow linear features such as dirt roads from multiscale satellite images. The spatiotemporal analysis detected that dramatic land activities occurred in far eastern Mongolian steppe in the period of 2005-2018, consequently, the area of pristine steppe converted to land for oil exploitation and associated dirt roads and infrastructure increased by 88% with its largest expansion by 47% in the period 2005–2010. As a result of land cover/use change analysis, the time series dataset of dirt road networks was created for further land degradation mapping of Eastern Mongolian steppe.

Research question 2: How do the dirt road network, transportation corridors and steppe fire effect to the surrounding ecosystem of eastern Mongolia steppe?

To answer this question, **chapter 2.2** explains a case study including vegetation field surveys and an associated aerial surveys using UAV that has been conducted at four sites along the main railroad and dirt road transportation corridor between province center to border crossing. Sampling sites were divided into burned by steppe fire and unburned. Vegetation cover was delineated at dominant plant functional group level with reasonable accuracy on a small scale from very high spatial resolution UAV data using Random Forest. Within this RGB image

analysis, the predictive power of explanatory variables including spectral metrics, vegetation index and texture metrics were evaluated for vegetation cover mapping. Then, vegetation cover maps derived from UAV data were integrated to PlanetScope data to create vegetation cover maps for impact assessments at a local scale. In this spatially aggregation process, a pixel-wise manner was carried out to minimize the typical scale effect that often impedes classification. With this technique, it is furthermore possible to spatially aggregate high resolution map products that are needed to be integrated with coarse resolution data. After the aggregation process, Random Forest regression was employed to successfully estimate the fractional cover of plant functional groups from PlanetScope multi-temporal data at a local scale. Finally, estimates on the created maps of plant functional groups demonstrated that dirt roads ecologically affects up to 60–100 m of roadside vegetation cover, whereas railroads transportation corridor affect up to 120 m distance in typical Mongolian steppes. The degradation rate of affected roadside vegetation area can be determined according to shifts in the dominance of graminoids, forbs, and shrubs. For steppe fires, a comparison between burned and unburned areas in different years indicates that wildfires affect the composition of pant functional groups in reducing the fractional cover of graminoids and forbs, and that increasing cover of bare ground leads to a distinct and patchy mosaic of different vegetation types.

Research question 3: What is the current condition of vegetation cover and land degradation in the eastern Mongolia steppe, and what drivers have potential to map land degradation with reasonable accuracy?

In **chapter 2.3** potential drivers including the novel road dataset for land degradation were evaluated taking the new knowledge on ecological effect of infrastructure into account. In the context of land degradation mapping, a comprehensive understanding of current vegetation cover is important, therefore, current fractional vegetation cover, aboveground biomass and NDVI trends were analyzed. The fractional vegetation cover and aboveground biomass were predicted by training Random Forest regression models against 256 field samples and Sentinel 2 data which obtained good accuracies (R^2=0.76-0.81). Regarding the trend analysis of NDVI time series, the Mann-Kendall trend test statistics were obtained from the Landsat data in 2010-2020. Results indicated that a statistically significant decreasing trend occurred on 59% of the whole study area, which was mostly clustered around the central, middle-eastern and northeastern parts.

Potential driver variables were grouped into ecological, geomorphometric, environmental and anthropogenic factors. Most of the geomorphometric and environmental explanatory variables were derived from geospatial and statistical data and other sources of remotely sensed data. Additionally, estimated fractional vegetation cover, aboveground biomass and NDVI trends were used as ecological variables. For land degradation mapping, a separate random forest classification model was trained using all potential explanatory variables and field measurements of degradation rates as response variable in eastern Mongolian steppe (n = 200). The classification model obtained a reasonable overall accuracy of 73%. Amongst the 20 potential explanatory variables, annual soil loss, slope, soil erodibility and AGB were the most important variables for the estimation of current land degradation status. The land degradation map shows that most of the study area is generally affected by some degree of degradation, of which 2,472 km2 (2%) are severely degraded, 7,416 km2 (6%) are heavily degraded, 35,843 km2 (29%) are moderately degraded, and 71,687 km2 (58%) are slightly

degraded. Pristine and undegraded grassland sums to an area of 6180 km2 (5%). Additionally, Spearman correlation analysis between AGB and all other land degradation drivers except FVC showed that no strong relationship could be found over the entire study area; however, strong correlations have been detected at local scales. In other word, results showed that the land degradation driving forces are not constant over the entire study area. For instance, AGB is positively correlated with elevation, NDVI trends, distance to mining and oil exploitation sites, distance to road network, soil types, distance to water body, precipitation sum, precipitation change and road corridors around the areas of interest in study region. However, it is not constant at all area; for instance, it is observed negative relation between some of these degradation drivers and AGB in some locations.

Understanding changes of anthropogenic drivers and its associated consequences on ecosystem is the basis for mapping degraded area while combating land degradation. To achieve this, this research gained scientific knowledge about ecological effects of transportation corridors on surrounding steppe that had never been estimated before in Mongolia. This estimate is particularly essential for land degradation assessment, environmental conservation, and decision making in future infrastructure development. Also, the thesis provided an effective approach for future integrations of UAV and satellite imagery data in studies of vegetation cover and land degradation. Additionally, results of fractional vegetation cover and aboveground biomass contribute to the usage of Mongolian pasture photo-monitoring data for producing vegetation cover maps from regional to country-wide scales. In the future, vegetation cover estimates based on the best practice of this thesis may be employed as one of the potential methods to analyze the accumulated database of Mongolian pasture photo monitoring. Finally, this thesis provided an effective model that allows integrating land degradation field measurements, proxies and potential drivers for land degradation mapping. In this context, the relationships between land degradation proxy and their potential drivers at local to regional level have been clarified; consequently, it was illustrated which drivers strongly contribute to ongoing land degradation in Eastern Mongolia steppe. Most of geospatial data provided in land degradation mapping are available free of charge for whole Mongolia, therefore, the model in this thesis can be used to extent land degradation maps to other regions or the entire country in future. For further research in the future, more underlying drivers that stand for socio-economic effects (e.g. income and poverty) should be considered in combination with land degradation mapping.

Overall, this thesis presents the first spatially explicit grassland degradation classification which is fully validated against field samples. In addition, it contributes to a better understanding of natural and anthropogenic factors driving grassland degradation in Eastern Mongolian steppe. This knowledge is key for maintaining of and/or development toward sustainable land-use in Mongolia. Since the conservation of the grassland ecosystems guarantees the welfare of a high proportion of the Mongolian people directly or indirectly depending on livestock productivity, this thesis transports products and knowledge which are of utmost importance for Mongolian society. This is especially important in light of the societal changes currently occurring in Mongolia. The result of these changes is the concentration of population in and around cities and other permanent settlements reducing the mobility of herders. Presumably, this will lead to local increase in degradation in the future. With the tools and products developed in this thesis, hence, it will be possible to project future grassland status considering societal and climate changes in Mongolia.

References

Agboola, O., Babatunde, D.E., Isaac Fayomi, O.S., Sadiku, E.R., Popoola, P., Moropeng, L., Yahaya, A., Mamudu, O.A., 2020. A review on the impact of mining operation: Monitoring, assessment and management. Results Eng. https://doi.org/10.1016/j.rineng.2020.100181

Anderson, W., Johnson, T., 2015. Evaluating global land degradation using ground-based measurements and remote sensing, in: Economics of Land Degradation and Improvement - A Global Assessment for Sustainable Development. Springer, Cham, pp. 85–116. https://doi.org/10.1007/978-3-319-19168-3_5

Anees, S.A., Zhang, X., Shakeel, M., Al-Kahtani, M.A., Khan, K.A., Akram, M., Ghramh, H.A., 2022. Estimation of fractional vegetation cover dynamics based on satellite remote sensing in pakistan: A comprehensive study on the FVC and its drivers. J. King Saud Univ. - Sci. 34, 101848. https://doi.org/10.1016/j.jksus.2022.101848

Asian Development Bank, 2014. Making Grasslands Sustainable in Mongolia International Experiences with Payments for Environmental Services in Grazing Lands and Other Rangelands.

Asian Development Bank, 2013. Making Grasslands Sustainable in Mongolia Adapting to climate and encironmental change.

Asian Development Bank, 2011. Mongolia: Road Sector Development to 2016.

Bai, Z., Dent, D.L., Olsson, L., Schaepman, M.E., 2008. Global assessment of land degradation and improvement 1: identification by remote sensing. Rep. 2008/01, FAO/ISRIC-Rome/Wageningen 78.

Bai, Z.G., Dent, D.L., Olsson, L., Schaepman, M.E., 2008. Proxy global assessment of land degradation. Soil Use Manag. https://doi.org/10.1111/j.1475-2743.2008.00169.x

Bao Le, Q., Nkonya, Ephraim, Mirzabaev, Alisher, Le, Q., Nkonya, E, Mirzabaev, A, 2016. Biomass Productivity-Based Mapping of Global Land Degradation Hotspots. Econ. L. Degrad. Improv. - A Glob. Assess. Sustain. Dev. 55–84. https://doi.org/10.1007/978-3-319-19168-3_4

Bardgett, R.D., Bullock, J.M., Lavorel, S., Manning, P., Schaffner, U., Ostle, N., Chomel, M., Durigan, G., L. Fry, E., Johnson, D., Lavallee, J.M., Le Provost, G., Luo, S., Png, K., Sankaran, M., Hou, X., Zhou, H., Ma, L., Ren, W., Li, X., Ding, Y., Li, Y., Shi, H., 2021. Combatting global grassland degradation. Nat. Rev. Earth Environ. https://doi.org/10.1038/s43017-021-00207-2

Batkhishig, O., 2013. Human impact and land degradation in Mongolia, in: Dryland East Asia: Land Dynamics amid Social and Climate Change. pp. 265–281.

Batmunkh, I., 2021. Environmental Issues in the Mining Sector of Mongolia. J. Environ. Prot. (Irvine,. Calif). 12, 415–427. https://doi.org/10.4236/jep.2021.126025

Batsaikhan, N., Buuveibaatar, B., Chimed, B., Enkhtuya, O., Galbrakh, D., Ganbaatar, O., Lkhagvasuren, B., Nandintsetseg, D., Berger, J., Calabrese, J.M., Edwards, A.E., Fagan, W.F., Fuller, T.K., Heiner, M., Ito, T.Y., Kaczensky, P., Leimgruber, P., Lushchekina, A., Milner-Gulland, E.J., Mueller, T., Murray, M.G., Olson, K.A., Reading, R., Schaller,

G.B., Stubbe, A., Stubbe, M., Walzer, C., Von Wehrden, H., Whitten, T., 2014. Conserving the World's Finest Grassland Amidst Ambitious National Development. Conserv. Biol. 28, 1736–1739. https://doi.org/10.1111/cobi.12297

Bayarsaikhan, T., Kim, S.T., Gim, T.H.T., 2020. International tourists' destination choice differences according to Plog's personality types: analyzing the case of Mongolia based on the recreation opportunity spectrum. Int. J. Urban Sci. 24, 485–515. https://doi.org/10.1080/12265934.2020.1771195

Bazha, S.N., Gunin, P.D., Danzhalova, E. V., Drobyshev, Y.I., Prishcepa, A. V., 2012. Pastoral Degradation of Steppe Ecosystems in Central Mongolia, in: Eurasian Steppes. Ecological Problems and Livelihoods in a Changing World. Springer, Dordrecht, pp. 289–319. https://doi.org/10.1007/978-94-007-3886-7_10

Behrend, H., 2016. Land Degradation and Its Impact on Security, Land Restoration: Reclaiming Landscapes for a Sustainable Future. Academic Press. https://doi.org/10.1016/B978-0-12-801231-4.00004-5

Bengtsson, J., Bullock, J.M., Egoh, B., Everson, C., Everson, T., O'Connor, T., O'Farrell, P.J., Smith, H.G., Lindborg, R., 2019. Grasslands—more important for ecosystem services than you might think. Ecosphere 10, e02582. https://doi.org/10.1002/ecs2.2582

Biancalani, R., Nachtergaele, F., Petri, M., Bunning, S., 2013. Land degradation assessment in drylands methodology and results, LADA.

Bilsborrow, R.E., 1992. Population growth, internal migration, and environmental degradation in rural areas of developing countries. Eur. J. Popul. 8, 125–148. https://doi.org/10.1007/BF01797549

Borrelli, P., Robinson, D.A., Fleischer, L.R., Lugato, E., Ballabio, C., Alewell, C., Meusburger, K., Modugno, S., Schütt, B., Ferro, V., Bagarello, V., Oost, K. Van, Montanarella, L., Panagos, P., 2017. An assessment of the global impact of 21st century land use change on soil erosion. Nat. Commun. 8, 1–13. https://doi.org/10.1038/s41467-017-02142-7

Carlson, T.N., Ripley, D.A., 1997. On the relation between NDVI, fractional vegetation cover, and leaf area index. Remote Sens. Environ. 62, 241–252. https://doi.org/10.1016/S0034-4257(97)00104-1

Caspari, T., van Lynden, G., Bai, Z., Databases, D. not cite information about, 2015. Land Degradation Neutrality: An Evaluation of Methods 57 p.

Chen, Y., Lee, G., Lee, P., Oikawa, T., 2007. Model analysis of grazing effect on above-ground biomass and above-ground net primary production of a Mongolian grassland ecosystem. J. Hydrol. 333, 155–164. https://doi.org/10.1016/j.jhydrol.2006.07.019

Cherlet, M., Hutchinson, C., Reynolds, J., Hill, J., Sommer, S. and Von Maltitz, G., 2018. World atlas of desertification: Limits to Sustainability, Publications Office of the European Union. Publications Office of the European Union, Luxembourg. https://doi.org/10.2760/06292

Chimed-Ochir B., Hertzman T., Batsaikhan N., Batbold D., Sanjmyatav D., O.Y. and M.B., 2010. Filling the gaps to Protect the Biodiversity of Mongolia.

Chu, D., 2020. Fractional Vegetation Cover, in: Remote Sensing of Land Use and Land Cover

in Mountain Region. Springer, Singapore, pp. 195–207. https://doi.org/10.1007/978-981-13-7580-4_10

Chuluun, T., Altanbagana, M., Ojima, D., Tsolmon, R., Suvdantsetseg, B., 2017. Vulnerability of pastoral social-ecological systems in mongolia, in: Rethinking Resilience, Adaptation and Transformation in a Time of Change. Springer, Cham, pp. 73–88. https://doi.org/10.1007/978-3-319-50171-0_6

Coffin, A.W., Ouren, D.S., Bettez, N.D., Borda-de-água, L., Daniels, A.E., Grilo, C., Jaeger, J.A.G., Navarro, L.M., Preisler, H.K., Rauschert, E.S.J., 2021. The Ecology of Rural Roads: Effects, Management & Research. Ecol. Soc. Am. 1036.

Conant, R.T., 2012. Grassland soil organic carbon stocks: Status, opportunities, vulnerability, in: Recarbonization of the Biosphere: Ecosystems and the Global Carbon Cycle. Springer Nature, pp. 275–302. https://doi.org/10.1007/978-94-007-4159-1_13

D'Odorico, P., Ravi, S., 2016. Land Degradation and Environmental Change, in: Biological and Environmental Hazards, Risks, and Disasters. Academic Press, pp. 219–227. https://doi.org/10.1016/B978-0-12-394847-2.00014-0

Dagvadorj, D., Natsagdorj, L., Dorjpurev, J. and Namkhainyam, B., 2009. Assessment Report on Climate Change (MARCC), Ministry of Environment, Nature and Tourism, Mongolia. Ministry of Environment, Nature and Tourism, Mongolia.

Dagvadrj, D., Batjargal, Z., Natsagdorj, L., 2014. Mongolia Second Assessment Report on Climate Change, Ministry of Environment and Green Development of Mongolia. Ulaanbaatar.

Danzhalova, E. V., Bazha, S.N., Gunin, P.D., Drobyshev, Y.I., Kazantseva, T.I., Prischepa, A. V., Slemnev, N.N., Ariunbold, E., 2012. Indicators of Pasture Digression in Steppe Ecosystems of Mongolia. Erforsch. Biol. Ressourcen der Mongolei / Explor. into Biol. Resour. Mong. 12, 297–306.

Densambuu, B., Sainnemekh, S., Bestelmeyer, B., Ulambayar, B., Batjargal, E., 2018. National report on the rangeland health of Mongolia: Second Assessment. Ulaanbaatar.

Dorjgotov, D. (Ed.), 2009. Mongolian National Atlas, The Institute of Geography, Mongolian Academy of Sciences. The Institute of Geography, Mongolian Academy of Sciences, Ulaanbaatar.

Dregne, H.E., 2002. Land degradation in the drylands. Arid L. Res. Manag. 16, 99–132. https://doi.org/10.1080/153249802317304422

Dubovyk, O., 2017a. The role of Remote Sensing in land degradation assessments: opportunities and challenges. Eur. J. Remote Sens. https://doi.org/10.1080/22797254.2017.1378926

Dubovyk, O., 2017b. The role of Remote Sensing in land degradation assessments: opportunities and challenges. Eur. J. Remote Sens. https://doi.org/10.1080/22797254.2017.1378926

Dudley, N., Eufemia, L., Petersen, I., Fleckenstein, M., Campari, J., Eugenia Periago, M., O. Miñarro, F., Siqueira, C., François Timmers, J., Rincón, S., Musálem, K., Rendón, E., Caterine Forero, D., Kauffman, M., Miaro III, L., Burns, A., Ge, Z., Pereladova, O., Buyanaa, C., Serdyuk, A., Thapa, K., de Valença, A., Doornbos, S., McConnel, I., 2020.

GRASSLAND AND SAVANNAH ECOSYSTEMS An urgent need for conservation and sustainable management. Ger. WWF 90.

Easdale, M.H., Bruzzone, O., Mapfumo, P., Tittonell, P., 2018. Phases or regimes? Revisiting NDVI trends as proxies for land degradation. L. Degrad. Dev. 29, 433–445. https://doi.org/10.1002/ldr.2871

Egoh, B.N., Bengtsson, J., Lindborg, R., Bullock, J.M., Dixon, A.P., Rouget, M., 2018. The Importance of Grasslands in Providing Ecosystem Services, in: Routledge Handbook of Ecosystem Services. Routledge, pp. 421–441. https://doi.org/10.4324/9781315775302-37

Elbegjargal, N., Khudulmur, S., Tsogtbaatar, J., Dash, D., Mandakh, N., 2014. Desertification Atlas of Mongolia, Institute of Geoecology, Mongolian Academy of Sciences.

ELD Initiative, 2015. The value of land: Prosperous lands and positive rewards through sustainable land management.

Endicott, E., 2012. A history of land use in Mongolia: The thirteenth century to the present, A History of Land Use in Mongolia: The Thirteenth Century to the Present. Palgrave Macmillan. https://doi.org/10.1057/9781137269669

Environmental Information Center Mongolia [WWW Document], 2021. . Inf. Res. Inst. Meteorol. Hydrol. Environ. URL https://www.eic.mn/ (accessed 1.21.22).

FAO, 2017. The future of food and agriculture – Trends and challenges. Food and Agricultural Organization, Rome, Italy.

Fernandez-Gimenez, M., Allen-Diaz, B., 2001. Vegetation change along gradients from water sources in three grazed Mongolian ecosystems. Plant Ecol. 157, 101–118. https://doi.org/10.1023/A:1014519206041

Fernandez-Gimenez, M.E., 2006. Land use and land tenure in Mongolia: A brief history and current issues. USDA For. Serv. Proc. 39.

Foley, J.A., 2011. Can We Feed the World and Sustain the Planet?: A five-step global plan could double food production by 2050 while greatly reducing environmental damage. Sci. Am. 305, 60–65.

Foley, J.A., Ramankutty, N., Brauman, K.A., Cassidy, E.S., Gerber, J.S., Johnston, M., Mueller, N.D., O'Connell, C., Ray, D.K., West, P.C., Balzer, C., Bennett, E.M., Carpenter, S.R., Hill, J., Monfreda, C., Polasky, S., Rockström, J., Sheehan, J., Siebert, S., Tilman, D., Zaks, D.P.M., 2011. Solutions for a cultivated planet. Nature 478, 337–342. https://doi.org/10.1038/nature10452

Food and Agricultural Organization (FAO), 2015. Status of the World's Soil Resources. Rome, Italy.

Food and Agriculture Organization of the United Nations (FAO), W.W.F. (WWF), 2020. Environmental and Social Management Framework for "Promoting Dryland Sustainable Landscapes and Biodiversity Conservation in The Eastern Steppe of Mongolia" Project. Ulaanbaatar.

Forman, R.T.T., Alexander, L.E., 1998. Roads and their major ecological effects. Annu. Rev. Ecol. Syst. 29, 207–231. https://doi.org/10.1146/annurev.ecolsys.29.1.207

Gang, C., Zhou, W., Chen, Y., Wang, Z., Sun, Z., Li, J., Qi, J., Odeh, I., 2014. Quantitative assessment of the contributions of climate change and human activities on global grassland degradation. Environ. Earth Sci. 72, 4273–4282. https://doi.org/10.1007/s12665-014-3322-6

Gantumur, B., Wu, F., Vandansambuu, B., Munaa, T., Itirititphan, F., Zhao, Y., 2018. Land degradation assessment of agricultural zone and its causes: a case study in Mongolia, in: Https://Doi.Org/10.1117/12.2325164. SPIE, p. 72. https://doi.org/10.1117/12.2325164

Gao, J., O'Neill, B.C., 2020. Mapping global urban land for the 21st century with data-driven simulations and Shared Socioeconomic Pathways. Nat. Commun. 11, 1–12. https://doi.org/10.1038/s41467-020-15788-7

Gao, L., Wang, X., Johnson, B.A., Tian, Q., Wang, Y., Verrelst, J., Mu, X., Gu, X., 2020. Remote sensing algorithms for estimation of fractional vegetation cover using pure vegetation index values: A review. ISPRS J. Photogramm. Remote Sens. https://doi.org/10.1016/j.isprsjprs.2019.11.018

Gemma Shepherd, Enric Terradellas, Alexander Baklanov, U.K., William A. Sprigg, S.N., Ali Darvishi Boloorani, A.A.-D., 2016. Global Assessment of Sand and Dust Storms, United Nations Enviromental Program.

Gerber, N., Nkonya, E., Von Braun, J., 2014. Land degradation, poverty and marginality, in: Marginality: Addressing the Nexus of Poverty, Exclusion and Ecology. Springer, Dordrecht, pp. 181–202. https://doi.org/10.1007/978-94-007-7061-4_12

Gibbs, H.K., Salmon, J.M., 2015. Mapping the world's degraded lands. Appl. Geogr. https://doi.org/10.1016/j.apgeog.2014.11.024

Ginin P.D. Saandar M. (Eds). (Ed.), 2019. Ecosystems of Mongolia Atlas, A.N Severtsov Institute of Ecology and Evolution, Russian Academy of Science. A.N Severtsov Institute of Ecology and Evolution, Russian Academy of Science, Moscow - Ulaanbaatar.

Girvetz, E.H., McDonald, R., Heiner, M., Kiesecker, J., Davaa, G., Pague, C., Durnin, M., Oidov, E., 2014. Eastern mongolian grassland steppe, in: Climate and Conservation: Landscape and Seascape Science, Planning, and Action. Island Press-Center for Resource Economics, pp. 92–103. https://doi.org/10.5822/978-1-61091-203-7_8

Gitay, H., Noble, I.R., 1997. What are functional types and how should we seek them? Int. Geosphere-biosph. Program. B. Ser. Plant Funct. types Their Relev. to Ecosyst. Prop. Glob. Chang. 1, 3–19. https://doi.org/10.3/JQUERY-UI.JS

Global Mechanism of the UNCCD, 2018. Country Profile of Mongolia. Investing in Land Degradation Neutrality: Making the Case. An Overview of Indicators and Assessments. Bonn, Germany.

Goyal, H.D., 1999. A Development Perspective on Mongolia. Asian Surv. 39, 633–655. https://doi.org/10.2307/3021242

Greenwood, K.L., McKenzie, B.M., 2001. Grazing effects on soil physical properties and the consequences for pastures: A review. Aust. J. Exp. Agric. https://doi.org/10.1071/EA00102

GUERRA, A.J.T., FULLEN, M.A., JORGE, M. do C.O., BEZERRA, J.F.R., SHOKR, M.S.,

2017. Slope Processes, Mass Movement and Soil Erosion: A Review. Pedosphere 27, 27–41. https://doi.org/10.1016/S1002-0160(17)60294-7

Gunin, P.D., Bazha, S.N., Danzhalova, E. V., Dmitriev, I.A., Drobyshev, Y.I., Kazantseva, T.I., Miklyaeva, I.M., Ogureeva, G.N., Slemnev, N.N., Titova, S. V., Ariunbold, E., Battseren, C., Jargalsaikhan, L., 2012. Expansion of Ephedra sinica Stapf. in the arid steppe ecosystems of Eastern and Central Mongolia. Arid Ecosyst. 2, 18–33. https://doi.org/10.1134/S2079096112010052

Han, J., Dai, H., Gu, Z., 2021. Sandstorms and desertification in Mongolia, an example of future climate events: a review. Environ. Chem. Lett. https://doi.org/10.1007/s10311-021-01285-w

Hilbig, W., Narantuya, N., 2016. Plant Communities in Eastern Mongolia. Erforsch. Biol. Ressourcen der Mongolei / Explor. into Biol. Resour. Mong. ISSN 0440-1298.

Hilker, T., Natsagdorj, E., Waring, R.H., Lyapustin, A., Wang, Y., 2014. Satellite observed widespread decline in Mongolian grasslands largely due to overgrazing. Glob. Chang. Biol. 20, 418–428. https://doi.org/10.1111/gcb.12365

Hosonuma, N., Herold, M., De Sy, V., De Fries, R.S., Brockhaus, M., Verchot, L., Angelsen, A., Romijn, E., 2012. An assessment of deforestation and forest degradation drivers in developing countries. Environ. Res. Lett. https://doi.org/10.1088/1748-9326/7/4/044009

Huang, J., Yu, H., Guan, X., Wang, G., Guo, R., 2016. Accelerated dryland expansion under climate change. Nat. Clim. Chang. 6, 166–171. https://doi.org/10.1038/nclimate2837

Huang, S., Tang, L., Hupy, J.P., Wang, Y., Shao, G., 2021. A commentary review on the use of normalized difference vegetation index (NDVI) in the era of popular remote sensing. J. For. Res. https://doi.org/10.1007/s11676-020-01176-w

IFRC, 2021. Climate Change Impacts on Health and Livelihoods: Mongolia Assessment.

IPBES, 2019. Global Assessment Report on Biodiversity and Ecosystem Services, Global Assessment Summary for Policymakers. IPBES secretariat, Bonn, Germany. https://doi.org/https://doi.org/10.5281/zenodo.3831673

Jamsran, B.E., Lin, C., Byambakhuu, I., Raash, J., Akhmadi, K., 2019. Applying a support vector model to assess land cover changes in the Uvs Lake Basin ecoregion in Mongolia. Inf. Process. Agric. 6, 158–169. https://doi.org/10.1016/j.inpa.2018.07.007

John, R., Chen, J., Giannico, V., Park, H., Xiao, J., Shirkey, G., Ouyang, Z., Shao, C., Lafortezza, R., Qi, J., 2018. Grassland canopy cover and aboveground biomass in Mongolia and Inner Mongolia: Spatiotemporal estimates and controlling factors. Remote Sens. Environ. 213, 34–48. https://doi.org/10.1016/j.rse.2018.05.002

Jugder, D., Gantsetseg, B., Davaanyam, E., Shinoda, M., 2018. Developing a soil erodibility map across Mongolia. Nat. Hazards 92, 71–94. https://doi.org/10.1007/s11069-018-3409-6

Kairis, O., Karavitis, C., Salvati, L., Kounalaki, A., Kosmas, K., 2015. Exploring the Impact of Overgrazing on Soil Erosion and Land Degradation in a Dry Mediterranean Agro-Forest Landscape (Crete, Greece). Arid L. Res. Manag. 29, 360–374. https://doi.org/10.1080/15324982.2014.968691

Kaneko, K., Nohara, S., 2014. Review of Effective Vegetation Mapping Using the UAV

(Unmanned Aerial Vehicle) Method. J. Geogr. Inf. Syst. 06, 733–742. https://doi.org/10.4236/jgis.2014.66060

Kapalanga, T.S., 2008. A Review of Land Degradation Assessment Methods 17–68.

Kemper, J., MacDonald, S., 2009. Effects of contemporary winter seismic exploration on low arctic plant communities and permafrost. Arctic, Antarct. Alp. Res. 41, 228–237. https://doi.org/10.1657/1938-4246-41.2.228

Keshkamat, S.S., Tsendbazar, N.E., Zuidgeest, M.H.P., Shiirev-Adiya, S., van der Veen, A., van Maarseveen, M.F.A.M., 2013. Understanding transportation-caused rangeland damage in Mongolia. J. Environ. Manage. 114, 433–444. https://doi.org/10.1016/j.jenvman.2012.10.043

Keshkamat, S.S., Tsendbazar, N.E., Zuidgeest, M.H.P., Van Der Veen, A., De Leeuw, J., 2012. The environmental impact of not having paved roads in arid regions: An example from Mongolia. Ambio 41, 202–205. https://doi.org/10.1007/s13280-011-0155-3

Kim, Jungrack, Dorjsuren, M., Choi, Y., Purevjav, G., 2020. Reconstructed Aeolian Surface Erosion in Southern Mongolia by Multi-Temporal InSAR Phase Coherence Analyses. Front. Earth Sci. 8, 458. https://doi.org/10.3389/feart.2020.531104

Kim, Jaebeom, Kang, S., Seo, B., Narantsetseg, A., Han, Y., 2020. Estimating fractional green vegetation cover of Mongolian grasslands using digital camera images and MODIS satellite vegetation indices. GIScience Remote Sens. 57, 49–59. https://doi.org/10.1080/15481603.2019.1662166

Kinugasa, T., Suzuyama, Y., Tsuchihashi, N., Nachinshonhor, G.U., 2015. Colonization and expansion of grassland species after abandonment of dirt roads in the Mongolian steppe. Landsc. Ecol. Eng. 11, 19–27. https://doi.org/10.1007/s11355-013-0230-y

Kirui, O.K., Mirzabaev, A., von Braun, J., 2021. Assessment of land degradation 'on the ground' and from 'above.' SN Appl. Sci. 3, 1–13. https://doi.org/10.1007/s42452-021-04314-z

Kouba, Y., Merdas, S., Mostephaoui, T., Saadali, B., Chenchouni, H., 2021. Plant community composition and structure under short-term grazing exclusion in steppic arid rangelands. Ecol. Indic. 120, 106910. https://doi.org/10.1016/j.ecolind.2020.106910

Kowal, V.A., Ahlborn, J., Jamsranjav, C., Avirmed, O., Chaplin-Kramer, R., 2021. Modeling integrated impacts of climate change and grazing on mongolia's rangelands. Land 10, 397. https://doi.org/10.3390/land10040397

Kriegler, F.J., Malila, W.A., Nalepka, R.F., Richardson, W., 1969. Preprocessing transformations and their effects on multispectral recognition. Proc. 6th Int. Symp. Remote Sens. Environ. 97–131.

Kumar, L., Mutanga, O., 2017. Remote sensing of above-ground biomass. Remote Sens. https://doi.org/10.3390/rs9090935

Lal, R., Moldenhauer, W.C., 1987. Effects of soil erosion on crop productivity. CRC. Crit. Rev. Plant Sci. 5, 303–367. https://doi.org/10.1080/07352688709382244

Lamchin, M., Lee, J.Y., Lee, W.K., Lee, E.J., Kim, M., Lim, C.H., Choi, H.A., Kim, S.R., 2016. Assessment of land cover change and desertification using remote sensing technology in a local region of Mongolia. Adv. Sp. Res. 57, 64–77.

https://doi.org/10.1016/j.asr.2015.10.006

Langdon, R.J., Yousefi, P.D., Relton, C.L., Suderman, M.J., 2006. Global impacts of land degradation. Overseas Dev. Gr. (ODG), Norwich. https://doi.org/10.2/JQUERY.MIN.JS

Le, Q.B., Nkonya, E., Mirzabaev, A., 2015. Biomass productivity-based mapping of global land degradation hotspots, in: Economics of Land Degradation and Improvement - A Global Assessment for Sustainable Development. Springer, Cham, pp. 55–84. https://doi.org/10.1007/978-3-319-19168-3_4

Lemaire, G., Hodgson, J., Chabbi, A., 2011. Grassland productivity and ecosystems services, Grassland Productivity and Ecosystems Services. CABI. https://doi.org/10.2989/10220119.2014.955878

Li, C., de Jong, R., Schmid, B., Wulf, H., Schaepman, M.E., 2020. Changes in grassland cover and in its spatial heterogeneity indicate degradation on the Qinghai-Tibetan Plateau. Ecol. Indic. 119, 106641. https://doi.org/10.1016/j.ecolind.2020.106641

Li, S.G., Tsujimura, M., Sugimoto, A., Davaa, G., Sugita, M., 2006. Natural recovery of steppe vegetation on vehicle tracks in central Mongolia. J. Biosci. 31, 85–93. https://doi.org/10.1007/BF02705239

Liang, S., Wang, J., 2020a. Fractional vegetation cover, in: Advanced Remote Sensing. Academic Press, pp. 477–510. https://doi.org/10.1016/b978-0-12-815826-5.00012-x

Liang, S., Wang, J., 2020b. Aboveground biomass, in: Advanced Remote Sensing. Academic Press, pp. 543–580. https://doi.org/10.1016/b978-0-12-815826-5.00014-3

Liu, Y., Lu, C., 2021. Quantifying grass coverage trends to identify the hot plots of grassland degradation in the tibetan plateau during 2000-2019. Int. J. Environ. Res. Public Health 18, 1–18. https://doi.org/10.3390/ijerph18020416

Liu, Y., Yang, Y., Wang, Q., Khalifa, M., Zhang, Z., Tong, L., Li, J., Shi, A., 2019. Assessing the Dynamics of Grassland Net Primary Productivity in Response to Climate Change at the Global Scale. Chinese Geogr. Sci. 29, 725–740. https://doi.org/10.1007/s11769-019-1063-x

Liu, Y.Y., Evans, J.P., McCabe, M.F., de Jeu, R.A.M., van Dijk, A.I.J.M., Dolman, A.J., Saizen, I., 2013. Changing Climate and Overgrazing Are Decimating Mongolian Steppes. PLoS One 8, e57599. https://doi.org/10.1371/journal.pone.0057599

Lkhagva, A., Boldgiv, B., Goulden, C.E., Yadamsuren, O., Lauenroth, W.K., 2013. Effects of grazing on plant community structure and aboveground net primary production of semiarid boreal steppe of northern Mongolia. Grassl. Sci. 59, 135–145. https://doi.org/10.1111/grs.12022

Luckeneder, S., Giljum, S., Schaffartzik, A., Maus, V., Tost, M., 2021. Surge in global metal mining threatens vulnerable ecosystems. Glob. Environ. Chang. 69, 102303. https://doi.org/10.1016/j.gloenvcha.2021.102303

Luo, J., Liu, X., Yang, J., Liu, Y., Zhou, J., 2018. Variation in plant functional groups indicates land degradation on the Tibetan Plateau. Sci. Rep. 8, 1–9. https://doi.org/10.1038/s41598-018-36028-5

Ma, Q., Wu, J., He, C., Fang, X., 2021. The speed, scale, and environmental and economic impacts of surface coal mining in the Mongolian Plateau. Resour. Conserv. Recycl. 173,

105730. https://doi.org/10.1016/j.resconrec.2021.105730

Mandakh, N., Tsogtbaatar, J., Dash, D., Khudulmur, S., 2016. Spatial assessment of soil wind erosion using WEQ approach in Mongolia. J. Geogr. Sci. 26, 473–483. https://doi.org/10.1007/s11442-016-1280-5

Maus, V., Giljum, S., Gutschlhofer, J., da Silva, D.M., Probst, M., Gass, S.L.B., Luckeneder, S., Lieber, M., McCallum, I., 2020. A global-scale data set of mining areas. Sci. Data 7, 289. https://doi.org/10.1038/s41597-020-00624-w

McCarter, S.S., Rudy, A.C.A., Lamoureux, S.F., 2017. Long-term landscape impact of petroleum exploration, Melville Island, Canadian High Arctic. Arct. Sci. https://doi.org/10.1139/as-2016-0016

Mehring, M., Batbuyan, B., Bolortsetseg, S., Buuveibaatar, B., Dashpurev, T., Drees, L., Enkhtuvshin, S., Ganzorig, G., Hickler, T., Lehnert, L.W., Liehr, S., Miehe, G., Munkhbolor, G., Müller, T., Nandintsetseg, D., Olson, K., Ring, I., Tarne, A., Wang, Y., Wesche, K., 2018. Keep on moving - How to facilitate nomadic pastoralism in Mongolia in the light of current societal transformation processes, ISOE Policy Brief.

Meng, X., Gao, X., Li, Sen, Li, Shengyu, Lei, J., 2021. Monitoring desertification in Mongolia based on Landsat images and Google Earth Engine from 1990 to 2020. Ecol. Indic. 129, 107908. https://doi.org/10.1016/j.ecolind.2021.107908

Meusburger, K., Bänninger, D., Alewell, C., 2010. Estimating vegetation parameter for soil erosion assessment in an alpine catchment by means of QuickBird imagery. Int. J. Appl. Earth Obs. Geoinf. 12, 201–207. https://doi.org/10.1016/j.jag.2010.02.009

Miao, L., Müller, D., Cui, X., Ma, M., 2017. Changes in vegetation phenology on the Mongolian Plateau and their climatic determinants. PLoS One 12, e0190313. https://doi.org/10.1371/journal.pone.0190313

Millennium Ecosystem Assessment, 2005. Ecosystems and Human Well-being: Scenarios.

Millennium Ecosystem Assessment (Program), 2005. Ecosystems and Human Well-Being. Island Press, Washington, DC.

Mineral Resources Authority of Mongolia, 2021. Mining and Geology Statistics 2021 data, Mineral Resources Authority of Mongolia. Ulaanbaatar.

Mineral Resources Authority of Mongolia, 2016. Annual Bulletin of Mining and Geology - Mongolia 2016, Mineral Resources Authority of Mongolia. Ulaanbaatar.

Mineral Resources Authority of Mongolia, 2015. Mining and Geology Statistics 2015 data, Mineral Resources Authority of Mongolia.

Ministry of Environment and Tourism of Mongolia, 2018. National Report on Voluntary Target Setting To Achieve Land Degradation, UNCCD.

Mirzabaev, A., Nkonya, E., Goedecke, J., Johnson, T., Anderson, W., 2015. Global drivers of land degradation and improvement, in: Economics of Land Degradation and Improvement - A Global Assessment for Sustainable Development. Springer, Cham, pp. 167–195. https://doi.org/10.1007/978-3-319-19168-3_7

Mongolia EITI, 2020. Mongolia Fourteenth EITI Reconciliation Report 2019. Ulaanbaatar.

Montanarella, L., Scholes, R., Brainich, A., 2018. The IPBES assessment report on land

degradation and restoration, Companion to Environmental Studies. Bonn, Germany.

Mortimore, M., 1993. Population growth and land degradation. GeoJournal 31, 15–21. https://doi.org/10.1007/BF00815897

Mu, H., Battsetseg, B., Ito, T.Y., Otani, S., Onishi, K., Kurozawa, Y., 2011. Health effects of dust storms: Subjective eye and respiratory system symptoms in inhabitants in Mongolia. J. Environ. Health.

Mu, H., Otani, S., Shinoda, M., Yokoyama, Y., Onishi, K., Hosoda, T., Okamoto, M., Kurozawa, Y., 2013. Long-term effects of livestock loss caused by dust storm on mongolian inhabitants: A survey 1 year after the dust storm. Yonago Acta Med. 56, 39–42.

Munkhzul, O., Oyundelger, K., Narantuya, N., Tuvshintogtokh, I., Oyuntsetseg, B., Wesche, K., Jäschke, Y., 2021. Grazing Effects on Mongolian Steppe Vegetation—A Systematic Review of Local Literature. Front. Ecol. Evol. https://doi.org/10.3389/fevo.2021.703220

Murray, P., Crotty, F., Eekeren, N. van, 2013. Management of Grassland Systems, Soil, and Ecosystem Services, in: Soil Ecology and Ecosystem Services. Oxford University Press, pp. 282–294. https://doi.org/10.1093/acprof:oso/9780199575923.003.0024

Na, Y., Li, J., Hoshino, B., Bao, S., Qin, F., Myagmartseren, P., 2018. Effects of different grazing systems on aboveground biomass and plant species dominance in typical Chinese and Mongolian steppes. Sustain. 10, 4753. https://doi.org/10.3390/su10124753

Nakano, T., Bat-Oyun, T., Shinoda, M., 2020. Responses of palatable plants to climate and grazing in semi-arid grasslands of Mongolia. Glob. Ecol. Conserv. 24, e01231. https://doi.org/10.1016/j.gecco.2020.e01231

Nandintsetseg, B., Boldgiv, B., Chang, J., Ciais, P., Davaanyam, E., Batbold, A., Bat-Oyun, T., Stenseth, N.C., 2021. Risk and vulnerability of Mongolian grasslands under climate change. Environ. Res. Lett. 16, 034035. https://doi.org/10.1088/1748-9326/abdb5b

Nandintsetseg, B., Shinoda, M., 2015. Land surface memory effects on dust emission in a Mongolian temperate grassland. J. Geophys. Res. Biogeosciences 120, 414–427. https://doi.org/10.1002/2014JG002708

Nandintsetseg, D., Bracis, C., Olson, K.A., Böhning-Gaese, K., Calabrese, J.M., Chimeddorj, B., Fagan, W.F., Fleming, C.H., Heiner, M., Kaczensky, P., Leimgruber, P., Munkhnast, D., Stratmann, T., Mueller, T., 2019. Challenges in the conservation of wide-ranging nomadic species. J. Appl. Ecol. 56, 1916–1926. https://doi.org/10.1111/1365-2664.13380

Nanzad, L., Zhang, J., Batdelger, G., Sharma, T.P.P., Koju, U.A., Wang, J., Nabil, M., 2021. Analyzing npp response of different rangeland types to climatic parameters over mongolia. Agronomy 11, 647. https://doi.org/10.3390/agronomy11040647

Nasanbat, E., Sharav, S., Sanjaa, T., Lkhamjav, O., Magsar, E., Tuvdendorj, B., 2018. Frequency analysis of MODIS NDVI time series for determining hotspot of land degradation in Mongolia, in: International Archives of the Photogrammetry, Remote Sensing and Spatial Information Sciences - ISPRS Archives. International Society for Photogrammetry and Remote Sensing, pp. 1299–1304. https://doi.org/10.5194/isprs-archives-XLII-3-1299-2018

National Statistical Office of Mongolia, 2020. Mongolian Statistical Yearbook 2020.

National Statistics Office of Mongolia, 2021. Mongolian statistical information service: Number of livestock by region [WWW Document]. Natl. Stat. Off. Mong. URL http://1212.mn/tables.aspx?tbl_id=DT_NSO_1001_021V1&BAG_select_all=0&BAGSingleSelect=_4_421_422_423_0&TYPE_OF_LIVESTOCK_select_all=0&TYPE_OF_LIVESTOCKSingleSelect=_01&YearY_select_all=0&YearYSingleSelect=_1990_2019_2020_2018_2017_2016_2015_2014_2013_2012_ (accessed 12.30.21).

Nkonya, E., Anderson, W., Kato, E., Koo, J., Mirzabaev, A., Von Braun, J., Meyer, S., 2015. Global cost of land degradation, in: Economics of Land Degradation and Improvement - A Global Assessment for Sustainable Development. Springer, Cham, pp. 117–165. https://doi.org/10.1007/978-3-319-19168-3_6

Nuissl, H., Siedentop, S., 2021. Urbanisation and Land Use Change, in: Sustainable Land Management in a European Context. Springer, Cham, pp. 75–99. https://doi.org/10.1007/978-3-030-50841-8_5

Nyamtseren, M., Jamsran, T., Khudulmur, S., 2015. The assessment and mapping of desertification in Mongolia, in: 3rd Scientific Conference of UN CCD. Cancun, Mexico.

Oldeman, L.R., Hakkeling, R.T.A., Sombroek, W.G., 1990. World map of the status of human-induced soil degradation: an explanatory note. World map status human-induced soil Degrad. an Explan. note.

Olson, D.M., Dinerstein, E., 2002. The global 200: Priority ecoregions for global conservation, in: Annals of the Missouri Botanical Garden. Missouri Botanical Garden, pp. 199–224. https://doi.org/10.2307/3298564

Olson, D.M., Dinerstein, E., Wikramanayake, E.D., Burgess, N.D., Powell, G.V.N., Underwood, E.C., D'Amico, J.A., Itoua, I., Strand, H.E., Morrison, J.C., Loucks, C.J., Allnutt, T.F., Ricketts, T.H., Kura, Y., Lamoreux, J.F., Wettengel, W.W., Hedao, P., Kassem, K.R., 2001. Terrestrial ecoregions of the world: A new map of life on Earth. Bioscience. https://doi.org/10.1641/0006-3568(2001)051[0933:TEOTWA]2.0.CO;2

Olson, K.A., Fuller, T.K., Mueller, T., Murray, M.G., Nicolson, C., Odonkhuu, D., Bolortsetseg, S., Schaller, G.B., 2010. Annual movements of Mongolian gazelles: Nomads in the Eastern Steppe. J. Arid Environ. 74, 1435–1442. https://doi.org/10.1016/j.jaridenv.2010.05.022

Olson, K.A., Mueller, T., Kerby, J.T., Bolortsetseg, S., Leimgruber, P., Nicolson, C.R., Fuller, T.K., 2011. Death by a thousand huts? Effects of household presence on density and distribution of Mongolian gazelles. Conserv. Lett. 4, 304–312. https://doi.org/10.1111/j.1755-263X.2011.00180.x

Onda, Y., Kato, H., Tanaka, Y., Tsujimura, M., Davaa, G., Oyunbaatar, D., 2007. Analysis of runoff generation and soil erosion processes by using environmental radionuclides in semiarid areas of Mongolia. J. Hydrol. 333, 124–132. https://doi.org/10.1016/j.jhydrol.2006.07.030

Otani, S., Kurosaki, Y., Kurozawa, Y., Shinoda, M., 2017. Dust storms from degraded drylands of Asia: Dynamics and health impacts. Land 6. https://doi.org/10.3390/land6040083

Otgonbayar, M., Atzberger, C., Chambers, J., Damdinsuren, A., 2019. Mapping pasture

biomass in Mongolia using Partial Least Squares, Random Forest regression and Landsat 8 imagery. Int. J. Remote Sens. 40, 3204–3226. https://doi.org/10.1080/01431161.2018.1541110

P.R. Shukla, J. Skea, E. Calvo Buendia, V.M.-D., H.-O. Pörtner, D. C. Roberts, P. Zhai, R. Slade, S. Connors, R. van Diemen, M. Ferrat, E. Haughey, S. Luz, S. Neogi, M. Pathak, J.P., J. Portugal Pereira, P. Vyas, E. Huntley, K. Kissick, M. Belkacemi, J. Malley, (eds.), 2019. IPCC, 2019: Climate Change and Land: an IPCC special report on climate change, desertification, land degradation, sustainable land management, food security, and greenhouse gas fluxes in terrestrial ecosystems, IPCC.

Pacheco, F.A.L., Sanches Fernandes, L.F., Valle Junior, R.F., Valera, C.A., Pissarra, T.C.T., 2018. Land degradation: Multiple environmental consequences and routes to neutrality. Curr. Opin. Environ. Sci. Heal. 5, 79–86. https://doi.org/10.1016/J.COESH.2018.07.002

Pfeiffer, Martin, Dulamsuren, C., Jäschke, Y., Wesche, K., 2021. Grasslands of China and Mongolia: Spatial Extent, Land Use and Conservation, in: Grasslands of the World. CRC Press, pp. 182–210. https://doi.org/10.1201/9781315156125-15

Pfeiffer, M., Dulamsuren, C., Wesche, K., 2020. Grasslands and Shrublands of Mongolia, in: Encyclopedia of the World's Biomes. Elsevier, pp. 759–772. https://doi.org/10.1016/B978-0-12-409548-9.12057-3

Plaza-Toled, M., 2018. The Mineral Industry of Mongolia, in: USGS Minerals Yearbook 2015. pp. 19.1-19.6.

Priess, J.A., Schweitzer, C., Batkhishig, O., Koschitzki, T., Wurbs, D., 2015. Impacts of agricultural land-use dynamics on erosion risks and options for land and water management in Northern Mongolia. Environ. Earth Sci. 73, 697–708. https://doi.org/10.1007/s12665-014-3380-9

Pring, I., Polunin, N., 2010. Effects of Seismic Exploration on Mangrove Habitat in Tanzania. West. Indian Ocean J. Mar. Sci. 9, 57–73.

Qi, Y.Q., Liu, J.Y., Shi, H.D., Hu, Y.F., Zhuang, D.F., 2008. Using 137Cs tracing technique to estimate wind erosion rates in the typical steppe region, northern Mongolian Plateau. Chinese Sci. Bull. 53, 1423–1430. https://doi.org/10.1007/s11434-008-0070-6

Raynolds, M.K., Jorgenson, J.C., Jorgenson, M.T., Kanevskiy, M., Liljedahl, A.K., Nolan, M., Sturm, M., Walker, D.A., 2020. Landscape impacts of 3D-seismic surveys in the Arctic National Wildlife Refuge, Alaska. Ecol. Appl. 30, e02143. https://doi.org/10.1002/eap.2143

Reading, R.P., Bedunah, D., Amgalanbaatar, S., 2010. Conserving mongolia's grasslands, with challenges, opportunities, and lessons for north america's great plains. Gt. Plains Res. 20, 85–107.

Sainnemekh, S., Barrio, I.C., Densambuu, B., Bestelmeyer, B., Aradóttir, Á.L., 2022. Rangeland degradation in Mongolia: A systematic review of the evidence. J. Arid Environ. https://doi.org/10.1016/j.jaridenv.2021.104654

Sheehy, D.P., 1993. Grazing management strategies as a factor influencing ecological stability of Mongolian grasslands. Nomad. People. 33, 17–30.

Shi, H., Gao, Q., Qi, Y., Liu, J., Hu, Y., 2010. Wind erosion hazard assessment of the

Mongolian Plateau using FCM and GIS techniques. Environ. Earth Sci. 61, 689–697. https://doi.org/10.1007/s12665-009-0381-1

Shukherdorj, B., Shiga, T., Batlai, O., Wesche, K., Ritz, C.M., Khurelbaatar, K., Kim, J.Y., Jo, H.J., Nyam-Osor, B., Chung, G.Y., Choi, H.J., 2019. Contribution to the knowledge on the flora of Numrug Strictly Protected Area and some parts of East Mongolia. J. Asia-Pacific Biodivers. 12, 284–301. https://doi.org/10.1016/j.japb.2019.01.005

Sterk, G., Riksen, M., Goossens, D., 2001. Dryland Degradation by Wind Erosion and its Control. Ann. Arid Zone 40, 351–367.

Sternberg, T., Tsolmon, R., Middleton, N., Thomas, D., 2011. Tracking desertification on the Mongolian steppe through NDVI and field-survey data. Int. J. Digit. Earth 4, 50–64. https://doi.org/10.1080/17538940903506006

Stevens, C.J., 2018. Recent advances in understanding grasslands. F1000Research 7, 1363. https://doi.org/10.12688/F1000RESEARCH.15050.1

Suttie, J.M., Reynolds, S.G., Batello, C., 2005. Grasslands of the World, Grasslands of the World. https://doi.org/10.1201/9781315156125

Sutton, P.C., Anderson, S.J., Costanza, R., Kubiszewski, I., 2016. The ecological economics of land degradation: Impacts on ecosystem service values. Ecol. Econ. 129, 182–192. https://doi.org/10.1016/j.ecolecon.2016.06.016

Suzuki, Y., 2013. Conflict Between Mining Development and Nomadism in Mongolia, in: The Mongolian Ecosystem Network: Environmental Issues Under Climate and Social Changes. Springer, Tokyo, pp. 269–294. https://doi.org/10.1007/978-4-431-54052-6_20

Tao, S., Fang, J., Zhao, X., Zhao, S., Shen, H., Hu, H., Tang, Z., Wang, Z., Guo, Q., Turner, B.L., 2015. Rapid loss of lakes on the Mongolian Plateau. Proc. Natl. Acad. Sci. U. S. A. 112, 2281–2286. https://doi.org/10.1073/pnas.1411748112

The World Bank Group and the Asian Development Bank, 2021. Climate Risk Country Profile: Mongolia (2021), The World Bank Group and the Asian Development Bank. Washington DC and Manila.

Thomas, H.J.D., Myers-Smith, I.H., Bjorkman, A.D., Elmendorf, S.C., Blok, D., Cornelissen, J.H.C., Forbes, B.C., Hollister, R.D., Normand, S., Prevéy, J.S., Rixen, C., Schaepman-Strub, G., Wilmking, M., Wipf, S., Cornwell, W.K., Kattge, J., Goetz, S.J., Guay, K.C., Alatalo, J.M., Anadon-Rosell, A., Angers-Blondin, S., Berner, L.T., Björk, R.G., Buchwal, A., Buras, A., Carbognani, M., Christie, K., Siegwart Collier, L., Cooper, E.J., Eskelinen, A., Frei, E.R., Grau, O., Grogan, P., Hallinger, M., Heijmans, M.M.P.D., Hermanutz, L., Hudson, J.M.G., Hülber, K., Iturrate-Garcia, M., Iversen, C.M., Jaroszynska, F., Johnstone, J.F., Kaarlejärvi, E., Kulonen, A., Lamarque, L.J., Lévesque, E., Little, C.J., Michelsen, A., Milbau, A., Nabe-Nielsen, J., Nielsen, S.S., Ninot, J.M., Oberbauer, S.F., Olofsson, J., Onipchenko, V.G., Petraglia, A., Rumpf, S.B., Semenchuk, P.R., Soudzilovskaia, N.A., Spasojevic, M.J., Speed, J.D.M., Tape, K.D., te Beest, M., Tomaselli, M., Trant, A., Treier, U.A., Venn, S., Vowles, T., Weijers, S., Zamin, T., Atkin, O.K., Bahn, M., Blonder, B., Campetella, G., Cerabolini, B.E.L., Chapin, F.S., Dainese, M., de Vries, F.T., Díaz, S., Green, W., Jackson, R.B., Manning, P., Niinemets, Ozinga, W.A., Peñuelas, J., Reich, P.B., Schamp, B., Sheremetev, S., van Bodegom, P.M., 2019. Traditional plant functional groups explain variation in economic but not size-related traits across the tundra biome. Glob. Ecol. Biogeogr. 28, 78–95.

https://doi.org/10.1111/geb.12783

Trombulak, S.C., Frissell, C.A., 2000. Review of ecological effects of roads on terrestrial and aquatic communities. Conserv. Biol. 14, 18–30. https://doi.org/10.1046/j.1523-1739.2000.99084.x

Tsedev, B.-E., 2021. Land Use and Nature Conservation in Mongolia. Springer, Cham, pp. 195–211. https://doi.org/10.1007/978-3-030-61434-8_11

Tucker, C.J., Sellers, P.J., 1986. Satellite remote sensing of primary production. Int. J. Remote Sens. 7, 1395–1416. https://doi.org/10.1080/01431168608948944

Tully, J., Barnwell, A., 2014. Mongolia – Potential in an Emerging Economy. Geo ExPro 11, 48–52.

Tumur, E., Heijman, W., Gurjav, E.-A., Agipar, B., Heerink, N., 2020. Options for Increasing Mongolia's Livestock Sector Exports - A Revealed Comparative Advantage Analysis. Mong. J. Agric. Sci. 30, 38–50. https://doi.org/10.5564/MJAS.V30I2.1490

Tuvshintogtokh, I., Ariungerel, D., 2013. Degradation of Mongolian Grassland Vegetation Under Overgrazing by Livestock and Its Recovery by Protection from Livestock Grazing, in: The Mongolian Ecosystem Network. Springer, Tokyo, pp. 115–130. https://doi.org/10.1007/978-4-431-54052-6_10

Ulziibaatar, M., Matsui, K., 2021. Herders' perceptions about rangeland degradation and herd management: A case among traditional and non-traditional herders in khentii province of mongolia. Sustain. 13, 7896. https://doi.org/10.3390/su13147896

UNCCD, 2017. The Global Land Outlook, first edition., UNCCD.

UNDP, 2021. Independent Country Programme Review: Mongolia, The Independent Evaluation Office (IEO) of the United Nations Development Programme (UNDP).

UNDP, 2011. Assessment of Development Results - Mongolia, United Nations Development Programme, Assessment of Development Results. UN. https://doi.org/10.18356/a9b537c9-en

UNESCO, 2021. Mongol Daguur Biosphere Reserve, Mongolia [WWW Document]. UNESCO. URL https://en.unesco.org/biosphere/aspac/mongol-daguur (accessed 12.28.21).

United Nations, 2021. World Population Prospects - Population Division - United Nations [WWW Document]. United Nations. URL https://population.un.org/wpp/ (accessed 12.16.21).

United Nations Convention to Combat Desertification, 2019. The Global Land Outlook, Northeast Asia Thematic Report, United Nations Convention to Combat Desertification. United Nations Convention to Combat Desertification, Bonn, Germany.

United Nations Economic Commission for Europe, 2019. Environmental Performance Review: Mongolia - First Review, United Nations. United Nations publication, New York and Geneva.

Van Lynden, G.W.J., Mantel, S., 2001. The role of GIS and remote sensing in land degradation assessment and conservation mapping: Some user experiences and expectations. ITC J. 3, 61–68. https://doi.org/10.1016/S0303-2434(01)85022-4

Wang, J., Cheng, K., Liu, Q., Zhu, J., Ochir, A., Davaasuren, D., Li, G., Wei, H., Chonokhuu, S., Namsrai, O., Bat-Erdene, A., 2019. Land cover patterns in Mongolia and their spatiotemporal changes from 1990 to 2010. Arab. J. Geosci. 12, 1–13. https://doi.org/10.1007/s12517-019-4893-z

Wang, J., Wei, H., Cheng, K., Ochir, A., Davaasuren, D., Li, P., Shun Chan, F.K., Nasanbat, E., 2020. Spatio-Temporal Pattern of Land Degradation from 1990 to 2015 in Mongolia. Environ. Dev. 34, 100497. https://doi.org/10.1016/j.envdev.2020.100497

Wang, J., Wei, H., Cheng, K., Ochir, A., Shao, Y., Yao, J., Wu, Y., Han, X., Davaasuren, D., Chonokhuu, S., Zhou, Y., Zhang, M., Cao, X., Gao, M., Zhu, J., Li, Y., Li, Q., Liang, X., Li, K., 2022. Updatable dataset revealing decade changes in land cover types in Mongolia. Geosci. Data J. 00, 1–14. https://doi.org/10.1002/gdj3.149

Wei, H., Wang, J., Cheng, K., Li, G., Ochir, A., Davaasuren, D., Chonokhuu, S., 2018. Desertification information extraction based on feature space combinations on the Mongolian plateau. Remote Sens. 10, 1614. https://doi.org/10.3390/rs10101614

Widana, A., 2019. Environmental Impacts of the Mining Industry : A literature review. United Nations Dev. Progr. J. 1, 2–3.

World Bank, 2006. Mongolia: A Review of Environmental Social Impacts of the Mining Sector. Washington, DC.

World Bank Group, 2017. Mongolia - Mining Sector Institutional Strengthening Technical Assistance Project (English), World Bank Group. Washington, D.C.

World Food and Agriculture, 2021. World Food and Agriculture – Statistical Yearbook 2021, World Food and Agriculture – Statistical Yearbook 2021. FAO. https://doi.org/10.4060/cb4477en

Wright, J.P., Naeem, S., Hector, A., Lehman, C., Reich, P.B., Schmid, B., Tilman, D., 2006. Conventional functional classification schemes underestimate the relationship with ecosystem functioning. Ecol. Lett. 9, 111–120. https://doi.org/10.1111/j.1461-0248.2005.00850.x

Xiaoyu, M., Gao, X., Li, S., Lei, J., 2020. Spatial and Temporal Characteristics of Vegetation NDVI Changes and the Driving Forces in Mongolia during 1982–2015. Remote Sens. 2020, Vol. 12, Page 603 12, 603. https://doi.org/10.3390/RS12040603

Yembuu, B., 2021a. The Physical Geography of Mongolia, Springer Nature.

Yembuu, B., 2021b. Climate and Climate Change of Mongolia, in: The Physical Geography of Mongolia. Springer, Cham, pp. 51–76. https://doi.org/10.1007/978-3-030-61434-8_4

Yengoh, G.T., Dent, D., Olsson, L., Tengberg, A.E., Tucker, C.J., 2015a. Applications of NDVI for Land Degradation Assessment, in: Use of the Normalized Difference Vegetation Index (NDVI) to Assess Land Degradation at Multiple Scales. Springer, Cham, pp. 17–25. https://doi.org/10.1007/978-3-319-24112-8_3

Yengoh, G.T., Dent, D., Olsson, L., Tengberg, A.E., Tucker, C.J., 2015b. Main Global NDVI Datasets, Databases, and Software. Use Norm. Differ. Veg. Index to Assess L. Degrad. Mult. Scales 45–50. https://doi.org/10.1007/978-3-319-24112-8_8

Ykhanbai, H., 2010. Mongolia Forestry Outlook Study, Asia-Pacific Forestry Sector Outlook Study II.

Yong, M., Shinoda, M., Nandintsetseg, B., Bi, L., Gao, H., Wang, Y., 2021. Impacts of Land Surface Conditions and Land Use on Dust Events in the Inner Mongolian Grasslands, China. Front. Ecol. Evol. 9, 531. https://doi.org/10.3389/fevo.2021.664900

Zabel, F., Delzeit, R., Schneider, J.M., Seppelt, R., Mauser, W., Václavík, T., 2019. Global impacts of future cropland expansion and intensification on agricultural markets and biodiversity. Nat. Commun. 10, 1–10. https://doi.org/10.1038/s41467-019-10775-z

Zainelabdeen, Y.M., Yan, R., Xin, X., Yan, Y., Ahmed, A.I., Hou, L., Zhang, Y., 2020. The impact of grazing on the grass composition in Temperate Grassland. Agronomy 10, 1230. https://doi.org/10.3390/agronomy10091230

Zhao, Y., Liu, Z., Wu, J., 2020. Grassland ecosystem services: a systematic review of research advances and future directions. Landsc. Ecol. 2020 354 35, 793–814. https://doi.org/10.1007/S10980-020-00980-3

Zhao, Yujin, Sun, Y., Chen, W., Zhao, Yanping, Liu, X., Bai, Y., 2021. The potential of mapping grassland plant diversity with the links among spectral diversity, functional trait diversity, and species diversity. Remote Sens. 13, 3034. https://doi.org/10.3390/rs13153034

Zika, M., Erb, K.H., 2009. The global loss of net primary production resulting from human-induced soil degradation in drylands. Ecol. Econ. 69, 310–318. https://doi.org/10.1016/j.ecolecon.2009.06.014